Comparative anatomy of the pig brain -

An integrative magnetic resonance imaging (MRI) study of the porcine brain with special emphasis on the external morphology of the cerebral cortex

VERENA SCHMIDT

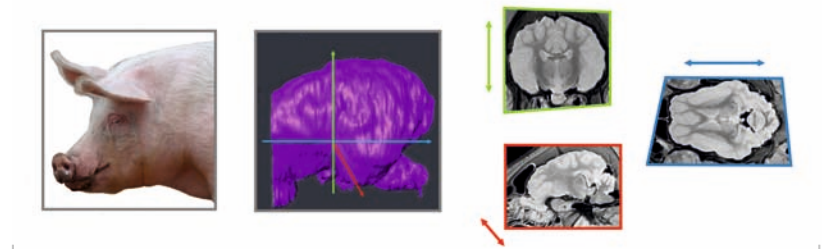

Inauguraldissertation zur Erlangung des Grades eines
Dr. med. vet.
beim Fachbereich Veterinärmedizin der Justus-Liebig-Universität Gießen

édition scientifique
VVB LAUFERSWEILER VERLAG

1. Auflage 2015

1st Edition 2015

Printed in Germany

édition scientifique
VVB LAUFERSWEILER VERLAG

STAUFENBERGRING 15, D-35396 GIESSEN
Tel: 0641-5599888 Fax: 0641-5599890
email: redaktion@doktorverlag.de

www.doktorverlag.de

Aus dem Klinikum Veterinärmedizin
Klinik für Kleintiere - Chirurgie
der Justus-Liebig-Universität Gießen

Betreuer: PD Dr. med.vet.(habil.) M. Schmidt

Comparative anatomy of the pig brain -

An integrative magnetic resonance imaging (MRI) study of the porcine brain with special emphasis on the external morphology of the cerebral cortex

INAUGURAL-DISSERTATION
zur Erlangung des Grades
eines Dr. med. vet.
beim Fachbereich Veterinärmedizin
der Justus-Liebig-Universität Gießen

eingereicht von

Verena Schmidt

Tierärztin aus Bonn

Gießen 2014

Mit Genehmigung des Fachbereichs Veterinärmedizin
der Justus-Liebig-Universität Gießen

Dekan: Prof. Dr. Dr. h.c. Martin Kramer

Gutachter:
PD Dr. med. vet. (habil.) M.J. Schmidt
Prof. Dr. Dr.med.vet. (habil.) G. Reiner
Prof. Dr. C. Herden

Tag der Disputation
16.04.2015

meiner Familie und meinen Freunden

Contents

1 Abbreviations

A

ab: amygdaloid body (*corpus amygdaloideum*; Fig. 34-37)

acn: accumbens nucleus (nucleus accumbens) (Fig. 11, Fig. 27-28, Fig. 31-32)

alv: alveus (Fig. 14-16, Fig. 24, Fig. 39-42)

Ans: ansate sulcus (*sulcus ansatus*; Fig. 57 G and 58 C (horse), Fig.77)

ans: ansiform lobule (*lobulus ansiformis*; Fig. 11-16, Fig. 21-27 , Fig. 47-52)

aob: accessory olfactory bulb (*bulbus olfactorius accessories*; Fig. 54)

aq: mesencephalic aqueduct (*aqueductus mesencephali*; Fig. 11-12, Fig. 30, Fig. 40-45, Fig. 72)

Aur: internal ear (*auris*; Fig. 7-9)

B

bcc: brachium of the caudal colliculus (*brachium colliculi caudalis*; Fig. 10, Fig. 42-45)

boc: basioccipital bone (*os basioccipitale*; Fig. 30)

brc: brachium of the rostral colliculus (*brachium of the rostral colliculus*; Fig. 41)

bsp: basisphenoid bone (*os basisphenoidale*; Fig. 30)

C

ca: cortical aplasia of the cerebellum (Fig. 28-29)

Cal: calcarine fissure (*fissura calcarine*; Fig 63)

cam: cornu ammonis (Fig. 10-17, Fig. 20-28, Fig. 38-43)

cc: corpus callosum (Fig. 14, Fig. 25-30, Fig. 31-38)

ccc: commissure of the caudal colliculi (*commissura colliculi caudalis*; Fig. 12, Fig. 28, Fig. 44)

ccl: caudal colliculus (*colliculus caudalis*; Fig. 10-12, Fig. 24-26 , Fig. 46-47)

Cco: cerebellar cortex (*cortex cerebelli*; Fig.74)

ccr: commissure of the rostral colliculli (*commissura colliculi rostralis*; Fig. 42)

cdc: caudal commissure (*commissura caudalis*; Fig. 12-13, Fig. 30, Fig. 40-41)

cec: central canal (*canalis centralis* Fig. 30)

cf: column of fornix (*columna fornicis*; Fig. 9, Fig. 33-37, Fig. 41)

cfo: corpus of fornix (*corpus fornicis*; Fig. 13-14, Fig. 33-35)

cgs: central grey substance (*substantia grisea centralis*; Fig. 10-12, Fig. 28-29, Fig. 40-45)

cho: optic chiasm (*chiasma opticum*; Fig. 6-8, Fig. 28-30, Fig. 32-33)

ci: cingulated gyrus (*gyrus cinguli*; Fig. 16-17, Fig. 28-30 , Fig. 32)

cin: cingulum (Fig. 17)

cl: central lobule (*lobulus centralis*; Fig. 12-13, Fig. 28-30, Fig. 46-48, Fig. 72)

cla: claustrum (Fig. 33)

cm: central white substance of the cerebellum (*corpus medullare cerebelli*; Fig.74)

cmf: commissure of the fornix (commissura fornicis Fig. 36-40)

cn: caudate nucleus (*nucleus caudatus*; Fig. 13-15, Fig. 25-29, Fig. 31-37)

con: cochlear nucleus (*nucleus cochlearis*; Fig. 50-52)

Cor: coronal sulcus (*sulcus coronalis*; Fig. 12-18, Fig. 23-26, Fig. 32-33, Fig. 57-58)

cpi: piriform cortex (*cortex piriformis* Fig. 27)

crc: cerebral crus (*crus cerebri*; Fig. 9-10, Fig. 35-42)

Cru: cruciate sulcus (*sulcus cruciatus*, Fig. 57)

cu: culmen vermis (Fig. 14-16, Fig. 29-30, Fig. 47-48, Fig. 72)

D

dbb: diagonal band of broca (*stria/gyrus diagonalis*; Fig. 25, Fig. 32)

de: declive vermis (Fig. 13-14, Fig. 29-30, Fig. 49-52, Fig. 72)

Dia: diagonal sulcus (*sulcus diagonalis*; Fig. 15-17, Fig. 21-24, Fig. 57-58)

dg: dentate gyrus (*gyrus dentatus*; Fig. 13-15, Fig. 39)

dpc: decussation of the rostral cerebellar peduncle (decussatio pedunculorum cerebellarium rostralium; Fig. 8-9, Fig. 28-30, Fig. 42-43)

dt: descending tracts- corticospinal and corticobulbar (*tractus corticospinalis, tractus cortico bulbaris*; Fig. 6, Fig. 43)

E

ec: external capsule (*capsula externa*; Fig. 13-14, Fig. 23-25, Fig. 31-38)

Ecg: ectogenual sulcus (*sulcus sctogenualis*; Fig. 13-17)

Ecm: ectomarginal sulcus (*sulcus ectomarginalis*; Fig. 15-18, Fig. 19-21, Fig. 32-40, Fig. 57-60)

Ecs: ectosylvian sulcus (*sulcus ectosylvius*; Fig. 14-18, Fig. 19, Fig. 35-41, Fig. 57-60)

Eng: endogenual sulcus (*sulcus endogenualis;* Fig. 13-14, Fig. 29-30, Fig. 57)

Enm: endomarginal sulcus (*sulcus endomarginalis*; Fig. 18, Fig. 24-25, Fig. 42-51, Fig. 57-60)

Enspl: endosplenial sulcus (*sulcus endosplenalis*; Fig. 59)

F

fh: fimbria of hippocampus (*fimbria hippocampi*; Fig. 10-15, Fig. 20-26, Fig. 38-39)

Flc: longitudinal cerebral fissure (*fissura longitudinalis cerebri*; Fig. 17-18)

flm: medial longitudinal fasciculus (*fasciculus longitudinalis medialis*; Fig. 6-9, Fig. 29-30, Fig. 42-52)

fmt: mammillothalamic fasciculus (*fasciculus mammilo-thalamicus*; Fig.10-13, Fig. 28-29, Fig. 35-37)

flo: flocculus (Fig. 9, Fig. 21-22, Fig. 48-52, Fig. 72)

fo: fornix (Fig.10-12,15, Fig. 27-30)

fol: folium vermis (Fig. 29-30, Fig. 72)

fos: fibrae olfactorii septales (Fig. 10-12; Fig. 32)

fsc: subcallosal fasciculus (*fasciculus subcallosus*; Fig. 31-39)

fte: fasciculus tegmenti (forel) (Fig. 27, Fig. 40-47)

ftp: transverse fibres of the pons (*fibrae transversae pontis* Fig. 42-44)

G

gcc: genu of the corpus callosum (genu corporis callosi Fig. 29-30)

Gen: genual sulcus (*sulcus genualis*; Fig. 13-17, Fig. 30, Fig. 57)

gnf: genu of the facial nerve (*genu nervi facialis*, VII; Fig. 7-8, Fig. 49-50)

gp: globus pallidus (Fig. 12, Fig. 31-33)

H

ha: habenula (Fig. 38-40)

hit: habenulo-interpedumcular tract (*tractus habenulo-interpeduncularis*; Fig. 10-13, Fig. 28-29, Fig. 39)

I

ic: internal capsule (*capsula interna*; Fig. 14-16, Fig. 22-26, Fig. 31-37)

idg: induseum griseum (Fig. 36-38)

in: insula (Fig. 14-15, Fig. 33, Fig. 56)

inc: insulae callejae (Fig. 31)

ipd: interpeduncular nucleus (*nucleus interpeduncularis*; Fig. 30, Fig. 42-43)

ir: infundibular recess (*recessus infundibularis*; Fig. 6)

ita: interthalamic adhesion (*adhaesio interthalamica*; Fig. 35-39)

L

lal: lateral lemniscus (*lemniscus lateralis*; Fig. 8-9, Fig. 25 , Fig. 44-45)

lgb: lateral geniculate body (*corpus geniculatum laterale*; Fig. 40-41)

lme: external medullary lamina (*lamina medullaris externa*; Fig. 12-14, Fig. 24, Fig. 36-40)

lmi: internal medullary lamina (*lamina medullaris interna*; Fig. 38)

Lms: lateral mesencephalic sulcus (*sulcus lateralis mesencephali*; Fig. 41)

lot: lateral olfactory tract (*tractus olfactorius lateralis*; Fig. 7-10, Fig. 23-24, Fig. 31-32)

li: lingua vermis (Fig. 9-11, Fig. 28-30, Fig. 46-51, Fig. 72)

lv: lateral ventricle (*ventriculus lateralis*; Fig. 23-26, Fig. 34-39)

M

Mar: marginal sulcus (*sulcus marginalis;* Fig. 18, Fig. 21-27, Fig. 34-51, Fig. 57-60)

mb: mamillary body (*corpus mammillare*; Fig. 28-30, Fig. 38)

mgb: medial geniculate body (*corpus geniculatum mediale*; Fig. 10-12, Fig. 40-41)

ml: medial lemniscus (*lemniscus medialis*; Fig. 6, Fig. 26, Fig. 42-47)

mot: medial olfactory tract (*tractus olfactorius medialis*; Fig7-9)

N

nab: nucleus of the abducent nerve (*nucleus nervi abducentis*; Fig. 7, Fig. 49)

nde: dentate nucleus (*nucleus dentatus*; Fig. 24-25,Fig. 49-51)

nf: fastigial nucleus (nucleus fastigii; Fig. 11, Fig. 51-52)

nip: interposed nucleus (*nucleus interpositus*; Fig. 11, Fig. 28, Fig. 49-51)

nmv: vestibular nucleus (*nucleus vestibularis medialis*; Fig. 50-52)

nml: lateral vestibular nerve (*nucleus nervi vestibularis lateralis, Deiters's;* Fig. 50)

nnf: facial nerve (*nucleus nervi facialis*; Fig. 50-52)

nno: oculomotor nerve (*nucleus nervi occulomotorii*; Fig. 42)

nnt: trigeminal nerve (*nuclei nervi trigemini*; Fig. 46-48)

no: nodulus vermis (Fig. 28-30, Fig. 72)

npo: pontine nuclei (*nuclei pontis*; Fig. 26-27, Fig. 45)

nrt: reticular nucleus of thalamus (*nucleus reticularis thalami*; Fig. 26)

nts: nucleus of the spinal tract of the trigeminal nerve (*nucleus tractus spinalis nervi trigemini*; Fig. 25; Fig. 49)

O

ob: olfactory bulb (*bulbus olfactorius*; Fig. 6-9, Fig. 21-27)

Obl: oblique sulcus (sulcus obliquus; Fig. 58)

Oc: oculus, eye (Fig. 7-14)

ocm: external ocular muscles (Fig. 22)

olf: olfactory fibres (*fibrae olfactoriae*; Fig. 6-10, Fig. 19-30)

oli: olivaris nucleus (*nucleus olivaris*; Fig. 30)

olr: olfactory recess (*recessus olfactorius*; Fig. 54)

omn: oculomotor nerve (*nervus oculomotorius*; Fig. 27)

Op: operculum (Fig. 60)

opn: optic nerve (*nervus opticus*; Fig. 6-8, Sagittal Fig. 21-27)

or: optic radiation (*radiatio optica*; Fig. 15, Fig. 19-20, Fig. 38-41)

ot: optic tract (*tractus opticus*; Fig. 8-14, Fig. 21-26, Fig. 34-40)

otu: olfactory tubercle (*tuberculum olfactorium*; Fig. 23-26, Fig. 31)

ox: obex region (*obex;* Fig. 30)

P

paf: paraflocculus (Fig. 9-10, Fig. 19-21, Fig. 46-52, Fig. 72)

pb: pineal body (*corpus pineale*; Fig. 14, fig. 30, Fig. 40)

pcc: caudal cerebellar peduncle (pedunculus cerebellaris caudalis Fig. 8-9, Fig. 23-26, Fig. 52)

Pcf: preculminalte fissure (*fissura praeculminata*; Fig. 72)

pcm: medial cerebellar peduncle (*pedunculus cerebellaris medialis* Fig. 8-10, Fig. 23-24, Fig. 45-47)

pcr: rostral cerebellar peduncle (*pedunculus cerebellaris rostralis* Fig. 9-10, Fig. 25-27, Fig. 46-49)

pg: pituitary gland (*hypophysis*; Fig. 7, Fig. 28-30, Fig. 34-40)

phg: parahippocampal gyrus (*gyrus parahippocampalis*; Fig. 10-13, Fig. 38-43)

pir: piriform lobe (*lobus piriformis*; Fig. 7-13, Fig. 19-21, Fig. 43-42)

pml: paramedian lobule (*lobulus paramedianus*; Fig. 10-13, Fig. 22-26)

prpc: prepiriform cortex (*cortex praepiriformis*; Fig. 11)

Ppf: prepyramidal fissure (*fissura praepyramidalis*; Fig. 72)

Prf: primary fissure (*fissura prima*; Fig. 27-30, Fig. 72)

Prr: prorean sulcus (*sulcus proreus*; Fig. 57)

Prs: presylvian sulcus (*sulcus praesylvius*; Fig. 11-13, Fig. 25, Fig. 57A,B,C)

put: putamen (Fig. 13-15, Fig. 22-24, Fig. 31-36)

pul: pulvinar (*nucleus pulvinaris*; Fig. 25, Fig. 40-41)

po: pons (Fig. 28-30, Fig. 45, Fig. 72)

pta: pretectal area (*area praetectalis*; Fig. 27)

py: pyramis vermis (Fig. 27-30, Fig. 72)

pyr: pyramidal tracts (*tractus pyramidalis*; Fig. 29; Fig. 48)

R

rc: rostral commissure (*commissura rostralis*; Fig. 11-12, Fig. 26-28, Fig. 50-52)

rcc: radiation of the corpus callosum (*radiatio corporis callosi*; Fig. 22-25, Fig. 31-42)

rcl: rostrum of the corpus callosum (*rostrum corporis callosi*; Fig. 13, Fig. 28-30)

rf: reticular formation (*formatio reticularis*; Fig. 27)

Rfi: rhinal fissure (*fissura rhinalis lateralis*; Fig. 13-14, Fig. 19-22, Fig. 31-48)

rm: rete mirabile (Fig. 28-30)

rmt: radix motoria of the trigeminal nerve (Fig. 23)

rn: red nucleus (nucleus ruber; Fig. 27-28, Fig. 41)

rnf: radix of the facial nerve (*radix nervi fascialis*, VII; Fig. 6, Fig. 49)

roc: rostral colliculus (*colliculus rostralis*; Fig. 13, Fig. 25-30, Fig. 42-45)

rtv: recessus tecti of the fourth ventricle (*recessus tecti ventriculi quarti*; Fig. 72)

S

Scl: callosal sulcus (*sulcus corporis callosi*; Fig. 30)

scc: splenium of the corpus callosum (*splenium corporis callosi*; Fig. 28-29; Fig. 41-42)

Scf: secundary fissure (*fissura secunda*; Fig. 72, Fig. 28-30)

si: substantia innominata (Fig. 33)

sl: lateral septal nuclei (*nuclei septi laterales;* Fig. 31-32)

smt: stria medullaris of the thalamus (*stria medullaris thalami*; Fig. 14, Fig. 29-30, Fig. 33-38)

sn: septal nuclei (*nuclei septales*; Fig. 30)

sng: substantia nigra (Fig. 9, Fig. 25-26, Fig. 38-41)

spe: septum pellucidum (Fig. 39-40)

Spl: splenial sulcus (sulcus splenialis; Fig. 17-18, Fig. 23-30, Fig. 31-48, Fig. 57-60)

Spl*: connecting sulcus between splenial and suprasylvian sulcus (Fig. 25-30, Fig. 32-37, Fig. 59)

spt: spinal tract of the trigeminal nerve (*tractus spinalis nervi trigemini*; Fig. 6-7, Fig. 24-25)

Sss: suprasylvian sulcus (sulcus suprasylvius; Fig. 14-18, Fig. 19-26, Fig. 31-46**,** Fig. 57-60)

stb: striate body (*corpus striatum*; Fig. 25-26)

sto: stratum opticum of the rostral colliculus (Fig. 42).

Syl: sylvian fissure (*fissura sylvii*; Fig. 14-18, Fig. 19-20, Fig. 33-38, Fig. 57-59)

T

tb: trapezoid body (*corpus trapezoideum*; Fig. 26, Fig. 48)

th: thalamus (Fig. 12-14, Fig. 24-30, Fig. 35-38)

tl: terminal lamina (*lamina terminalis*; Fig. 28-30)

tu: tuber of vermis (*tuber vermis*; Fig. 14-16, Fig. 25-26, Fig. 72)

U

uv: uvula vermis (Fig. 28-30, Fig. 72)

Unf: uvulonodular fissure (*fissura uvulonodularis*; Fig. 72)

V

vn: vestibular nuclei (*nuclei vestibulares*)

vtx: decussatio tegmenti ventralis (*Forel*; Fig. 38)

Z

zi: zona incerta (Fig. 38)

Roman figures

V: trigeminal nerve (*nervus trigeminus*; Fig. 6-7, Fig. 21-24, Fig. 35-45)

Vmd: mandibular nerve of the trigeminal nerve (*nervus mandibularis*; Fig. 6, Fig. 21)

Vmx: maxillary nerve of the trigeminal nerve (*nervus maxillaris*; Fig. 6, Fig. 20-21)

VII: facial nerve (*nervus facialis*; Fig. 7-9)

VIII: vestibulocochlear nerve (*nervus vestibulocochlearis*; Fig. 6-7, Fig. 48-49)

Arabic figures

3: third ventricle (*ventriculus tertius*; Fig. 8-9, Fig. 29-30)

4: fourth ventricle (*ventriculus quartus*; Fig. 7-9, Fig. 30)

2 Introduction

Since its domestication around 7000 BC the pig (*sus scrofa domesticus*) has always been of great economical importance. Due to the discovery of significant structural and metabolic similarities to the human body, the pig has also become the subject of biomedical research (Landy et al. 1961, Douglas 1972, Book and Bustad 1974, Tumbleson 1986; Swindle et al. 1988, Swindel et al. 1994, Munkeby et al. 2006). Therefore detailed anatomical knowledge of the pig brain is invaluable to researchers and a number of anatomical and histological pig brain atlases exist (Salinas-Zeballos et al. 1986, Makita and Tominaga 1987, Félix et al. 1999). The experimental biomedical and neuro-radiological approach remains the main source of the documentation of the MRI anatomy of the pig brain (Marcilloux 1989, 1993, Duhaime et al. 2000, Sørensen et al. 2000, Rhode 2001, Watanabe et al 2001, Makiranta et al. 2002, Duhaime et al. 2003, Grate et al. 2003, Bjarkam et al. 2004, Munkeby 2004, Fang et al. 2005, 2006, Duhaime et al. 2006, Lidegran et al. 2006, Munkeby 2006, Cohen et al. 2007, Gizewski et al. 2007, Hata et al. 2007, Moxon-Lester et al. 2007, Rosendal et al. 2009, Oto et al 2011).

Standard anatomical atlases in veterinary medicine and comparative anatomy are based on macroscopic and/or histological examination. Most of them contain few drawings of the porcine brain or concentrate only on parts of the pig brain. It is their aim to give an overview of the anatomy or the evolutionary relationship of several domestic animal species (Franck and Martin 1894, Flatau and Jakobsohn 1899, Schellenberg 1900, Martin 1904, Bolk 1906, Ellenberger and Baum 1942, Sisson 1953, Koch 1965, Yoshikawa 1968, Brauer and Schober 1970, Romer and Parson 1991, Nickel et al. 1992, Dyce et al. 2002).

In veterinary medicine results of MRI investigations of other species, such as companion animals (Buonnano et al. 1982, Kraft et al. 1989, Hudson et al. 1995, Assheuer and Sager 1997, Smith et al. 2001, Leigh et al. 2008), ruminants (Gordon and Dennis 1995, Karger 1998, Tzuka and Taura 1999, Yamada et al. 2005, Schmidt et al. 2006, Schenk 2007, Schmidt et al. 2008, Schmidt et al. 2009, Schmidt et al. 2011) and horses (Chaffin 1997, Arencibia et al. 2001) are available as a result of the ongoing effort to collect morphological data for the currently expanding field of magnetic resonance imaging (MRI). The existing histological atlases of the pig brain

are useful for anatomical and biomedical studies. They have however limitations when it comes to the identification of porcine brain structures in MRI scans. The translation of morphological data into the identification of cortical sections of the porcine brain (in MRI) remains a challenge, because a structure highlighted by a certain staining technique does not necessarily have an intense signal in MRI scans.

Furthermore morphological nomenclature of the sulci of the porcine brain is not standardized. Terminology changes and varies between research groups. This may be because of progress in research and advances in technology, but also because of differences in opinion. This problem is highlighted in this study with the aim to spark renewed discussions, that will ultimately lead to a standardized terminology.

This study presents anatomical details of the porcine brain as revealed in MRI and includes a synopsis of historical and recent data on the morphology of the porcine brain. In addition the morphology of the porcine brain in MRI is compared with the MR images of other ungulates and members of the suidae and other mammals, including rare MRI scans of a female babirusa. Similarities and differences are pointed out. The description of specific features in MRI scans of the domestic pig brain complements existing data for veterinary diagnostic imaging.

3 The pig in biomedical research

The idea of using the pig as a model to help understand the physiology and anatomy of the human body is not new (Gross 1998), but lay more or less forgotten until the 20th century. Scientific research over the last five decades has shown the great potential of pigs in biomedical research because of biological homologies to the human body and the pig's suitability as a laboratory animal (Lind et al. 2007).

First scientists focused on the similarities of human and porcine nutritional and physiological functions. This included studies of the reproductive tract. Pigs were also used in pediatric research (Landy et al. 1961, Douglas 1972, Book and Bustad 1974). Furthermore the pig became popular as a model in cardiovascular research and currently plays an important role in experimental surgery, such as cardiac surgery, organ transplantation and plastic and reconstructive surgery. In cardiology the pig model is used to conduct research into myocardial infarction (Checkley 1987, Williams 1988). But the pig is also used in the fields of anaesthesiology (Mäkiranta et al. 2002) and orthopaedic research (Robinson et al. 1988). Pigs have been used to study sudden infant's death (Waters et al. 1996) and metabolic disorders (Cesta et al. 2006, Danielsen et al. 2001). The pig is also used frequently in surgical training (Swindel et al. 1994). Much today's understanding of human neonatal physiology derives from studies conducted in animal models (Munkeby et al. 2004, Munkeby et al. 2006) and a large body of data concerning the newborn pig has been gathered for this purpose. Research shows that the piglet's anatomy and physiology are in many respects close to that of humans (Mc Cellan et al. 1968, Tumbleson 1986, Roohey et al. 1997, Swindle et al. 1998, Munkeby et al. 2006).

3.1 General advantages of the pig model in biomedical research

When selecting a suitable animal model for human brain research, primate brains, such as *macacca* brains, seem to be the obvious choice, because of the close human-primate phylogenetic relationship (Rosendal et al. 2009).

Although the fully grown domestic pig‘s (*sus scrofa domesticus*) weight and size could be seen as a disadvantage, piglets or small purpose bred minipigs are considered to be an alternative (Swindel et al. 1994, Roohey et al. 1997). As a laboratory animal the pig is less expensive to keep and more accessible, it produces larger litters and is more easily handled than primates. Pigs also seem to have fewer health problems in a laboratory environment (Book and Bustad 1974, Swindle et al. 1994, Bjarkam et al. 2004, Fang et al. 2005). Non-human primate models have also the disadvantage of unresolved ethical issues (Roohey et al. 1997). It is easier and less expensive to keep pigs under controlled conditions (Vodička et al. 2005).

As early as the 1960s the first specific pathogen free (SPF) pigs were bred (Landy et al. 1961) and pigs were raised under germ-free conditions (Meyer et al. 1964). In addition to that, pigs have been already transgenically modified by somatic cell nuclear transfer (Dai et al. 2002, Lai et al. 2002), this allows the establishment of knockout piglets and facilitates xenotransplantation and the creation of transgenic disease models (Lind 2007). The pig’s lifespan of 12-18 years also allows long term research, like the evaluation of safety and efficacy of therapeutic methods (Lind et al. 2007). Minipigs are nowadays purposely bred as laboratory animals (Yucatan, Hanford, Göttingen, Sinclair or Chinese breeds like Xiang, Wuzhishan, Diannan Small-Ear, Tibetan and Banna). Desired traits are placidity and size (Lind et al. 2007).

3.2 The pig brain in neuroscience

Although the pig was used for pediatric brain research in the sixties and seventies of the last century (Landy et al. 1961, Douglas 1972, Book and Bustad 1974), it took decades until the pig's use in neuroscience was fully recognised (Lind et al 2007). Today the porcine brain is viewed as an excellent non primate, gyrencephalic model for the human brain (Hofman 1985, Hashimoto et al. 1996, Mun-Bryce et al. 2001, Lidegran et al. 2006, Nielsen et al. 2009). The nuclei of the pig brain are larger in comparison to the nuclei of a rat- or rodent brain (Marcilloux et al. 1989 and 1993). The pig brain is also large enough to allow the identification of cortical and subcortical structures using conventional imaging techniques like magnetic resonance imaging (MRI), functional magnetic resonance imaging (fMRI) and positron emission tomography (PET) (Watanabe et al. 2001, Bjarkam et al 2004, Jelsing et al. 2005, Lind et al. 2007). The porcine brain also allows well- localised lesions (surgical procedures) or stimulations (using neural stimulation devices) in anatomically defined structures (Dalmose et al. 2005).

The gyrated pig brain is more similar to the primate brain than the lissencephalic brain of smaller laboratory animals (Jelsing et al. 2006, Lind et al. 2007). The shape and gyral pattern of a piglet's brain is basically comparable to that of humans, as is the distribution of grey and white matter. The changes in brain morphology during development also show similarities (Mäkiranta et al. 2002, Grate et al. 2003, Munkeby et al. 2004, Munkeby et al. 2006, Lind et al. 2007, Lodygensky et al. 2007). The porcine brain is seen as an appropriate model for the brain of human infants. Advantages of piglets as experimental animals in pediatric research have been investigated by Glauser (1966). The growths spurt of the porcine brain, like that of human brains, extents from late prenatal to early postnatal life (Dickerson and Dobbing 1967, Pond et al. 2000). The pig brain is furthermore a model for recovery after brain trauma (Armstead and Kurth 1994, Wagner et al. 1996, Duhaime et al. 2000, Raghupathi and Margulies 2002, Duhaime et al. 2003, Grate et al. 2003, Munkeby et al. 2004, Munkeby et al. 2006). The brain injury responses of Yorkshire piglets of 5 days of age, 1month of age and 4month of age were found to correspond developmentally to brain injury responses of human infants, toddlers and early adolescents (Duhaime et al. 2003). Brains of three to five day old piglets were used as models for infant brains less than 3 month of age, while investigating traumatic

axonal injury (Raghupathi and Margulies 2002).

Brain hypoxia or brain ischemia can cause severe an irreversible brain damage with often fatal outcome for the patient. The lack of oxygen/blood supply to the brain can be for example caused by stroke or by complications during birth. The pig is used in a large number of studies concerning brain hypoxia and ischemia (Chang et al. 1998, Imai et al. 2006, Lidegran et al. 2006, Moxon-Lester et al. 2007, Rosen et al. 1992, Sakoh and Gjedde 2003). Munkeby et al. 2006 while investigating neonatal hypoxia ischemia demonstrated the value of MRI in morphological research and published pictures of the Haderian gland in piglets as revealed by MRI images (1.5 Tesla). This gland - though large enough - in size had only been investigated in rodents and lower vertebrates before. MRI is also used as a guiding tool in surgery (Rhode et al. 2001, Hata et al. 2007). Magnetic resonance imaging-guided focused ultrasound for thermal ablation of brain tumours was for example tested using a swine model (Cohen et al. 2007).

3.3 Steretotactic studies of the pig brain

Stereotaxy is important for a large number of in vivo studies of the central nervous system. It often involves the fitting of a specially designed apparatus (Fig. 1, Fig. 2).
To know the exact position of brain structures (such as nuclei) is very important, because stereotactic coordinates are the key to accurate cranio-encephalic topography- whether it involves surgical or pathological procedures or morphological research (Andersen et al. 2005, Bjarkam et al. 2004, Dalmose et al. 2005, Félix et al. 1999, Jelsing et al. 2006, Lim et al. 1960, Marcilloux et al. 1993, Poceta et al. 1981, Saito et al. 1998, Salinas-Zeballos et al. 1986, Sørensen et al. 2000, Szteyn et al. 1980, Talairach et Tournoux 1988, Tindal et al. 1968, Watanabe et al. 2001).
The porcine brain was studied using stereotactic methods. Stereotactic brain atlases, including a stereotactic atlas of the pig brain and stereotactic studies of selected structures of the porcine brain are available to researchers (Marcilloux et al. 1989 and1993, Felix et al. 1999, Bjarkam et al. 2004, Saito et al. 1998). In 1986 Salinas-Zeballos et al. published a stereotactic atlas of the developing swine brain, because detailed studies of the nervous system in development (e.g. postnatal development of neural control of visceral function) need accuracy and reproducibility of electrode placement. To aid the localization of the porcine hippocampus, stereotactic coordinates were also determined (Saito et al. 1998).
A detailed stereotactic atlas of the pig brain was published in 1999. The atlas consists of transversal and sagittal drawings and photographs (Felix et al. 1999). Stereotactic procedures were for example established to locate hypothalamic nerve centres in the porcine brain (Szteyn et al. 1980), to place cannulae in cerebral ventricle in experimental settings (Poceta et al. 1981), to map cerebral blood flow (Andersen et al. 2005) and to allow stereotactic electrical stimulation of the pontine micturition centre in the pig (Dalmose et al. 2005).

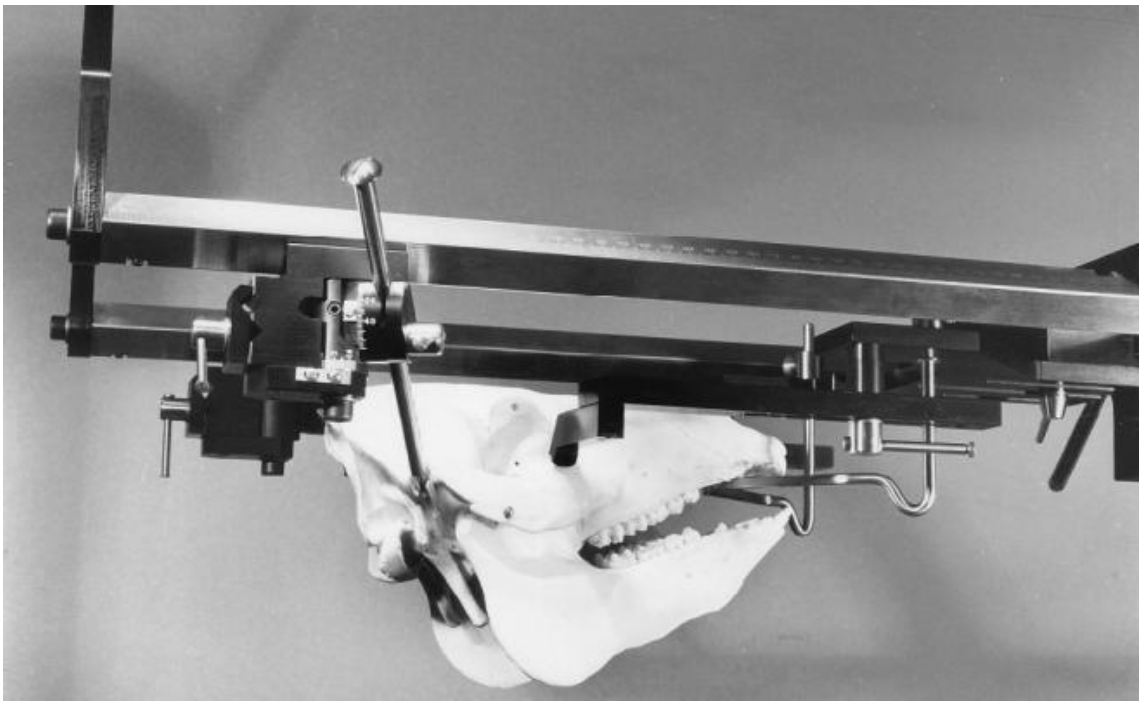

Figure 1
Example of a stereotactic apparatus (from Félix et al.1999). The porcine skull is fixed by ear- bars and mouth and orbital pieces. This was necessary to be able to produce a detailed stereotactic atlas of the pig brain. The atlas consists of transversal and sagittal drawings and photographs of the porcine brain.

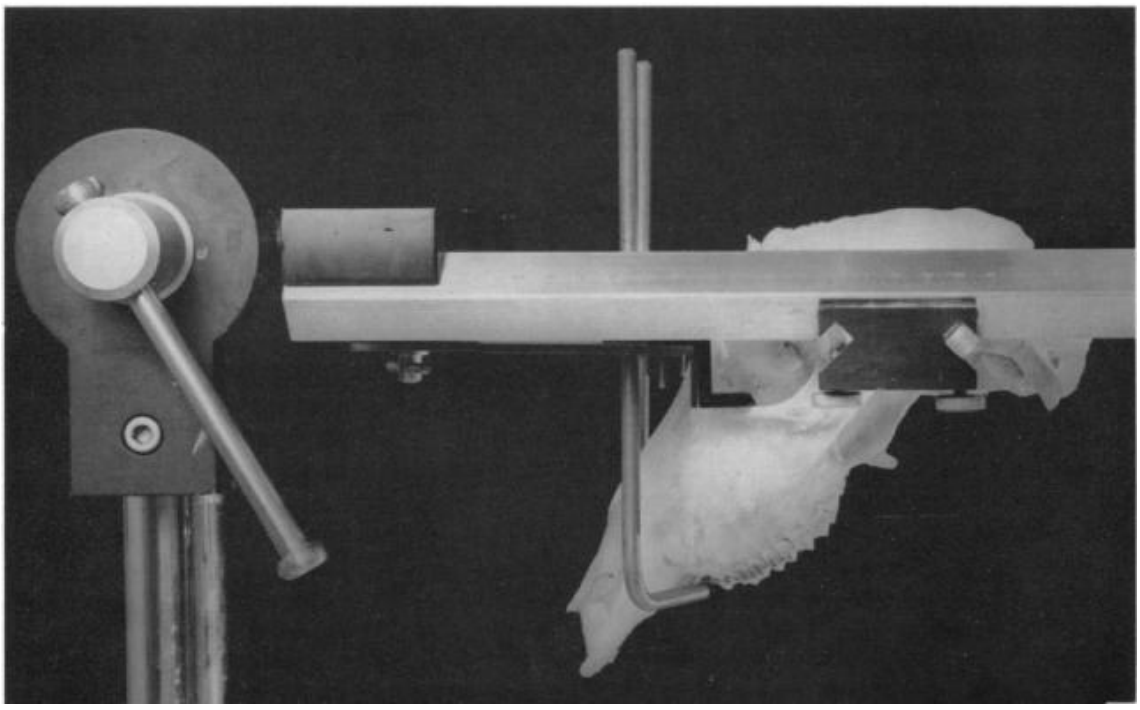

Figure 2
The scull of a goat is fitted into a stereotactic apparatus (from Tindal et. al 1986). Stereotactic coordinates and techniques are essential for the accurate insertion of electrodes, or cannulae bearing steroids or drugs, into specific brain structures.

3.4 Morphological details of the pig brain in literature

Interest in the anatomy of the porcine brain started at the beginning of the last century. Since then the porcine brain has been featured in a large number of comparative anatomical atlases and comparative anatomical studies of the central nervous system of mammals. Today a variety of anatomical studies of the porcine brain, based on macroscopic studies and studies investigating the brain function, are available (Franck and Martin 1894, Flatau and Jakobsohn 1899, Ziehen 1899, Schellenberg 1900, Martin 1904, Gegenbauer 1909, Kappers 1921, Kuhlenbeck 1927, Anthony and De Grzybowski 1931, Haller v. Hallerstein V 1934, Ellenberger and Baum 1942, Stephan 1951, Sisson 1953, Koch 1965, Yoshikawa 1968, Brauer and Schober 1970, Dellmann and Mc Clure 1975, Lauer 1982, Stark 1982, Romer and Parson 1991, Nickel et al. 1992, Nieuwenhuys et al. 1998, Dyce et al. 2002).

A comparative anatomical investigation into the cerebellum of mammals was delivered by Bolk (1906). He describes the porcine cerebellum comprehensively. The development of the cerebellum of the pig was described by Larsell in 1954. And the topography and cytoarchitecture of the cerebellum (boar) was investigated by Bujak in 1974. Bujak describes a partial aplasia of the cerebellar cortex that is caused mechanically during the brain development of the domestic pig and the wild boar (also mentioned by Schulz 1953 and Cohrs and Schulz 1952). The absolute and relative growth curves for the foetal cerebellum of the pig and the entire brain of the foetal pig (from 45 days to term) were determined by Done and Herbert (1968). Bradley (1903) examined the cerebellum of pig embryos from day 40 to day 70, as well as the adult cerebellum of the pig. The porcine cerebellum was also compared with cerebelli of other domestic mammals including the cerebelli of horse, dog, goats and sheep. The mesencephalon of domestic mammals was described by Chromiak in 1963. This paper gives information about nuclear topography of the brains of domestic mammals and includes the porcine brain.

Myelo- and cytoarchitectonics of the domestic pig’s mesencephalon and pons were also studied (Freund 1969, Freund 1973). The nuclear pattern of the non-tectal portions of the midbrain and isthmus in ungulates was examined (Gillian 1943). This study features the study of the midbrain of a 16 cm pig. The morphology and cytoarchitecture of red nucleus (nucleus ruber) of the domestic pig was described (Otabe and Horowitz 1970). The structure and the topography of the diencephalon

and its different nuclear groups were described by different authors. Studies include the nuclei of the posterior group of the thalamus (Welento 1964), the thalamus (Solnitzky 1037), the nuclei of the hypothalamus (Welento 1964) and the nuclei of the ventromedial hypothalamus (Seeger 1990). A study of the hypothalamus and subthalamus of sus scrofa also exists (Solnitzky 1939), as well as a more recent study of the subthalamic nucleus. The subthalamic nucleus was evaluated using immunohistochemistry and design-based stereology (Larsen et al. 2004). The porcine retinal projections were investigated with the aid of histological staining techniques. In that context nuclei of the diencephalon were described, including the dorsal and ventral nuclei of the lateral geniculate body. The retinal projections of the pig were also compared with the retinal projections of sheep (Karamanlidis and Magras 1972). The thalamus of the pig was compared with the thalamus of the sheep. Cellular and fibrous structures were investigated (Rose 1942).

The structure of the mammalian corpus callosum was described and species differences and similarities of that structure were pointed out (Olivares et al. 2001).

The sulci of the cerebral cortex of ungulates were studied as early as 1878. The study includes the description of features of the porcine brain. The system of the sulci of ungulates was also compared with the system of sulci of carnivores (Krueg 1878).

The motor cortex of the domestic pig was studied by Breazile et al. (1966) and the primary- and secondary somatosensory cortex of the new born pig were both described by Craner and Ray in 1991. They confirmed the similarity of the organization of these cortical areas to those of other mammals. Earlier investigations into the same areas were performed by Adrian in 1943 and Woolsey and Fairman in 1946. The primary somatosensory cortex was recently studied using functional magnetic resonance imaging in piglets (Duhaime et al. 2006).

The prefrontal cortex of the minipig brain (Göttingen minipig) was described using neural projection criteria and concentrating on cytoarchitecture (Jelsing et al. 2006 a). The same year the development of glia cells and neocortical neurons of the domestic pig and the Göttingen minipig were studied (Jelsing et al. 2006 b).

Hofman (1985) proposed a dimensionless index of cortical folding, rather than the use of a single allometric relation, to study the effect of size increase on the geometry of the brain. He compared the size of various brain structures in mammals, including sus scrofa.

The morphological characteristics of the gyrus dentatus (archipallium) in some animal species and in man were described (Dilberovic et al. 1986).

The olfactory system of the porcine brain is well developed and was investigated by a number of researchers. They have concentrated on the olfactory tubercle and the nucleus of the diagonal fasciculus of Broca (Hereć 1967). Within the olfactory bulb of the pig, the luteinizing hormone-releasing hormone was localised immuncytochemically (Leshin et al. 1991). The accessory olfactory bulb of the pig is the subject of another research project (Salazar et al. 2004).

A comprehensive study of the early development of the olfactory nerve of pigs can be found (Edgar and Bedford 1904).

The brainstem of the domestic pig is the research subject of Breazile (Breazile 1967). He delivers a description of the cytoarchitecture of this part of the porcine central nervous system. He later examined the ventrolateral spinal cord afferents to the brain stem of the pig (Breazile and Kitchell 1986).

Furthermore the course and termination of the pyramidal tract of the porcine brain were determined (Palmieri et al. 1987). A fiber and numerical analysis of the pyramidal tract of ungulates was performed (Lassek 1941). It also features the pig.

There is an interest in the brain growth of the pig during ontogeny. The development of the porcine cerebellum was examined in the foetal pig (Done and Herbert 1968).

Descriptions of the pre- and postnatal development of the porcine central nervous system (Dickerson and Dobbing 1967, Pond et al. 2000) can be found.

It was possible to identify postnatal changes in functional activities of the porcine brain using functional magnet resonance imaging (Fang et al. 2005 a). The post partal development of the porcine cerebellum was also studied by Fang et al. (2005 b) using f MRI.

3.5 The Göttingen minipig brain in literature

Minipigs are a popular animal model in neuroscience (Lind et al. 2007, Rosendal et al. 2009). It is therefore not surprising that scientists are developing protocols to utilize MRI as tool to aid the determination of neuronal coordinates of the minipig brain (Rosendal et al. 2009). Rosendal et al. 2009 used a 3 Tesla MRI to produce in vivo visualization of the Göttingen minipig brain (focusing on nuclei that are of special interest in human medical research). The high quality scans allow the visualisation of important nuclear groups. Watanabe et al. (2001) published a MR based statistical atlas of the minipig brain after examining 22 male Göttingen minipigs to establish a basis for a planned systematic comparison of gender, age and strain differences of the minipig brain. He achieved (through 3 D image rendering) a model that pictures the statistical/ average shape of the of the minipig brain. Because of its value as a laboratory animal (see above) the brain of the Göttingen minipig was examined in detail. Age- weight relationships of selected organs and body weight were established in the early seventies (Thomas and Beamer 1971). Auditory- and somatosensory cortex of minipigs were mapped (Andrews et al. 1990). A volumetric screening procedure for the Göttingen minipig brain was developed in 2005 (Jelsing et al. 2005). The prefrontal cortex of the Göttingen minipig was described by neural projection criteria and cytoarchitecture. Cytoarchitectonic and connectional data of this study suggest that the Göttingen minipig has a structurally divided prefrontal cortex (Jelsing et al. 2006 a). Using stereological principles, the development of overall number- and perikaryon volume of the Purkinje cells post partum were estimated in the Göttingen minipig brain. The cells were found to be considerably larger in comparison with human Purkinje cells and the Purkinje cells of other mammals. The volume of the perikaryon and the increase in cell number was considered to be part of the growth and development of the cerebellum in this breed (Jelsing et al. 2006 c). Glia cells and neocortical neurons of the Göttingen minipig and the domestic pig were compared. In this study the researchers focused on the postnatal development (Jelsing et al. 2006 b). As part of the research into the Parkinson disease, the pars compacta of the substantia nigra was studied in the Göttingen minipig (Nielsen et al. 2009). A MRI protocol for the visualization of the minipigs brain was established experimentally. As a consequence the determination of coordinates necessary in experimental neurosurgery in the Göttingen minipig was

considerably improved (Rosendal et al. 2009).

3.6 Comparative brain studies of the porcine brain

Scientists have been interested in interested the anatomy of the wild boar brain (Hadziselimovic and Dilberovic 1977) and changes of the brain during domestication. A special interest in the anatomical differences between the brain of the domestic pig and its wild relative exists. As early as 1939 brains of the wild boar and domestic pig breeds were examined anatomically and compared (Rawiel 1939). These studies were continued by a comparison of the cytoarchitectonic composition of brains of the European wild boar and the domestic pig (Kruska et al. 1970). Researchers were keen on finding out how domestication changes the structure of the brain and consequently the behaviour of the animal (Stephan 1951, Kruska 1988). The brains of feral pigs and European domestic pigs were examined to establish whether the effects of domestication on the porcine brain are reversible or not (Kruska and Röhrs 1974, Röhrs and Ebinger 1999). A description of the brain of the *Sus (Porcula) salvanius hodgson*, a miniature wild pig, discusses the difficulties of comparative anatomy of mammal brains of different body size (Kruska 1982). Auditory structures of the European wild boar and the domestic pig were also compared (Plogmann and Kruska 1990). In 1987 Makita and Tominaga developed a pig brain atlas to aid the interpretation of CT scan slices. It contains drawings and photographs of dorsal and transversal brain sections. It was followed by a study comparing CT scans of the brains of pigs under anaesthesia with formalin fixed brains of wild boar in 1988.
Brauer und Schober compare the system of sulci und gyri of the Warthog (*Phacochoerus africanus*), pekaris (Tayassuidae), wild boar and the pot belly pig (Brauer und Schober 1970).

4 Materials and methods

4.1 Specimens

The intracranial central nervous system of 10 pigs (hybrids for meat production, 5 month old) is described in this study. The pigs were received post mortem. They had undergone surgery at the Giessen School of Endoscopy (human medicine) and were euthanized after the endoscopic procedures. One animal was flushed with 0.9% saline via the jugular vein, followed by 4% formaldehyde in phosphate buffer. After fixation and hardening of the tissue, the head was dissected between the first and second cervical vertebrae and stored in the same fixation solution. After 2 weeks of post fixation, imaging was performed using Phillips brilliance, 1 Tesla MRI scanner, with a Phillips surface coil (C3) at the Department of Veterinary Clinical Science - Clinic for Small Animals, Justus Liebig-University (Fig. 3). The other 9 pigs were scanned directly post mortem without fixation.

The head of a female babirusa (Indonesian member of the suinae), also known as “pig deer” was received from the “Hessisches Untersuchungsamt”. The animal had been euthanized because of a uterine neoplasia at Frankfurt Zoo (Fig. 62). The female was 27 years old. The babirusa did not show any neurological disorders ante mortem. The head was removed from the babirusa’s body post mortem and taken to the Department of Veterinary Clinical Science - Clinic for Small Animals, Justus Liebig-University (JLU) in Giessen. Here it underwent MRI examination. The scans were taken 2-3 hours after death and before preparation and fixation of the brain in formalin for future examinations.

The head of a Wiesenauer minipig was obtained post mortem from the Clinic for Swine at the Justus-Liebig-University, Giessen. The pig was euthanized because of complicated pelvic fractures. Native MRI scans were taken directly after death.

The head of a wild boar (sus scrofa) was kindly donated by Dr. Markus Müller. The animal was killed during a hunt and in accordance with the German game law (“Jagdrecht”).

The scans of the porcine brain were also compared with available scans of post-mortem bovine, equine and ovine brains that had previously undergone MRI examination at the Clinic for small animals (JLU). CT Images of all porcine heads

were taken with a CT scanner, Phillips Brilliance (Fig. 3) to identify the position of the brain within the skull and to help with orientation.
All animals scanned for the purpose of this study, were obtained after their death. Therefore it was not necessary to apply for permission according to the German animal welfare act (Tierschutzgesetz § 8 from the 18th of May 2006 (BGBI. I S. 1206, 2013)). All other MR images (including brains scans of red deer and alpaca) were found in the archives of the small animal surgery department of the JLU in Giessen. The images were used with the kind permission of Prof. Dr.Dr. h.c. M. Kramer and PD Dr. med.vet. (habil.) M. Schmidt.

4.2 MR-imaging of the formalin fixed specimens

Magnetic resonance images of the entire head were acquired in dorsal, sagittal and transverse planes, using a 3D gradient echo sequence. To achieve a sufficient signal-to-noise ratio (SNR), 32 averages were accumulated overnight (approx. 8 h) obtaining slices of 1mm thickness with 130 mm field of view (FOV) at 256/256 matrix size. After acquisition each dimension was additionally extrapolated by a factor 2. This resulted in an image size of 1024x1024, with 0,25 mm in-plane resolution and 1.0 mm slice distance. Optimum contrast was obtained with 1800 milliseconds (ms) repetition time (TR) and a 90° flip angle, while the echotime (TE) was adjusted to 35 ms. Proton density (PD) weighted images were produced with these parameters. The chosen 3D sequence facilitates the generation of pictures with high signal intensity because each impulse excites the volume of the brain. It was shown that greater sensitivity is achieved with 3D sequences because each signal acquisition represents an average of the entire sample volume, resulting in a substantial increase in the signal-to-noise ratio (Toga and Mazziotta 1996).

4.3 MR-Imaging of unfixed specimen

The other species were examined using routine imaging protocols for living animals. T2- weighted turbo spinecho sequences were used with TE: 10,0 ms, TR 4567,0 ms

and a 90 ° flip angle. Image matrix and field of view (FOV) were adjusted on the size of the head of the animal.

4.4 Assembly of the 3D brain model

Computer-generated volume reconstruction of the brain surface was carried out using AMIRA® and AVIZO 6® (Mercury Computer Systems) graphical software. The 3D model of the outer brain surface (Fig. 4) was assembled by manual image segmentation of the original scans. This method provides greater accuracy of the results compared with automatic segmentation. The AMIRA® and AVIZO® programs are essential for the manual and semi-automated image segmentation of the individual slice. This can be achieved by manuall or automated creation of an image mask. All of the voxels corresponding to a single anatomical structure in the scans were selected. The multiplanar projection of all planes in one image could then be used to label the images. By placing the crosshair tool (Fig.5) on one point of interest in one plane, it marks the same structure in the two remaining planes. A 3D surface model of the porcine brain was also constructed. It helps to identify the position of one slice of the brain in relation to the two remaining orthogonal planes. This method was used to identify the gyri and sulci in the 2D images (Fig. 4). The terminology used in this study complies with the Nomina Anatomica (1989), Nomina Anatomica Veterinaria (1994), and Terminologia Anatomica (1998). 13 dorsal, 12 sagittal and 22 transverse MRI slices were selected and labelled. The scans were furthermore compared with MRI brain scans of other domestic animal species (for example canine, equine, ovine and bovine) and the wild boar, Wiesenauer minipig and babirusa. Veterinary textbooks, anatomical atlases and studies of the porcine brain were used to identify structures before labelling (Krueg 1878, Franck 1894, Flatau and Jakobsohn 1899, Schellenberg 1900, Martin 1904, Black 1915, Kappers 1921, Rawiel 1939, Ellenberger Baum 1943, Stephan 1951, Sisson 1953, Koch 1965, Breazile 1966, Yoshikawa 1968, Brauer and Schober 1970, Kruska 1970, Lauer 1982, Salinas-Zeballos et al. 1986, Makita and Tominaga 1987, Palmieri et al. 1987, Craner and Ray 1991, Nickel et al. 1992, Felix et al. 1999, Watanabe et al. 2001, Dyce et al. 2002, Lind et al. 2007).

Figure 3

A: MRI scanner (Phillips), B: CT scanner (Phillips) at the clinic for small animals, Justus Liebig-University, Giessen. CT Images of all porcine heads were taken with a Phillips CT scanner to identify the position of the brain within the skull and to help with orientation. MRI images were produced using a Phillips Brilliance, 1 Tesla MRI scanner, with a Phillips surface coil (C3) © Verena Schmidt.

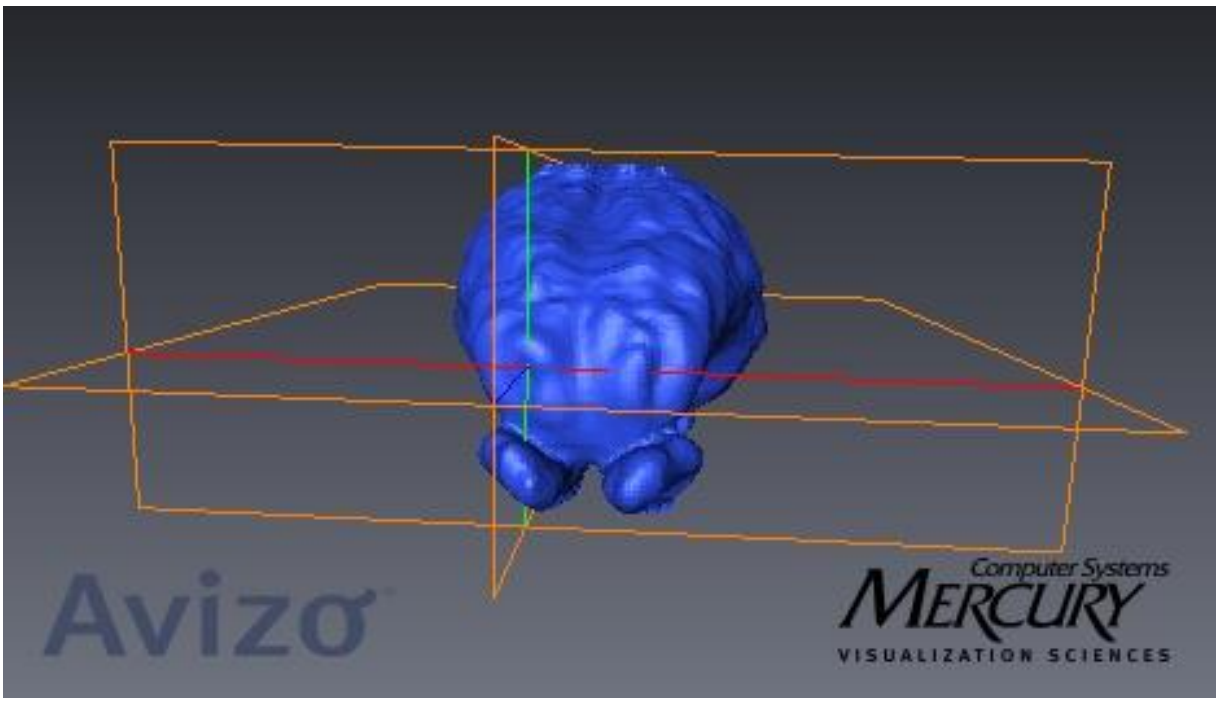

Figure 4

A 3D- surface model of the pig brain was created with the Avizo® program. The identification of the sulci was possible with the aid of the multiplanar modus. The right presylvian sulcus is positioned at the crossing of the blue (dorsal), red (transversal) and green (sagittal) orthogonal planes. ©Verena Schmidt

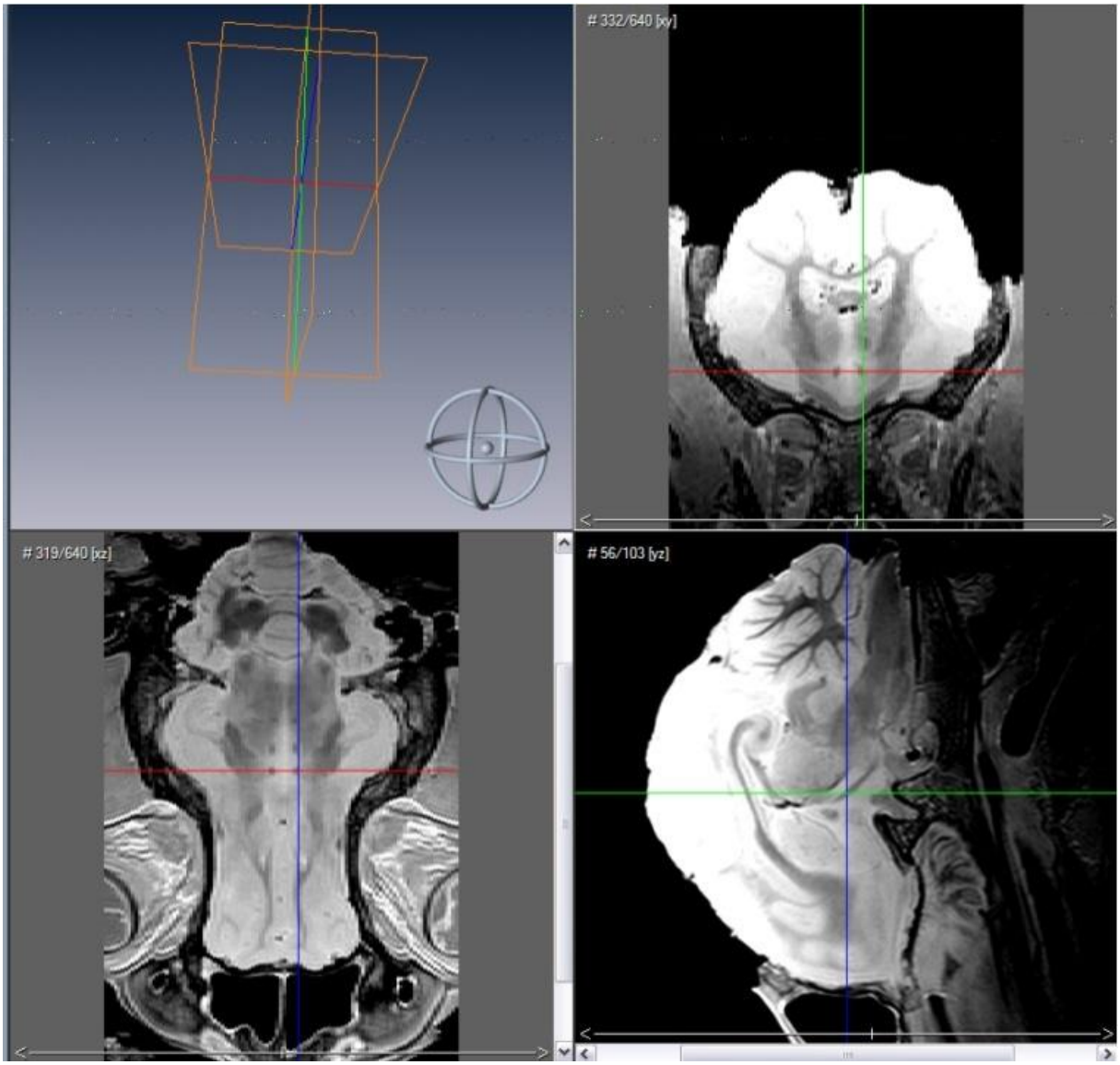

Figure 5

The three- dimensional identification of porcine brain structures is possible with the AMIRA® multiplanar reconstruction program and the "cross hair tool". Top left: cross hair tool. Identification of the fornix in the transversal plane (top right) helps to identify the same position in the dorsal (bottom left) and the sagittal plane (bottom right) of the MRI dataset. ©Verena Schmidt

5 Results

5.1 High detailed morphology of the porcine brain as revealed by MRI

5.1.1 General external morphology

In the pig the caudal poles of the medially flattened hemispheres are wider than the rostral poles. The hemispheres together give the cerebrum an oval shape in dorsal scans (Fig. 18). Images of the same orientation through the piriform lobe reveal two kidney shaped hemispheres (Fig. 11-13). In rostral transverse scans the hemispheres are ventrally narrow and dorsally wider. Put together they appear almost heartshaped (see Fig. 31).

5.1.2 Cerebral cortex (pallium)

5.1.2.1 Paleopallium

The paleopallium is the basal part of the brain. In the pig it is very prominent with massive olfactory bulbs which are long, flat and situated ventrally from the frontal cortex. The hypointens olfactory tract is divided into a medial- (mot: Fig. 7-9) and a lateral (lot: Fig. 7-10, Fig. 23-24, Fig. 31-32) tract. The medial tract reaches the precommissural area. One part of the fibres terminates there surrounded by cortical gyri, but other fibers stretch beyond the hypointense rostral commissure (rc: Fig. 11-12, Fig. 26-30, Fig. 31-33) to reach the corresponding region of the opposite hemisphere. The lateral part of the olfactory tract terminates in the prominent piriform lobe (pir: Fig. 7-13, Fig. 19-21, Fig. 34-42) of the pig (olfactory cortex). Most cranially positioned the prominent olfactory bulbs are visible in MRI scans (transverse scans

not included), along with their olfactory fibers (olf: Fig. 6-10, Fig. 19-30). The hypointens olfactory fibers extend in ventral, rostral and lateral direction. While the olfactory bulb appears as a dorsoventrally flattened oval in sagittal aspects (Fig. 21-27) they are triangular in dorsal sections at the level of the optic chiasm (Fig. 6). The paired bulbs don't touch in midline. The accessory olfactory bulbs, that are situated in the middle region of the olfactory bulbs can not be identified in the atlas, but are featured in a native scan (Fig. 54). The olfactory bulbs of the pig are ventrally positioned. The lamina cribrosa is horizontally positioned and the olfactory fibres stretch out in rostral direction from the surface of the bulbs. The two tracts flank a prominent olfactory tubercle (otu: Fig. 23-26, Fig. 31). Caudally bordered by the diagonal band of broca (diagonal gyrus; dbb: Fig. 25, Fig. 32) forming the trigone.

5.1.2.2 Neopallium

The neopallium is laterally separated from the paleopallium by the rhinal fissure (Rfi: Fig. 13-14, Fig. 19-22, Fig. 31-48) and medially separated from the archipallium by the splenial sulcus (Spl: Fig. 16-18, Fig. 23-30, Fig. 31-48, Fig. 57-60). The pig's gyrencephalic brain is characterized by a pattern of alternating furrows (sulci) and ridges (gyri). The sulci of the porcine brain can be identified as hyperintens lines in the images of the atlas. They are accompanied either side by the corresponding hypointens gyri. The longitudinal cerebral fissure (Flc: Fig. 17-18) divides the hemispheres. On the lateral surface of the hemispheres of our formalin fixed specimen we are able to identify the deep, long sylvian fissure that points caudodorsally (Syl: Fig. 14-18, Fig. 19-20, Fig. 33-38, Fig. 57-59). It originates near the middle of the rhinal sulcus. The sylvian gyrus obscures the insula (in: Fig. 14-15, Fig. 33, Fig. 56) bordering the sylvian fissure. Caudal to the sylvian fissure the shorter caudal ectosylvian sulcus (Ecs: Fig. 14-18, Fig. 19, Fig. 35-41, Fig. 57-60) can be identified pointing dorsocaudally, almost running parallel to the sylvian fissure. The diagonal sulcus (Dia: Fig. 15-17, Fig. 21-24, Fig. 57-58) crosses the rostral part of the lateral surface pointing in caudoventral direction. The suprasylvian sulcus (Sss: Fig. 14-18, Fig. 19-26, Fig. 31-46, Fig. 57-60) is positioned dorsally to the sylvian sulcus and the ectosylvian sulci. It positioned parallel to the mediodorsal border of the hemisphere. A dorsal branch of the rostral suprasylvian sulcus (ramus dorsalis) can be identified. Further caudal the marginal sulcus (Mar: Fig. 18, Fig. 21-27, Fig.

34-5, Fig. 57-60) can be found, medial the endomarginal sulcus (Enm: Fig. 18, Fig. 24-25, Fig. 42-5, Fig. 57-60) and lateral the ectomarginal sulcus (Ecm: Fig. 15-18, Fig. 19, Fig. 32-40, Fig. 57-60) can be identified. The ectomarginal sulcus is positioned dorsocaudally to the suprasylvian sulcus and ventrolaterally to the marginal sulcus. The endomarginal sulcus is positioned mediodorsal to the marginal sulcus. The coronal sulcus (Cor: Fig. 12-18, Fig. 23-26, 57-58) emerges from dorsal margin of the hemispheres and can be connected caudomedially with the ansate sulcus (not visible in MRI atlas).

Medially the hyperintens sulcus of the corpus callosum (Scl: Fig. 30) surrounds the corpus callosum rostrally, dorsally and ventrally and separates the corpus callosum (cc: Fig. 14, Fig. 25-30, Fig. 31-38) from the cingulate cortex above. It is framed dorsally by the cingulate gyrus that appears to be hypointens in comparison. The caudal splenial sulcus (Spl: Fig. 17-18, Fig. 23-30, Fig. 31-48, Fig. 57-60) extends around the splenium of the corpus callosum (scc: Fig. 28-29; Fig. 41-42) and also extends cranially above the trunk of the corpus callosum. The genual sulcus (Gen: Fig. 13-17, Fig. 30, Fig. 57) is positioned rostrally and extends around the genu of the corpus callosum (gcc: Fig. 29-30) and lies in the middle between the endo- (Eng: Fig. 13-14, Fig. 29-30, Fig. 57) and ectogenual (Ecg: Fig. 13-17) sulcus. Another sulcus connects the medial splenial sulcus with the lateral suprasylvian sulcus. For the purpose of this study it is called “connecting sulcus” (Spl*: Fig. 25-30, Fig. 32-37, Fig. 59). The nomenclature concerning this sulcus in literature is controversial and will be examined in the discussion chapter of the thesis.

5.1.2.3 Basal nuclei

The ventrolateral part of each hemisphere contains the basal nuclei (caudate nuclei, putamen, globus pallidus, claustrum, accumbens nucleus). The accumbens nucleus (acn: Fig.11, Fig. 27-28, Fig. 31-32) is situated in close proximity to the caudate-putamen complex (rostroventromedial). It is not easily distinguishable from its surroundings. The caudate nucleus (cn: Fig. 13-15, Fig. 25-29, Fig. 31-37) is large and easy to identify, it is elongated, laterally flattened and does not bulge into the lateral ventricle. In dorsal and transverse scans the caudate nuclei form a butterfly shaped structure. The caudate nucleus of the pig is not as curved as the caudate

nucleus of humans or other domestic mammals (see also comparative morphology below). Therefore the tail end of the nucleus, that follows the curve of the lateral ventricle, does not appear twice in transverse scans. Body and tail of the nucleus can't be seen together in the same scan. The basal nuclei are hyperintens and embedded in hypointens fibre bundles (white substance). They form the characteristic stripes of the striate body. The caudate nucleus (cn: Fig. 13-15, Fig. 25-29, Fig. 31-37) is separated from the lentiform nucleus or lenticular nucleus by hypointens fibres of the internal capsule (ic: Fig. 14-16, Fig. 22-26, Fig. 31-37). The hyperintens lentiform nucleus consists of the medial globus pallidus or pallidum (gp: Fig. 12, Fig. 31-33) -part of the palaeostriatum- and the lateral putamen (put: Fig. 13-15, Fig. 22-24, Fig. 31-36). The lentiform and the caudate nucleus combined form the neostriatum. Laterally the claustrum (cla: Fig. 33), a narrow structure, is separated from the neopallium by the extreme capsule or capsule extrema (not featured). The amygdaloid body (ab: Fig. 34-37) is usually described as part of the basal nuclei, but is located caudoventrally from the lenticular nucleus at the top of the piriform lobe and is functionally part of the rhinencephalon. Medially it is connected with the hippocampus and with the lateral olfactory tract (lot: Fig. 7-10, Fig. 23-24, Fig. 31-32) and the claustrum (cla: Fig. 33).

5.1.2.4 Archipallium

The cingulated (ci: Fig. 16-17, Fig. 28-30, Fig. 32) and supracallosal gyri form the medio-dorsal part of the pig's archipallium. They are situated between the dorsal splenial sulcus (Spl: Fig. 16-18, Fig. 23-30, Fig. 31-48) and the ventral corpus callosum. The archipallium's ventrolateral part is known as the cornu ammonis or "Ammonshorn" housing the hippocampus. The archipallium embraces the dorsal caudal and ventral aspects of the thalamus. The cornu ammonis is hyperintens (but isointense to the piriform lobe, best seen in transverse and dorsal images) and resembles the horn of a ram (cam: Fig. 10-17, Fig. 20-30, Fig. 38-43). In our transverse scans the arched cornu ammonis appears as two separate stuctures in the same slice (dorsally and ventrally; Fig. 39-40).

The fornix (arch) is formed by a bundle of fibres (fo: Fig. 10-12,15, Fig. 27-30; cf: Fig. 9, Fig. 41; cfo: corpus of fornix Fig. 13-14, Fig. 33-35). These fibres are longitudinal association fibres and originating from the cingulum, white matter originating from the

cingulate gyrus (ci: Fig. 16-17, Fig. 28-30, Fig. 32). The association fibres enter the hippocampus caudally and are parting from it rostrally. Rostrally the fornix is situated below the corpus callosum (cc: Fig. 14, Fig. 25-30, Fig. 31-38). From there it continues in ventral direction (around the rostral aspect of the thalamus). Further caudal it reaches the mamillary bodies (mb: Fig. 28-30, Fig. 38) of the hypothalamus. All the way the fornix remains connected to the corpus callosum by the septum telencephali, also known as septum pellucidum (spe: Fig. 39-40). It forms parts of the medial wall of the lateral ventricle. The septum also contains the septal nuclei (sn: Fig. 30). The pronounced rhinencephalon contains the limbic system, consisting of the dentate gyrus (dg: Fig. 13-15, Fig. 39) cingulate gyrus (ci: Fig. 16-17, Fig. 28-30, Fig 32), supracallosal gyrus, geniculate gyrus and the hippocampal formation, is well developed.

5.1.2.5 Commissures

One of the most striking features in the midsagittal MR image is the corpus callosum that connects most parts of the neopallium of the two hemispheres. Its rostrum (rcl: Fig. 28-30) connects caudoventrally with the lamina terminalis. Its most rostral part is the genu of corpus callosum (gcc: Fig. 29-30). From there its trunk runs along the bottom of the longitudinal fissure, caudally forming the splenium of the corpus callosum (scc: Fig. 28-29). The hypointens fibres of the corpus callosum run transversally, entering the corpus medullare of the hemispheres. Here they spread out to frontal and occipital cortical areas. The corpus callosum (trunk and splenium) also forms the roof of the lateral ventricles. The corpus callosum of the pig forms a very long narrow arch in sagittal scans. In some parts it is not thicker than the fornix.

The hypointens rostral commissure (rc: Fig. 11-12, Fig. 26-30, Fig. 31-33) of the paleopallium is located just ventrally to the connection between the rostrum of the corpus callosum (rcl: Fig. 28-30) and the terminal lamina (tl: Fig. 28-30). Rostrally the commissure leads to the olfactory tracts and septal area, while the caudal part connects laterally with the piriform lobe. The commissure of the fornix joins the hippocampus of the left and right hemisphere. It is part of the archipallium (cmf: Fig. 36-40) and is also known as the commissure of the hippocampus.

5.1.3 Diencephalon

The rostral part of the brain stem is called diencephalon. The diencephalon is divided into thalamus, metathalamus, epithalamus and hypothalamus. It is mostly hidden from view by the telencephalon and is situated directly below the hypointens fibres of the fornix (fo: Fig. 10-12,15, Fig. 27-30) and the hyperintens cornu ammonis (cam: Fig. 10-17, Fig. 20-28, Fig. 38-43), a three dimensional structure shaped like the horn of a ram. Only the most ventral aspect- the hypothalamus is visible. A midsagittal MR image reveals a better view (Fig. 30). A region called the subthalamus is positioned dorsal to the hypothalamus and is a continuation of the mesencephalic tegmentum. The different parts of the fornix can be best viewed in transverse scans. Here we can distinguish between the columna fornicis (cf: Fig. 9, Fig. 33-37, Fig. 41), the commissure of the fornix (cmf: Fig. 36-40) and the corpus of the fornix (cfo: Fig. 13-14, Fig. 33-35).

5.1.4 Mesencephalon

The mesencephalon is part of the brain stem. The pig's arched mesencephalon is mostly covered by the rostral part of the cerebellum; a smaller section is covered by the occipital lobe. The ventral aspect is exposed. The hyperintens narrow mesencephalic aqueduct (aq: Fig. 11-12, Fig. 30, Fig. 40-45) runs through it joining the 3rd and 4th ventricle rostrally. It is surrounded by the more hypointens central grey substance (cgs: Fig. 10-12, Fig. 28-29, Fig. 40-45). Together they form of the large arched aqueduct. This can be viewed in sagittal slices. The mesencephalon can be divided into a dorsal (tectum), medial (tegmentum) and ventral (crura cerebri) part. The tectum is the dorsal aspect with the aqueduct (aq: Fig. 11-12, Fig. 29-30, Fig. 40-45) positioned below. It forms the caudal (part of the auditory pathway) and rostral colliculi (roc: Fig. 13, Fig. 25-30, Fig. 42-45) as part of the visual pathway. Four structures arranged as two pairs are forming the roof of the mesencephalon. The caudal colliculi are positioned further apart than the rostral colliculi. They are spherical structures. They are more ventrally positioned then the rostral colliculi.
The rostral colliculi (roc: Fig. 13, Fig. 25-30, Fig. 42-45) of the pig are larger than the caudal colliculi (ccl: Fig. 10-12, Fig. 24-26, Fig. 46-47) - similar to the rostral colliculi

of small ruminants- and are connected by the commissure of the rostral colliculi .This can also be observed in Fig. 41. In the pig the rostral and caudal colliculi are separated by a longitudinal medial sulcus from their contralateral counterpart and a transverse sulcus parts the rostral from the caudal colliculi. The rostral colliculi are connected to the hypointens optic tract (ot: Fig. 9-14, Fig. 21-26, Fig. 34-40) while the caudal colliculi are connected to the medial geniculate body (mgb: Fig. 10-12, Fig. 40-41) by the hypointens brachium of the caudal colliculi (bcc: Fig. 10, Fig. 42-45).
The medial longitudinal fasciculus (flm: Fig. 6-9, Fig. 29-30, Fig. 42-52) is positioned ventrally to the periaqueductal grey/central grey substance (cgs: Fig. 10-12, Fig. 28-29, Fig. 40-45). Ventrally the hypointens fibres of the rostral cerebellar peduncles (pcr: Fig. 9-10, Fig. 25-26, Fig. 46-49) are crossing over to the contralateral side, forming the decussation of the rostral cerebellar peduncles/decussation of the brachium conjunctivum/ interpeduncular decussation (dpc: Fig. 8-9, Fig. 28-30, Fig. 42-43) with the hyperintens central interpeduncular nucleus of the tegmentum just below, that was identified in the scans (ipd: Fig. 30, Fig. 42-43). In the MR images it is also possible to identify the substantia nigra (sng: Fig. 9, Fig. 25-26, Fig. 38-41). The red nucleus (rn: Fig. 27-28, Fig. 41) of the domestic pig was not easy to identify in our scans. The position had to be assumed due to the neighbouring easily identifiable features in the same plane such as the substantia nigra (sng: Fig. 9, Fig. 25-26, Fig. 38-41), aqueduct (aq: Fig. 11-12, Fig. 30, Fig. 40-45), the fasciculus tegmenti (fte: Fig. 27, Fig. 40-47) and the brachium of the rostral colliculus (brc: Fig. 41) in transverse images.
The pons of the pig (po: Fig. 28-30, Fig. 45) stretches far in rostral direction. In transverse scans it can be identified below the mesencephalon.

5.1.4.1 Thalamus

The thalamus of the pig is almost oval shaped in the midsagittal scan. The largest section of the third ventricle can be found ventrally from the intermediate mass of the thalamus. The thalamus can be seen just below the fornix (fo: Fig. 10-12,15, Fig. 27-30) building the floor of the lateral ventricle and bordering the internal capsule (ic: Fig. 14-16, Fig. 22-26, Fig. 31-37). It meets the terminal lamina (tl: Fig. 28-30) rostrally while it connects caudally with the mesencephalon. The thalamus of the pig consists of a number of hyperintens nuclei that could not be individually identified in

our scans. In the midsagittal picture (Fig. 30) the nuclei of the thalamus form a prominent circular structure (th: Fig. 12-14, Fig. 24-30, Fig. 35-38) that appears to be hypointens compared to the ventricle that is reduced to a hyperintense ring. The thalamus develops within the walls of the third ventricle. The connection of the thalamus of the left and right hemisphere is called interthalamic adhesion (ita: Fig. 35-39) or massa intermedia. In transverse and dorsal slices the thalamus is not circular but changes its shape from cranial to caudal and ventral to dorsal.

The thalamus is the most important connection and control point between the brainstem, the medulla oblongata and the telencephalon. The most striking afferent nerve is the optical nerve (opn: Fig. 6-8, Fig. 21-27). The left and right (mildly hypointense) parts converge and cross over to the contralateral side at the optic chiasm (cho: Fig. 6-8, Fig. 28-30, Fig. 32-33) and continue as the optic tract (ot: Fig. 9-13, Fig. 21-26, Fig. 24-40). Their destination is the metathalamic lateral geniculate body (lgb: Fig. 40-41). The strong hypointens optic tract and the optic chiasm form the rostral boundary of the diencephalon. In sagittal scans the optic chiasm appears oval shaped and dorsoventrally elongated (Fig. 30).

5.1.4.2 Metathalamus

The metathalamus is dominated by the hyperintens lateral (lgb: Fig. 40-41) - and medial (mgb: Fig. 10-12, Fig. 40-41) geniculate bodies. They contain nuclei that are a relay centres for acoustic and visual information. Unfortunately it is not possible to identify the nuclei individually. In the transverse scans the strongly hypointens optic tract arches over the geniculate bodies. The hypointens lamina medullaris externa (lme: Fig. 12-14, Fig. 24, Fig. 36-40) is visible ventromedial from the lateral geniculate body (lgb). The lateral geniculate body connects with the optic tract (ot: Fig. 9-13, Fig. 21-26, Fig. 24-40) while the medial geniculate body is met by fibres from the caudal colliculi (ccl: Fig. 10-12, Fig. 24-26 , Fig. 46-47). The fibres of the stongly developed optic nerve (opn: Fig. 6-8, Sagittal Fig. 21-27) are crossing over to the contralateral side. As a result the optic chiasm (cho: Fig. 6-8, Fig. 28-30, Fig. 32-33) is large and the lateral geniculate body is strongly developed.

5.1.4.3 Epithalamus

The epithalamus positioned dorsomedially of the brain. The pineal body (pb: Fig. 14, fig. 30, Fig. 40) is part of the epithalamus. The pineal body is a small structure and is indeed shaped like a pine cone. The structure is caudodorsally attached to the habenular commissure that could not be identified in our selected scans. The pineal body is connected to the diencephalon by the habenulae (ha: Fig. 38-40) a paired structure originating from a hypointens fibre bundle called the stria medullares thalami (smt: Fig. 14, Fig. 29-30, Fig. 33-38) also known as the habenular stria and connected by the habenular commissure. The stria also act as the major afferent tract to the habenulae from the telencephalon, while the main efferent tract, the fasciculus retroflexus or habenulo-interpeduncular tract (hit: Fig. 10-13, Fig. 28-29, Fig. 39) with a small round hypointens shape in dorsal sections travels through the dorsomedial parts of the dorsal thalamus and finally to the interpeduncular nucleus (ipd: Fig. 30, Fig. 42-44) in the brainstem. The habenular nuclei are interconnected with the limbic system. The caudal commissure (cdc: Fig. 12-13, Fig. 29, Fig. 40-41) is positioned caudoventrally to the cone shaped pineal body (pb). The small roundish hypointens caudal commissure forms the dorsal wall of the rostral entrance to the aqueduct (aq: Fig. 11-12, Fig. 30, Fig. 40-45). Unfortunately hypointens artefacts, caused by air are separating the cerebellum from the telencephalon, result in a gap between the rostral colliculus (roc: Fig. 13, Fig. 25-30, Fig. 42-45) and the pineal gland that would not be there had the pig’s head not been removed from the body prior to the scan. This was unfortunately necessary to facilitate the formalin fixating process.

5.1.4.4 Hypothalamus

The hypothalamus is the most ventral part of the diencephalon and forms the floor of the 3rd ventricle (3: Fig. 8-9, Fig. 29-30). The pituitary gland is elongated and is pointing in caudoventral direction (pg: Fig. 7, Fig. 28-30, Fig. 34-40). The pituitary gland is situated in a deep groove surrounded by the basiphenoid bone (bsp: Fig. 30). The caudoventral part of the groove is filled the blood vessels of the rete mirabile (rm: Fig. 29-30). The rete mirabile is hypointense in our scans. The rete mirabile takes up more space than the pituitary gland itself. The pituitary gland is positioned in the dorsal part of the groove. The tissue of the pituitary gland is hypointens to the cerebrospinal fluid (CSF) that fills the infundibular recess of the 3rd ventricle. It is isointense to the piriform lobes that emerge at the level of the nucleus of the abducent nerve (nab: Fig. 7, Fig. 49).

The tuber cinereum (a hollow structure consisting of gray matter and positioned between the optic chiasm and mammillary body) is not marked in the MR images, but the hyperintens infundibular recess (ir: Fig. 6) and the mammillary body (mb: Fig. 28-30, Fig. 38) are labelled. We can see the infundibular recess (ir: Fig. 6) of the pituitary gland caudal from the optic chiasm (cho Fig. 6-8, Fig. 28-30, Fig. 32-33). It is filled with cerebrospinal fluid (CSF) from the 3rd ventricle that is responsible for the hyperintens signal in PD weighed images of the formalin fixed brain.

5.1.4.5 Subthalamus

The subthalamic region is positioned dorsal to the hypothalamus and is a continuation of the mesencephalic tegmentum. The subthalamus is positioned between thalamus (dorsal) and hypothalamus (ventral and medial). The internal capsule (ic: Fig. 14-16, Fig. 22-26, Fig. 31-37) borders the subthalamus laterally on either side. It is bordered caudally by the tegmentum of the mesencephalon. The subthalamus is part of the extrapyramidal system. The subthalamic nucleus is connected with the putamen (put: Fig. 13-15, Fig. 22-24, Fig. 31-36) and pallidum (gp: Fig. 12, Fig. 31-33) by fibres of the ansa lenticularis (not identified in scans). The zona incerta can be identified dorsomedial of the subthalamic nucleus (zi: Fig. 38) in transverse scans. The hyperintens pallidum or globus pallidus (gp) consists of

loosely distributed nerve cells. It is a part of the diencephalon but is divided from it by the hypointens fibres of the internal capsule (ic: Fig. 14-16, Fig. 22-26, Fig. 31-37) and shifted towards the putamen (put) of the telencephalon. As mentioned above pallidum and putamen are forming the elongated lenticular nucleus of the porcine brain.

5.1.5 Metencephalon

The metencephalon consists of the tegmentum metencephali and the cerebellum (cb) (see below), they are divided by the 4th ventricle (4:Fig. 7-9, Fig. 30). The 4th ventricle emerges at the level of the nucleus of the abducent nerve (nab: Fig. 7, Fig. 49) in our scans. It is filled with hyperintens cerebrospinal fluid (CSF). We can identify two cranial nerves in dorsal scans of the metencephalic level (Fig. 7) and slightly ventral (Fig. 6). The fifth cranial nerve (trigeminal nerve) emerges here caudolaterally from the descending corticobulbar and corticospinal tracts and cranially from the floor of the 4th ventricle. The trigeminal nerve of the pig is is large, its roots extend laterally. In transversal scans the trigeminal nerve (with its hypointense white matter) can be identified as a bean shaped structure stretching in rostral direction (V: Fig. 6-7, Fig. 21-24, Fig. 35-45). In sagittal scans we can see that the nerve extends in cranioventral direction. The spinal tract of the trigeminal nerve (spt: Fig. 6-7) extends in caudal direction (towards the spinal cord Fig. 6) and laterally in the direction of the fasciculus longitudinalis medialis (flm: Fig. 6-9, Fig. 28-30, Fig. 42-52). The fibre bundle of the medial longitudinal fasciculus is isointense to the spinal tract of the trigeminal nerve and is situated ventral of the 4th ventricle (4: Fig. 7-9, Fig. 30) and the central canal (cec: Fig. 30). The 8th cranial nerve (vestibulocochlear nerve VIII: Fig. 6-7, Fig. 48-49) emerges caudolaterally from the trigeminal nerve (V) in Fig. 6 and innervates the ear (Aur: Fig. 7-9). We can also identify the well developed pons (po: Fig. 28-30, Fig. 45) with its hypointens transverse fibres (ftp: Fig. 42-44) and the embedded hyperintens pontine nuclei (npo: Fig. 26-27, Fig. 45). Easily distinguishable as an external ridge, the pons and its organisation can be seen as a continuation of the medulla oblongata. The pons is connected on either side with the cerebellum by the hypointens medial cerebellar peduncle (pcm: Fig. 8-10, Fig. 23-24, Fig. 45-47) also known as the brachium pontis. Caudal of the pons, the trapezoid body (tb: Fig. 26, Fig. 48) releases

vestibulocochlear nerve (VIII: Fig. 6-7, Fig. 48-49) and the facial nerve (VII: Fig. 25-27). The hypointense genu of the facial nerve (gnf: Fig. 7-8, Fig. 49-50) and the hypointense radix of the facial nerve (rnf: Fig. 6, Fig. 49) are captured in our scans. The hyperintense nucleus of the facial nerve is pictured in Fig. 50-52. The genu of the facial nerve wraps itself around the hyperintense nucleus of the abducent nerve (nab: Fig. 7, Fig. 49). In transverse scans the hypointense genu of the facial nerve forms an arch like sructure. The fiber bundle of the facial nerve extends in ventrolateral direction and ends in the radix of the facial nerve. Here they surface from the brainstem. Medially directly under the hypointens central grey substance (cgs: Fig. 10-12, Fig. 28, Fig. 40-45) runs the hypointens medial longitudinal fasciculus (flm: Fig. 6-9, Fig. 28-30, Fig. 42-52).

The trapezoid body appears hypointens and consists of transverse fibres (like the pons) that surround the dorsal and ventral trapezoid nuclei. The trapezoid body, as part of the auditory pathway, is continued rostrally by the lateral lemniscus (lal: Fig. 8-9, Fig. 25, Fig. 44-45). Fibers from the ventral cochlear nuclei pass through an ipsi- or contralateral nucleus of the trapezoid body. Some of the fibres reach the caudal colliculi (ccl: Fig. 10-12, Fig. 24-26, Fig. 46-47) via the hypointens lateral lemniscus (lal: Fig. 8-9, Fig. 25, Fig. 44-45), the other fibers reach the auditory cortex (temporal lobe) after passing through the medial geniculate body (mgb: Fig. 10-12, Fig. 40-41).

Fibres extending from the dorsal cochlear nucleus (con: Fig. 50-52) join the ipsi-or contralateral lateral lemniscus (lal: Fig. 8-9, Fig. 25, Fig. 44-45) directly. In the pig the small dorsal and ventral cochlear nuclei are embedded in the acoustic tubercle. The hyperintens medial (nmv: Fig. 50-52) - and lateral (nml: Fig. 50) vestibular nuclei form a part of the ventrolateral wall of the 4th ventricle (vestibular area). The pons can be divided into a dorsal and a ventral part. Ventrally we find the transverse fibres (ftp: Fig. 42-44) and pontine nuclei (npo: Fig. 26-27, Fig. 45). The majority of fibres are part of the descending tract. They originate in the cerebral cortex and from there pass through the cerebral crura (crc: Fig. 9-10, Fig. 35-42). They cross over to the contralateral cerebellar hemisphere via the hypointens middle cerebellar peduncles (pcm: Fig. 8-10, Fig. 23-24, Fig. 45-47) also known as pontocerebellar tracts. The transverse fibres of the pons are crossed by fibres of the hypointens longitudinal pyramidal tract (pyr: Fig. 28-30, Fig. 48-52). The dorsal aspect of the pons is mainly formed by the reticular formation (rf: Fig. 27) connecting the spinal cord with the forebrain.

5.1.5.1 Cerebellum

The cerebellum of the pig in midsagittal MRI (Fig. 30, Fig. 73) scans is characterized by the hypointens medulla that forms the “abor vitae” as it branches out into individual lobes, lobules and folia (smallest subdivision). The cortex of the cerebellum is hyperintens. The primary cerebellar fissure (Prf: Fig. 27-30, Fig. 73), the first fissure that divides the primordial cerebellum during ontogenesis into a rostral and caudal lobe, is easily identified in the MRI scans. The rostral lobe appears to be smaller than the caudal lobe. The classical subdivisions of the vermis in mammals can also be identified in the pig. The lingula (li: Fig. 9-11, Fig. 28-30, Fig. 46- 51, Fig. 73) is positioned cranial to the recessus tecti of the 4th ventricle, followed dorsorostrally by the central lobule (cl: Fig. 12- 13, Fig. 28-30, Fig. 46-48, Fig. 73). Culmen (cu: Fig. 14-16, Fig. 29-30, Fig. 47-48, Fig. 73) and declive (de: Fig. 13-14, Fig. 29-30, Fig. 49-52, Fig. 73) together form the monticulus (little hill), which is raised and pointed in the pig. They are separated by the primary cerebellar fissure and caudoventrally joined by the folium (fol: Fig. 29-30, Fig. 72) and the tuber (tu: Fig. 14-16, Fig. 25-26, Fig. 72). The prepyramidal fissure (Ppf: Fig. 72) separates the tuber from the pyramis (py: Fig. 27-30, Fig.74) and the secondary cerebellar fissure (Scf: Fig. 28-30, Fig. 72) divides the pyramis from the uvula (uv: Fig. 28-30, Fig. 72). The nodulus (no: Fig. 9-12, Fig. 27-30, fig. 52, Fig. 72) is positioned ventrally between the caudal uvolunonodular fissure (Unf: Fig.74) and the cranial recess. From the rostral and caudal truncus the medulla branches of into a number of lobes, lobules and folia (smallest subdivision). From dorsomedial to ventrolateral the declive (de: Fig. 13-17, Fig. 29-30, Fig. 49-52, Fig. 72), ansate gyrus, paraflocculus (paf: Fig. 9-10, Fig. 19-21, Fig. 46-52, Fig. 72) and flocculus (flo: Fig. 9, Fig. 21-22, Fig. 48- 52, Fig. 72) form an arch around the cerebellar nuclei. In midsagittal slices the vermis of the porcine brain is nearly circular. Cranially from the cerebellum we find the rostral (roc: Fig. 13, Fig. 25-30, Fig. 42-45) and caudal colliculi (ccl: 10-12, Fig. 24-26, Fig. 46-47) of the lamina quadrigemina. Within the medulla of the cerebellum we can identify a number of hyperintens nuclei. They are the nucleus fastigii (nf: Fig. 11, Fig. 51-52), the nucleus interpositus (nip: Fig. 11, Fig. 28, Fig. 49-51) and the dentate nucleus (nde: Fig. 24-25, Fig. 49-51). The hypointens fibres of the rostral (pcr: Fig. 9-10, Fig. 25-26, Fig. 46-49), medial (pcm: Fig. 8-10, Fig. 23-24, Fig. 45-47) and caudal (pcc: Fig. 8-9, Fig. 23-26, Fig. 52) cerebellar peduncles connect the cerebellum to the surrounding parts of the brain. In dorsal, sagittal and transverse scans we can see

that the cerebellum is composed of the central vermis and hemispheres. In dorsal scans the lateral lobules of the cerebellar hemispheres are lacking the symmetry of the telencephalic hemispheres due to the curved vermis. The curve of the vermis is not visible in midsagittal scans. We can identify on either side of the vermis the flocculus (flo: Fig. 9, Fig. 21-22, Fig. 48-52, Fig.74), paraflocculus (paf: Fig. 9-10, Fig. 19-21, Fig. 46-52, Fig. 72) ansiform lobule (ans: Fig. 11-16, Fig. 21-27, Fig. 47-52) and paramedian lobule (pml: Fig. 10-13, Fig. 22-26). Again we can identify the hypointens medulla and the hyperintens cortex. In the pig the ansiform lobule is especially easy to identify due to its medulla that runs at a transverse angle to the vermis stretching in rostrolateral direction.

5.1.5.2 Medulla oblongata

Because the pig's heads were removed from the rest of the body we could only detect the rostral part of the medulla oblongata. The caudal structures are partly destroyed in the preparation process. The medulla oblongata can be seen as an extension of the spinal cord. Together with the caudal medullary velum and the caudal part of the 4th ventricle (4: Fig. 7-9, Fig. 30) it forms the mylencephalon. In comparison with the spinal cord the medulla oblongata houses a larger number of nuclei (unidentified in our scans) responsible for an increase in width. The medulla oblongata is rostrally connected to the pons (po: Fig. 28-30, Fig. 45). It fills the medullar impression of the basioccipital bone (boc: Fig. 30) and reaches the foramen magnum caudally. On the ventral aspect runs the ventral median fissure ending at the caudal end of the pons.

5.2 Dorsal scans of the porcine brain

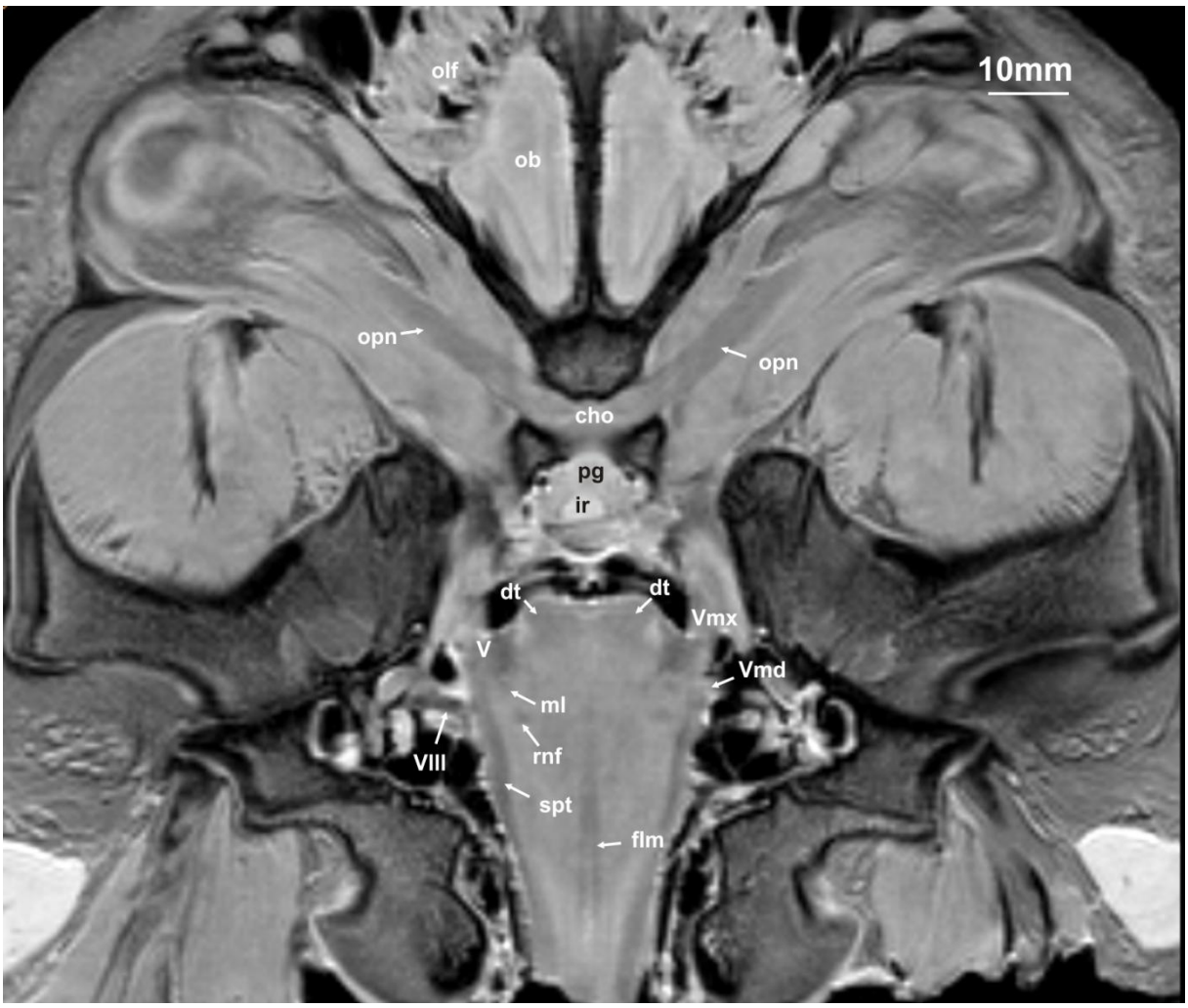

Figure 6
cho: optic chiasm; dt: descending tracts- corticospinal, corticobulbar; flm: medial longitudinal fasciculus; ir: infundibular recess; ml: medial lemniscus; ob: olfactory bulb; olf: olfactory fibers; opn: optic nerve; pg: pituitary gland; rnf: radix nervi fascialis; spt: spinal trct of the trigeminal nerve; V: trigeminal nerve; Vmd: nervus mandibularis of the trigeminal nerve; Vmx: nervus maxillaries of the trigeminal nerve; VIII: vestibulacochlear nerve.

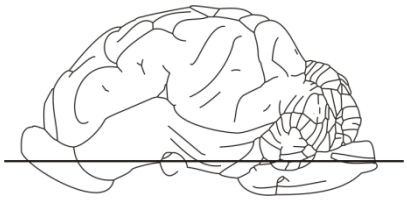

Figure 7

Aur: auris; cf: columna fornicis; cho: optic chiasm; crc: cerebral crus; flm: medial longitudinal fasciculus; gnf: genu nervi fascialis; lot: lateral olfactory tract; mot: medial olfactory tract; nab: nucleus of the abducent nerve; ob: olfactory bulb; Oc: oculus; olf: olfactory fibers; opn: optic nerve; pg: pituitary gland; pir: piriform lobe; spt: spinal tract of the trigeminal nerve; V: trigeminal nerve; VIII: vestibulocochlear nerve; 4: fourth ventricle.

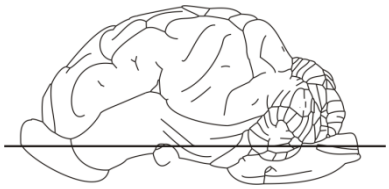

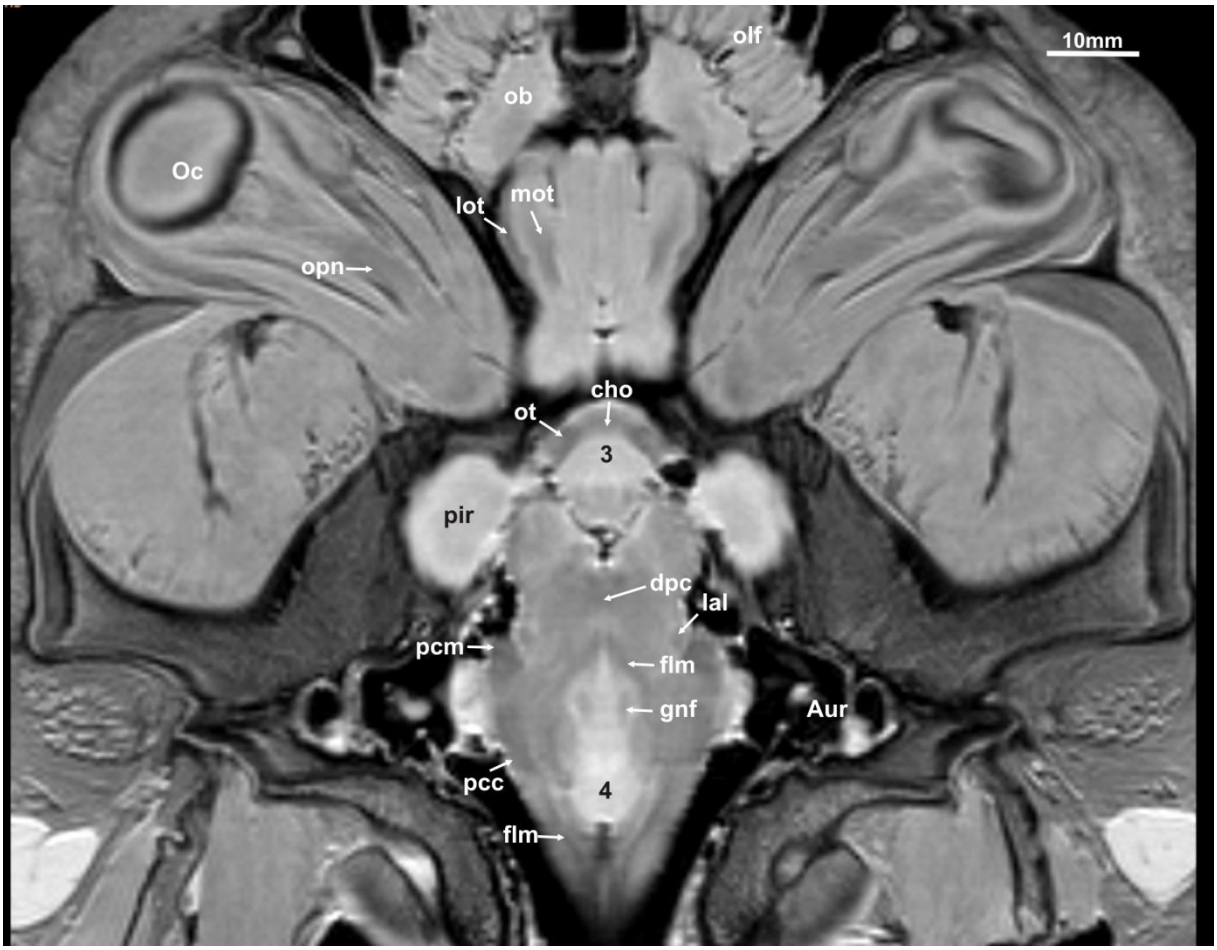

Figure 8

Aur: auris; cho: optic chiasm; dpc: decussatio pedunculorum cebellarium rostralium; flm: medial longitudinal fasciculus; gnf: genu nervi fascialis; lal: lateral lemniscus; lot: lateral olfactory tract; mot: medial olfactory tract; ob: olfactory bulb; Oc: oculus; olf: olfactory fibers; opn: optic nerve; ot: optic tract; pcc: pedunculus cerebellaris caudalis; pcm: pedunculus cerebellaris medialis; pir: piriform lobe; 3: third ventricle; 4: fourth ventricle.

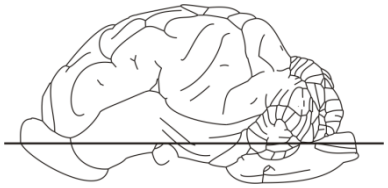

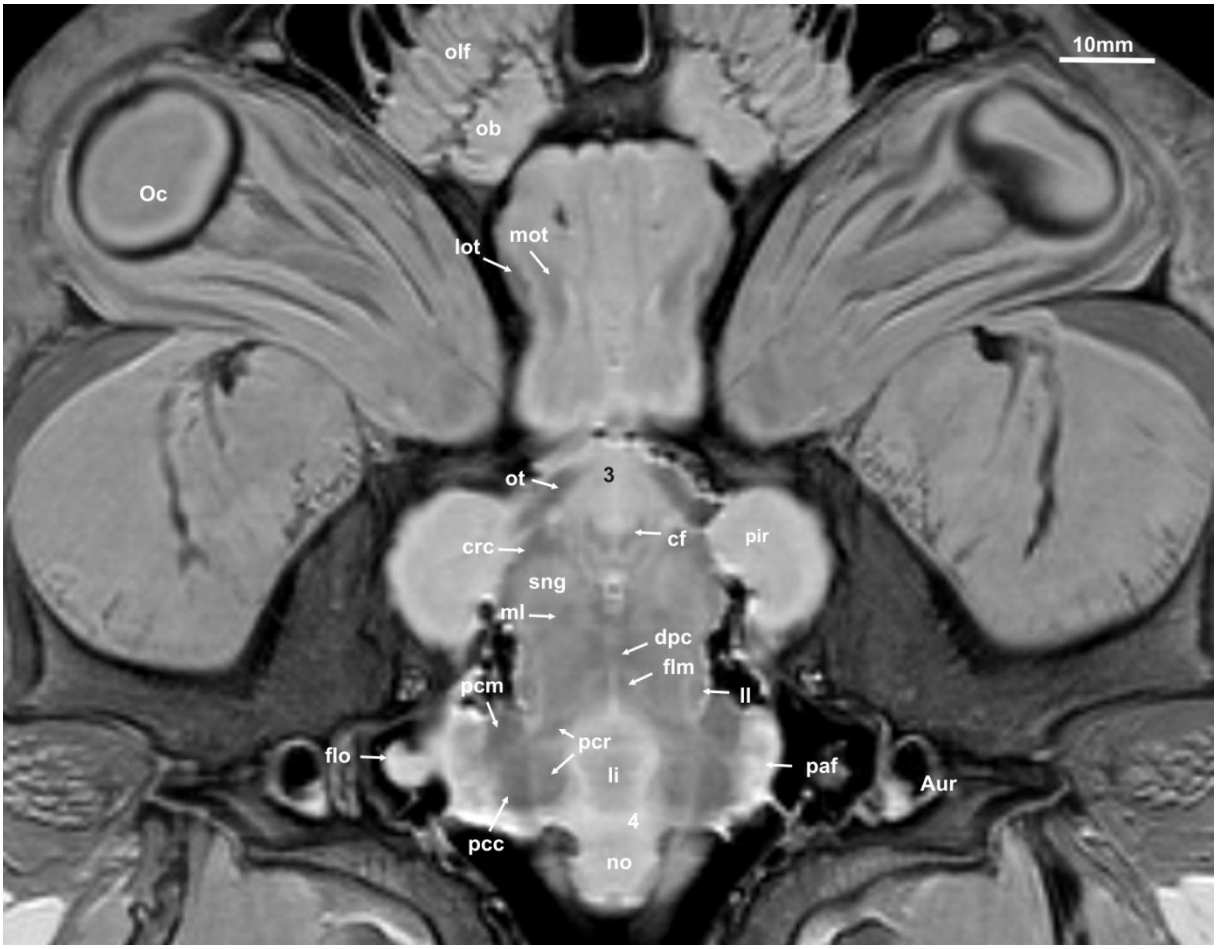

Figure 9

Aur: auris; cf: columna fornicis; crc: cerebral crus; dpc: decussatio pedunculorum cerebellarium rostralium; flm: medial longitudinal fasciculus; flo: flocculus; li: lingula; lot: lateral olfactory tract; ml: medial lemniscus; mot: medial olfactory tract; no: nodulus; ob: olfactory bulb; Oc: oculus; olf: olfactory fibers; ot: optic tract; pcc: pedunculus cerebellaris caudalis; pcm: pedunculus cerebellaris medialis; pcr: rostral cerebellar peduncle; pir: piriform lobe; sng: substantia nigra; 3: third ventricle; 4: fourth ventricle.

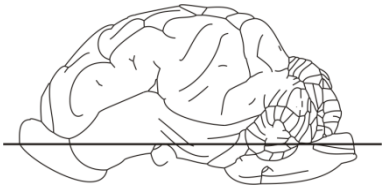

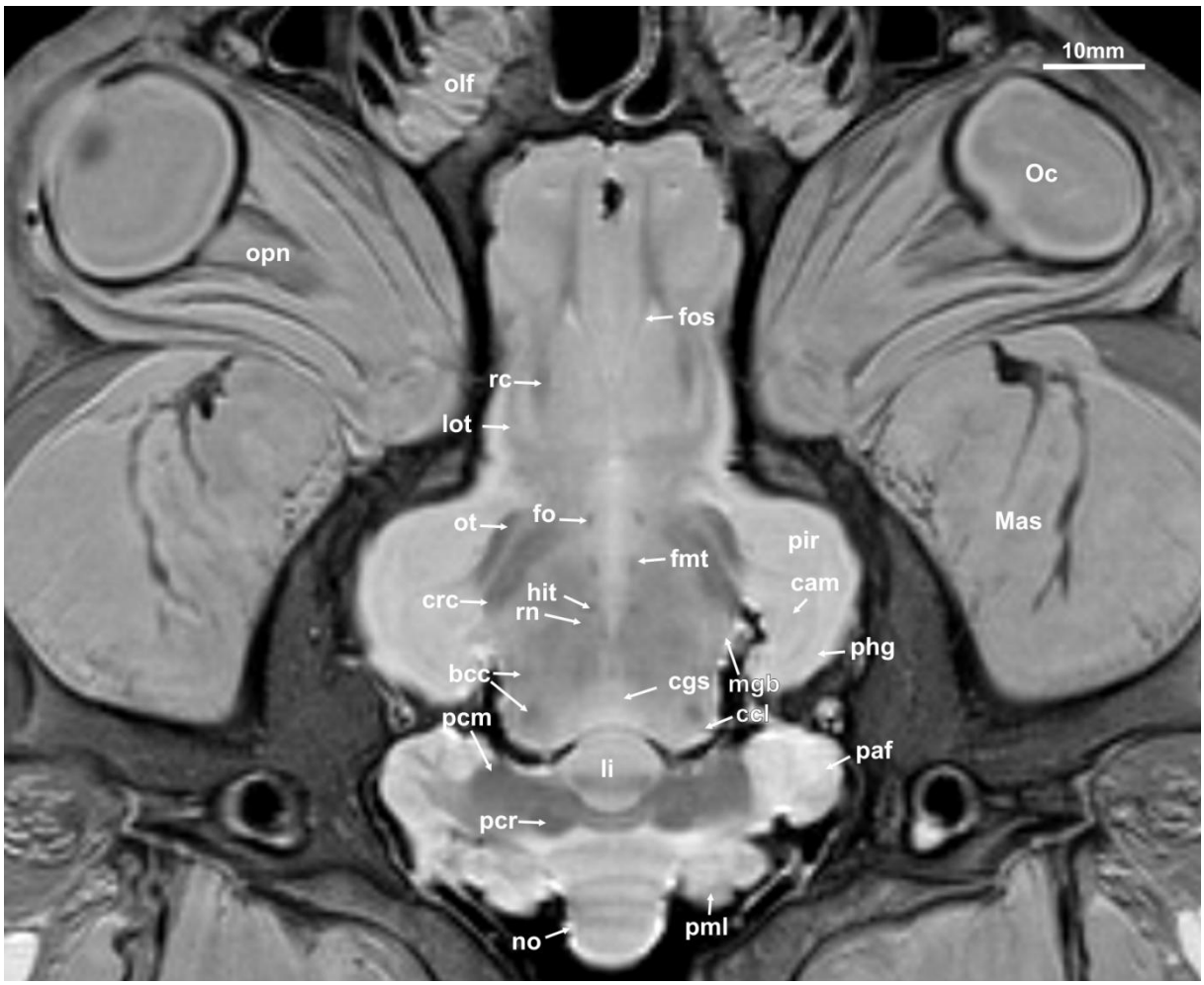

Figure 10

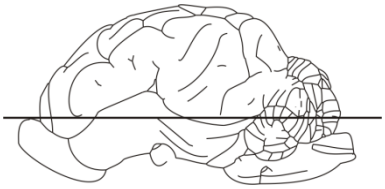

bcc: brachium colliculi caudalis; cam: cornu ammonis; ccl: caudal colliculus; mgb: medial geniculate body; cgs: central grey substance; crc: cerebral crus; fmt: fasciculus mammillothalamicus; fo: fornix; fos: fibrae olfactorii septalis; phg: parahippocampal gyrus; hit: habenulo-interpeduncular tract; li: lingula; lot: lateral olfactory tract; Mas: masseter muscle; mgb: medial geniculate body; no: nodulus; Oc: oculus; olf: olfactory fibers; opn: optic nerve; ot: optic tract; paf: paraflocculus; pcm: medial cerebellar peduncle; pcr: rostral cerebellar peduncle; pir: piriform lobe; phg: parahippocampal gyrus; pml: paramedian lobule.

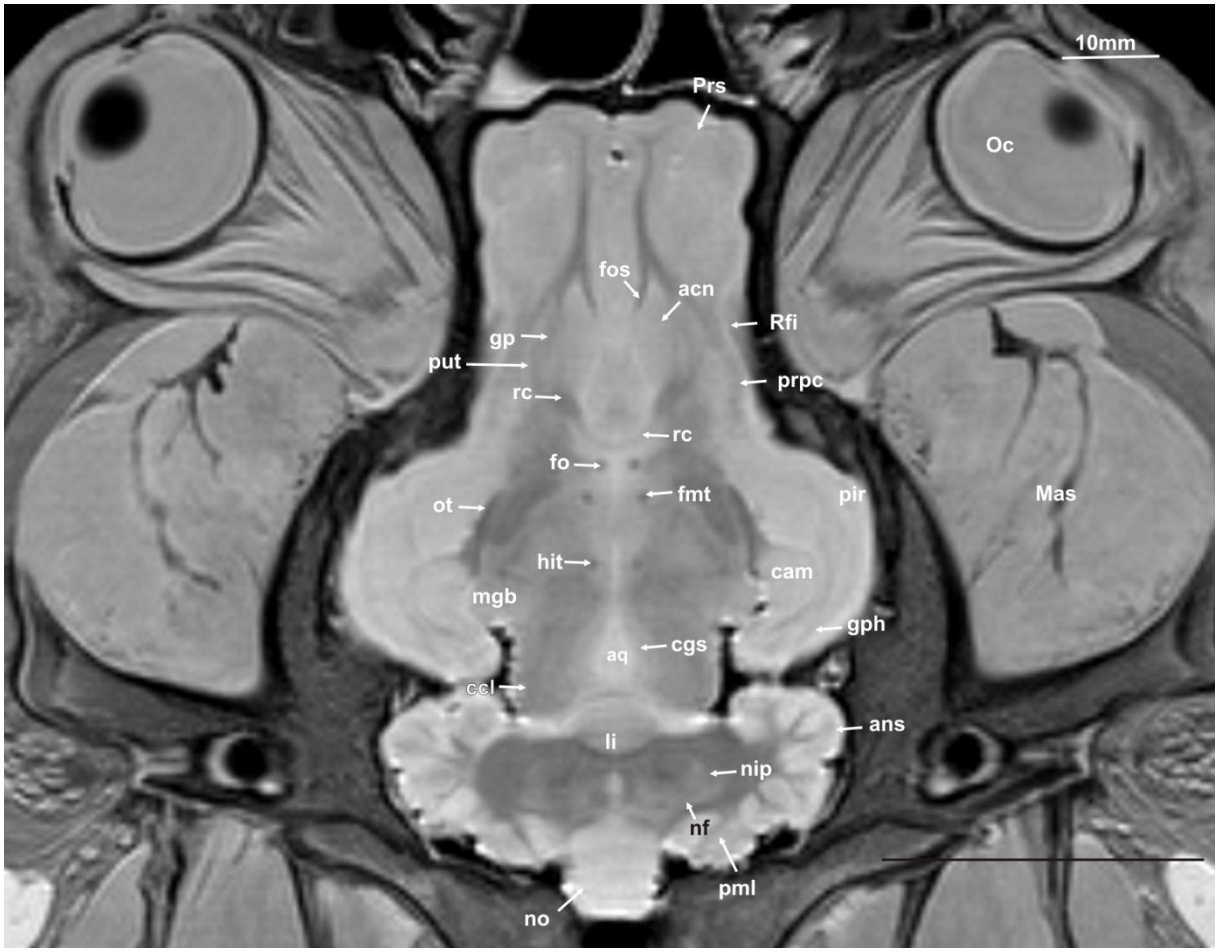

Figure 11

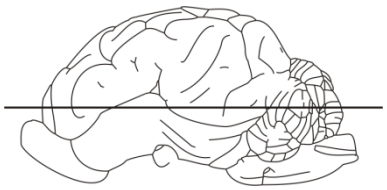

acn: accumbens nucleus; ans: ansiform lobule; aq: mesencephalic aqueduct; cam: cornu ammonis; ccl: caudal colliculus; cgs: central grey substance; fmt: fasciculus mammilo-thalamicus; fo: fornix; fos: fibrae olfactorii septalis; gp: globus pallidus; hit: habenulo-interpeduncular tract; li: lingula; Mas: masseter muscle; mgb: medial geniculate body; nde: nucleus dentatus; nf: nucleus fastigei; nip: nucleus interpositus; no: nodulus; Oc: oculus; ot: optic tract; paf: paraflocculus; prpc: praepiriform cortex; pir; piriform lobe; phg: parahippocampal gyrus; pml: paramedian lobule; Prs: presylvian sulcus; put: putamen; rc: rostral commissure; Rfi: rhinal fissure.

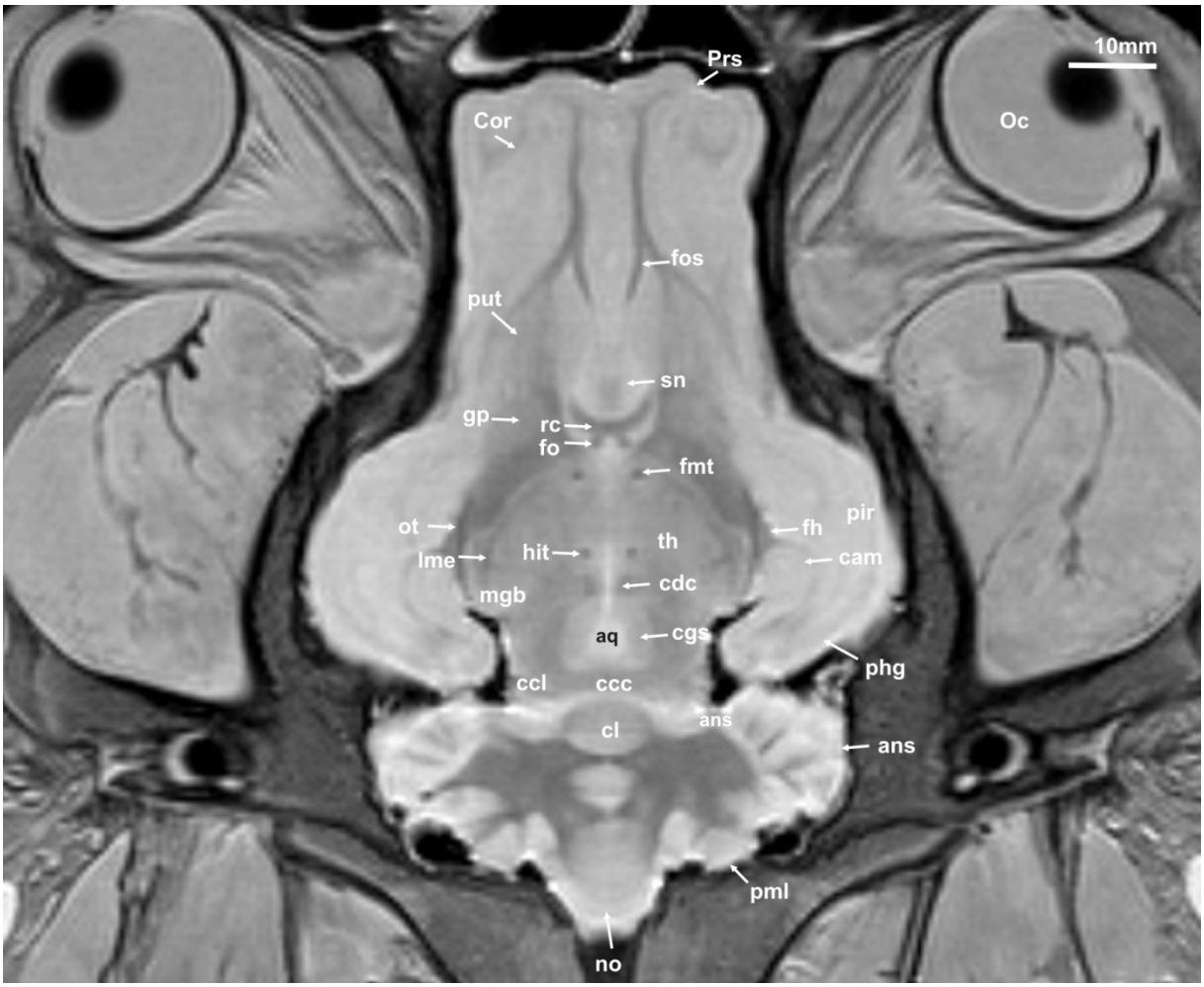

Figure 12

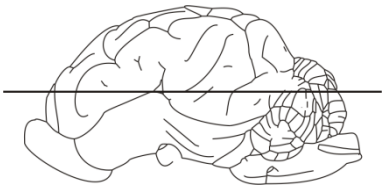

ans: ansiform lobule; aq: mesencephalic aqueduct; cam: cornu ammonis; ccc: commissura colliculi caudalis; ccl: caudal colliculus; cdc: caudal commissure; cgs: central grey substance; cl: central lobule; Cor: coronal sulcus; fh: fimbria hippocampi; fmt: fasciculus mammilo-thalamicus; fos: fibrae olfactorii septalis; gp: globus pallidus; gph: parahippocampal gyrus; hit: habenulo interpeduncular tract; lme: lamina medullaris externa; mgb: medial geniculate body; pml: paramedian lobule; no: nodulus; Oc: oculus; ot: optic tract: paf: paraflocculus; pir: piriform lobe; Prs: presylvian sulcus; put: putamen; th: thalamus.

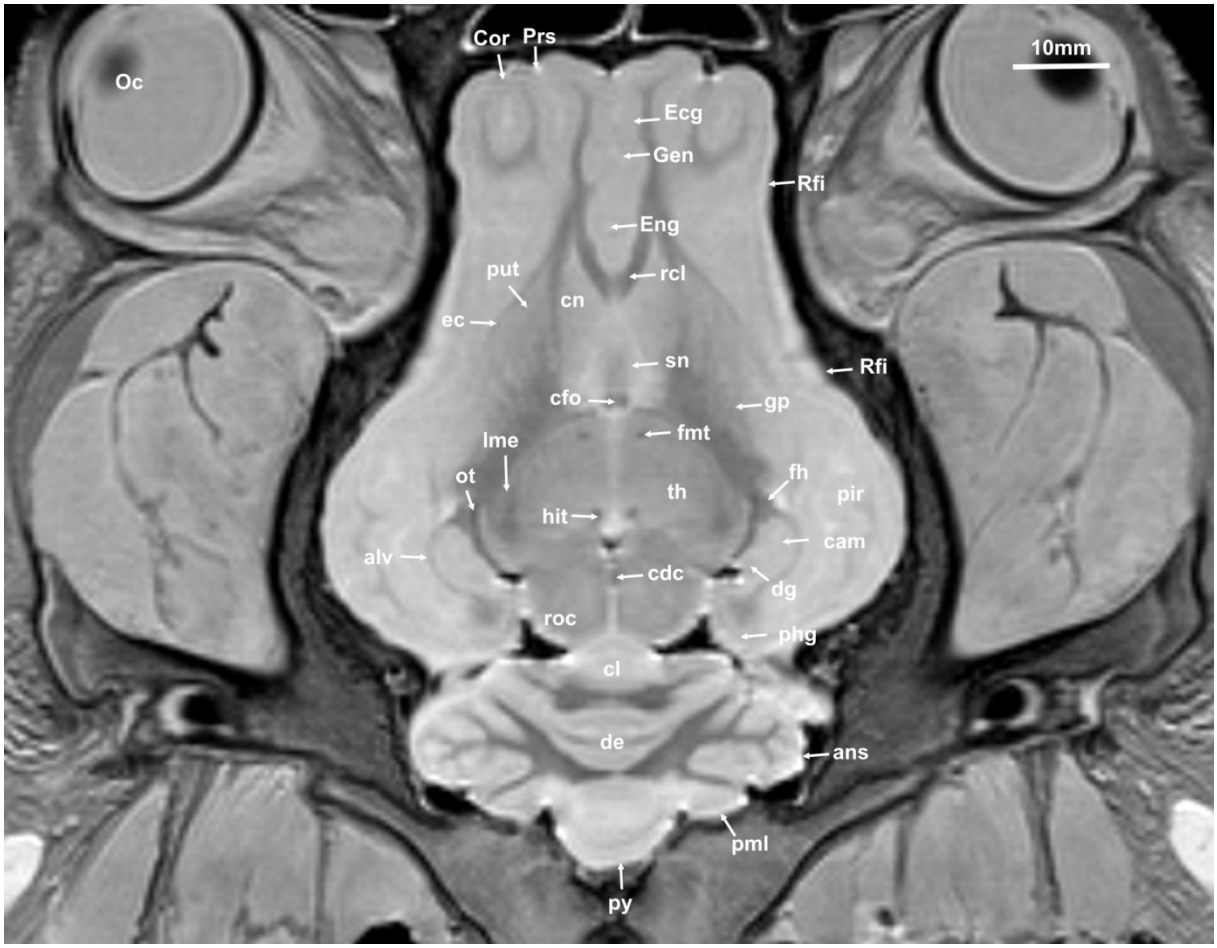

Figure 13

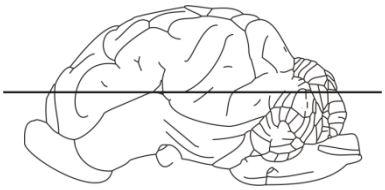

alv: alveus; ans: ansiform lobule; cam: cornu ammonis; cdc: caudal commissure; cfo: corpus of fornix; cl: central lobule; cn: caudate nucleus; Cor: coronal sulcus; dg: dentate gyrus; de: declive; ec: external capsule; Ecg: ectogenual sulcus; Eng: endogenual sulcus; fh: fimbria hippocampi; fmt: fasciculus mammilo-thalamicus; Gen: genual sulcus; gp: globus pallidus; hit: habenulo interpeduncular tract; lme: lamina medullaris externa; Oc: oculus; ot: optic tract; phg: parahippocampal gyrus; pir: piriform lobe; pml: paramedian lobule; Prs: Presylvian sulcus; put: putamen py: pyramis vermis; rcl: rostrum corporis callosi; Rfi: rhinal fissure; roc: rostral colliculus; sn: septal nuclei; th: thalamus.

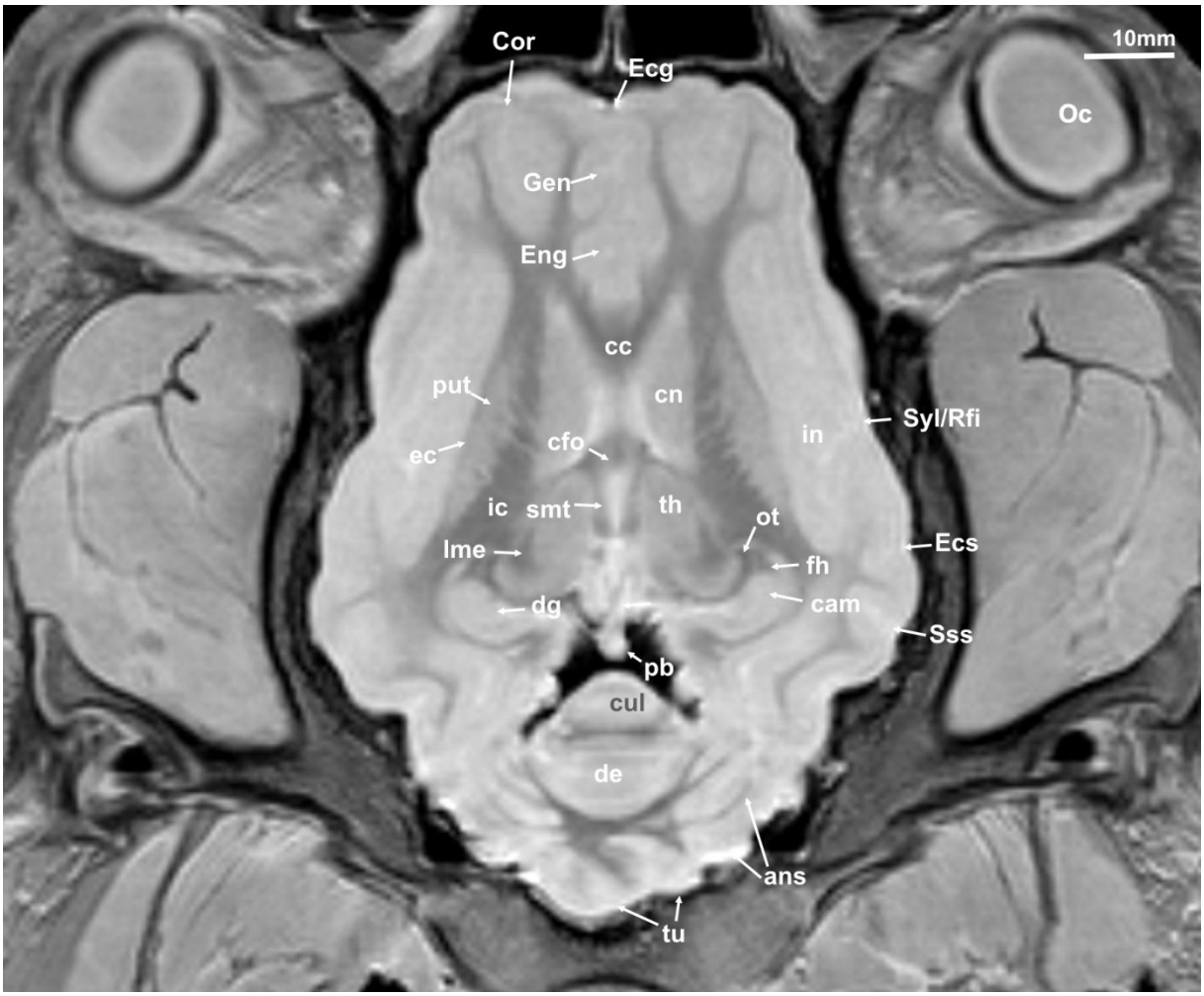

Figure 14

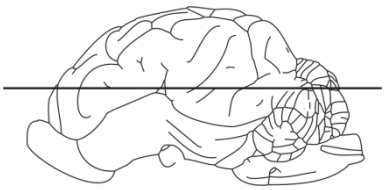

ans: ansiform lobule; cam: cornu ammonis; cc: corpus callosum; cfo: corpus of fornix; cn: caudate nucleus; Cor: coronal sulcus; cul: culmen; dg: dentate gyrus; ec: external capsule; Ecg: ectogenual sulcus; Ecs: ectosylvian sulcus; Eng: endogenual sulcus; fh: fimbria hippocampi; Gen: genual sulcus; ic: internal capsule; in: insula; lme: lamina medullaris externa; Oc: oculus; ot: optic tract; pb: pineal body; put: putamen; Rfi: rhinal fissure; smt: stria medullaris thalami; Sss: suprasylvian sulcus; Syl: sylvian fissure; th: thalamus; tu: tuber.

Figure 15

alv: alveus; ans: ansiform lobule; cam: cornu ammonis; cn: caudate nucleus; Cor: coronal sulcus; cul: culmen; Dia: sulcus diagonalis; dg: dentate gyrus; Ecs: ectosylvian sulcus; Ecm: ectomarginal sulcus; fh: fimbria hippocampi; fo: fornix; Gen: genual sulcus; ic: internal capsule; in: insula; or: optic radiation put: putamen; Sss: suprasylvian sulcus; Syl: sylvian fissure; tu: tuber.

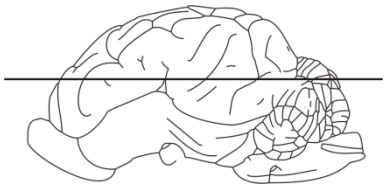

Figure 16

alv: alveus; ans: ansiform lobule; cam: cornu ammonis; cc: corpus callosum; ci: cingulated gyrus; coronal sulcus; cul: culmen; de: declive; Dia: sulcus diagonalis; Ecg: ectogenual sulcus; Ecs: Ectosylvian sulcus; Ecm: ectomarginal sulcus; fsc: fasciculus subcallosus; Gen; genual sulcus; ic: internal capsule; scc: splenium corporis callosi; Sss: suprasylvian sulcus; Syl: sylvian fissure; tu: tuber.

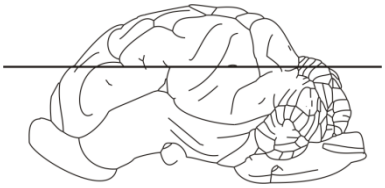

Figure 17

cam: cornu ammonis; ci: cingulated gyrus; cin: cingulum; Cor: coronal sulcus; de: declive; Dia: sulcus diagonalis; Ecg: ectogenual sulcus; Ecm: ectomarginal sulcus; Ecs: ectosylvian sulcus; Flc: longitudinal cerebral fissure; Gen: genual sulcus; or: optic radiation; Spl: splenial sulcus; Sss: suprasylvian sulcus; Syl: sylvian fissure.

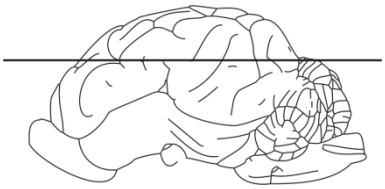

Figure 18

Cor: coronal sulcus; Ecm: ectomarginal sulcus; Ecs: ectosylvian sulcus; Enm: endomarginal sulcus; Flc: fissura longitudinalis cerebri; Mar: marginal sulcus; Spl: splenial sulcus; Sss: suprasylvian sulcus; Syl: sylvian fissure.

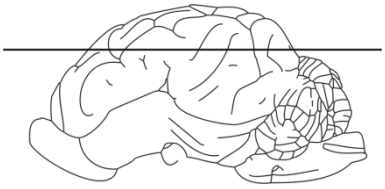

5.3 Sagittal scans of the porcine brain

Figure 19

Dia: diagonal sulcus; Ecs: ectosylvian sulcus; Ems: endomarginal sulcus; or: optic radiation; paf: parafloccullus; pir: piriform lobe; Rfi: rhinal fissure; Sss: suprasylvian sulcus; Syl: sylvian sulcus.

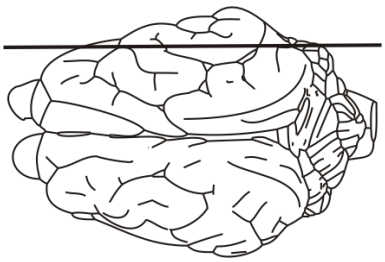

Figure 20

cam: cornu ammonis; Ecm: Ectomarginal sulcus; fh: fimbria hippocampi; olf: olfactory fibers; paf: paraflocculus; pir: piriform lobe; Rfi: rhinal fissure; or: optic radiation; Sss: suprasylvian fissure; Syl: Sylvian fissure; Vmx: maxillary nerve of the trigeminal nerve.

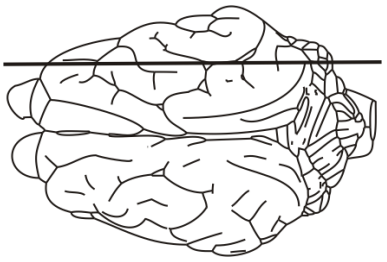

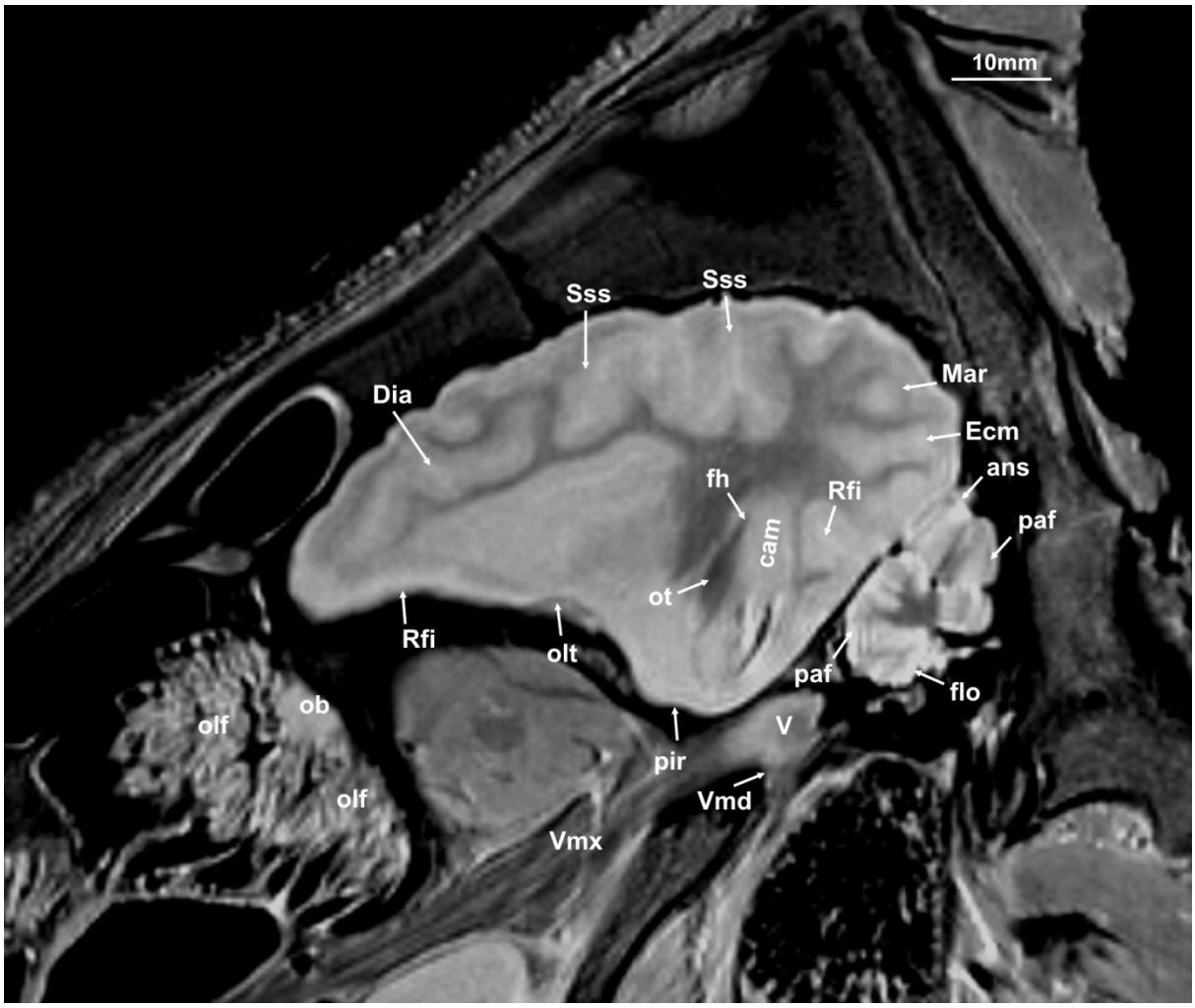

Figure 21

ans: ansiform lobule; cam: cornu ammonis; Dia: diagonal sulcus; Ecm: ectomarginal sulcus; fh: fimbria hippocampi; flo: flocculus; Mar: marginal sulcus; ob: olfactory bulb; olf: olfactory fibers; olt: olfactory tract; ot: optic tract; paf: paraflocculus; pir: piriform lobe; Rfi: rhinal fissure; Sss: suprasylvian sulcus; Vmd: mandibular nerve of the trigeminal nerve; V: trigeminal nerve (trunk); Vmx: maxillary nerve of the trigeminal nerve.

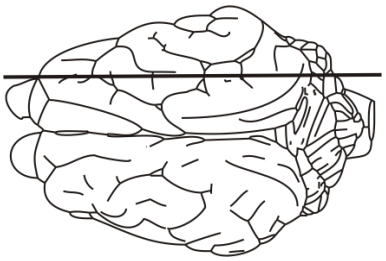

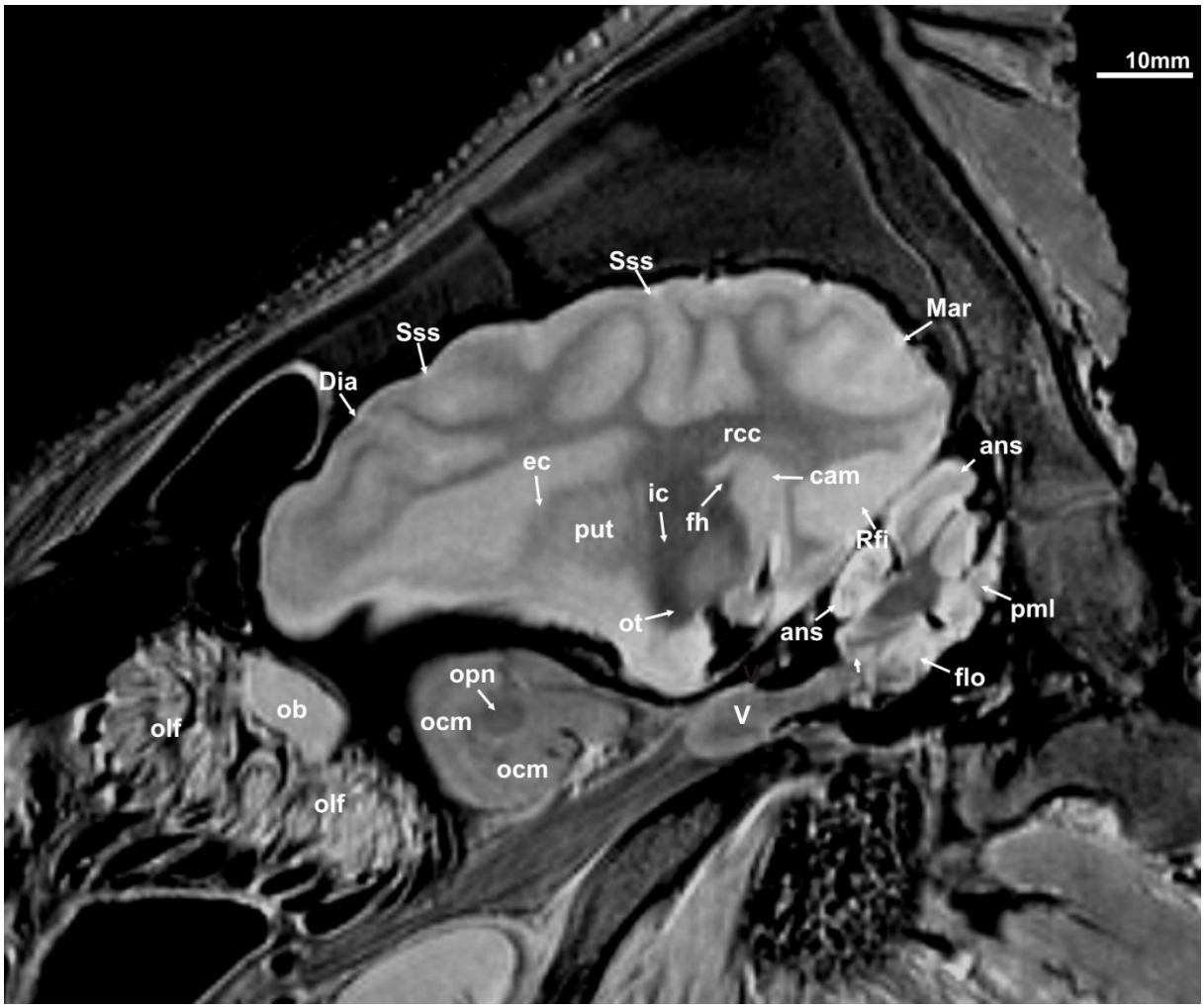

Figure 22

ans: ansiform lobule; cam: cornu ammonis; Dia: sulcus diagonalis; ec: external capsule; fh: fimbria hippocampi; flo: flocculus; ic: internal capsule; Mar: marginal sulcus; ob: olfactory bulb; ocm: external ocular muscles; olf: olfactory fibers; opn: optic nerve; ot: optic tract; pml: paramedian lobule; put: putamen; rcc: radiatio corporis callosi; Rfi: rhinal fissure (medial part); Sss: suprasylvian sulcus; V: trigeminal nerve.

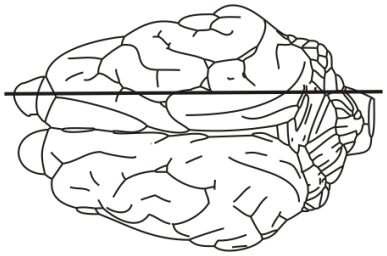

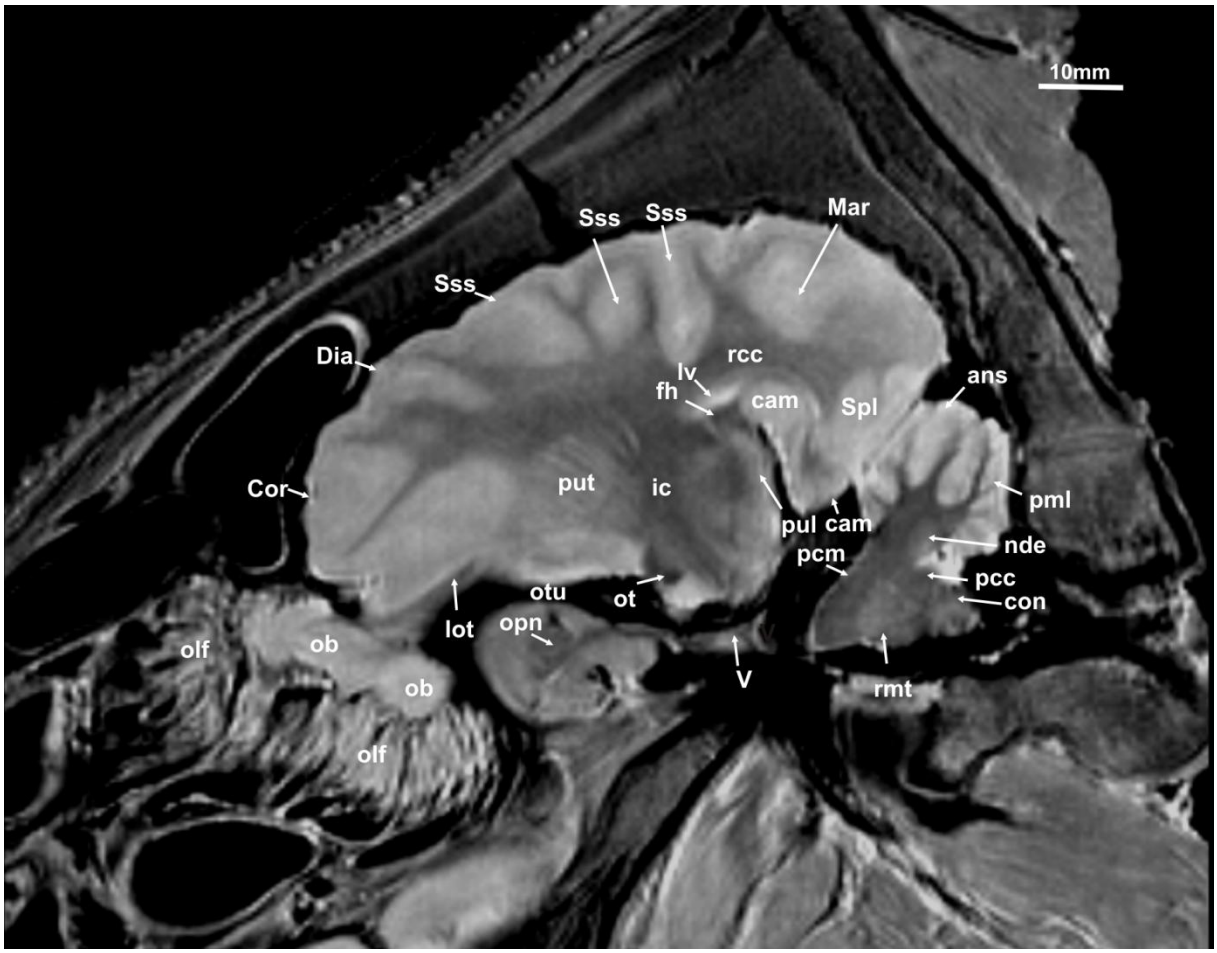

Figure 23

ans: ansform lobule; cam: cornu ammonis; con: cochlear nuclei; Cor: coronal sulcus; Dia: diagonal sulcus; fh: fimbria hippocampi; ic: internal capsule; lot: lateral olfactory tract; lv: lateral ventricle; Mar: marginal sulcus; nde: dentate nucleus; ob: olfactory bulb; olf: olfactory fibers; opn: optic nerve; ot: optic tract; otu: olfactory tubercle; pcc: caudal cerebellar peduncle; pcm: medial cerebellar peduncle; pml: paramedian lobule; pul: pulvinar; put: putamen; rcc: radiatio corporis callosi; rmt: radix motoria of the trigeminal nerve; Sss: suprasylvian sulcus, V: trigeminal nerve.

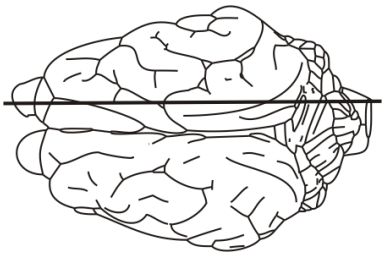

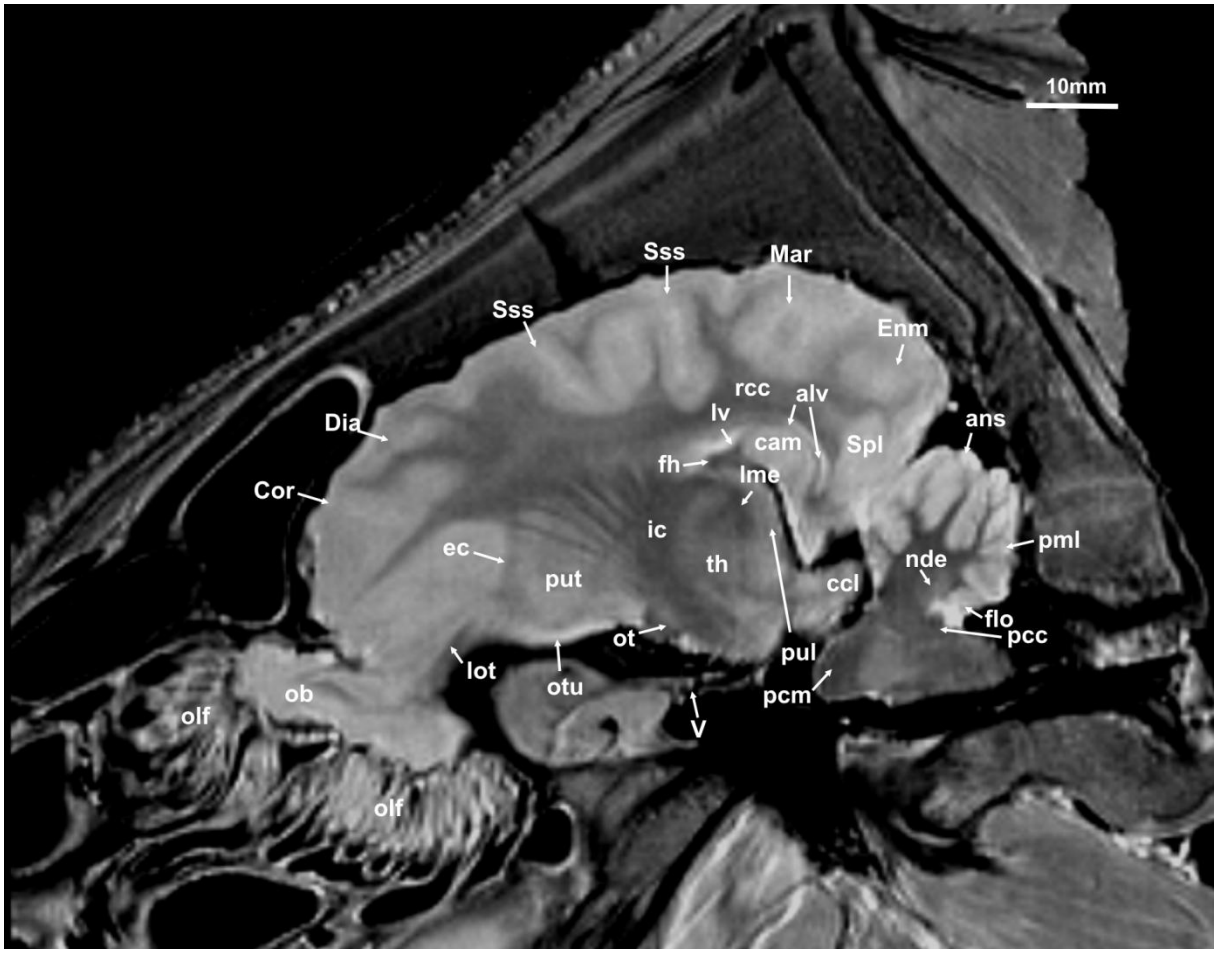

Figure 24

alv: alveus; ans: ansiform lobule; cam: cornu ammonis; ccl: caudal colliculus; Cor: coronal sulcus; Dia: diagonal sulcus; ec: external capsule; Enm: endomarginal sulcus; fh: fimbria hippocampi; flo: flocculus; ic: internal capsule; lme: lamina medullaris externa; lot: lateral olfactory tract; lv: lateral ventricle; Mar: marginal sulcus; nde: dentate nucleus; ob: olfactory bulb; olf: olfactory fibers; ot: optic tract; otu: olfactory tubercle; pcc: caudal cerebellar peduncle; pcm: medial cerebellar peduncle; pml: paramedian lobule; pul: pulvinar; put: putamen; rcc: radiation corporis callosi; Spl: splenial sulcus; Sss: suprasylvian sulcus; th: thalamus; V: trigeminal nerve.

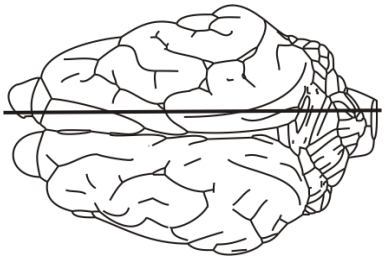

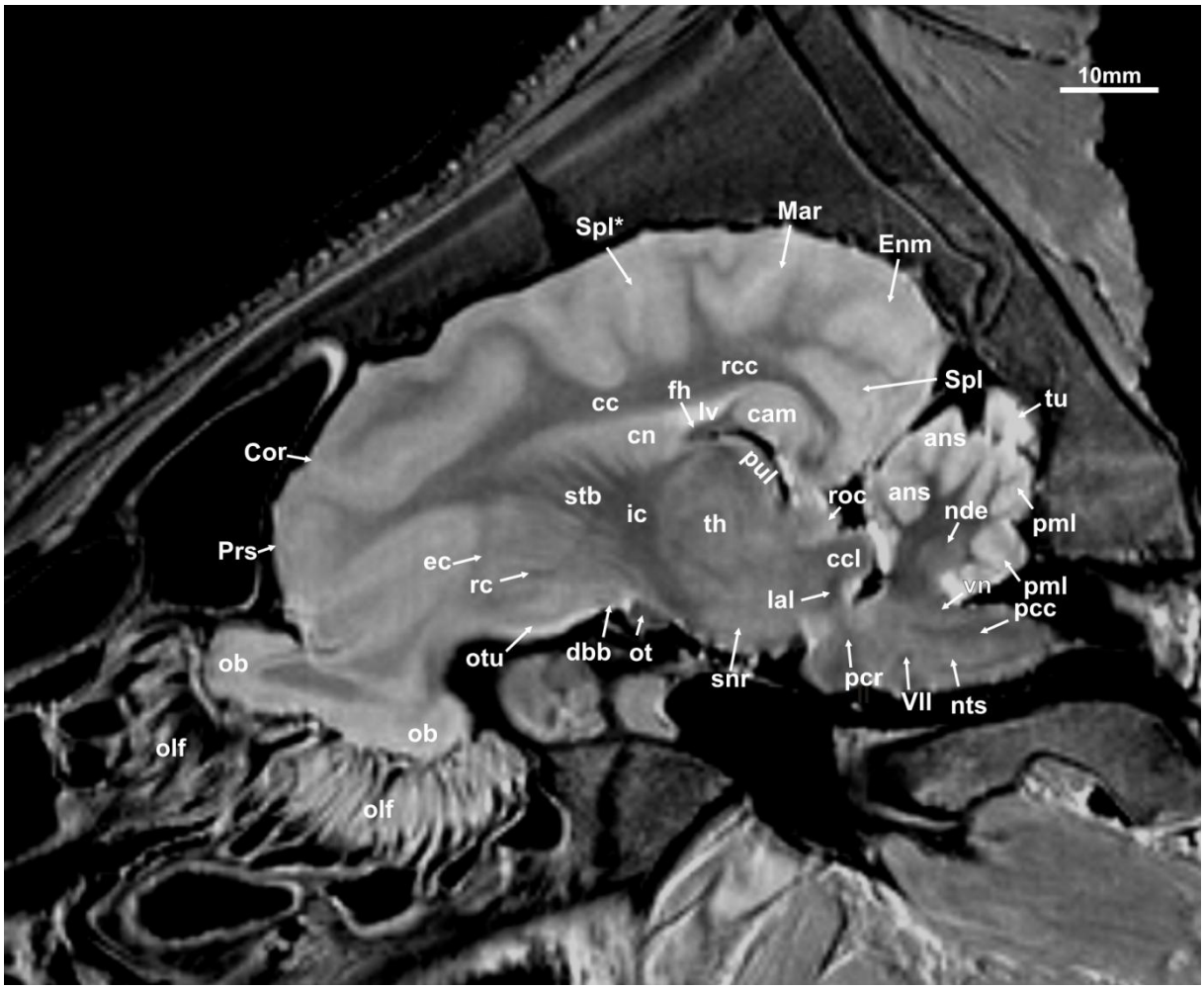

Figure 25

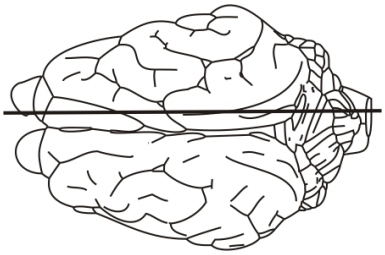

ans: ansiform lobule; cc: corpus callosum; ccl: caudal colliculus; cn: caudate nucleus; Cor: coronal sulcus; dbb: diagonal band of broca; ec: external capsule; Enm: endomarginal sulcus; fh: fimbria hippocampi; ic: internal capsule; lal: lateral lemniscus; lv: lateral ventricle; Mar: marginal sulcus; nde: dentate nucleus; nts: nucleus tractus spinalis nervi trigemini; ob: olfactory bulb; olf: olfactory fibers; ot: optic tract; otu: olfactory tubercle; pcc: caudal cerebellar peduncle; pcr: rostral cerebellar peduncle; pml: paramedian lobe; Prs: praesylvian sulcus; pul: pulvinar; rcc: radiatio corporis callosi; roc: rostral colliculus; snr: substantia nigra; Spl: splenial sulcus; Spl*: connecting sulcus; stb: striate body; th: thalamus; tu: tuber; vn: vestibular nuclei; VII: facial nerve.

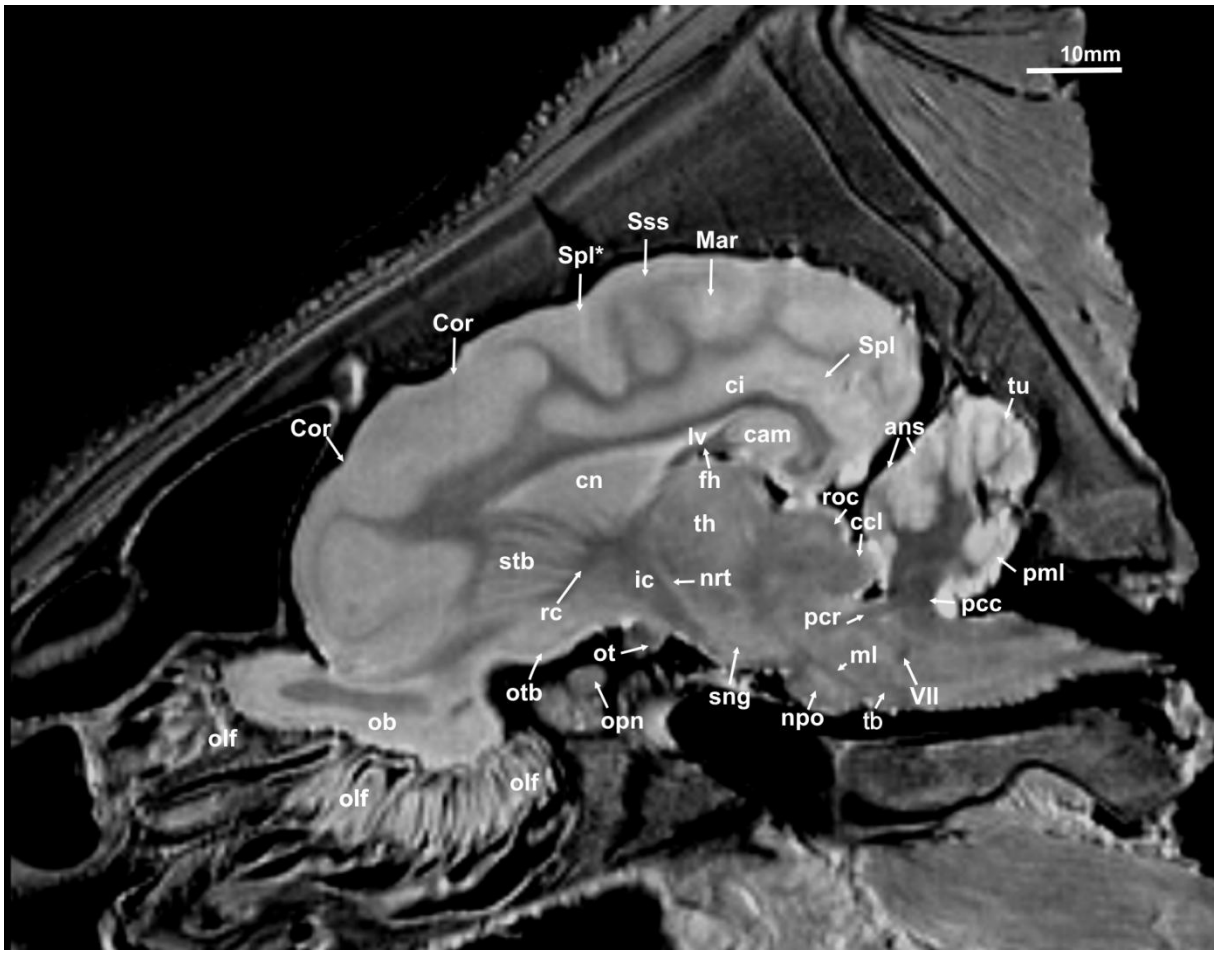

Figure 26

ans: ansiform lobule; cam: cornu ammonis; ccl: caudal colliculus; ci: cingulated gyrus; cn: caudate nucleus; Cor: coronal sulcus; fh: fimbria hippocampi; ic: internal capsule; lv: lateral ventricle; Mar: marginal sulcus; ml: medial lemniscus; npo: nuclei pontis; nrt: nucleus reticularis thalami; ob: olfactory bulb; olf: olfactory fibres; opn: optic nerve; ot: optic tract; otb: olfactory tubercle; pcc: caudal cerebellar peduncle; pcr: rostral cerebellar peduncle; pml: paramedian lobule; rc: rostral commissure; roc: rostral colliculus; sng: substantia nigra; Spl: splenial sulcus; Spl*: connecting sulcus; Sss: supra sylvian sulcus; stb: striate body; tb: trapezoid body; th: thalamus; tu: tuber; VII: facial nerve.

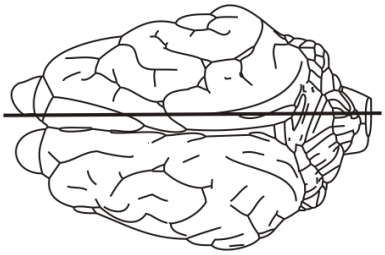

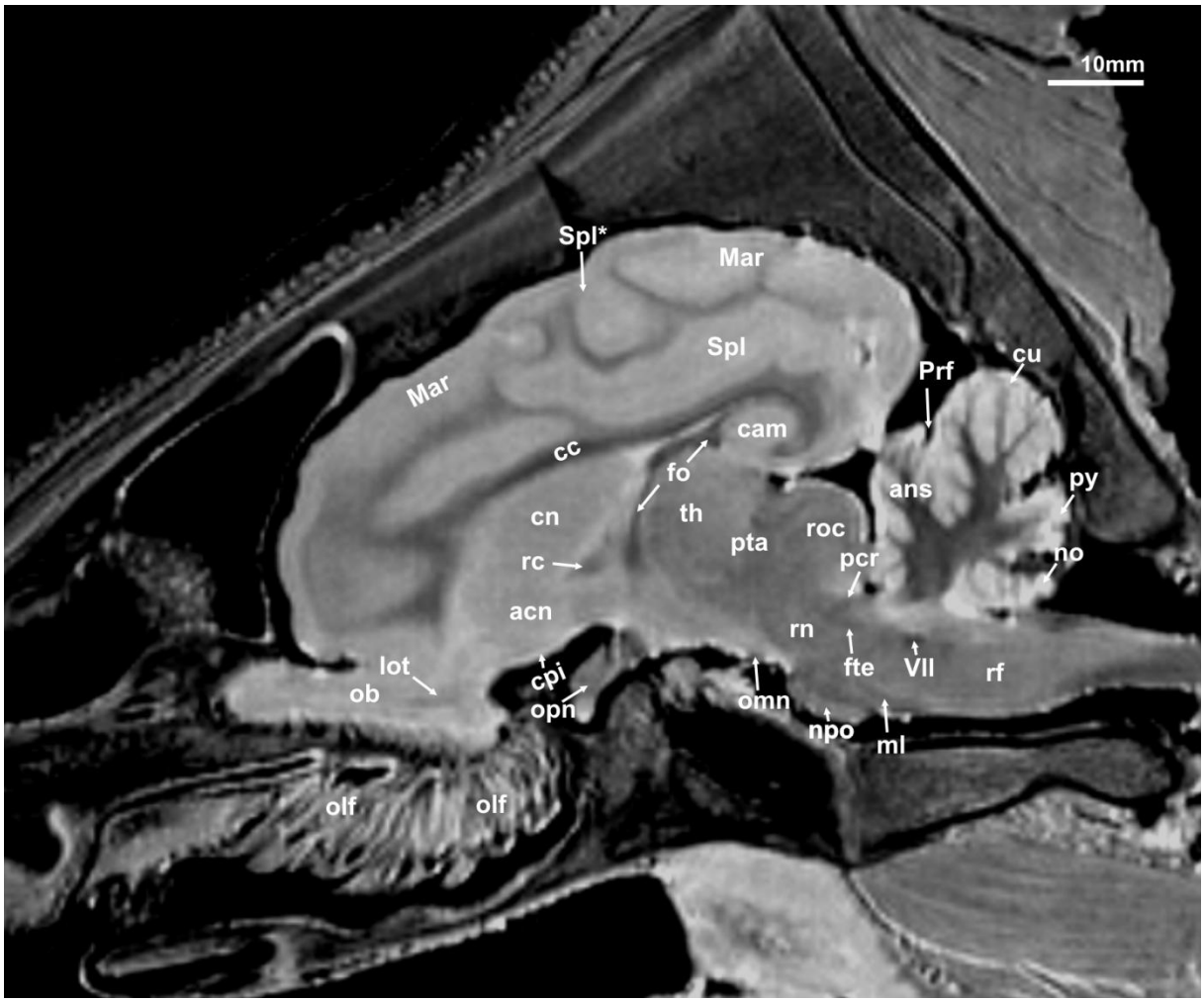

Figure 27

acn: accumbens nucleus; cu: culmen; ans: ansiform lobule; cam: cornu ammonis; cc: corpus callosum; cn: caudate nucleus; cpi: cortex piriformis; fo: fornix; fte: fasciculus tegmenti (forel); lot: lateral olfactory tract; Mar: marginal sulcus; ml: medial lemniscus; no: nodulus; npo: nuclei pontis; ob: olfactory bulb; olf: olfactory fibers; omn: oculomotor nerve; opn: optic nerve; pcr: rostral cerebellar peduncle; Prf: primary fissure; pta: pretectal area; py: pyramis vermis; rc: rostral commissure; rf: reticular formation; rn: red nucleus; roc: rostral colliculus; Spl: splenial sulcus; Spl*: connecting sulcus; th: thalamus; Vll: facial nerve.

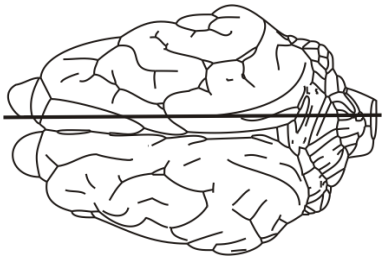

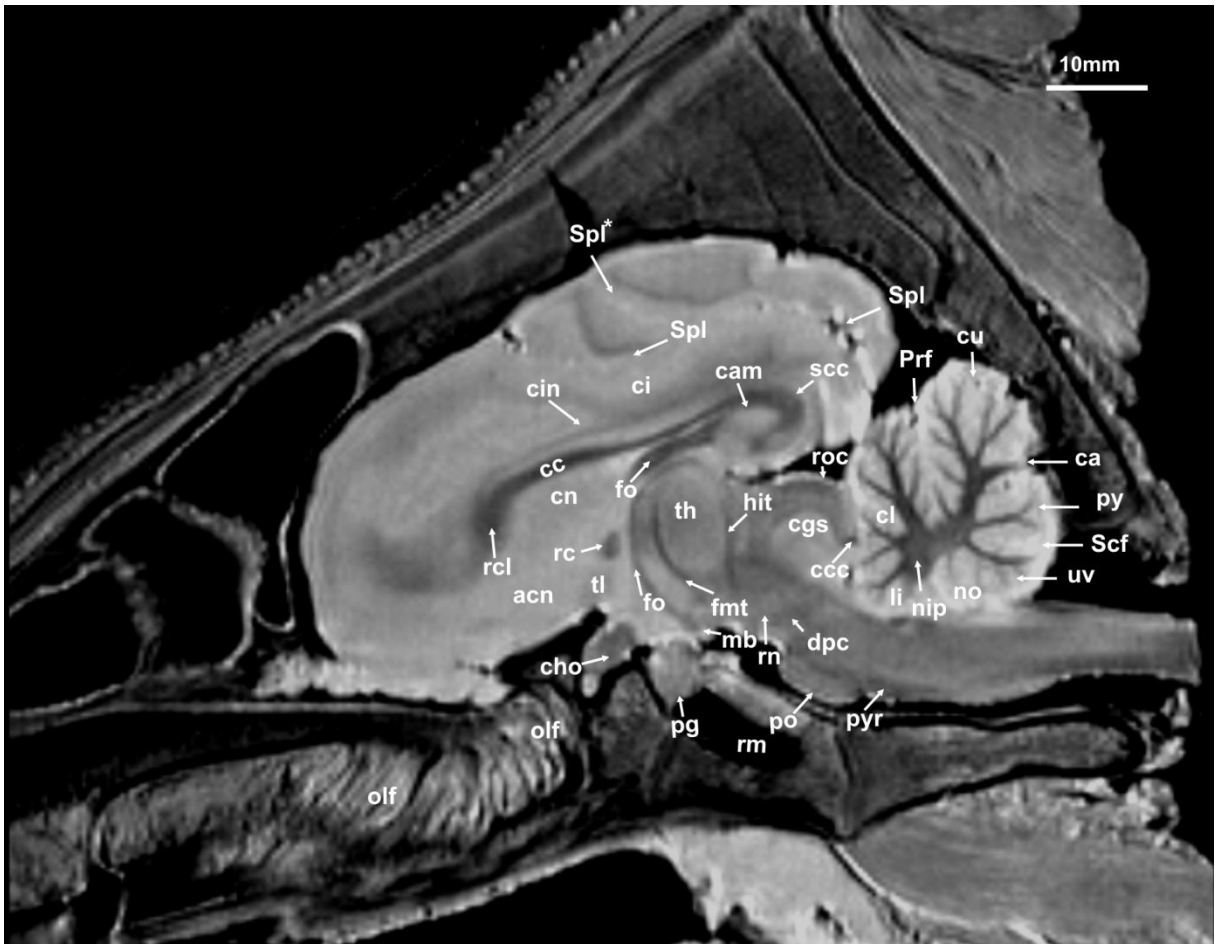

Figure 28

acn: accumbens nucleus, ca: cortical aplasia; cam: cornu ammonis; cc: corpus calosum; ccc: commissure of the caudal colliculi; cgs: central grey substance; cho: optic chiasm; cl: cetral lobule; ci: cingulated gyrus; cn: caudate nucleus; cu: culmen; fmt: fasciculus mammilo-thalamicus; fo: fornix; hit: habenulo-interpeduncular tract; li: lingula; mb: mammillary body; nip: interposed nucleus; no: nodulus; olf: olfactory fibers; pg: pituitary gland; po: pons; Prf: primary fissure; py: pyramis vermis; pyr: pyramidal tracts; rc: rostral commissue: rcl: rostrum of the corpus callosum; roc: rostral colliculus; scc: splenium of the corpus callosum; Scf: secondary fissure; Spl: splenial sulcus; Spl*: connecting sulcus; th: thalamus; tl: terminal lamina; uv: uvula.

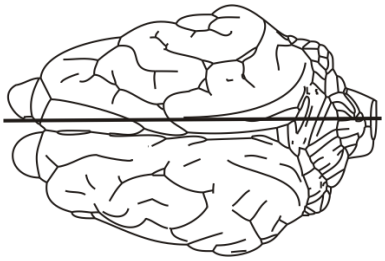

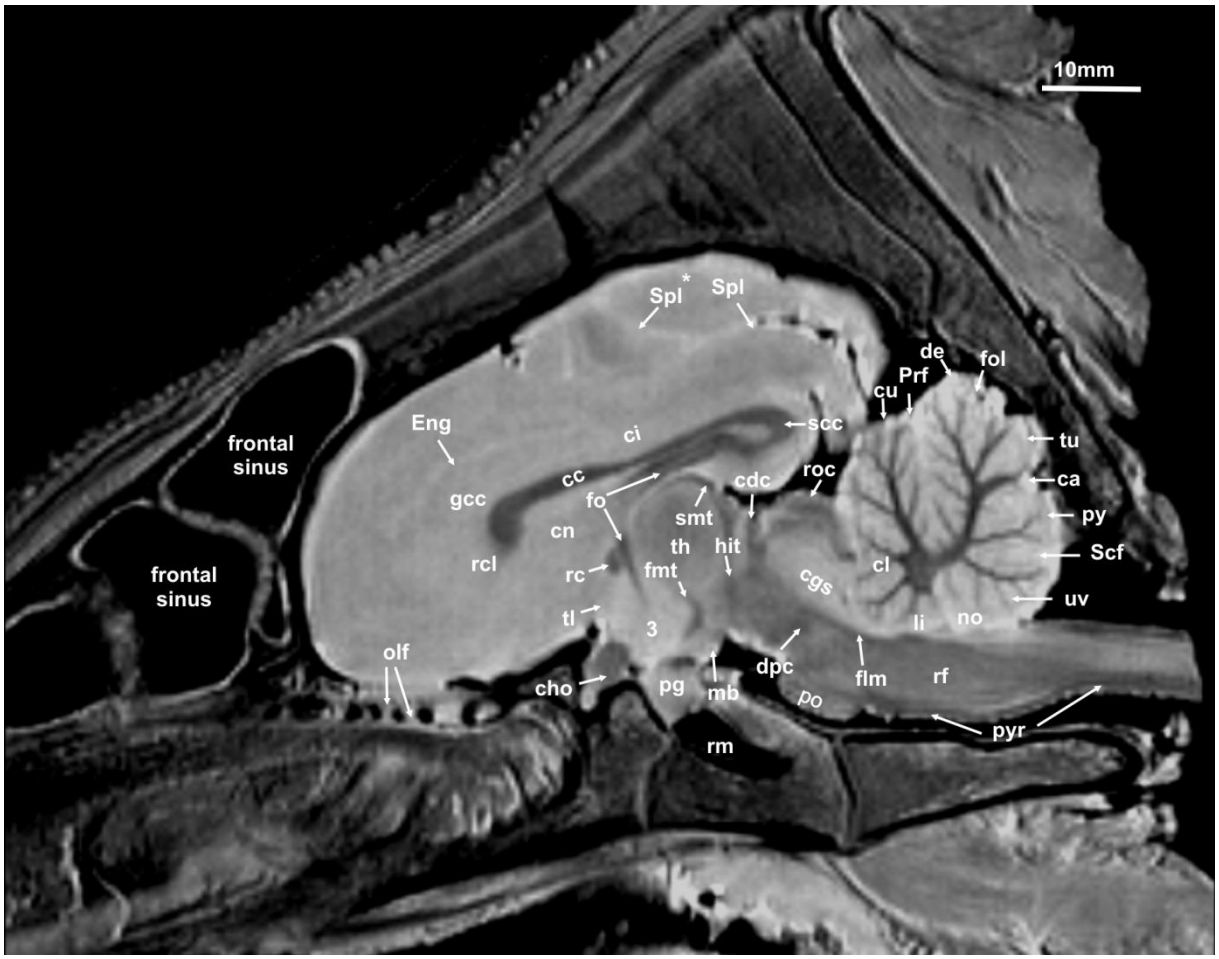

Figure 29

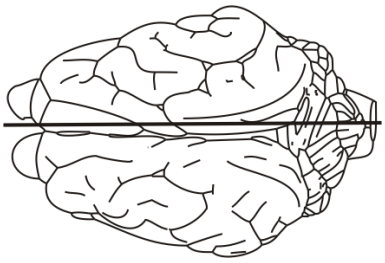

ca: cortical aplasia; cc: corpus calosum; cdc: caudal commissure; cgs: central gray substance; cho: optic chiasm; ci: cingulated gyrus; cl: cetral lobule; cn: caudate nucleus; cu: culmen; de: declive; dpc: decussatio pedunculorum cerebellarium rostralium; Eng: endogenual sulcus; flm: fasciculus longitudinalis medialis; fmt: fasciculus mammilo-thalamicus; fo: fornix; fol: folium; gcc: genu of the corpus callosum; hit: habenulo-interpeduncular tract; li: lingula; no: nodulus; olf: olfactory fibers; pg: pituitary gland; po: pons; Prf: primary fissure; py: pyramis vermis; pyr: pyramidal tracts; rc: rostral commissue: rcl: rostrum of the corpus callosum; rm: rete mirabile; roc: rostral colliculus; scc: splenium of the corpus callosum; Scf: secondary fissure; smt: stria medullaris thalami; Spl: splenial sulcus; Spl*: connecting sulcus; th: thalamus; tl: terminal lamina; tu: tuber; uv: uvula; 3: third ventricle.

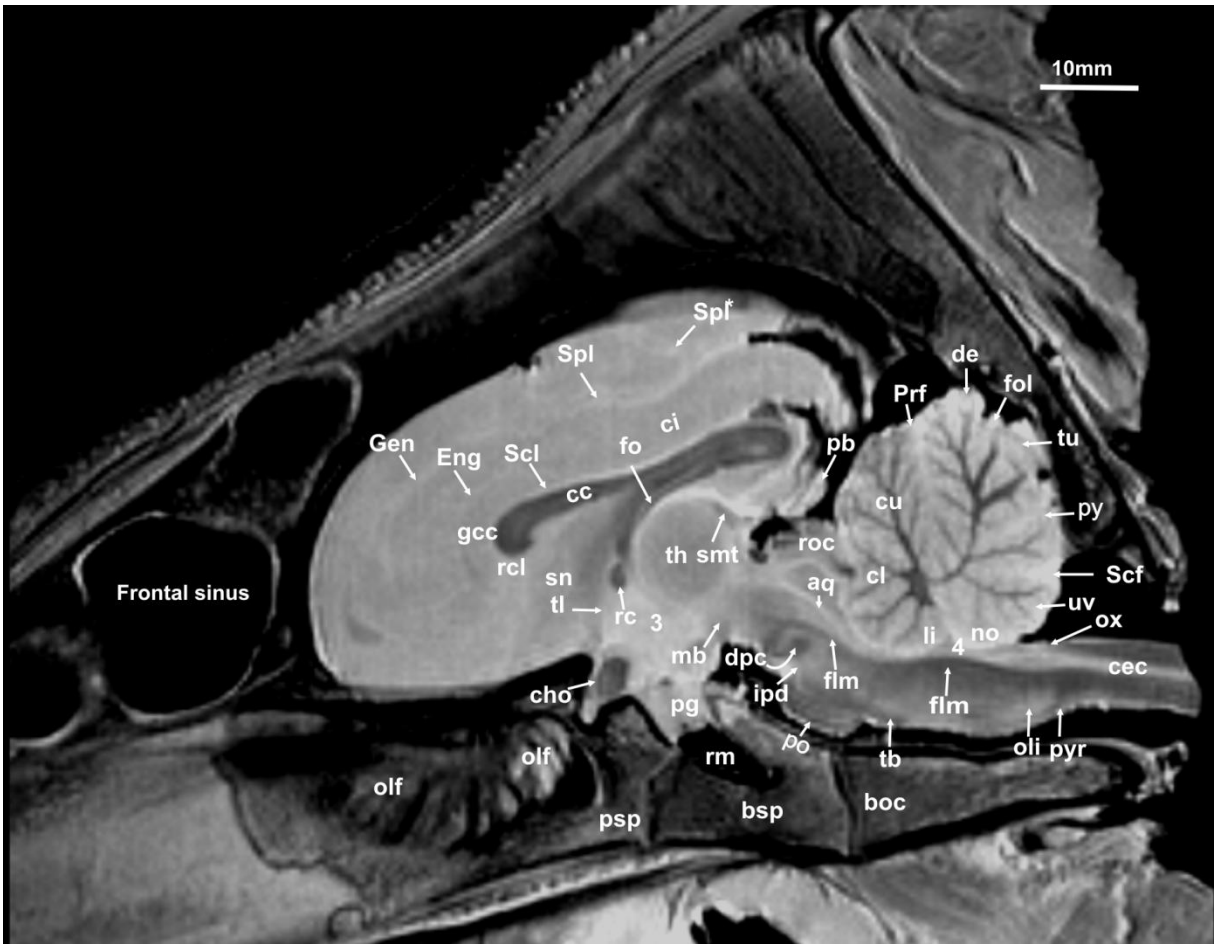

Figure 30

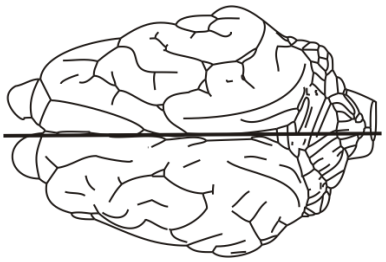

aq: mesencephalic aqueduct; boc: basioccipital bone; bsp: basisphenoidal bone; cc: corpus callosum; cec: central canal; cho: optic chiasm; ci: cingulated gyrus; cl: central lobule; cu: culmen; de: declive; dpc: decussatio pedunculorum cerebellarium rostralium; Eng: endogenual sulcus; flm: medial longitudinal fasciculus; fo: fornix; gcc: genu of the corpus callosum; Gen: genual sulcus; ipd: interpeduncular nucleus; li: lingula; mb: mammillary body; no: nodulus; psp: presphenoidal bone; olf: olfactory fibers; oli: olivary nucleus; ox: obex region ; pb: pineal body; pg: pituitary gland; po: pons; Prf: primary fissure; py: pyramis vermis; pyr: pyramidal tracts; rcl: rostrum of the corpus callosum; rm: rete mirabile; roc: rostral colliculus; Scf: secondary fissure; Scl: sulcus corporis callosi; smt: stria medullaris thalami; sn: septal nuclei; Spl: splenial sulcus; Spl*: connecting sulcus; tb: trapezoid body; th: thalamus; tl: terminal lamina; tu: tuber; uv: uvula; 3: third ventricle; 4: fourth ventricle.

5.4 Transverse scans of the porcine brain

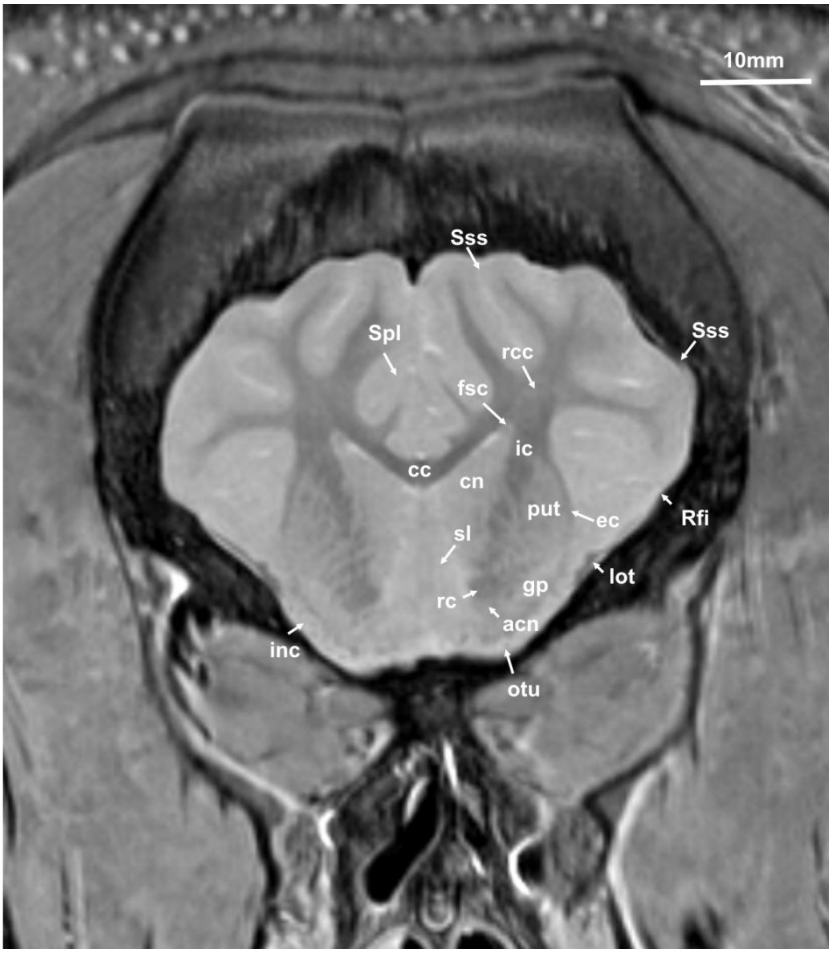

Figure 31
acn: accumbens nucleus; cc: corpus callosum; cn: caudate nucleus; ec: external capsule; fsc: fasciculus subcallosus; gp: globus pallidus; ic: internal capsule; inc: insulae callejae; lot: lateral olfactory tract; otu: olfactory tubercle; put: putamen; rc: rostral commissure; rcc: radiatio corporis callosi; Rfi: rhinal fissure; sl: lateral septal nuclei; Spl: splenial sulcus; Sss: suprasylvian sulcus.

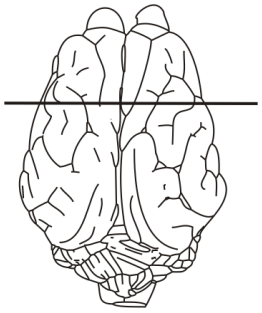

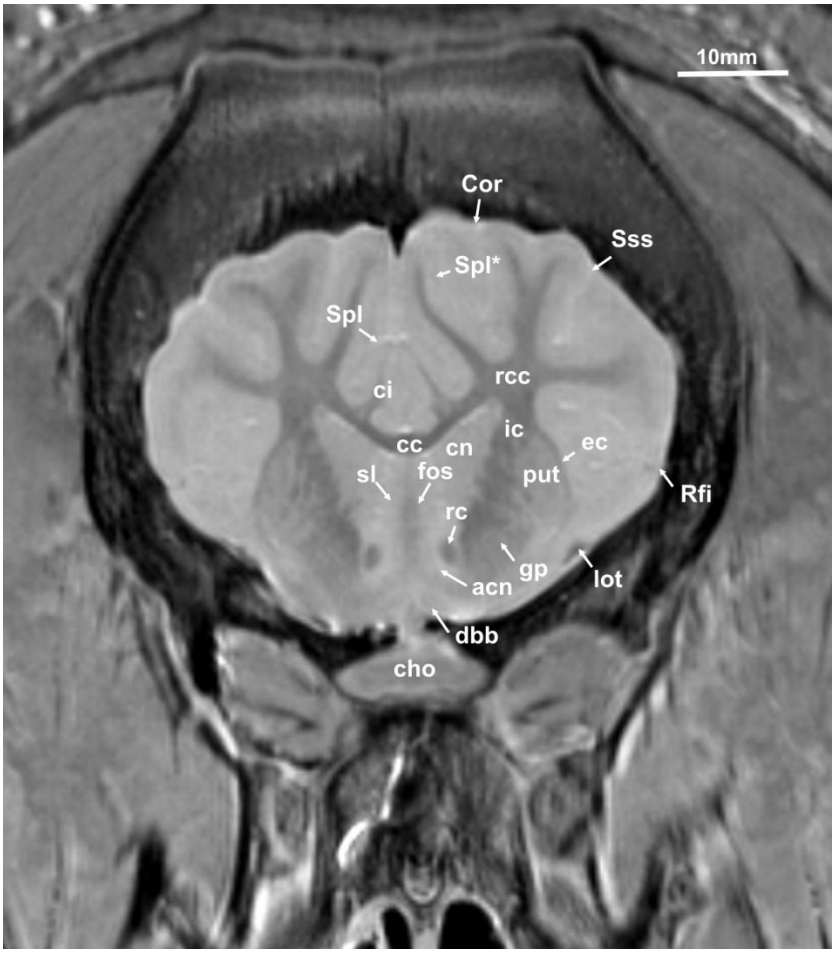

Figure 32

acn: accumbens nucleus; cc: corpus callosum; cho: optic chiasm; ci: cingulated gyrus; cn: caudate nucleus; Cor: coronal sulcus; dbb: diagonal band of broca; ec: external capsule; fos: fibrae olfactorii septales; gp: globus pallidus; ic: internal capsule; lot: lateral olfactory tract; put: putamen; rc: rostral commissure; rcc: radiatio corporis callosi; Rfi: rhinal fissure; sl: nuclei septi laterales; Spl: splenial sulcus; Spl*: connecting sulcus; Sss: suprasylvian sulcus.

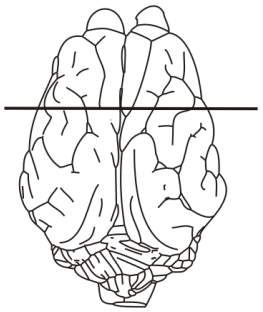

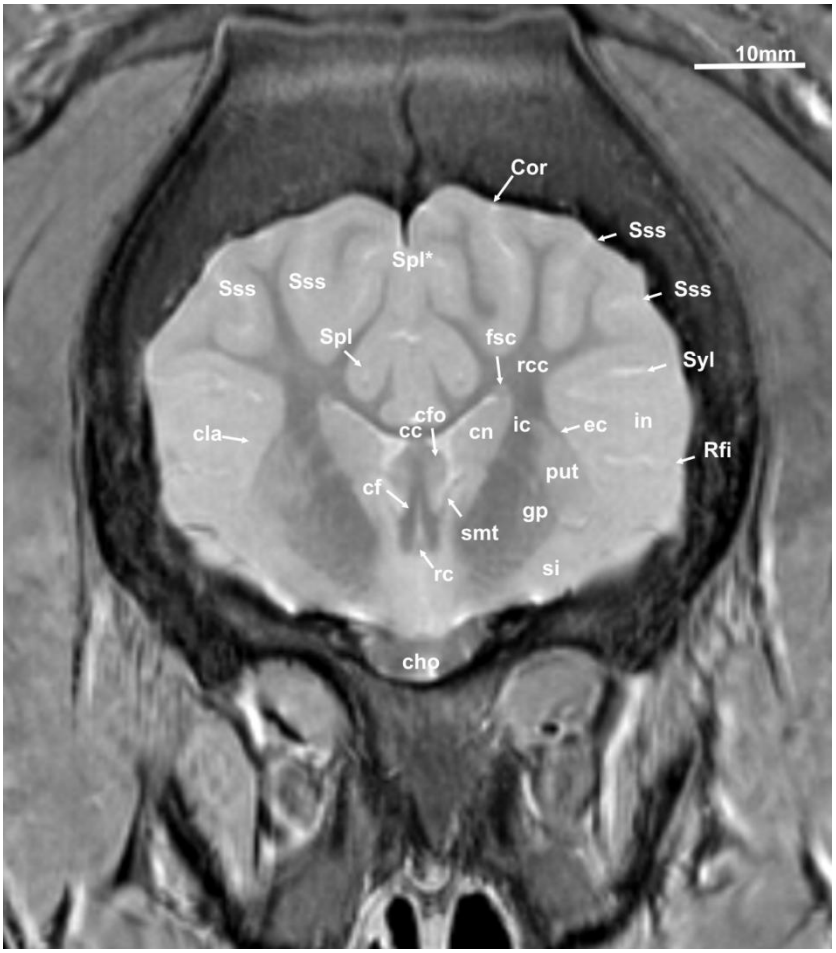

Figure 33

cc: corpus callosum; cfo: corpus of fornix; cf: columna fornicis; cho: optic chiasm; cla: claustrum; cn: caudate nucleus; Cor: coronal sulcus; ec: external capsule; fsc: fasciculus subcallosus; gp: globus pallidus; ic: internal capsule; in: insula; put: putamen; rc: rostral commissure; rcc: radiatio corporis callosi; Rfi: rhinal fissure; si: substantia innominata; smt: stria medullaris thalami; Spl: splenial sulcus; Spl*: connecting sulcus; Sss: suprasylvian sulcus; Syl: sylvian fissure.

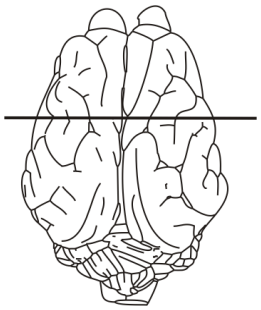

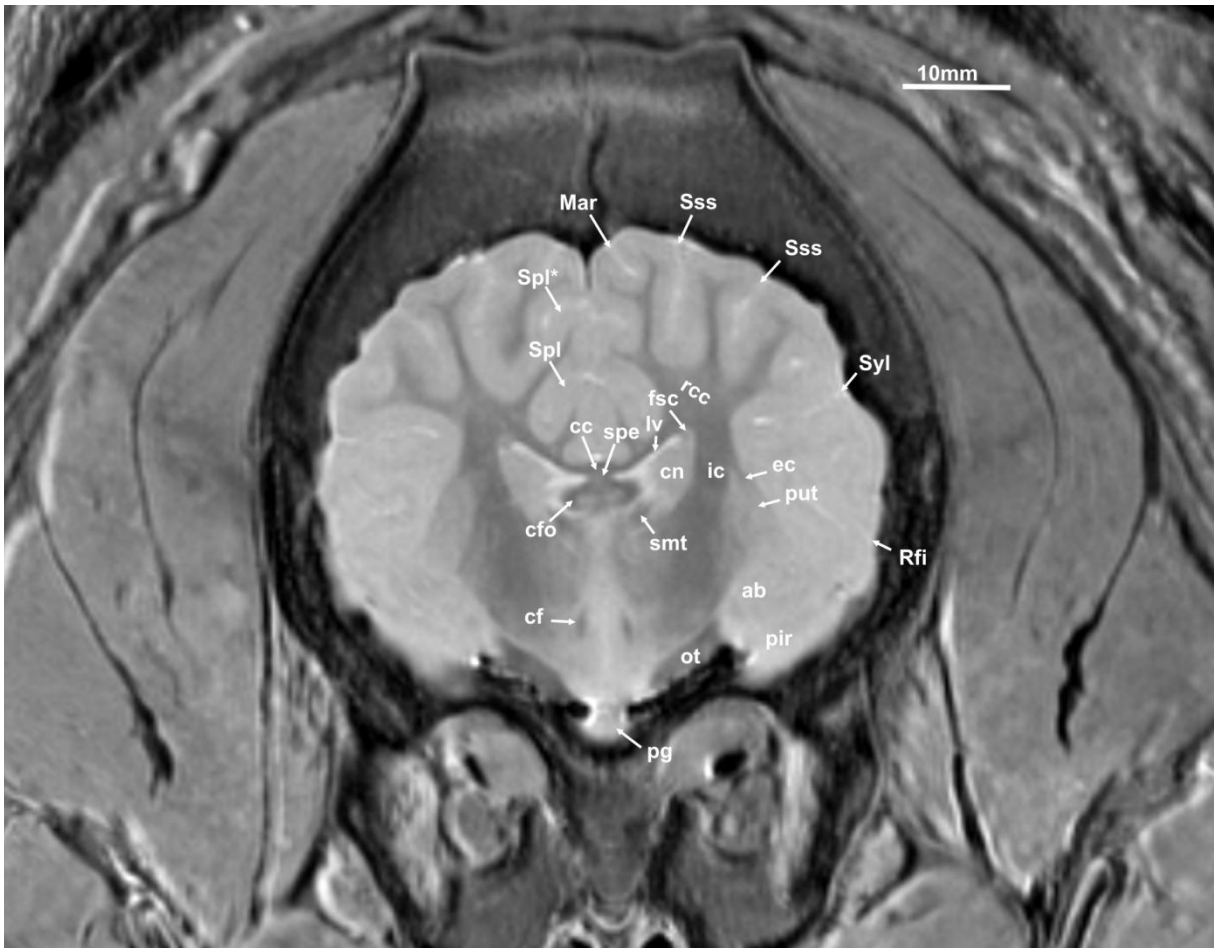

Figure 34

ab: amygdaloid body; cc: corpus callosum; cf: columna fornicis; cfo: corpus of fornix; cn: caudate nucleus; ec: external capsule; fsc: fasciculus subcallosus; ic: internal capsule; lv: lateral ventricle; Mar: marginal sulcus; ot: optic tract; pg: pituitary gland; pir: piriform lobe; put: putamen; rcc: radiatio corporis callosi; Rfi: rhinal fissure; smt: stria medullaris thalami; spe: septum pellucidum; Spl: splenial sulcus; Spl*: connecting sulcus; Sss: suprasylvian sulcus; Syl: sylvian fissure.

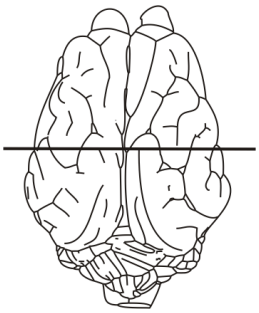

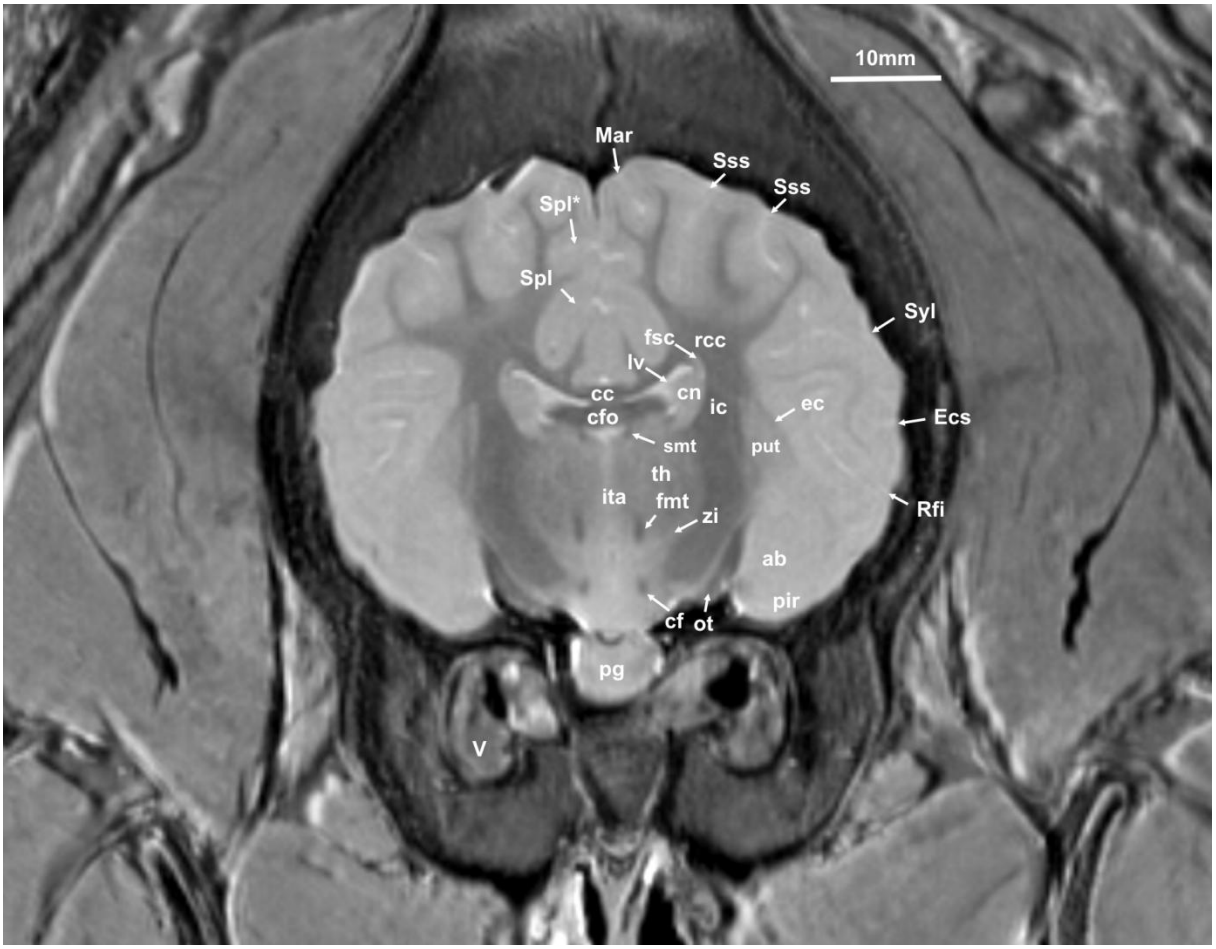

Figure 35

ab: amygdaloid body; cc: corpus callosum; cf: columna fornicis; cfo: corpus of fornix; cn: caudate nucleus; crc: cerebral crus; ec: external capsule; Ecs: ectosylvian sulcus; fmt: fasciculus mammilo-thalamicus; fsc: fasciculus subcallosus; ic: internal capsule; ita: interthalamic adhesion; lv: lateral ventricle; Mar: marginal sulcus; ot: optic tract; pg: pituitary gland; pir: piriform lobe; put: putamen; rcc: radiatio corporis callosi; Rfi: rhinal fissure; smt: stria medullaris thalami; Spl: splenial sulcus; Spl*: connecting sulcus; Sss: suprasylvian sulcus; Syl: sylvian fissure; th: thalamus; zi: zona incerta; V: trigeminal nerve.

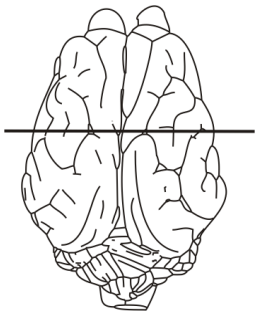

Figure 36

ab: amygdaloid body; cc: corpus callosum; cf: columna fornicis; cfo: corpus of fornix; cmf: commissure of the fornix; cn: caudate nucleus; crc: cerebral crus; ec: external capsule; Ecs: ectosylvian sulcus; fmt: fasciculus mammilo-thalamicus; fsc: fasciculus subcallosus; ic: internal capsule; idg: induseum griseum; ita: interthalamic adhesion; lv: lateral ventricle; lme: lamina medullaris externa; Mar: marginal sulcus; ot: optic tract; pg: pituitary gland; pir: piriform lobe; put: putamen; rcc: radiatio corporis callosi; Rfi: rhinal fissure; smt: stria medullaris thalami; Spl: splenial sulcus; Spl*: connecting sulcus; Sss: suprasylvian sulcus; Syl: sylvian fissure; th: thalamus; st: stria terminalis; V: trigeminal nerve.

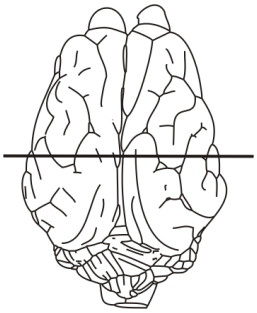

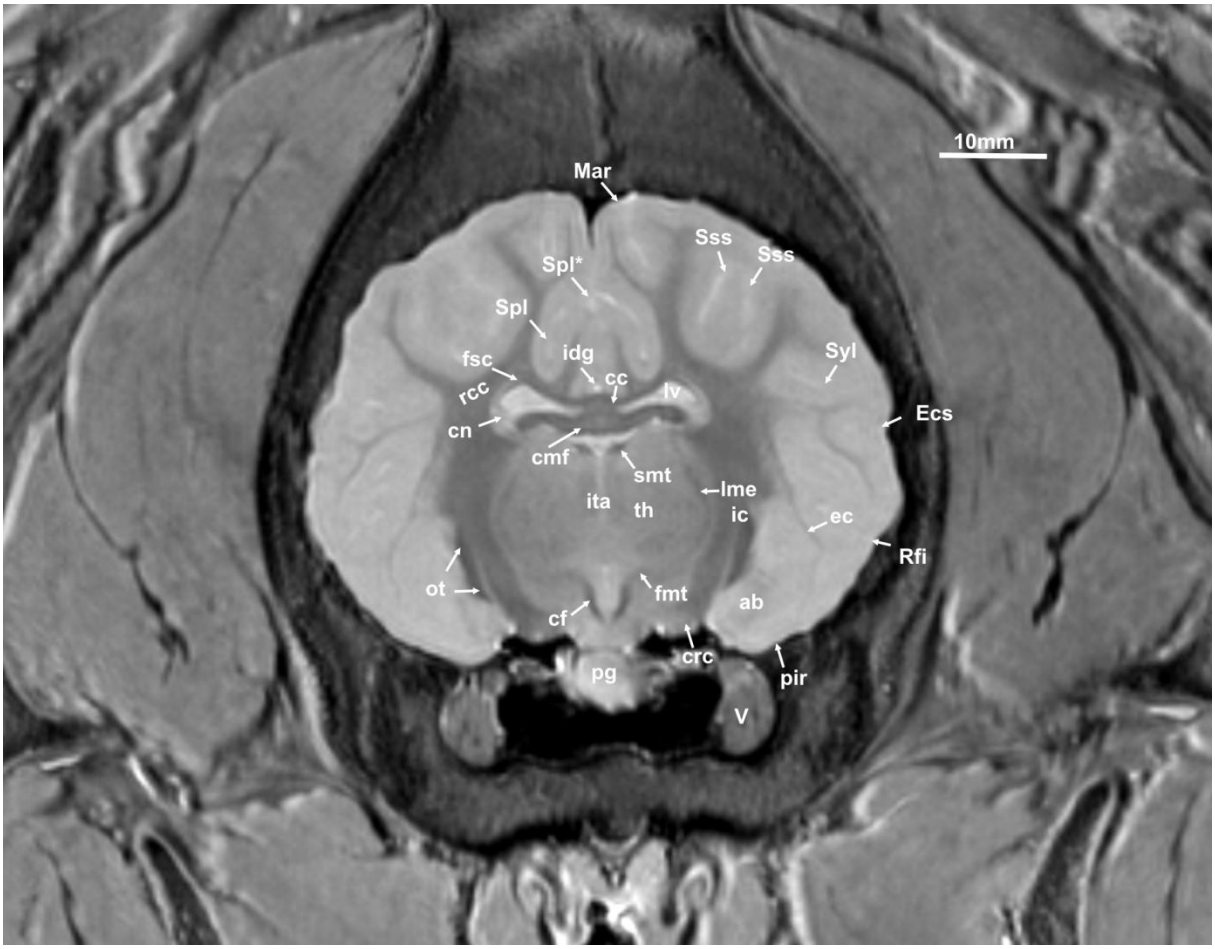

Figure 37

ab: amygdaloid body; cc: corpus callosum; cf: columna fornicis; cmf: commissure of the fornix; cn: caudate nucleus; crc: cerebral crus; ec: external capsule; Ecs: ectosylvian sulcus; fmt: fasciculus mammilo-thalamicus; fsc: fasciculus subcallosus; ic: internal capsule; idg: induseum griseum; ita: interthalamic adhesion; lv: lateral ventricle; lme: lamina medullaris externa; Mar: marginal sulcus; ot: optic tract; pg: pituitary gland; pir: piriform lobe; rcc: radiatio corporis callosi; Rfi: rhinal fissure; smt: stria medullaris thalami; Spl: splenial sulcus; Spl*: connecting sulcus; Sss: suprasylvian sulcus; Syl: sylvian fissure; th: thalamus; V: trigeminal nerve.

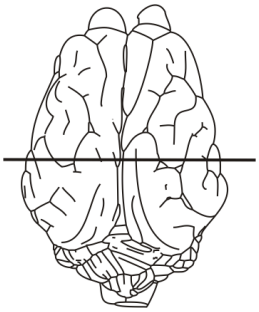

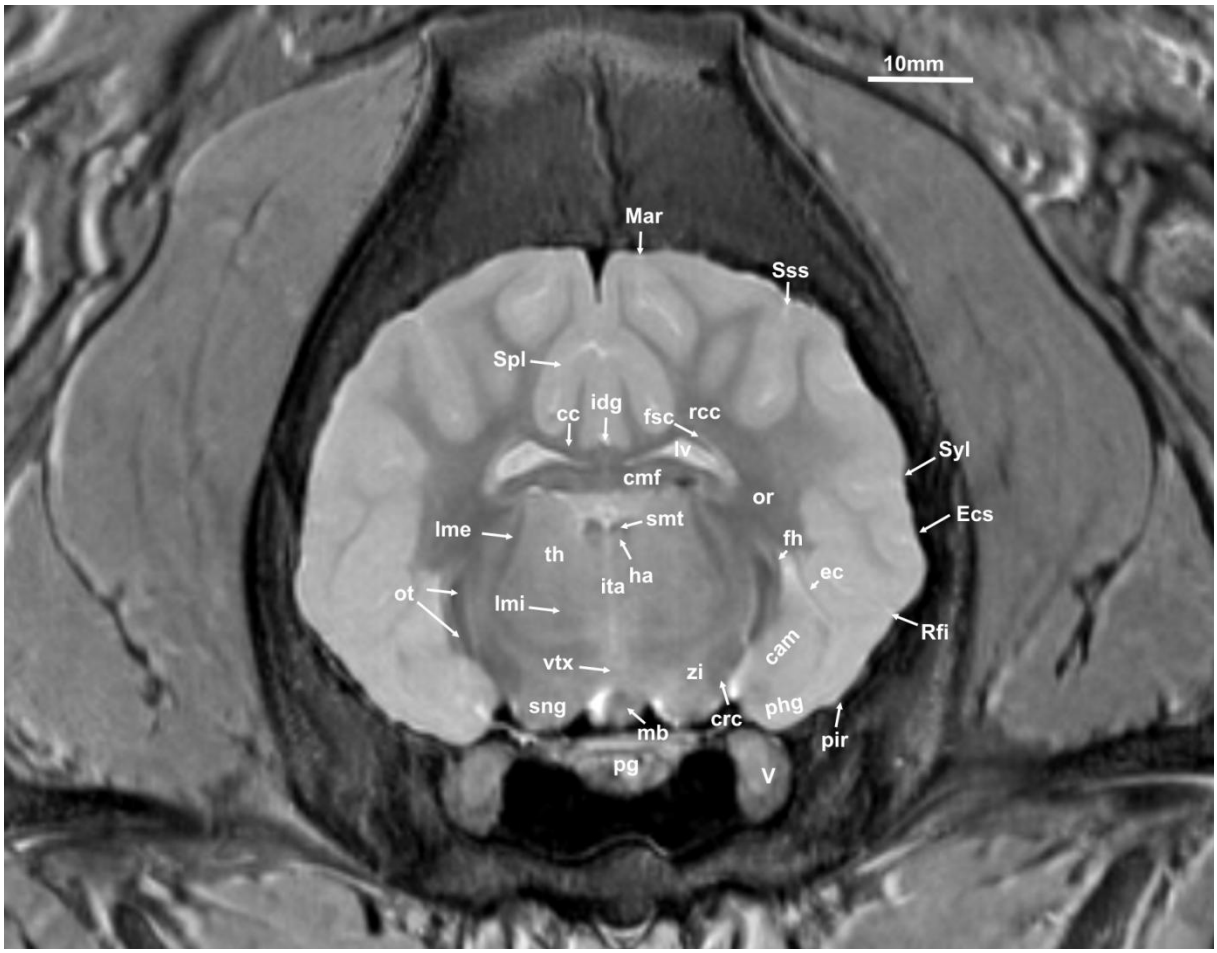

Figure 38

cam: cornu ammonis; cc: corpus callosum; cmf: commissura fornicis; crc: cerebral crus; ec: external capsule; Ecs: ectosylvian sulcus; fh: fimbria hippocampi; fsc: fasciculus subcallosus; idg: induseum griseum; ita: interthalamic adhesion; lv: lateral ventricle; lme: lamina medullaris externa; lmi: lamina medullaris interna; mb: mamillary body; Mar: marginal sulcus; ot: optic tract; pg: pituitary gland; pir: piriform lobe; or: optic radiation; rcc: radiatio corporis callosi; Rfi: rhinal fissure; smt: stria medullaris thalami; sng: substantia nigra; Spl: splenial sulcus; Sss: suprasylvian sulcus; Syl: sylvian fissure; th: thalamus; vtx: decussatio tegmenti ventralis; V: trigeminal nerve; zi: zona incerta.

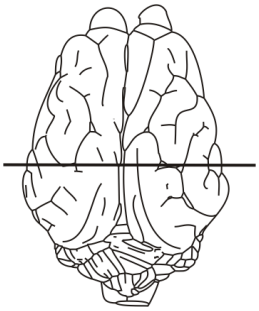

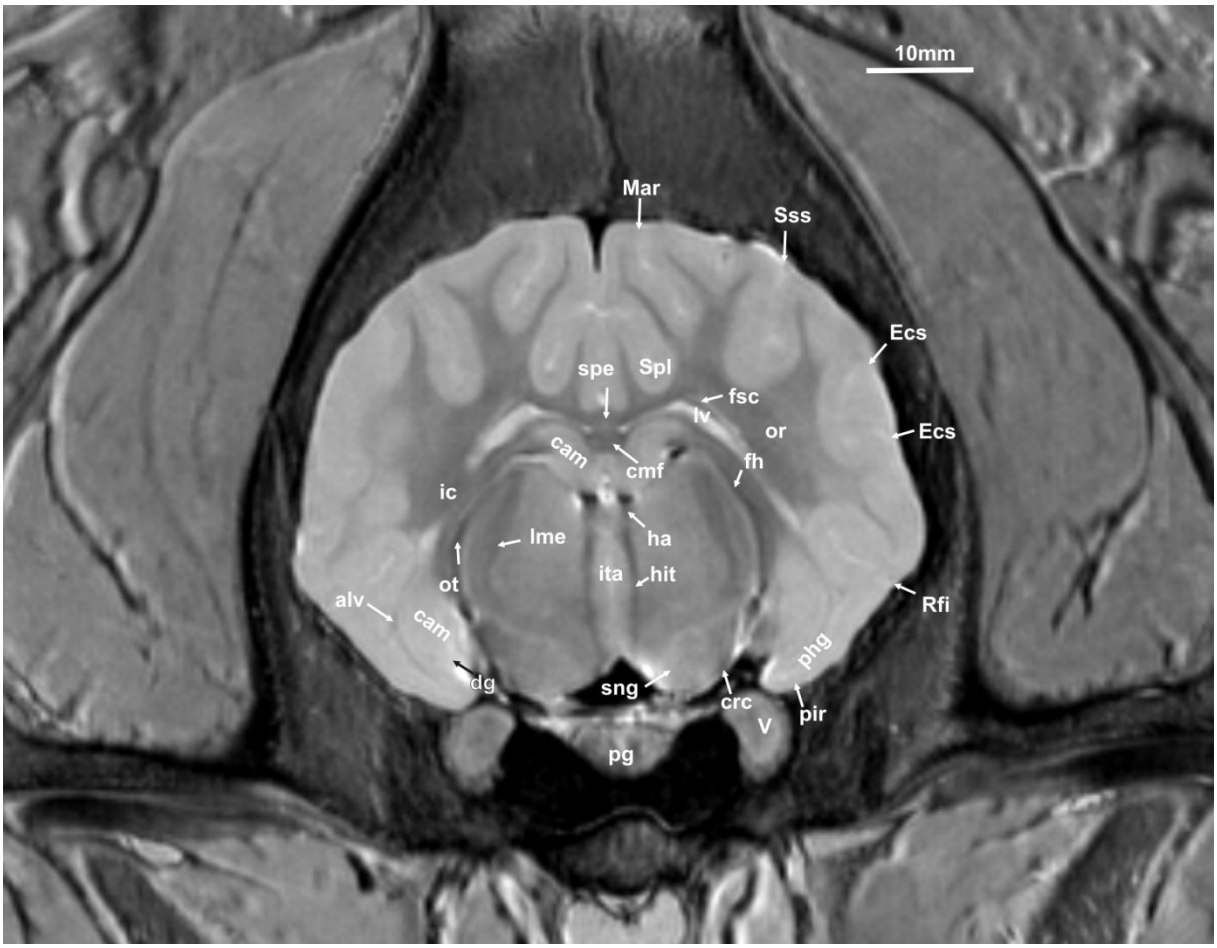

Figure 39

alv: alveus; cam: cornu ammonis; cmf: commissure of the fornix; crc: cerebral crus; dg: dentate gyrus; Ecs: ectosylvian sulcus; fh: fimbria hippocampi; fsc: fasciculus subcallosus; ha: habenulae; hit: habenulo-interpeduncular tract; ic: internal capsule; ita: interthalamic adhesion; lv: lateral ventricle; lme: lamina medullaris externa; Mar: marginal sulcus; or: optic radiation; ot: optic tract; pg: pituitary gland; phg: parahippocampal gyrus; pir: piriform lobe; Rfi: rhinal fissure; sng: substantia nigra; spe: septum pellucidum; Spl: splenial sulcus; Sss: suprasylvian sulcus; check: V: trigeminal nerve.

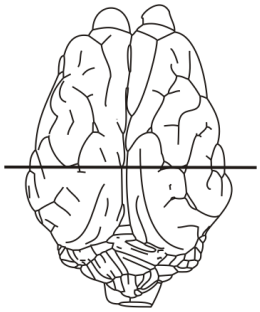

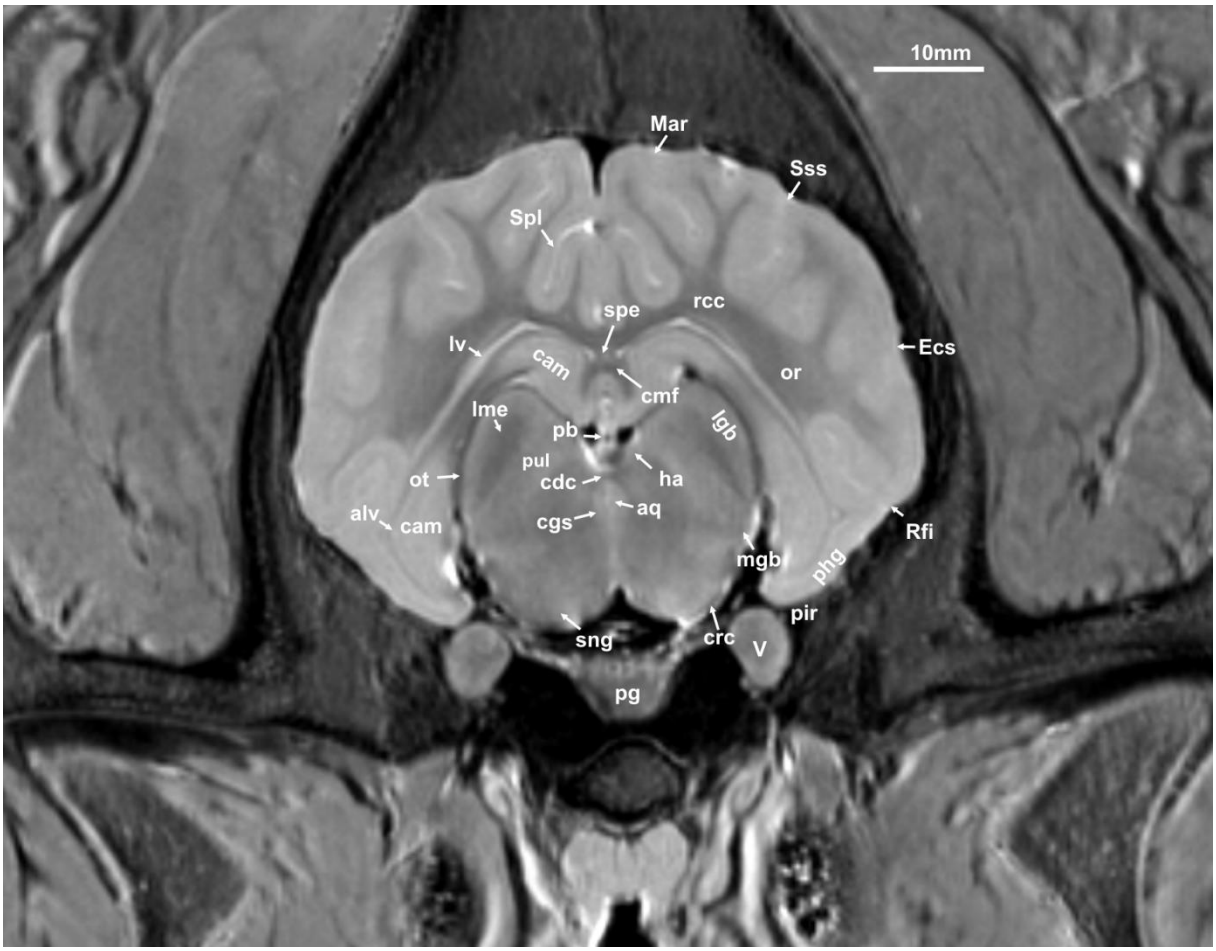

Figure 40

aq: mesencephalic aqueduct; alv: alveus; cam: cornu ammonis; cdc: caudal commissure; cgs: central grey substance; cmf: commissura fornicis; crc: cerebral crus; Ecs: ectosylvian sulcus; ha: habenulae; lgb: lateral geniculate body; lme: lamina medullaris externa; lv: lateral ventricle; Mar: marginal sulcus; mgb: medial geniculate body; or: radiatio optica; ot: optic tract; pg: pituitary gland; phg: parahippocampal gyrus; pir: piriform lobe; pul: pulvinar; rcc: radiatio corporis callosi; Rfi: rhinal fissure; sng: substantia nigra; spe: septum pellucidum; Spl: splenial sulcus; Sss: suprasylvian sulcus; V: trigeminal nerve.

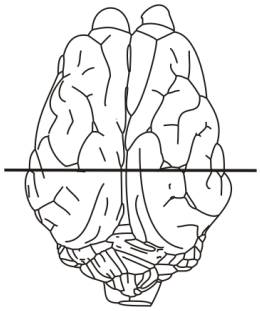

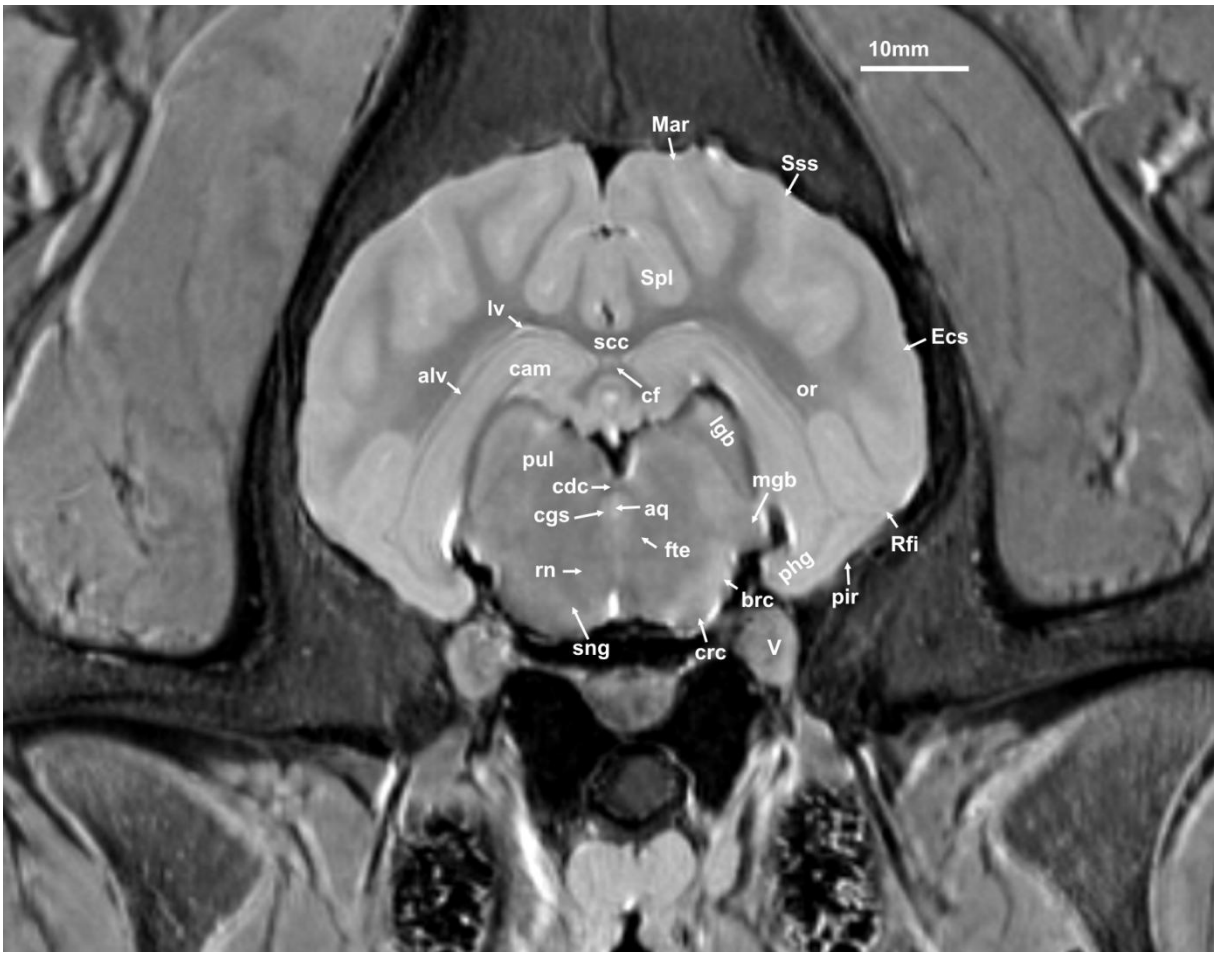

Figure 41

alv: alveus; aq: mesencephalic aqueduct; brc: brachium of the rostral colliculus; cam: cornu ammonis; cdc: caudal commissure; cgs: central grey substance; cf: columna fornicis; crc: cerebral crus; Ecs: ectosylvian sulcus; fte: fasciculus tegmenti; lgb: lateral geniculate body; lv: lateral ventricle; Mar: marginal sulcus; mgb: medial geniculate body; phg: parahippocampal gyrus; pir: piriform lobe; pul: pulvinar; or: optic radiation; rn: red nucleus; Rfi: rhinal fissure; red nucleus; sng: substantia nigra; scc: splenium corporis callosi; Spl: splenial sulcus; Sss: suprasylvian sulcus; V: trigeminal nerve.

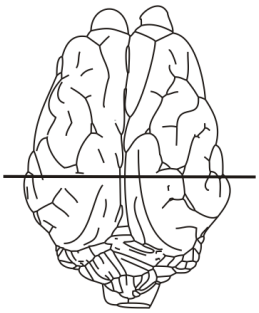

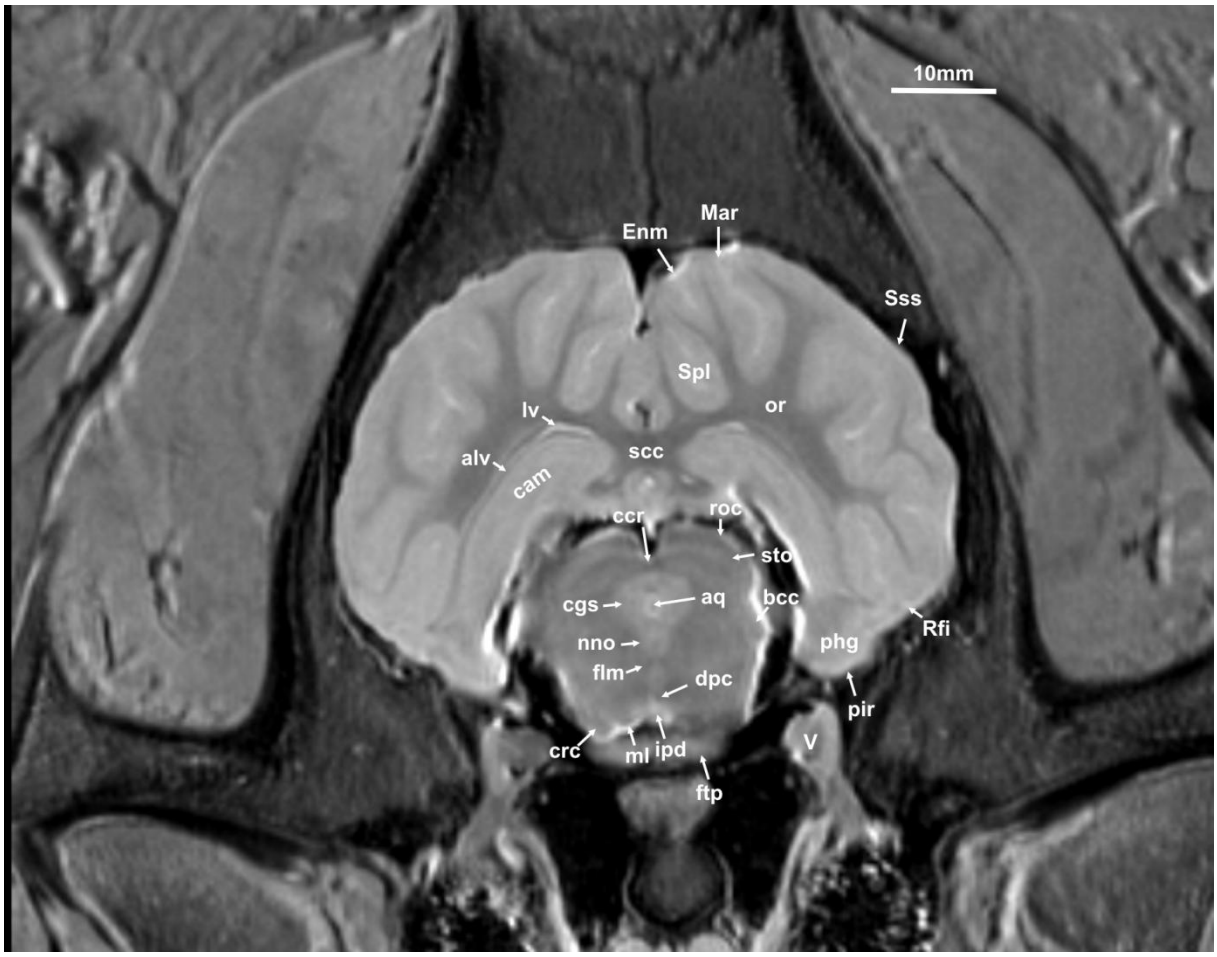

Figure 42

caudal colliculus; cam: cornu ammonis; ccr: commissure of the rostral colliculi; cgs: central grey substance; crc: cerebral crus; dpc: decussation of the rostral cerebellar peduncle; Enm: endomarginal sulcus; flm: fasciculus longitudinalis medialis; ftp: transverse fibers of the pons; ipd: interpeduncular nucleus; lv: lateral ventricle; Mar: marginal sulcus; ml: medial lemniscus; nno: nucleus nervi occulomotorius; or: optic radiation; phg: parahippocampal gyrus pir: piriform lobe; Rfi: rhinal fissure; roc: rostral colliculus; scc: splenium corporis callosi; Spl: splenial sulcus; Sss: suprasylvian sulcus; sto: striatum opticum of the rostral colliculus; V: trigeminal nerve.

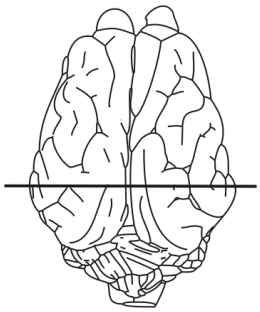

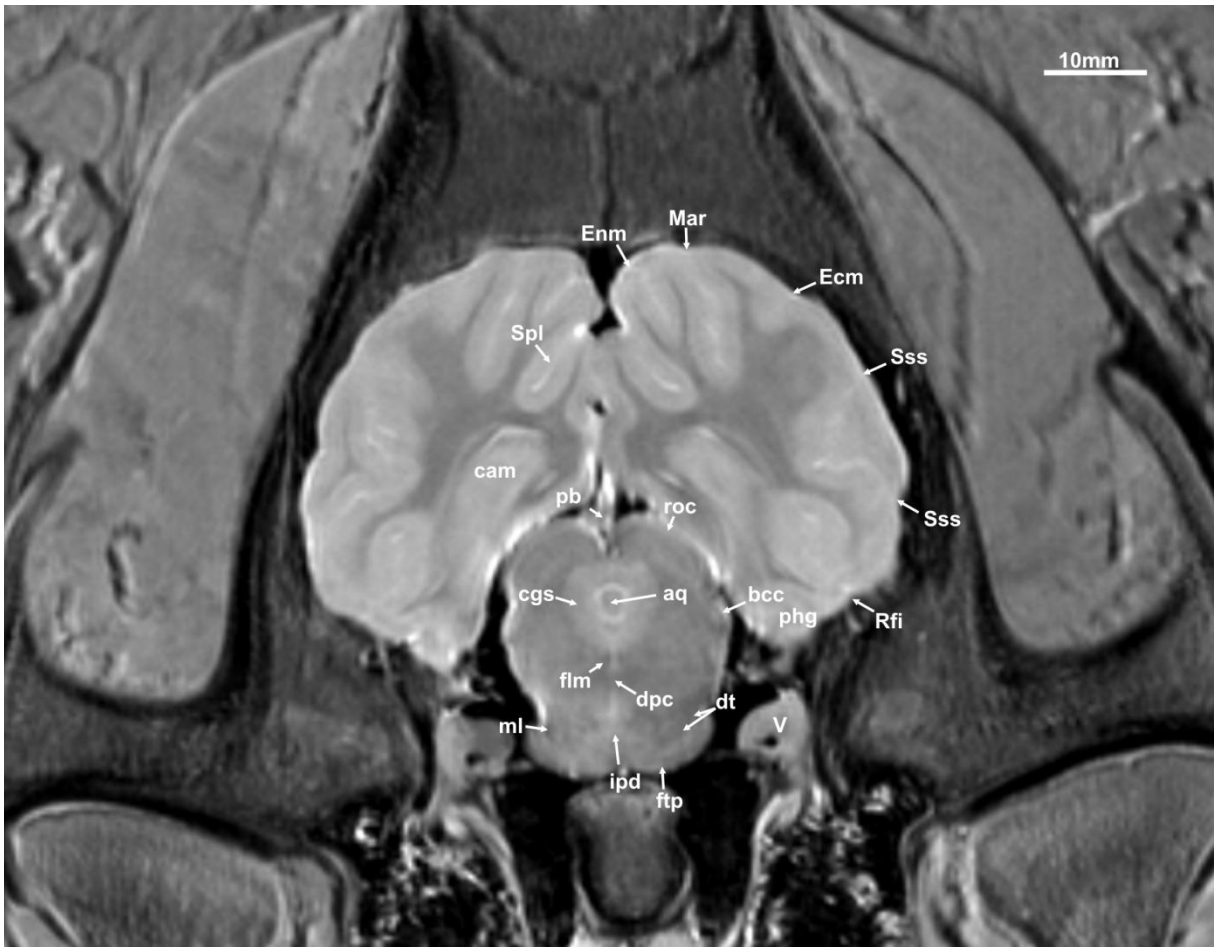

Figure 43

aq: mesencephalic aqueduct; bcc: brachium of the caudal colliculus; cam: cornu ammonis; cgs: central grey substance; dpc: decussation of the rostral cerebellar peduncle; dt: descending tracts (corticospinal and corticobulbar); Enm: endomarginal sulcus; Ecm: ectomarginal sulcus; flm: medial longitudinal fasciculus; ftp: transverse fibers of the pons; ipd: interpeduncular nucleus; Mar: marginal sulcus; ml: medial lemniscus; pb: pineal body; phg: parahippocampal gyrus; roc: rostral colliculus; Rfi: rhinal fissure; roc: rostral colliculus; Spl: splenial sulcus; Sss: suprasylvian sulcus, V: trigeminal nerve.

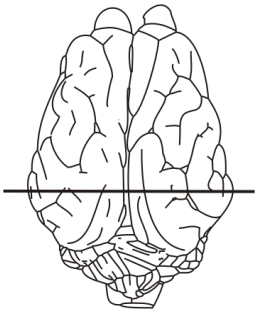

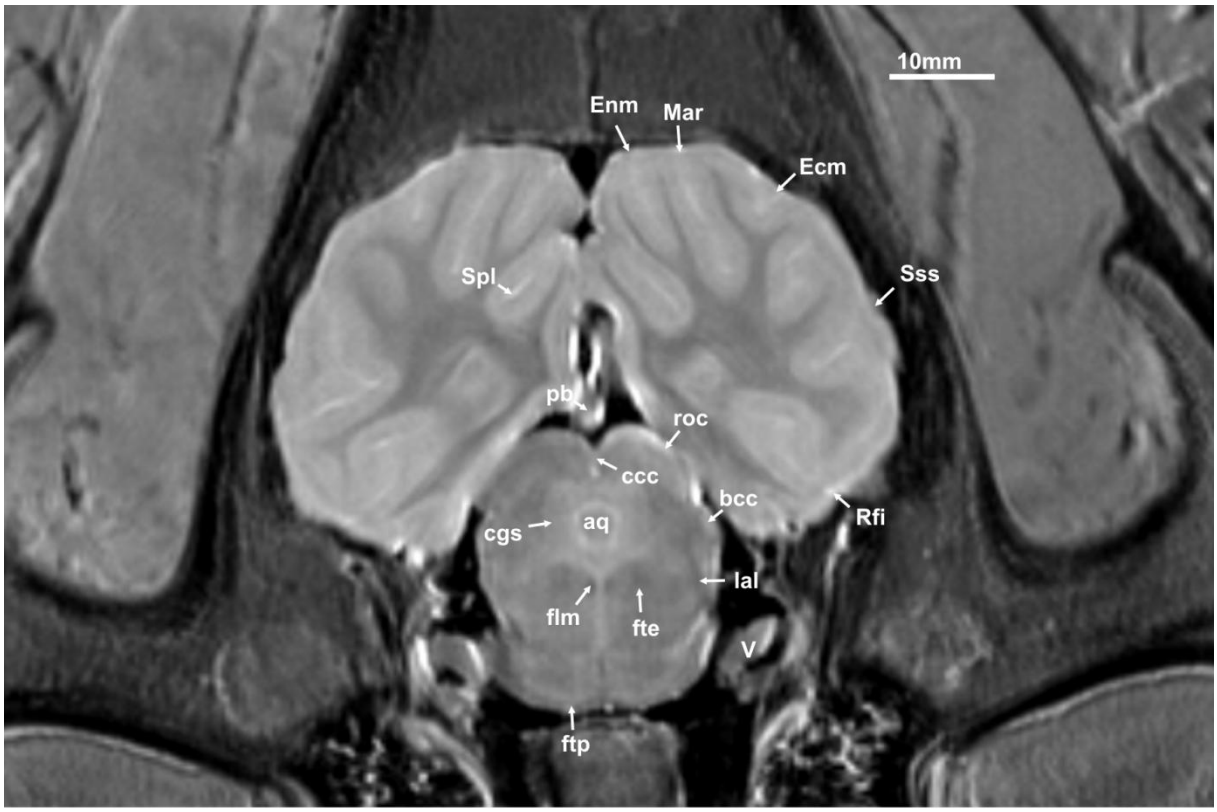

Figure 44

aq: mesencephalic aqueduct; bcc: brachium of the caudal colliculus; ccc: commissure of the caudal colliculi; cgs: central grey substance; Enm: endomarginal sulcus; Ecm: ectomarginal sulcus; flm: medial longitudinal fasciculus; fte: fasciculus tegmenti; ftp: fibrae transversae pontis; lal: lateral lemniscus; Mar: marginal sulcus; pb: pineal body; Rfi: rhinal fissure; roc: rostral colliculus; Spl: splenial sulcus; Sss: suprasylvian sulcus, V: trigeminal nerve.

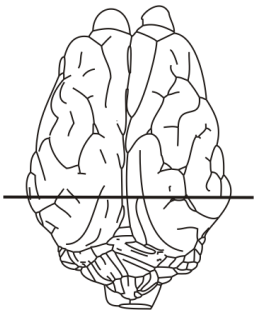

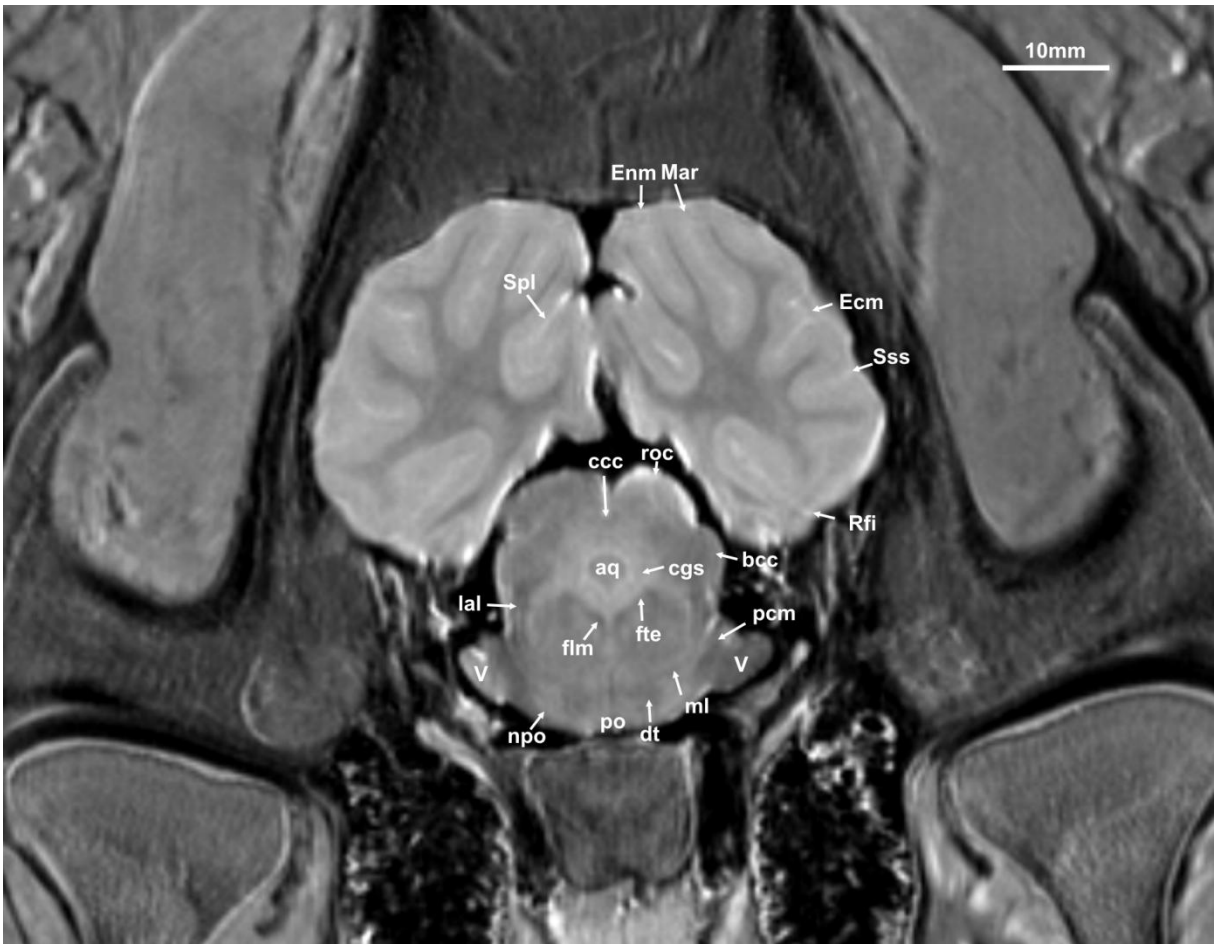

Figure 45

aq: mesencephalic aqueduct; bcc: brachium of the caudal colliculus; ccc: commissure of the caudal colliculus; cgs: central grey substance; dt: descending tracts; Enm: endomarginal sulcus; Ecm: ectomarginal sulcus; flm: fasciculus longitudinalis medialis; fte: fasciculus tegmenti; lal: lateral lemniscus; Mar: marginal sulcus; ml: medial lemniscus; npo: nuclei pontis; pcm: medial cerebellar peduncle; po: pons; Rfi: rhinal fissure; roc: rostral colliculus; Spl: splenial sulcus; Sss: suprasylvian sulcus, V: trigeminal nerve.

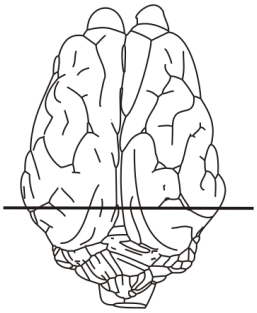

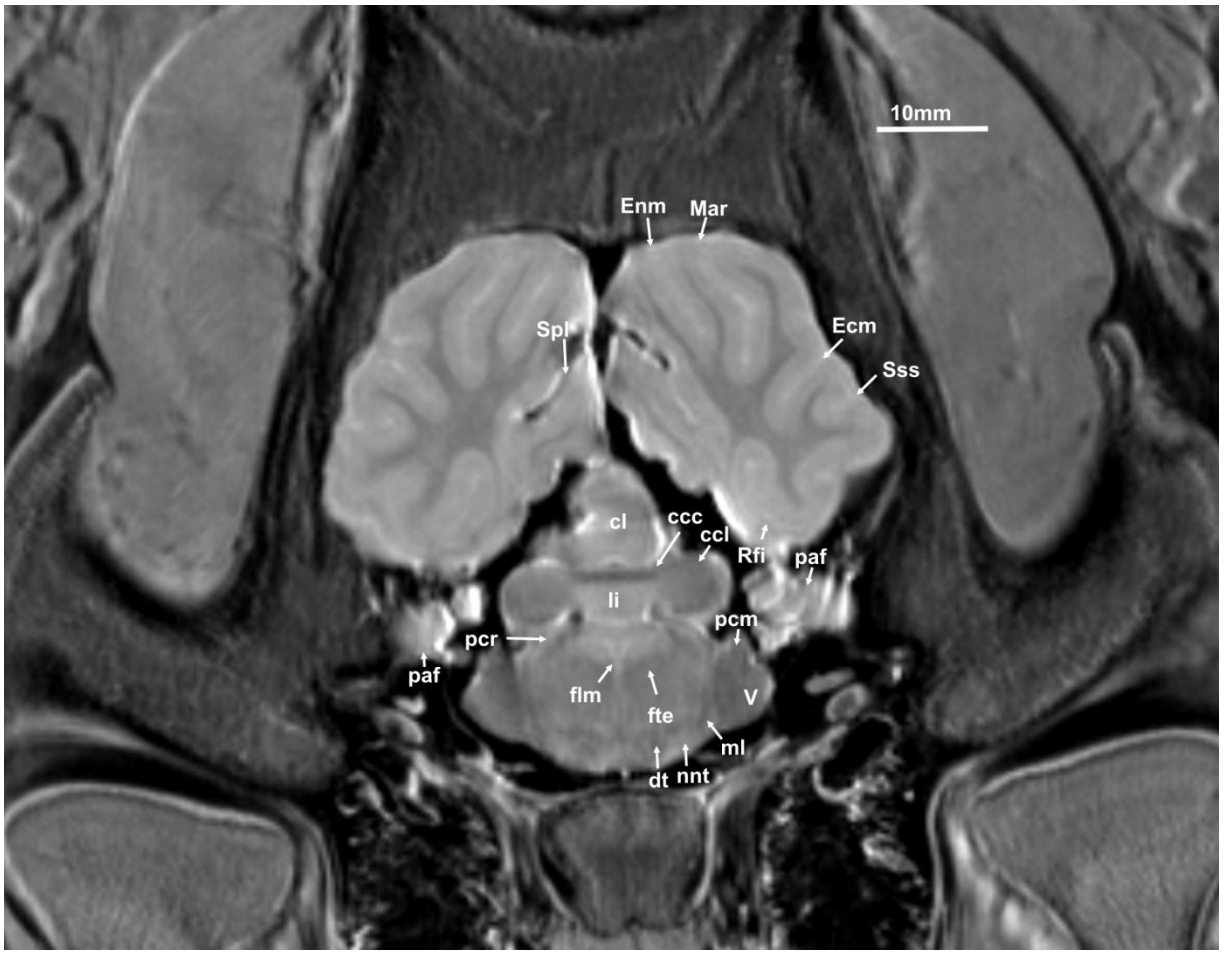

Figure 46

ccl: caudal colliculus; cl: central lobule; dt: descending tracts; Enm: endomarginal sulcus; Ecm: ectomarginal sulcus; Ems: ectomarginal sulcus; flm: medial longitudinal fasciculus; fte: fasciculus tegmenti; li: lingula; Mar: marginal sulcus; ml: medial lemniscus; nnt: nucleus nervi trigemini; paf: paraflocculus; pcm: medial cerebellar peduncle; pcr: rostral cerebellar peduncle; Spl: splenial sulcus; Sss: suprasylvian sulcus, V: trigeminal nerve.

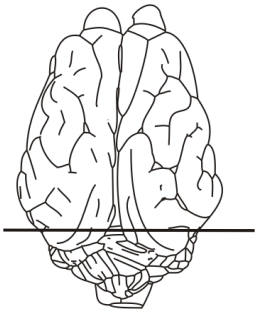

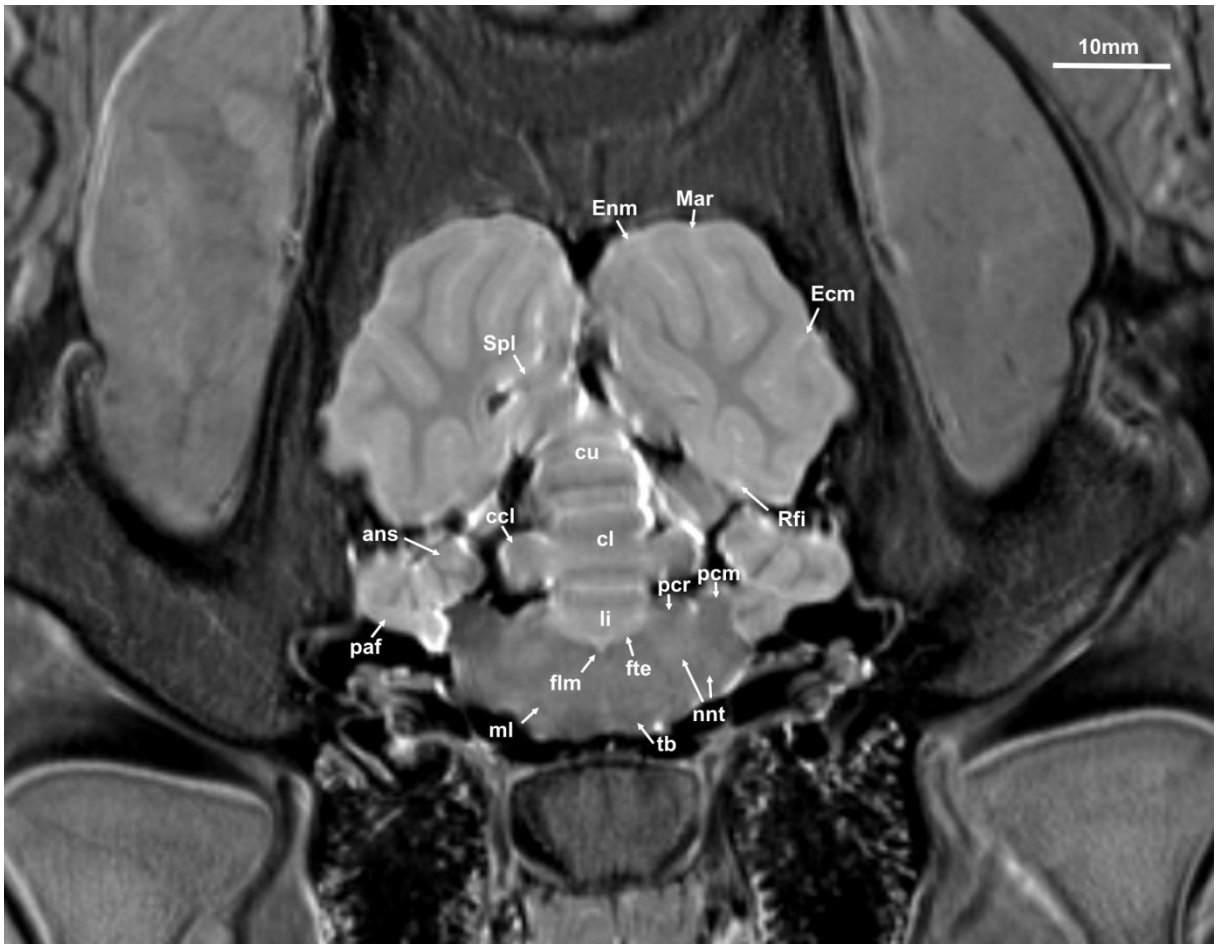

Figure 47

ans: ansiform lobule; ccl: caudal colliculus; cl: central lobule; cu: culmen; Enm: endomarginal sulcus; Ecm: ectomarginal sulcus; flm: medial longitudinal fasciculus; fte: fasciculus tegmenti; li: lingula; Mar: marginal sulcus; ml: medial lemniscus; nnt: nucleus nervi trigemini; paf: paraflocculus; pcm: medial cerebellar peduncle; pcr: rostral cerebellar peduncle; Rfi: rhinal fissure; Spl: splenial sulcus; tb: trapezoid body.

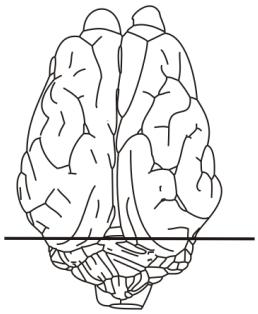

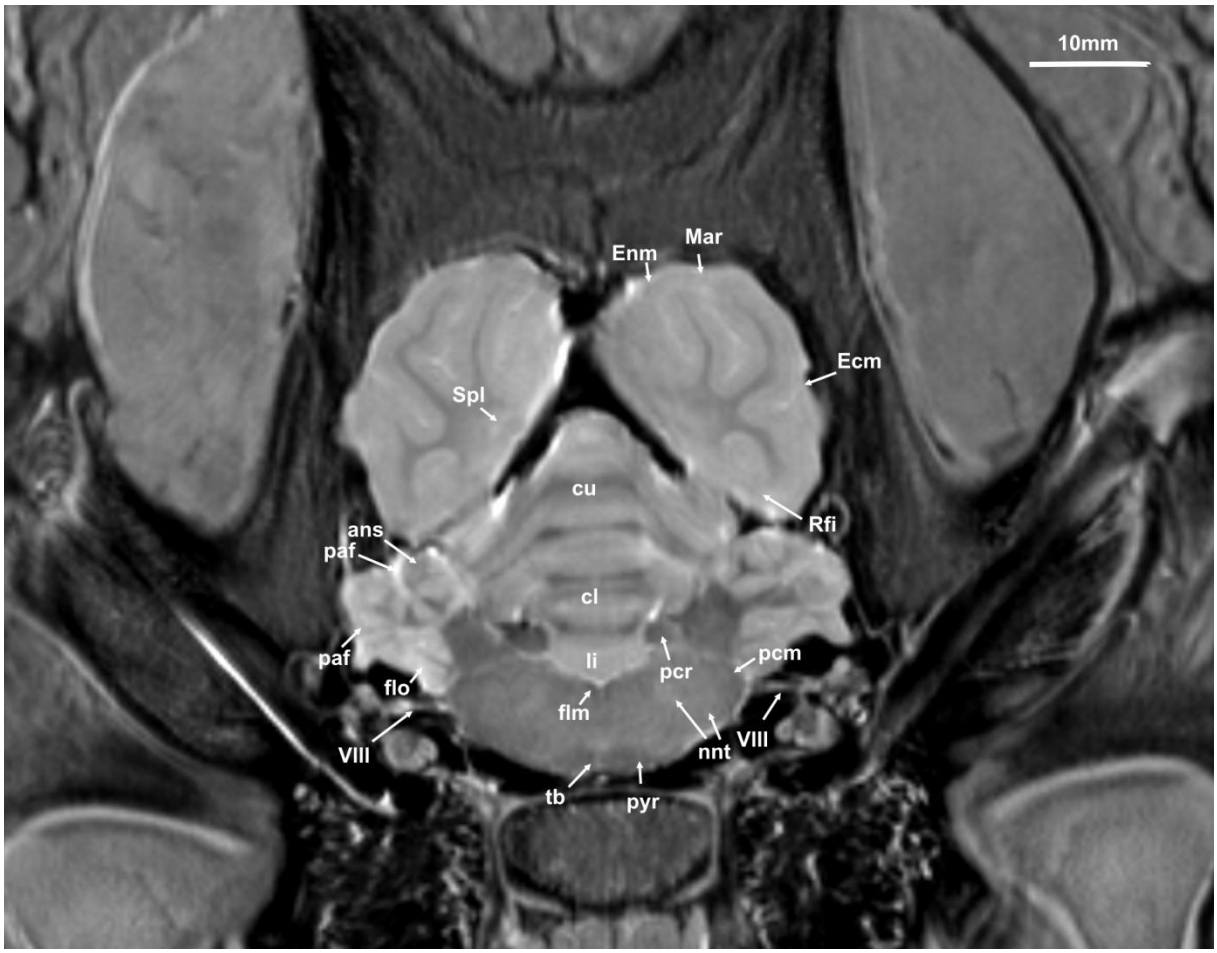

Figure 48

ans: ansiform lobule; cl: central lobule; cu: culmen; Enm: endomarginal sulcus; Ecm: ectomarginal sulcus; flm: medial longitudinal fasciculus; flo: flocculus; li: lingula; Mar: marginal sulcus; nnt: nucleus nervi trigemini; paf: paraflocculus; pcm: medial cerebellar peduncle; pcr: rostral cerebellar peduncle; pyr: pyramidal tracts; Rfi: rhinal fissure; Spl: splenial sulcus; tb: trapezoid body; VIII: vestibulocochlear nerve.

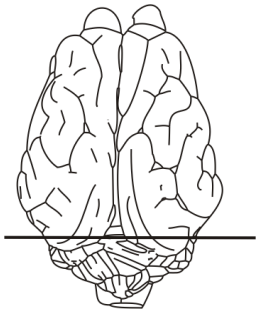

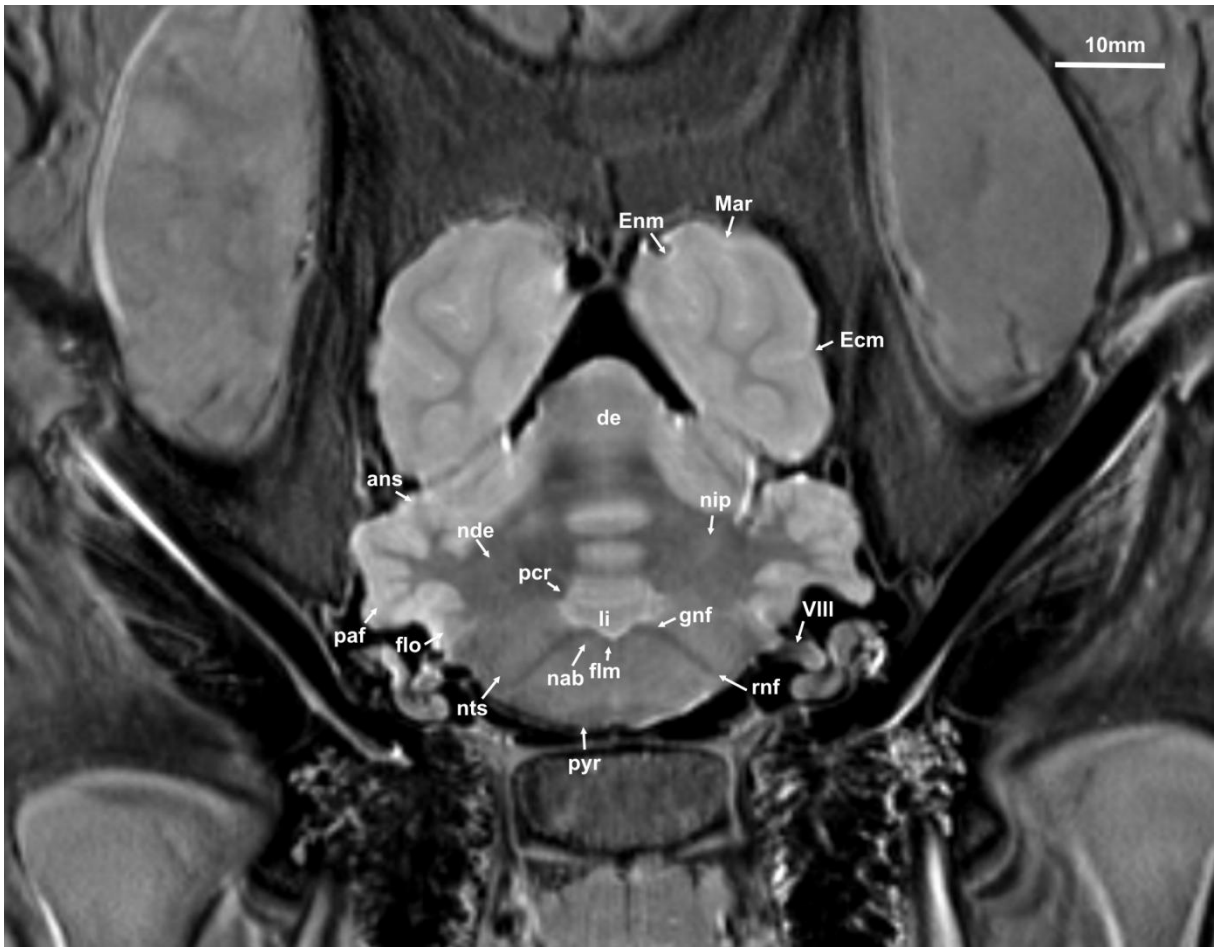

Figure 49

ans: ansiform lobule; de: declive; Enm: endomarginal sulcus; Ecm: ectomarginal sulcus; flm: medial longitudinal fasciculus; flo: flocculus; gnf: genu nervi facialis; li: lingula; Mar: marginal sulcus; nab: nucleus of the abducent nerve; nde: dentate nucleus; nts: nucleus tractus spinalis nervi trigemini; paf: paraflocculus; pcr: pedunculus cerebellaris rostralis; nab: nucleus of the abducent nerve; nip: interposed nucleus; pyr: pyramidal tracts; rnf: radix of the facial nerve; VIII: vestibulocochlear nerve.

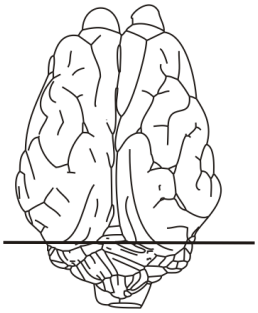

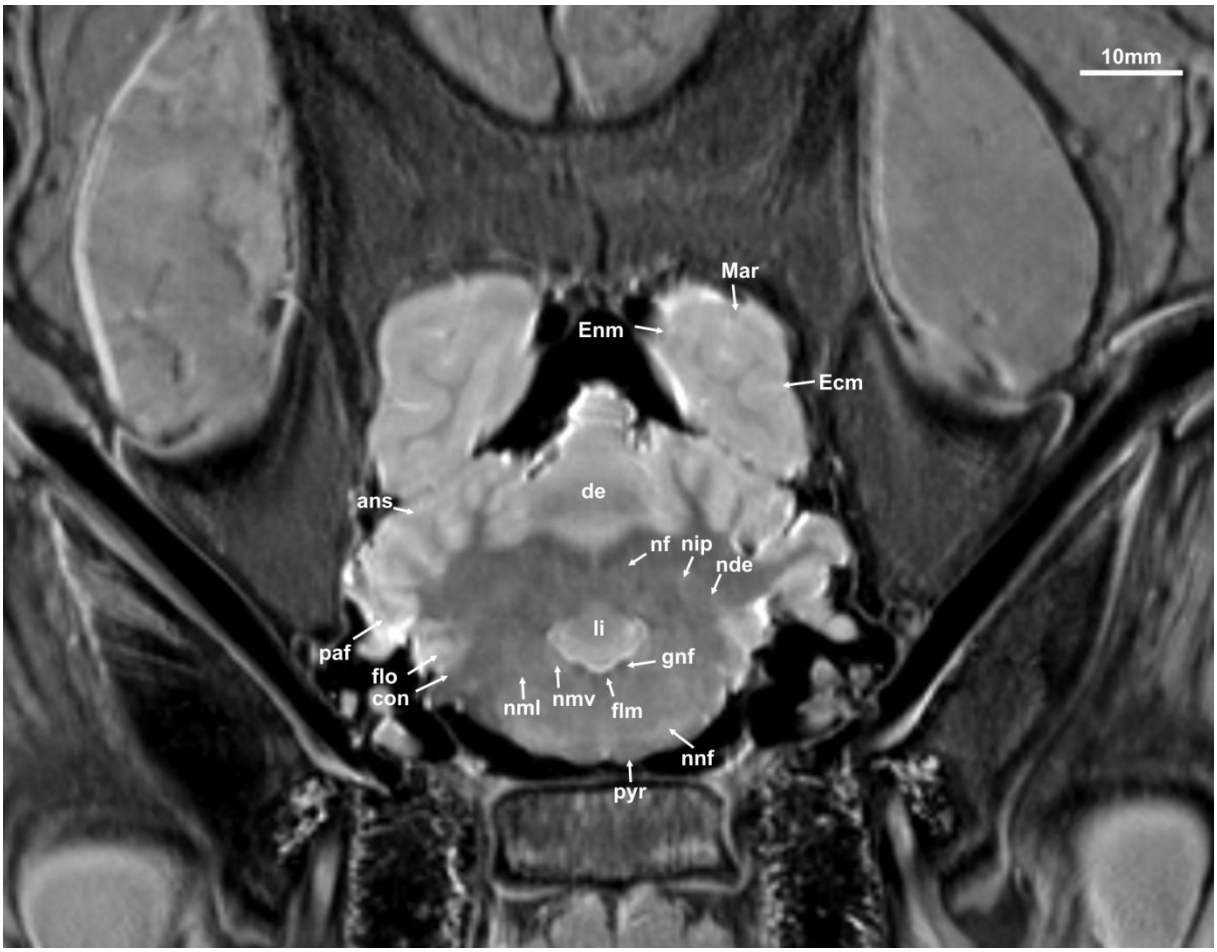

Figure 50

ans: ansiform lobule; con: cochlear nuclei; de: declive; Enm: endomarginal sulcus; Ecm: ectomarginal sulcus; flm: medial longitudinal fasciculus; flo: flocculus; gnf: genu nervi facialis; li: lingula; Mar: marginal sulcus; nf:fastigeal nucleus; nde dentate nucleus; nip: nucleus interpositus; nml: lateral vestibular nerve; nmv: medial vestibular nerve; nnf: nucleus of the facial nerve; paf: paraflocculus; pyr: pyramidal tract.

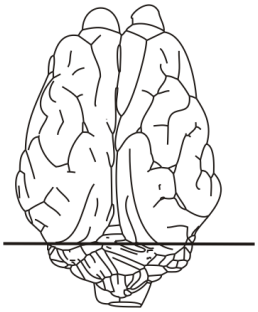

Figure 51

ans: ansiform lobule; de: declive; nde: dentate nucleus; Enm: endomarginal sulcus; Ecm: ectomarginal sulcus; flm: medial longitudinal fasciculus; flo: flocculus; li: lingula; Mar: marginal sulcus; con: cochlear nuclei; nf: nuclus fastigii; nip: nucleus interpositus; nmv: medial vestibular nerve; nnf: nucleus of the facial nerve; paf: paraflocculus; pcr: pedunculus cerebellaris rostralis; pyr: pyramidal tract.

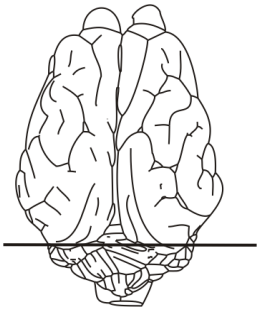

Figure 52

ans: ansiform lobule; de: declive; flm: medial longitudinal fasciculus; flo: flocculus; con: cochlear nuclei; nf: nuclus fastigii; nmv: medial vestibular nerve; nnf: nucleus of the facial nerve; no: nodulus; paf: paraflocculus; pcc: caudal cerebellar peduncle; pyr: pyramidal tract.

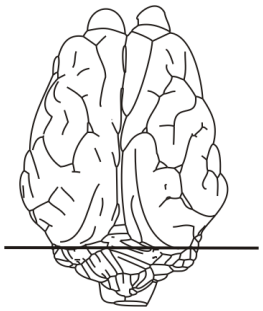

5.5 Comparative morphology of the porcine brain

Apart from giving a general overview of the porcine brain this study focuses on the surface of the brain (cerebrum and cerebellum) as revealed in MRI. It was also the aim to explore the system of sulci as detailed as possible while the brain remained in situ (within the cranial cavity). In addition selected structures of the porcine brain are featured that are visible in MRI, but that are usually damaged using traditional preparation techniques (removal of the brain from the cranial cavity etc.), such as the pituitary gland and the rete mirabile.

It would often have been desirable to deliver a more detailed comparison with the brains of other ungulates or brains of other species (e.g. carnivores) to highlight the unique features of the porcine brain. A more intense MRI study of other members of the suidae could have given more clues as to how closely members of the suidae are related, about the similarities and differences of brain shape and size and especially about the consistency of the system of gyri and sulci. Unfortunately brains of the domestic pig and especially the brains of rare breeds and rare members of the suinae are seldom available for veterinary research purposes. For this MRI study it was possible to obtain the brains of a babirusa, a member of the suidae. With this thesis it is therefore possible to deliver the results of a preliminary MRI study of the babirusa brain compared with brains of members of the suidae. A more detailed study of this interesting specimen was unfortunately beyond the scope of this study.

The hemispheres of the porcine telencephalon form the largest part of the brain. They cover the brainstem dorsally and reach the cerebellum caudally. They only cover a small rostral part of the cerebellum, leaving a larger caudal aspect uncovered. This is best seen in the midsagittal MRI scan (Fig. 30). The olfactory bulbs of the pig are impressively large and are dorsally approximately half covered by the hemispheres, while the bovine olfactory bulbs for example are nearly completely hidden from dorsal view (Nickel et al. 1992). Among the most distinctive morphological features of vertebrate brains is the evolutionary expansion of the cerebral cortex (Hofman 1985, Barton 2007). By comparing the scans of the pig brain with images of other domestic animals, the different degrees of gyrification as well as differences in size and shape of the hemispheres are apparent (Fig. 53). The pig's

rhinencephalon is large and dominates the forebrain. The porcine brain appears elongated and rostrally pointed. The lateral aspect is almost triangular. The brains of sheep, horse, deer, calf and alpaca appear to be wider, rounder and stockier in comparison. Even though all the studied brains are gyrencephalic, the equine and the ruminant brains show more gyri and sulci than the porcine brain (Fig. 53, Fig. 57-60). In the equine and ruminant brains second- and third degree gyri can be identified. The gyri of the pig are manly straight and longitudinally arranged. The basic arrangement of the “arcuate sulci”, as seen in lower ungulates (praeungulata, for example the hyrax), has been preserved. The brain of the deer is the most similar in shape and degree of gyrification (Fig. 53 C) in the dorsal scans.

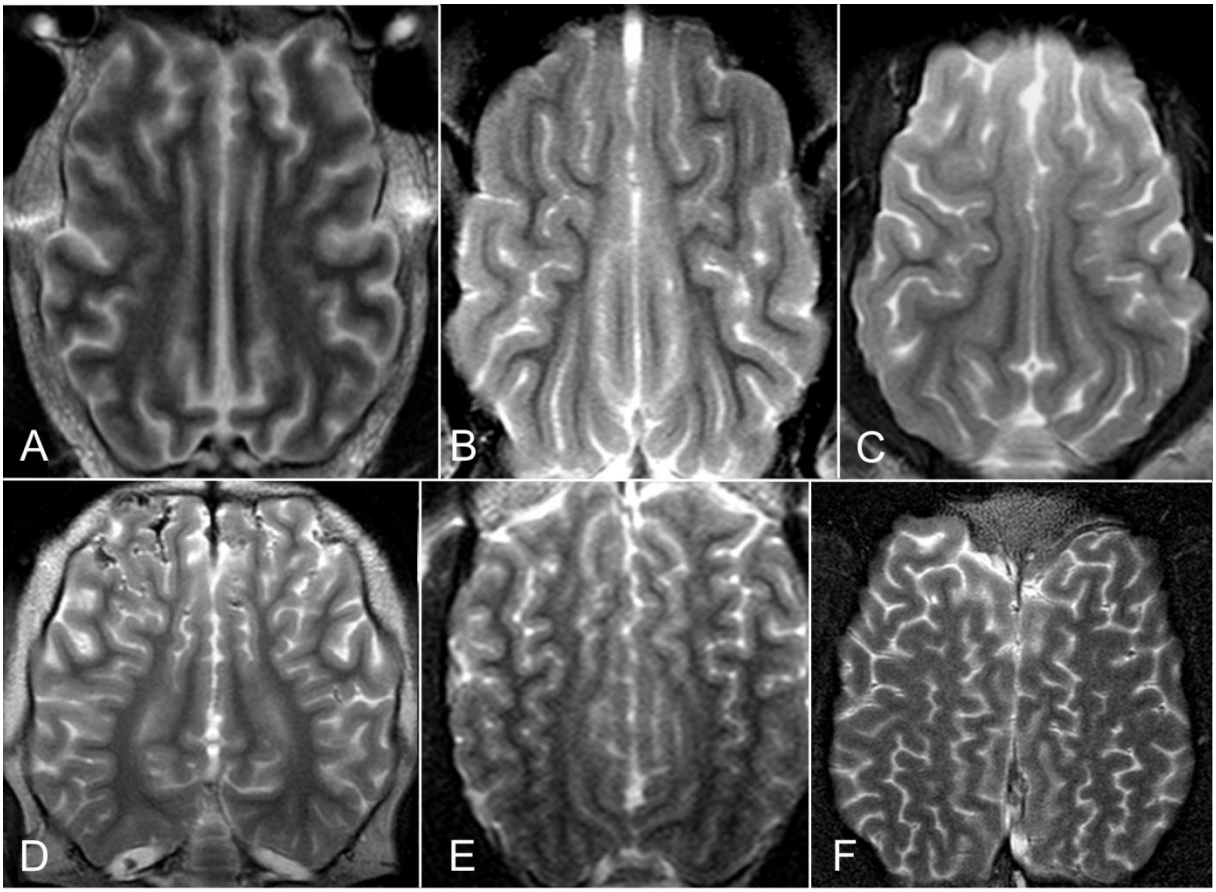

Figure 53

Dorsal scans highlighting differences in the degree of gyrification. A: sheep, *ovis ammon aries*; B: pig, *sus scrofa domestica* C: red deer, *cervus elaphus*; D: alpaca, *vicugna pacos*; E: calf, *bos taurus domestic*; F: horse, *equus caballus* (A-F courtesy of PD Dr. med.vet. (habil.) M. Schmidt).

5.5.1 The gross division of the cortex

As in other ungulates, the neopallium of the pig is laterally separated from the paleopallium by the lateral rhinal fissure (Rfi: Fig. 13-14, Fig. 19-22, Fig. 31-48) and medially separated from the archipallium by the splenial sulcus (Spl: Fig. 17-18, Fig. 23-30, Fig. 31-48, Fig. 57-60). The rhinal fissure is dorsally positioned and easy to identify. The piriform lobe of the pig is large and the olfactory tubercle (otu: Fig. 23-26, Fig. 31) is well developed. The pig's frontal cortex is situated below the large frontal sinus and the flat and elongated olfactory bulbs are positioned ventrally under the rostral pole of the brain. They extend caudally and almost reach the level of the terminal lamina, as can be seen in sagittal scans (tl: Fig. 28-30). The olfactory fibres (olf: Fig. 6-10, Fig. 19-30) of the pig are not confined to the rostral end of the bulb. Instead they spread out from the bulb's whole surface and are clearly visible in Fig. 30. The bulbs themselves house a large olfactory recess which seems to be collapsed in the fixed specimen scanned for the atlas, but can be visualized (more hyperintense than the surrounding tissue) in a native scan (Fig. 54 A). There is a gap between the two olfactory bulbs of the pig (ob: Fig. 6-9, Fig. 21-27), similar to the bovine olfactory bulbs and in contrast to the olfactory bulbs of the dog and cat that contact in midline (Nickel et al. 1992). The olfactory bulbs of other ungulates are dorsally covered by the cortex (according to Nickel et al. 1992). In the porcine brain an accessory olfactory bulb is located within the olfactory bulb. It is dorsally and slightly medially positioned (Fig. 54 A). The accessory olfactory bulb of the pig seems to be developed even before birth and might be involved in the essential nipple seeking behavior of neonatal pigs (Salazar et al. 2004). The rhinal fissure (Rfi: Fig. 13-14, Fig. 19-22, Fig. 31-48) of the lateral brain surface, with its rostral and caudal part forms the upper limit of the rhinencephalon. The rhinal fissure separates the neocortex from the paleocortex. With increasing gyrification the rhinal fissure is shifted ventrally (Fig. 55). The caudal part of the porcine rhinal sulcus is not covered by the temporal lobe.

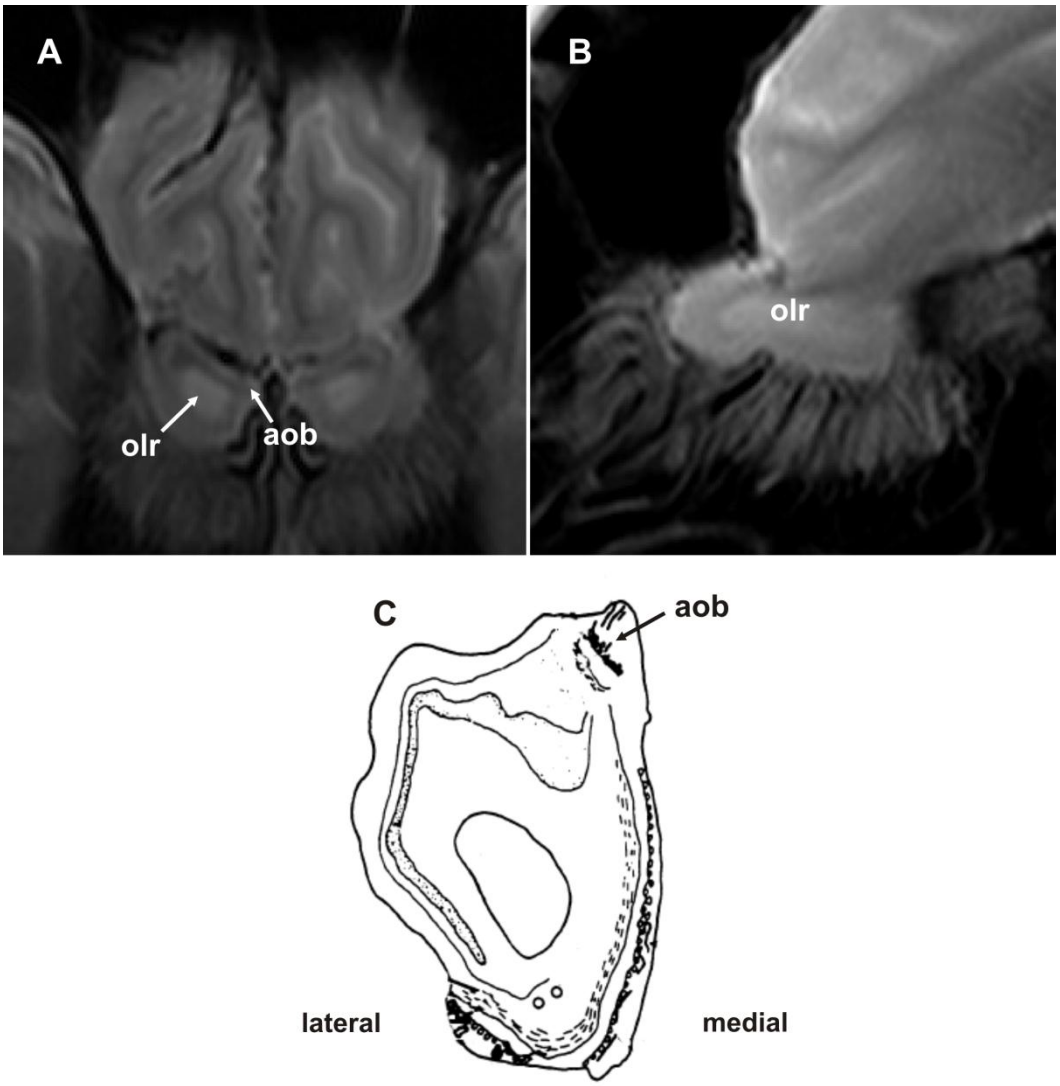

Figure 54
Accessory olfactory bulb and olfactory recess of the pig brain. A: native T2 weighted scan (transverse scan); B: native T2 weighted scan accessory olfactory bulb (sagittal scan); C: modified drawing from Leshin et al. 1991. The olfactory bulbs of the pig contain a large olfactory recess. In the porcine brain the accessory olfactory bulb is located within the olfactory bulb. It is dorsally and slightly medially positioned (A+B courtesy of PD Dr. med.vet. (habil.) M. Schmidt).

5.5.2 Expansion pattern of the cerebral cortex

The growth of the cortex during phylogenesis creates species specific expansion pattern. In the 19th century Krueg (1887) already mentioned, that the brains of ungulates and carnivores expand through different mechanisms which he describes as pronation and supination.

5.5.2.4 Pronation and supination

One can observe in the carnivore (feline) brain an expansion during development towards lateral aspect of the hemispheres (pronation). The medial surface of the hemisphere remains sparsely gyrated. As a result one can see (Fig. 55 C) that the corpus callosum is positioned in the top third of the brain. The hemispheres expand in lateral direction. We can also see (Fig. 55 A) an expansion of the cortex in the equine and bovine brain in medial direction (supination). This results in a large number of gyri and sulci on the medial surface of the hemispheres. Consequently the corpus callosum is shifted ventrally and towards the base of the skull. The pig's corpus callosum is positioned in the centre of the hemispheres and the brain. Compared with the brains of sheep and dogs, the brain gyrification- and development pattern of the pig seems to take up an intermediate position (Fig. 55 B). The pronation and supination process is described by Krueg (1878) and Kappers (1921).

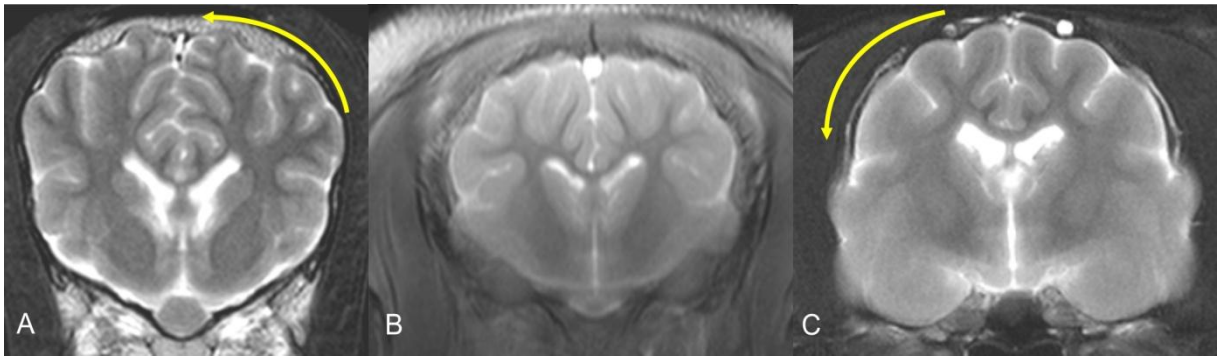

Figure 55

Increase of brain mass in dorso-medial orientation (A: bovine brain). Increase of brain mass latero-ventral orientation (C: feline brain). The brain of the pig takes an intermediate position (according to Krueg 1887 and Kappers 1921), (A-C courtesy of PD Dr. med.vet. (habil.) M. Schmidt).

5.5.2.5 Opercularisation

The insula is a part of the lateral brain surface (facies convexa). It was first described in the human brain by Vicq d'Azyr (1786) as "convolutions situated between sylvian fissure and striate body" (Clark 1896). This can also be seen in the scans of this study. In the pig the operculum covers only a part of the insula (Clark 1896, Kappers 1921, Nickel et al. 1992, Russo et al. 2007). The insula of the pig appears flattened and sparsely gyrated in the MRI scans (Fig. 56 C). In ungulates (such as bovines and sheep) insular gyri are developed (Fig. 56 A, B). The opercularisation in the pig brain is nearly complete (Lauer 1982). During the ontogenesis the smooth surface of the pallium starts to form the deep sylvian fissure (fissura lateralis cerebri/ fissura sylvina) and the insula. It is characterised by a considerable morphologic variability in mammals. During ontogenesis the insula together with the striate body remain in place, while the pallium growth arch like (caudoventrally) around this area in order to maximise its mass.

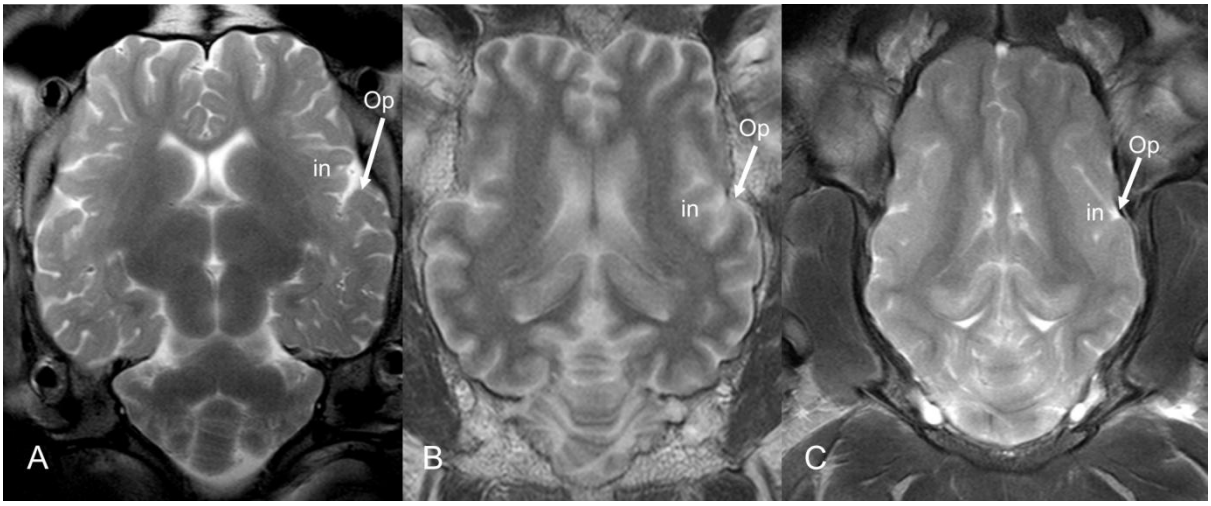

Figure 56

Comparison of dorsal T2 weighted images of the insular region of the A: bovine, B: ovine, C: porcine brain. The insula (in) and the operculum (Op) are not as gyrated in the porcine brain. The opercularisation of the porcine brain is almost complete. Only a small part of the insula remains uncoverd (A-C courtesy of PD Dr. med.vet. (habil.) M. Schmidt).

5.5.3 The porcine cortex in comparison with the cerebral cortex of other ungulates

Transverse brain scans of horse, sheep, calf and domestic pig at the level of the olfactory bulbs, the striatum, the optic chiasm, the pituitary gland, the mammillary bodies, the habenulae, the rostral colliculi and the lingula (cerebellum) were selected and compared. As mentioned above the brains of the horse, sheep and calf are more gyrated than the porcine brain. The paleopallium is the most developed part of the cerebral cortex. The opercularisation process of the porcine brain is advanced, while temporalisation is not as developed. Some sulci can be traced from rostral to caudal scans. The rhinal fissure is only missing at the level of the lingula. The rhinal fissure is most dorsally positioned in the porcine brain at every level. The diagonal sulcus of the horse and the calf can be traced caudally up to the level of the optic chiasm. The diagonal sulcus of the pig is shorter and is not as easily identified. The arched furrows (ectosylvian and suprasylvian sulci also known as “Bogenfurchen“) are preserved but not strongly developed in the porcine brain, especially at the rostral pole of the brain. Rostrally (Fig. 57 C) the forebrain of the horse is the most gyrated. The forebrain expands far in lateral direction. Together the hemispheres appear almost circular. The other transverse scans at the level of the olfactory bulbs are more triangular (Fig. 57 A, B, D). The porcine brain appears most elongated (dorsoventral direction). At the level of the striatum, the brains of the sheep and pig are trapezoid in transverse scans. The brains of the horse and the calf are more elliptical. The caudate nuclei of the calf are the most elliptical (Fig. 57 E). The caudate nucleus of the pig is more triangular and does not extend as far laterally (Fig. 57 H). The caudate nuclei of the horse are almost isointens to the surrounding tissue and therefore not easy to distinguish (Fig. 57 G). The sylvian fissures of the horse, sheep and calf are deep and more dorsally positioned than the sylvian fissure of the pig. The sylvian fissure of the horse is displayed twice in scan (57 E).At the level of the optic chiasm the brain of the pig starts to expand ventrolaterally. The caudate nucleus of the pig is still triangular in shape, whereas the caudate nuclei of the horse and sheep are oval and continue to expand laterally towards the putamen and pallidum. Further caudally, at the level of the pituitary gland, the porcine brain does not feature the oblique sulcus of the horse brain (Fig. 58 G).

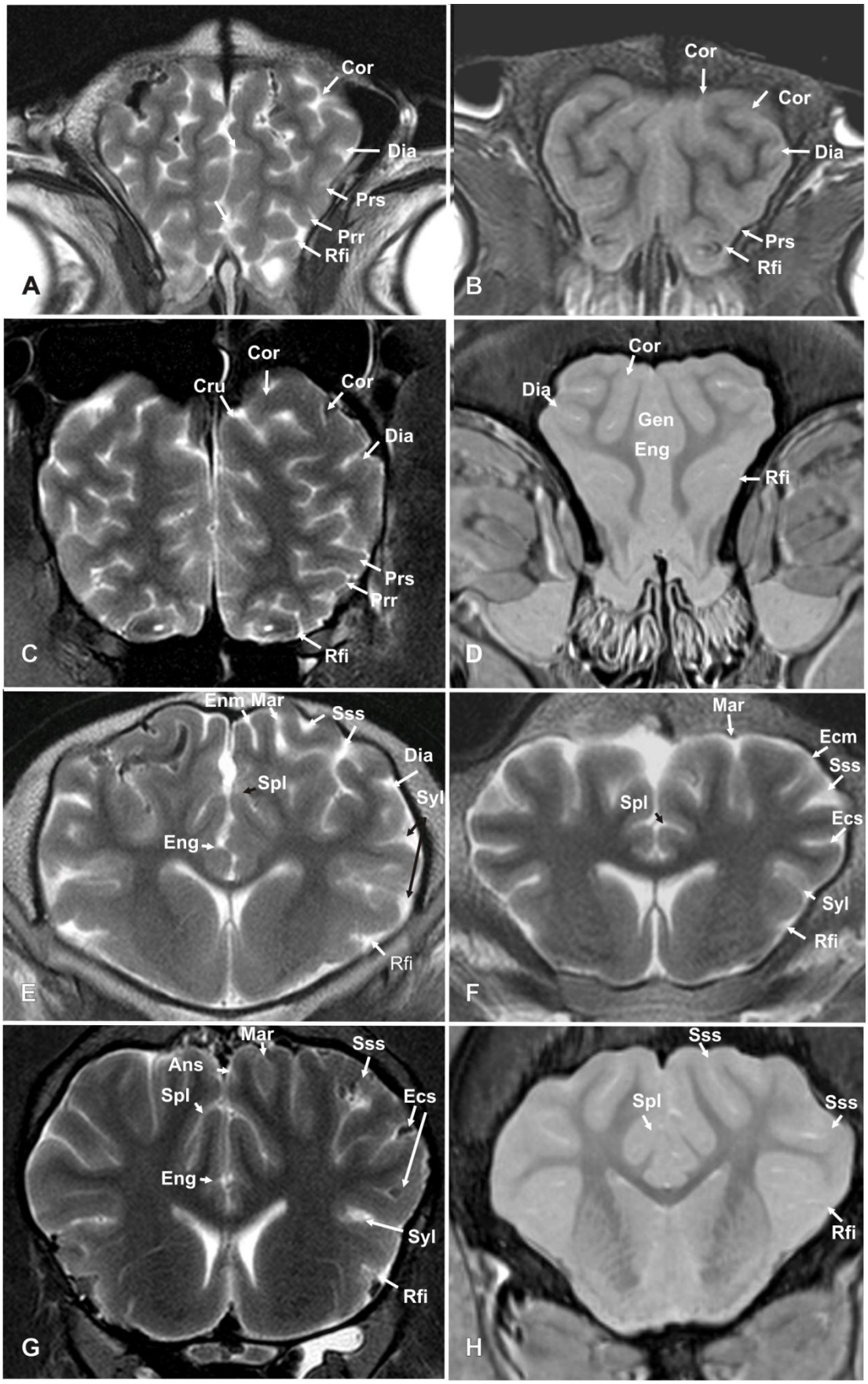

Figure 57

Transverse image of the brain of different ungulates on the level of the olfactory bulbs (A-D) and striatum (E-H); A: calf; B: sheep; C: horse; D: pig ; E: calf; F: sheep; G: horse; H: pig.

The brain of the pig is now almost round in the transverse scan. The corpora callosi of the horse and sheep seems to be more dorsally positioned. The system of gyri and sulci of horse, sheep and calf are dorsolaterally more gyrated. The gyri and sulci seem deeper and are more defined. At the level of the mammillary bodies (Fig. 59) the porcine brain is still round, while the brains of the horse, calf and sheep are dorsoventrally flattened. The endosplenial sulci of the horse and calf become visible at this level. The endosplenial sulcus is not a feature of the porcine brain. The horse, sheep and calf brains become more elliptical and dorsoventrally flattened. The ectosylvian sulcus (“Bogenfurche”) of the pig can be detected at this level (Fig. 59 D). In the pig it is rather shallow and not as long and complex as in the horse and the calf. In the porcine brain we can also find a sulcus (Spl*) connecting the splenial sulcus with the suprasylvian sulcus.

Marginal, endomarginal and ectomarginal sulci dominate the sulcal system in caudal transverse scans (Fig. 60). They seem to be the most conservative and are featured in all of our specimens.

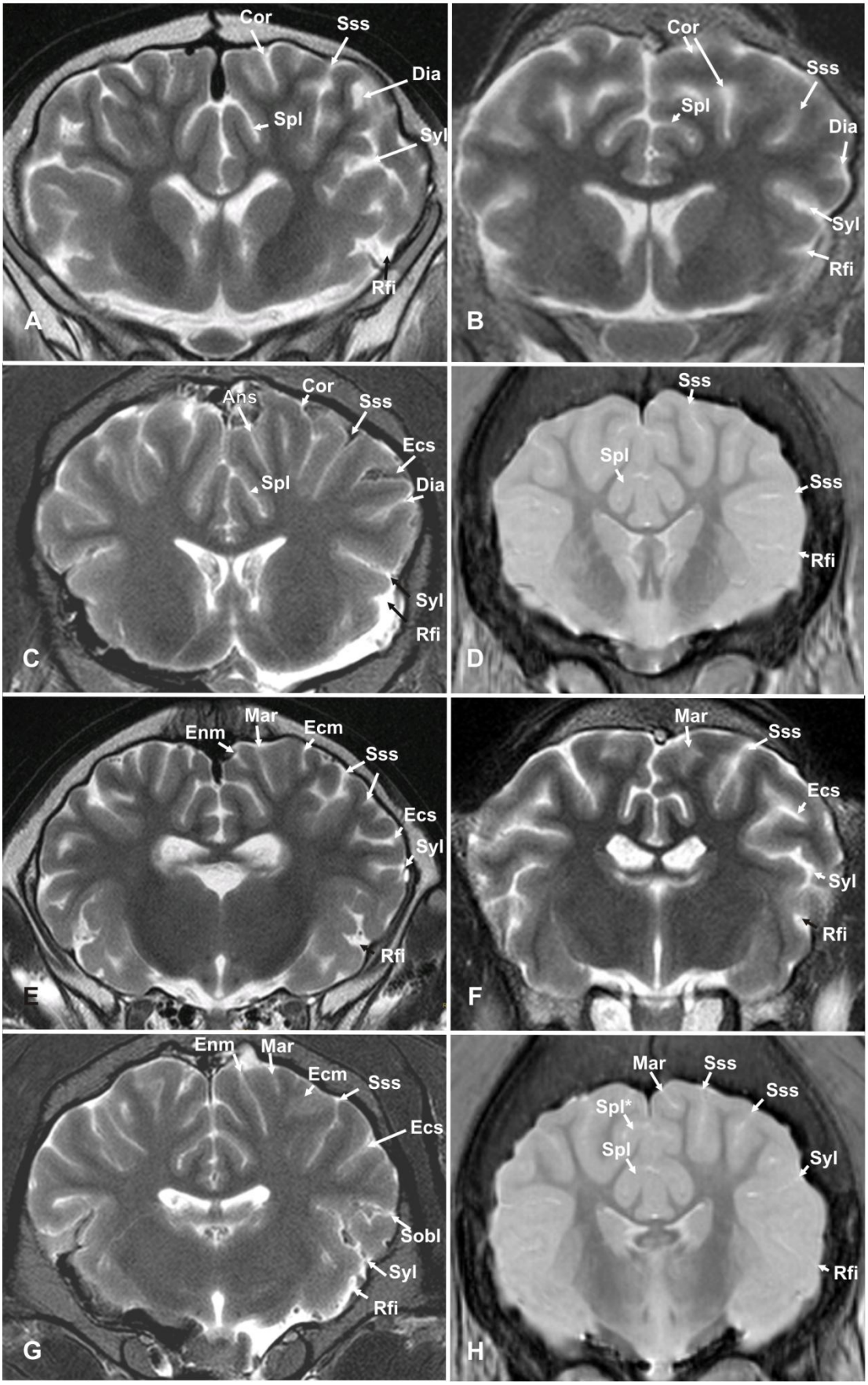

Figure 58

Transverse image of the brain of different ungulates on the level of the optic chiasm (A-D) and pituitary gland (E-H); A: calf; B: sheep; C: horse; D: pig ; E: calf; F: sheep; G: horse; H: pig.

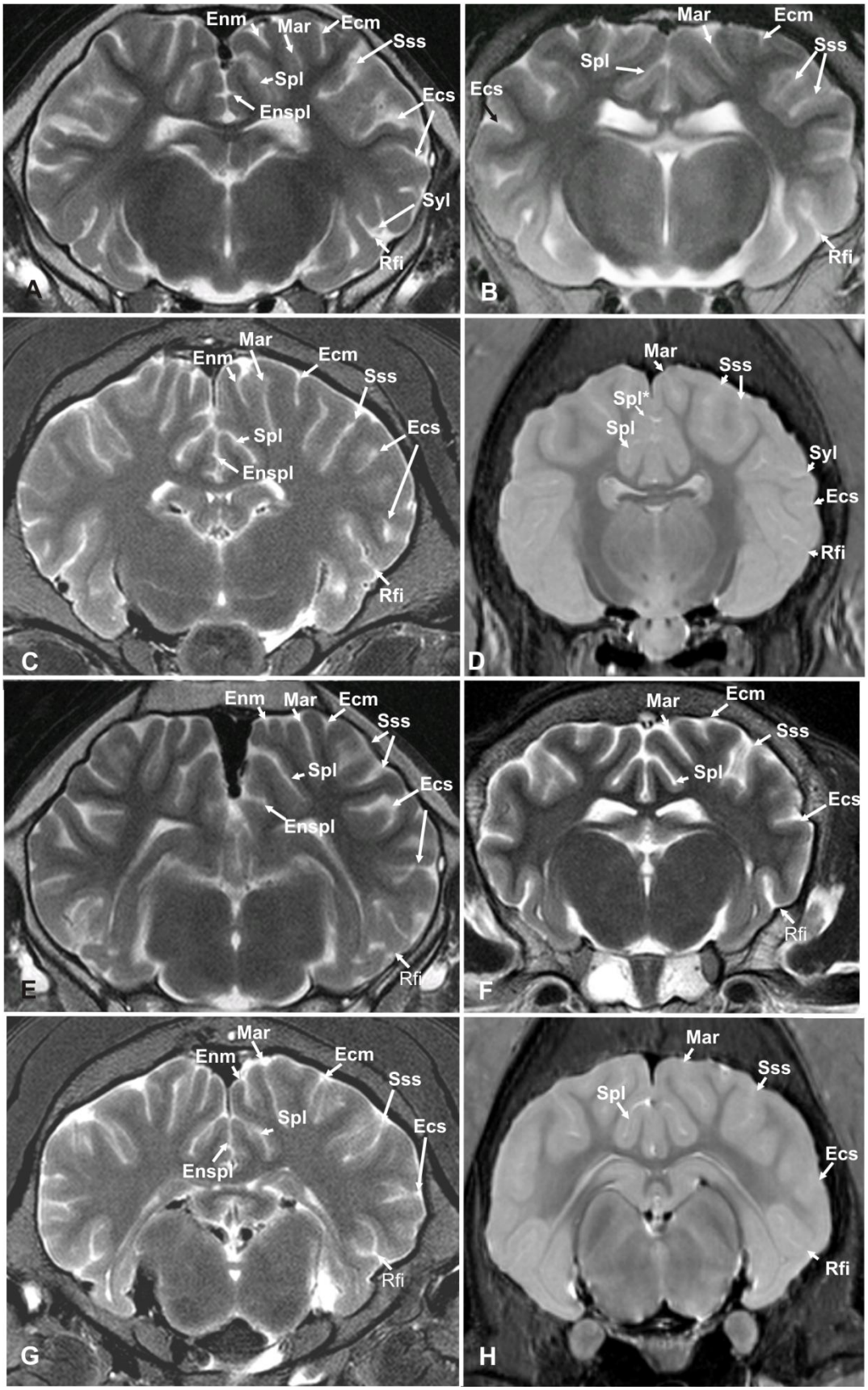

Figure 59

Transverse image of the brain of different ungulates on the level of the mammillary bodies (A-D) and habenulae (E-H); a: calf; B: sheep; C: horse; D: pig; E: calf; F: sheep; G: horse; H: pig.

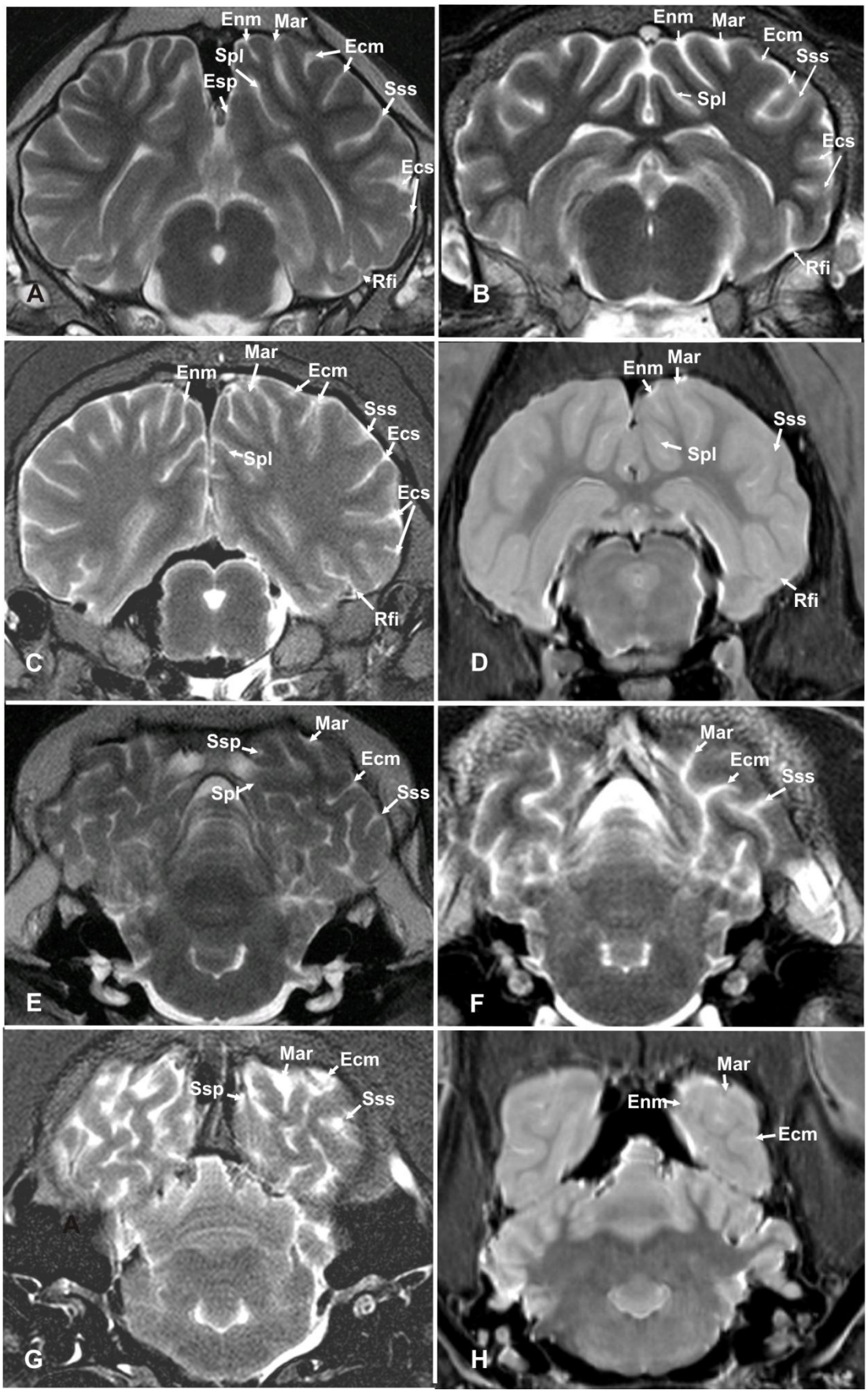

Figure 60

Transverse image of the brain of different ungulates on the level of the rostral colliculi (A-D) and of the lingula (E-H); A: calf; B: sheep; C: horse; D: pig ; E: calf; F: sheep; G: horse; H: pig.

Abbreviations figures 57-60:

Ans: ansate sulcus; Cor: coronal sulcus; Cru: cruciate sulcus; Dia: diagonal sulcus; Ecm: ectomarginal sulcus; Ecs: ectosylvian sulcus; Enm: endomarginal sulcus; Eng: endogenual sulcus; Enspl: endosplenial sulcus; Gen: genual sulcus; Mar: marginal sulcus; Obl: oblique sulcus; Prs: presylvian sulcus; Prr: prorean sulcus; Rfi: rhinal fissure; Scl: sulcus of the corpus callosum; Sss: suprasylvian sulcus; Spl: splenial sulcus; Spl*: connecting sulcus; Syl: sylvian fissure (pictures courtesy of PD Dr. med.vet. (habil.) M. Schmidt).

5.5.4 Comparative morphology of the cortex of pig breeds, wild boar and babirusa

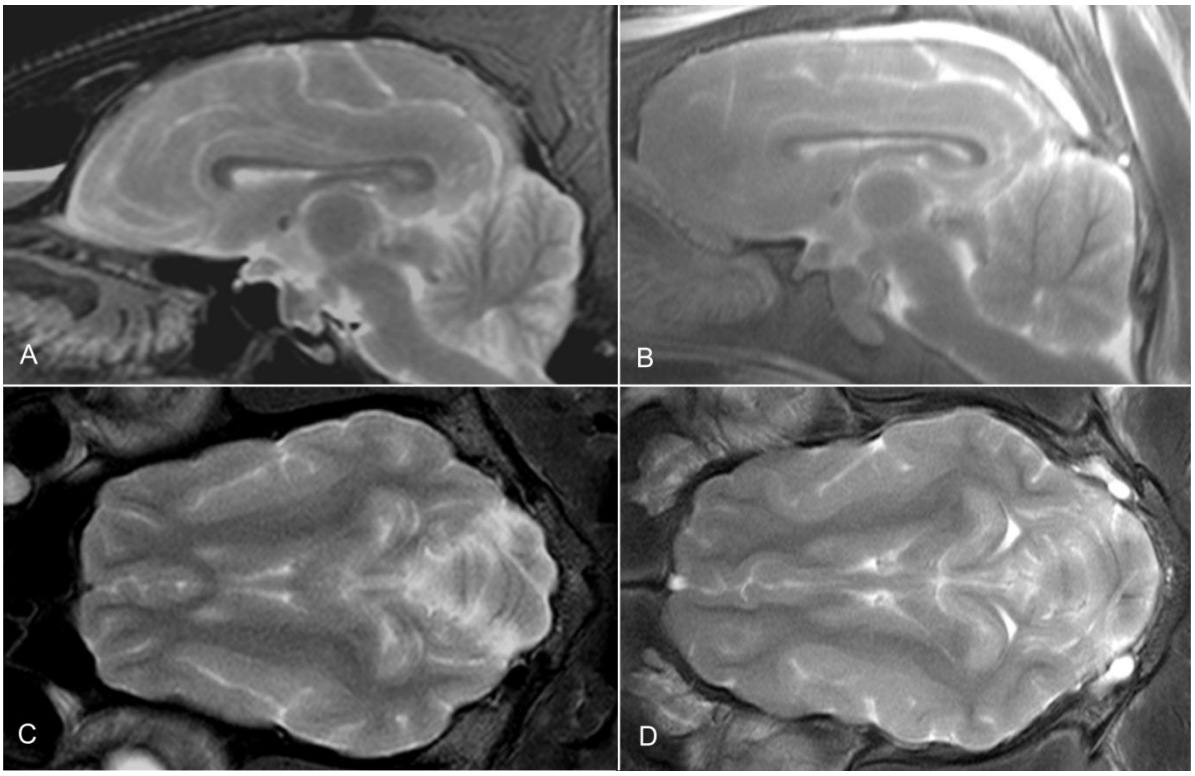

Figure 61

Comparison of the of the domestic pig brain with the brain of the wild boar: A: wild boar midsagittal scan, B: domestic pig midsagittal scan, C: wild boar dorsal scan, D: domestic pig dorsal scan. The main sulci of the domestic pig and the wild boar are very similarly positioned. Also the overall shape of the telencephalon and cerebellum is mostly preserved in the domestic pig. The dorsal curvature of the domestic pig's telencephalon seems less convex. The sulci of the wild boar appear longer and deeper (A-D courtesy of PD Dr. med.vet. (habil.) M. Schmidt).

In the MRI scans of Fig. 61 one can see that the main sulci of the domestic pig and the wild boar are very similarly positioned. Also the overall shape of the telencephalon and cerebellum is mostly preserved in the domestic pig, although the dorsal curvature of the domestic pig's telencephalon seems less convex (Fig. 61 B). The brains of both -domestic pig and the wild boar- present strongly developed olfactory bulbs and large pituitary glands. In the sagittal images one can see differences in the shape of the corpus callosum. The dorsal surface is almost concave in the wild boar. The gyri and sulci dorsal to the corpus callosum seem to be longer in the wild boar and appear to be more convoluted. This might be an explanation for the concave facies splenalis of the corpus callosum. As well as that the pons is more pronounced in the wild form than in the domestic pig. In the sagittal scan the sulci of the frontal cortex of the wild boar are more distinct (Fig.61 A and B). This observation was also made by Brauer and Schober (1970). The same observation is difficult to make in the dorsal images, since they are not taken in the exact same plane.

Differences between the brain of the domestic pig, Wiesenauer minipig, wild boar and the brain of the Indonesian babirusa (Fig. 63), a member of the suinae become apparent. Our MRI scans of the head show a massive frontal sinus extending dorsally over the telencephalon and cerebellum of the barbirusa. The telencephalon is relatively small when compared with the size of the cerebellum (Fig. 63 C). The shape of the cerebellum in MRI is almost square in the midsagittal scan. In contrast the cerebellum of the porcine brain is more dorsoventrally extended. The pons of the babirousa seems not as pronounced as the pons of the domestic pig, in spite of the large cerebellum. We propose that the corticocerebellar fibres of the pons are not as developed because of the smaller size of the telencephalon. The well developed cerebellum is responsible for vital coordination. The pituitary gland is large and points caudally like the pituitary gland of the domestic pig and wild boar. The corpora callosa of babirusa and pig are very similar in shape. The brain of the babirousa seems to be dorsoventrally compressed in transversal sections (Fig. 65). Compared with the porcine brain the corpus callosum the gyri of the babirusa are laterally more convoluted (transverse scans, Fig. 65-67). The telencephalon of the babirusa is elongated (sagittal scans, Fig.63), especially when compared with the brain of the Wiesenauer minipig. Out of the four specimens the Wiesenauer minipig features the least amount of olfactory fibres. The brain of this brachycephalic ("short headed") pig is rostrocaudally compressed. As a result the mesencephalon is shifted in dorsal

direction. The frontal lobe of the Wiesenauer minipig is positioned in a more rostral position than the olfactory bulbs (Fig. 63 B).

By comparing the brains of the dolichocephalic (“long headed”) domestic pig with the brains of Wiesenauer minipig, barbirusa and wild boar, it is apparent that the shape of the brain is influenced by the scull and either elongated or caudorostrally compressed. The sulci and gyri are stretched or compressed accordingly. As far as can be determined in MRI, the system of gyri and sulci varies little between the scanned specimens as can be seen in Fig. 65-67. The sulci emerge at approximately the same level. The variation is so slight, that is would be difficult to identify the individual specimens if the image was viewed out of the context of this study. The brain of the wild boar features the most secondary sulci and fissures. Volumetrical differences are not visible in the 2D images. The brain of the babirusa is dorsoventrally flattened and elongated compared with the other suidae. The cerebrum and cerebellum of the babirusa are in line.

Figure 62

Head of a babirusa (female), the specimen was scanned post mortem at the Justus Liebig University in Giessen. It was donated by the Hessisches Untersuchungsamt after the animal had been euthanized due to a neoplasia in the uterus at Frankfurt Zoo. © Verena Schmidt

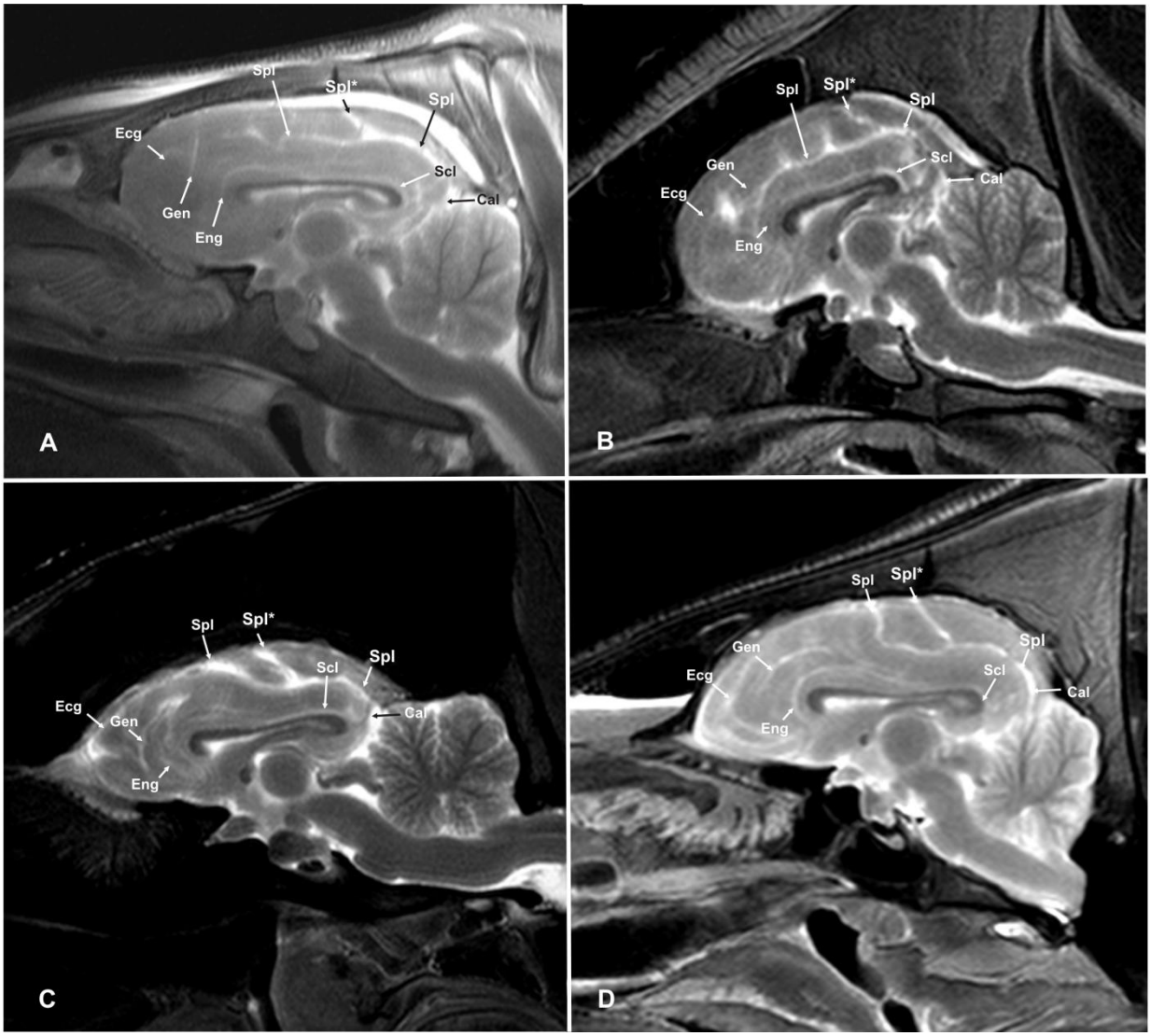

Figure 63
A: domestic pig, B: Wiesenauer minipig, C: babirousa D: wild boar in midsagittal scans.
Cal: calcarine fissure; Ecg: ectogenual sulcus; Eng: endogenual sulcus; Gen: genual sulcus; Scl: sulcus of the corpus callosum; Spl: splenial sulcus; Spl*: connecting sulcus (A-D courtesy of PD Dr. med.vet. (habil.) M. Schmidt).

The mesencephalon is elongated and the mammillary bodies are rostrally oriented. The babirusa displays the longest distance between the mammillary bodies and the pons. The Corpus callosum is long and thin in sagittal scans and the ventral surface is concave.

The cerebellum of the babirousa resembles the cerebellum of the bovine cerebellum in MRI-scans. It is cuboid in shape and very myelinated. In the Wiesenauer minipig, the wild boar and the domestic pig the cerebelli are rather cone shaped and rostrodorsally positioned

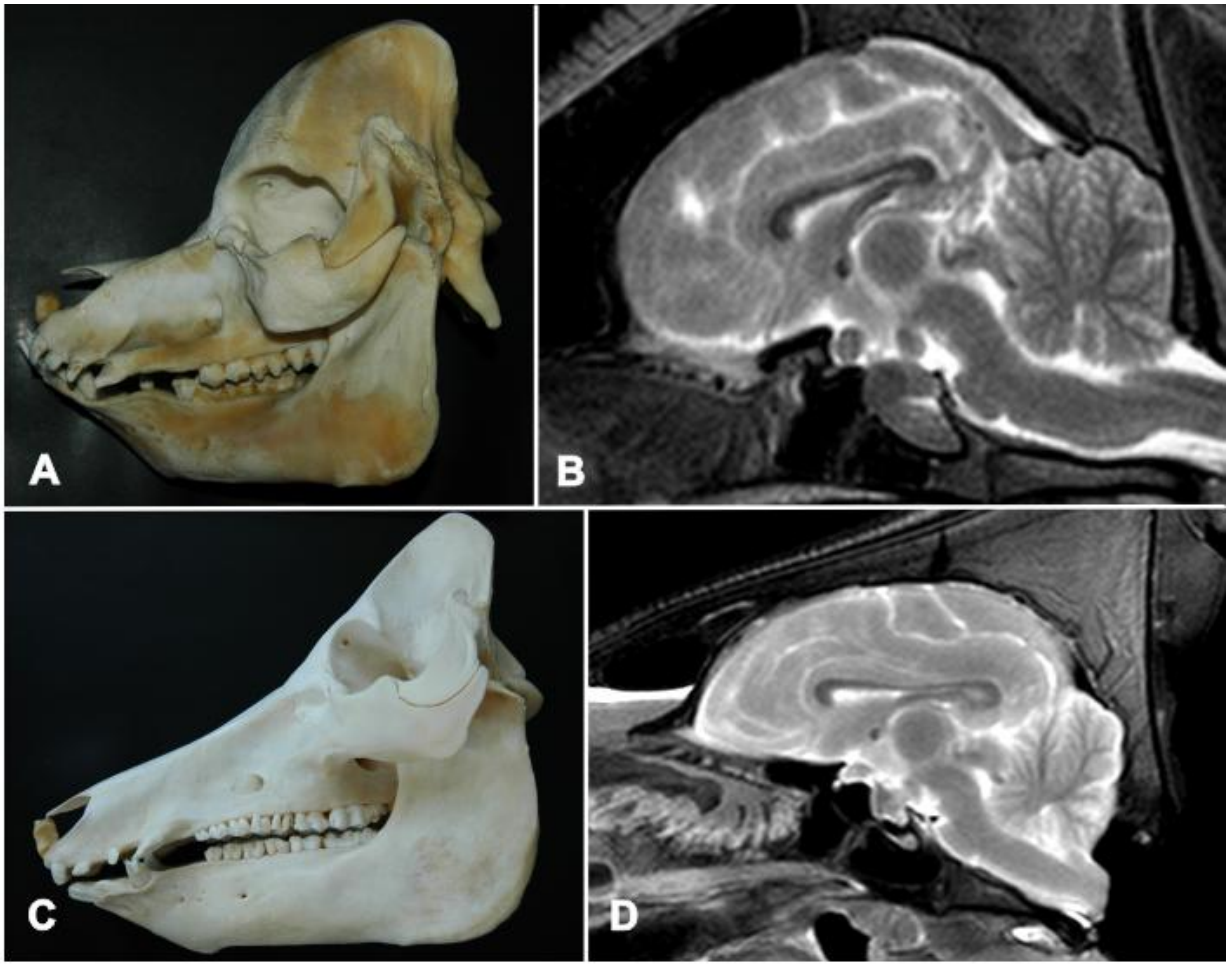

Figure 64

A: short nosed pig skull: B: Wiesenauer minipig MRI midsagittal; C: long nosed pig skull; D: wild boar brain midsagittal MRI. Note the differences in brain shape. The minipig brain seems rounder. The cerebellum appears to be rather square. The cranial and caudal lobes are of similar size, similar to the brachycephalic pug (Fig. 79 B) if not as pronounced the olfactory bulb and its fibres are shifted caudally (A-D courtesy of PD Dr. med.vet. (habil.) M. Schmidt).

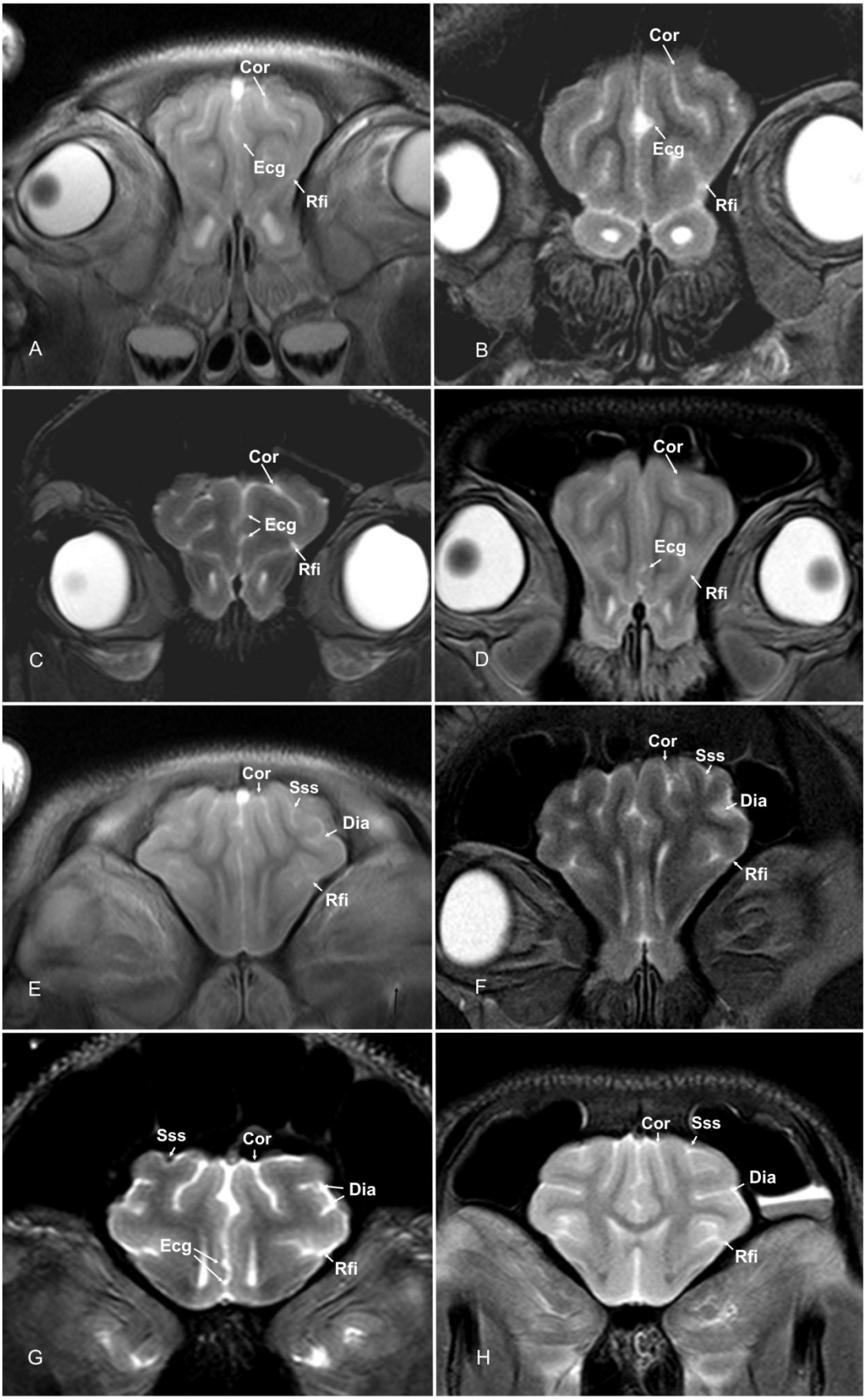
Cor
Ecg
Rfi
A
Cor
Ecg
Rfi
B
Cor
Ecg
Rfi
C
Cor
Ecg
Rfi
D
Cor
Sss
Dia
Rfi
E
Cor
Sss
Dia
Rfi
F
Sss
Cor
Dia
Ecg
Rfi
G
Cor
Sss
Dia
Rfi
H

Figure 65

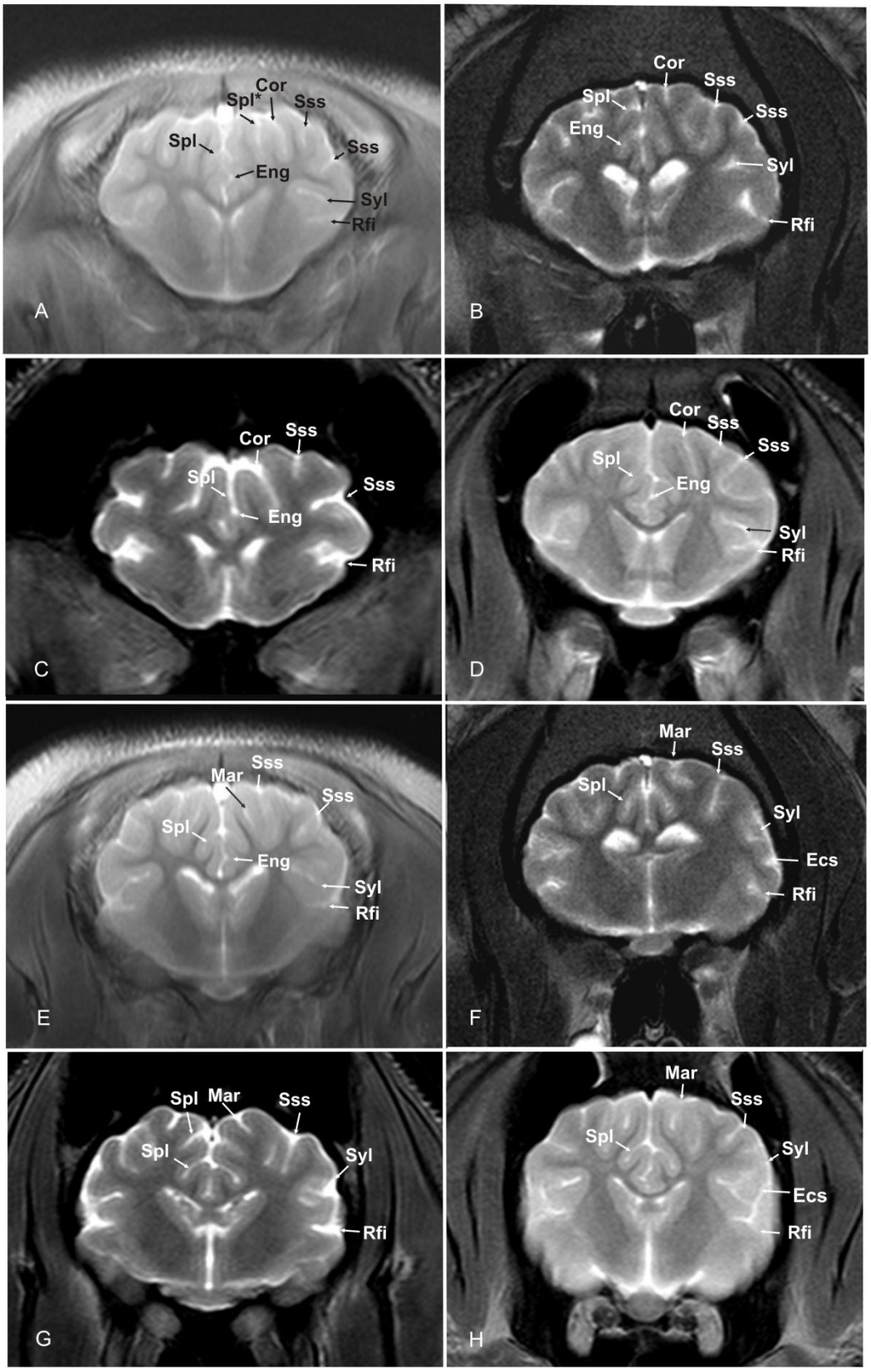
A
Spl*
Cor
Sss
Spl
Sss
Eng
Syl
Rfi
B
Cor
Sss
Spl
Sss
Eng
Syl
Rfi
C
Cor
Sss
Spl
Sss
Eng
Rfi
D
Cor
Sss
Sss
Spl
Eng
Syl
Rfi
E
Sss
Mar
Sss
Spl
Eng
Syl
Rfi
F
Mar
Sss
Spl
Syl
Ecs
Rfi
G
Spl
Mar
Sss
Spl
Syl
Rfi
H
Mar
Sss
Spl
Syl
Ecs
Rfi

Figure 66

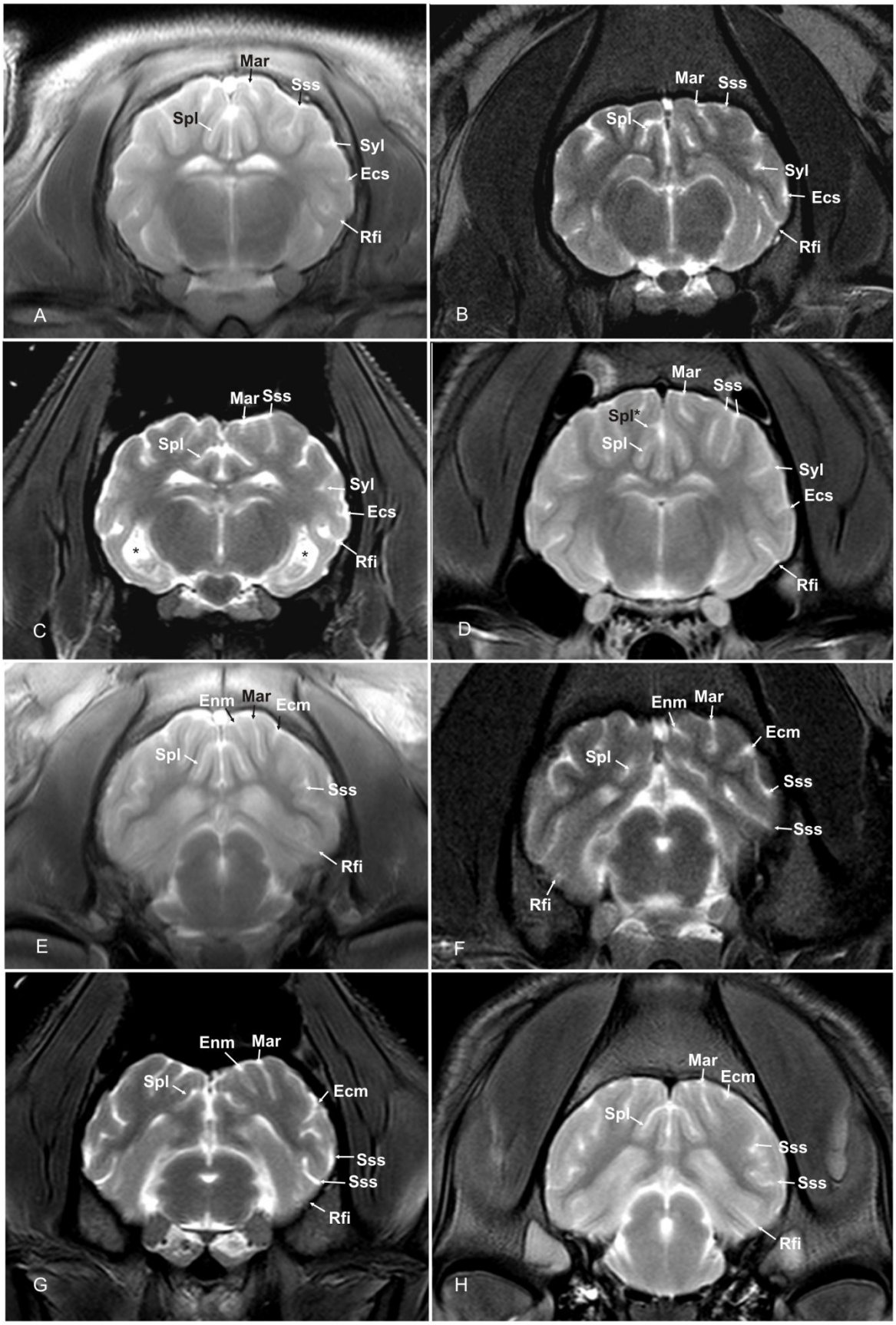
Mar
Sss
Spl
Syl
Ecs
Rfi
A
Mar
Sss
Spl
Syl
Ecs
Rfi
B
Mar
Sss
Spl
Syl
Ecs
Rfi
*
*
C
Mar
Sss
Spl*
Spl
Syl
Ecs
Rfi
D
Enm
Mar
Ecm
Spl
Sss
Rfi
E
Enm
Mar
Ecm
Spl
Sss
Sss
Rfi
F
Enm
Mar
Spl
Ecm
Sss
Sss
Rfi
G
Mar
Ecm
Spl
Sss
Sss
Rfi
H

Figure 67

Abbreviations figures 65-67:

A: Domestic pig, B: Wiesenauer minipig, C: Babirousa, D: Wild boar, E: Domestic pig, F: Wiesenauer minipig, G: Babirusa, H: Wild boar;
Cor: coronal sulcus; Dia: diagonal sulcus; Ecg: ectogenual sulcus; Ecs: ectosylvian sulcus; Eng: endogenual sulcus; Gen: genual sulcus; Mar: marginal sulcus; Rfi: rhinal fissure; Scl: sulcus of the corpus callosum; Sss: suprasylvian sulcus; Spl: splenial sulcus; Spl*: connecting sulcus; Syl: sylvian fissure (pictures courtesy of PD Dr. med.vet. (habil.) M. Schmidt).

5.5.5 Functional division of the pig's cortex

5.5.5.4 Frontal region of the cortex

The cortex of the rostral pole of the cerebrum is called prefrontal cortex (PFC). It was firstly described by Brodmann (1909) as an area specific to the primate brain. Since then, other scientists proposed that it could also be detected in other mammals (Jelsing et al. 2006 a). Rose and Woolsey (1948) characterized the prefrontal cortex as an area that is connected with the thalamic mediodorsal nucleus (Förstl 2005). For the purposes of a study conducted by Jelsing et al. (2006 a), the PFC was defined as the major reciprocal projection area from the thalamic mediodorsal nucleus (key definition according to Uylings and van Eden 1990). Jelsing et al. provide a map of the PFC in the young Göttingen minipig brain. The PFC seems to be rather large and seems to cover the rostral part of the superior frontal gyrus, the frontomedial cortex, the rostral cingulate gyrus and the rostral part of the insula inside the rhinal fissure (Fig. 68). Because of problems such as the precision of stereotactic injections and possible diffusion of injected tracer (manganese tracer) the result must be assessed with care. Jelsing et al. (2006 a) emphasise, that the reciprocal connectivity of the frontal cortex with the thalamic mediodorsal nucleus does not provide strict criteria for defining the PFC.

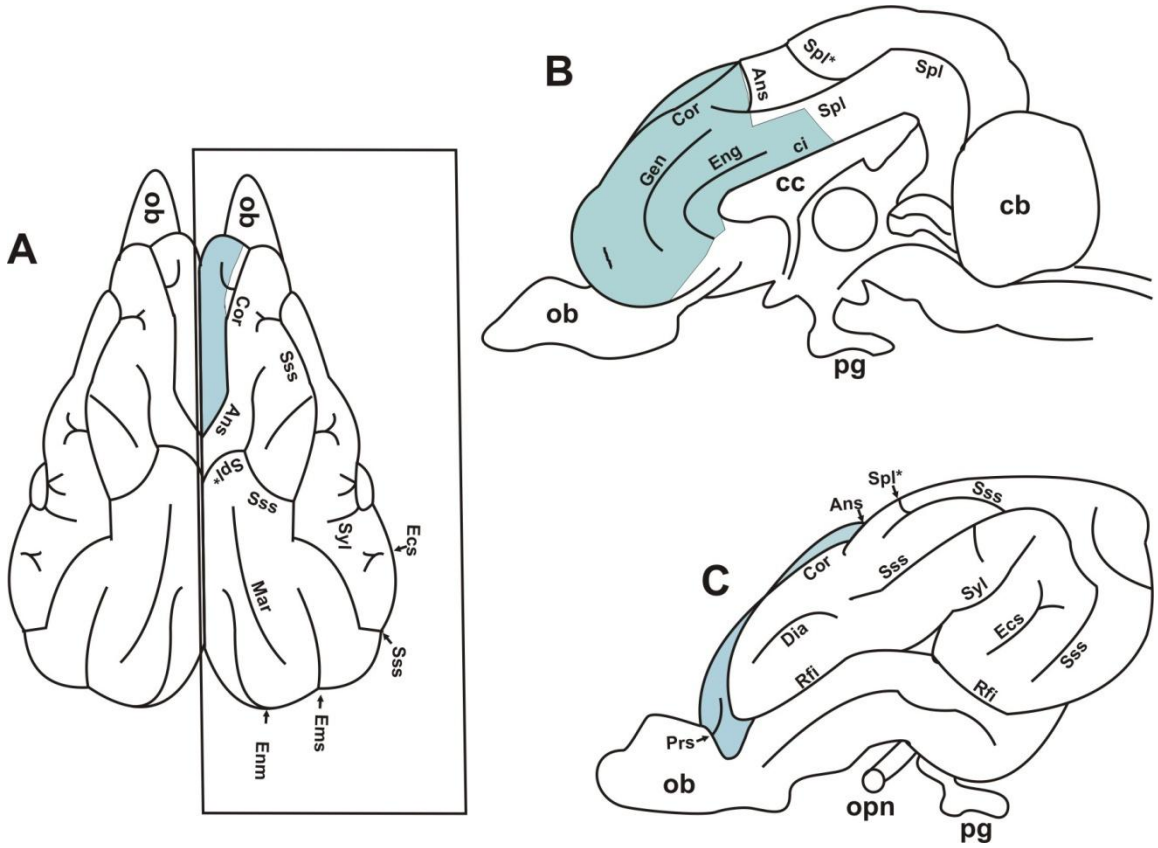

Figure 68

Prefrontal cortex of the Göttingen minipig brain (as proposed by Jelsing et al. 2006): Cytoarchitectonic and connectional data suggests that the Göttingen minipig has a structurally divided prefrontal cortex. The delineated PFC is rather large covering the rostral part of the superior frontal gyrus, the frontomedial cortex, the rostral cingulate gyrus as well as the rostral part of the insula (hidden within the deep rhinal fissure). A: dorsal view; B: medial view; C: lateral view of the prefrontal cortex (light blue areas);
Ans: ansate sulcus; cb: cerebellum; cc: corpus callosum; Cor: coronal sulcus; Dia: diagonal sulcus; Ecs: ectosylvian sulcus; Ems: ectomarginal sulcus; Eng: endogenual sulcus; Enm: endomarginal sulcus; Gen: genual sulcus; Mar: marginal sulcus; ob: olfactory bulb; opn: optic nerve; pg: pituitary gland; Rfi: rhinal fissure; Spl: splenial sulcus; Spl*: connecting sulcus; Sss: suprasylvian sulcus; Syl: sylvian fissure.

5.5.6 Primary and secondary somatosensory area of the porcine brain

The primary (S1) and secondary (S2) sensory cortex of the neonatal pig have been investigated by Craner et al. in 1991 and previously by Adrian in 1943 and Woolsey and Fairman (1946), who examined adult pig brains. The S1 of the pig seems to be very similar to the S1 of other mammals. The body surface projections are complete and somatotopically organized. They progress from hind limp to the head with medial to lateral locations in the cortex. The part of the body that is most important for the survival of the animal seems to have the largest cortical representation. This is supported by the fact that the rostrum of the pig used for rooting has a large representation (Craner and Ray 1991 a, Nickel et al. 1992). The representation of the rostrum region is located dorsal to the suprasylvian sulcus in the coronal gyrus (Fig. 69 A,B,C). Unlike SI, which possesses a disproportionately large representation of the rostrum, SII has no specialized representation of the rostrum. The secondary somatosensory region (SII) provides a more generalized representation of the total body surface and is located lateral to the rostral and middle suprasylvian sulci (Craner and Ray 1991 b).

5.5.7 Auditory cortex of the porcine brain

The auditory cortex and somatosensory cortex of the miniature swine (Andrews et al. 1990) and pig (Adrian 1943) were found to be comparable to those of other species (cat and monkey). The auditory region is positioned around sylvian fissure and the somatosensory cortex is placed around the central (dorsomedial suprasylvian) fissure (Fig.69 A).

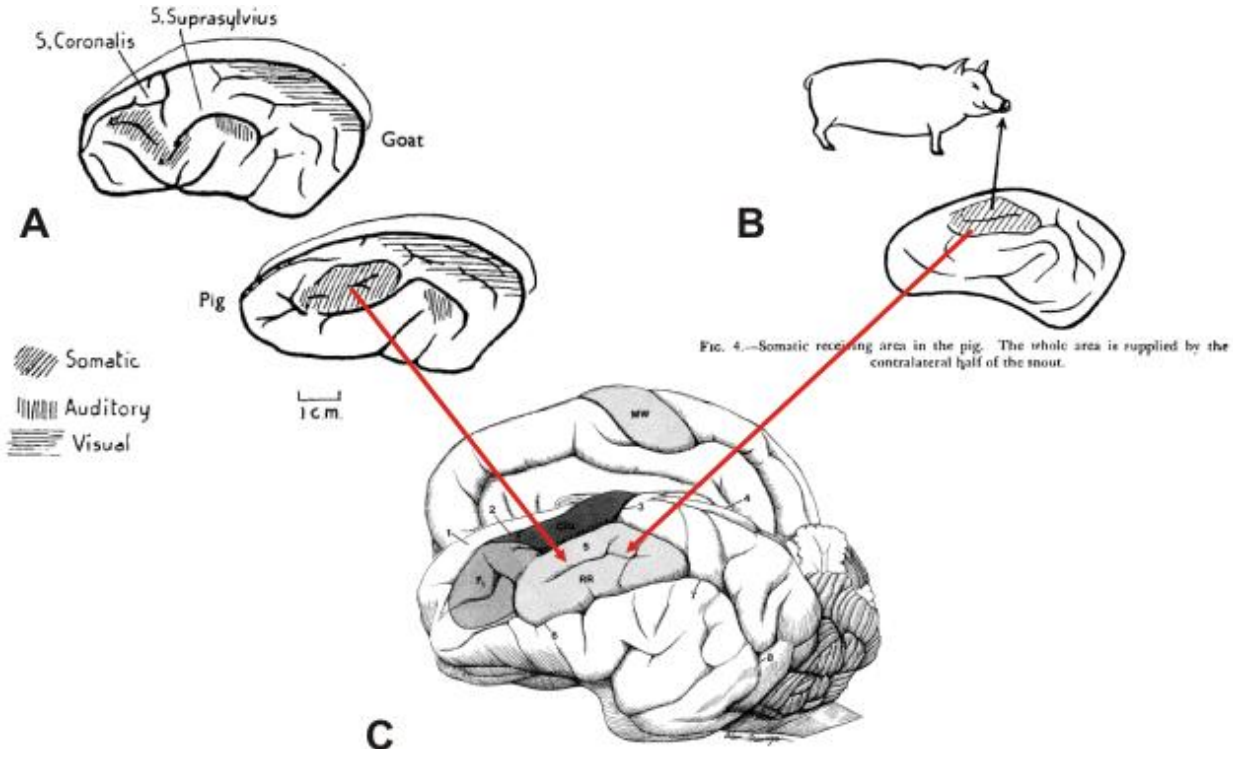

Fig. 4.—Somatic receiving area in the pig. The whole area is supplied by the contralateral half of the snout.

Figure 69
Somatosensory cortex of the porcine brain (taken from A+B: Adrian 1943 and C: Craner and Ray 1991). The representation of the rostrum region is located dorsal to the suprasylvian sulcus in the coronal gyrus.

5.5.8 Visual cortex of the porcine brain

The most characteristic and well defined area of the visual cortex (Fig. 69 A, Adrian 1943) is the so called area striata/striate area. On account of its special morphological character and its physiological importance, its relation to vision, the area striata has been investigated with high interest in a lot of species (Bright Funkhouser 1915, Adrian 1943, Lakshminarasimhan 1974, Barbier et al. 2002, Gizewski et al. 2007). In the human brain it is possible to identify with the naked eye a stripe of white fibrous matter lying tangentially within the grey substance. This

stripe is called the stripe of Gennari. In the pig and domestic mammals the visual cortex extends over the convexity of the occipital lobe including the endomarginal, marginal and splenial gyri (Fig. 69 A). Although secondary gyri complicate the identification in domestic herbivores, the visual cortex and its macroscopic structural representations in the mentioned gyri, seem to be very constant amongst the domestic animals (Nickel et al. 1992).

5.5.9 Motor cortex of the porcine brain

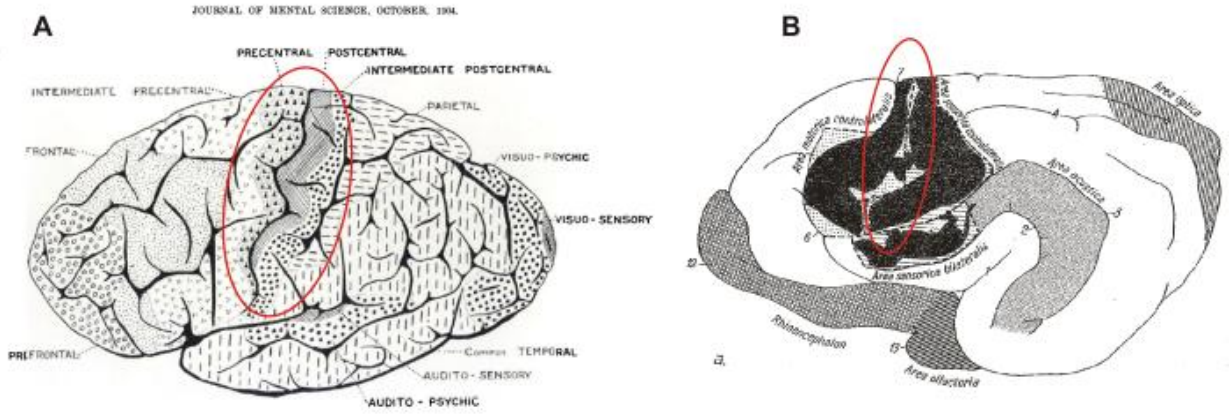

Figure 70
In literature the central sulcus (A) of humans and primates is often homogized with the cruciate sulcus of the dog (B). The central sulcus (A) and the cruciate sulcus (B) are marked with a red circle. The cruciate sulcus of the canine brain is positioned cranial to the motor area (marked by figure 7).
Pictures courtesy of Campbell 1905 (A) and Nickel et al.1992 (B, according to Campbell 1905, Marquis 1934, Tunturi 1950, Woolsey et al. 1952, Pinto et al. 1956 and Woolsey 1960.

In the porcine brain we find the motor area according to Breazile et al. 1966 and Palmieri et al. 1987 between cruciate and coronal sulci (Fig.71). The authors chose to name the sulcus cranial to the motor area “cruciate sulcus”. This seems to homologize this cruciate sulcus of the pig with the cruciate sulcus of the canine and feline brain, which is also positioned cranial to the motor area (Fig.70 B). The motor area of the human and primate brain is positioned rostrally to the central sulcus (Campbell 1905, Nickel et al. 1992) in the so called gyrus praecentralis, while

the somatosensory area is positioned caudally to the central sulcus in the postcentral gyrus (Fig. 70 A). In literature the cruciate sulcus of the canine and feline brain is often homologized with the central sulcus of the primate and human brain. But the somatosensory area of dog and cat includes the postcruciate and the rostral suprasylvian gyrus. Furthermore their cruciate sulcus is positioned in a praecentral position. It seems therefore problematic to homologize the central and cruciate sulcus and use the terms “precentral” and “postcentral” in domestic mammals (Fig. 70, Nickel et al. 1992).

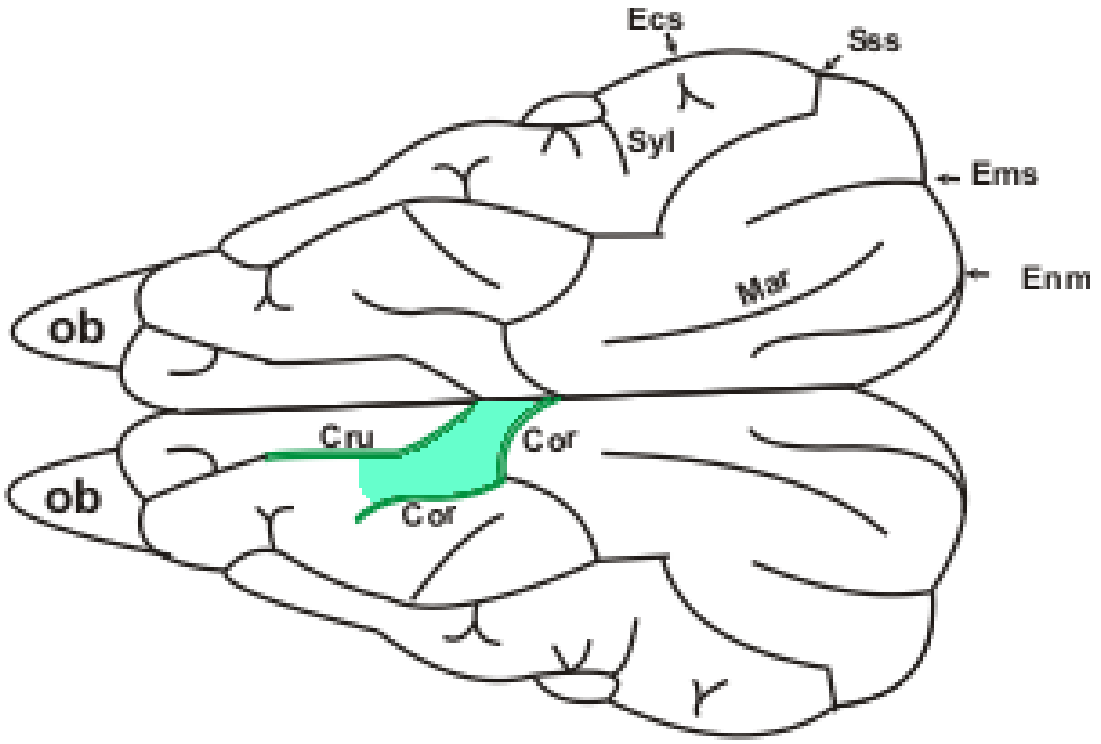

Figure 71

The motor area of the porcine brain is positioned on the lateral surface (according to Breazile et al.1966 and Palmieri et al. 1987). The motor area is positioned between the “cruciate” sulcus and the “coronal sulcus”. Compare with Fig. 70 (cruciate sulcus and central sulcus). ©Verena Schmidt.

5.5.10 Pituitary gland and rete mirabile in MRI

The hypothalamus of the pig was investigated by a number of authors (Solnitzky 1939, Welento 1964, Szteyn et al. 1980, Seeger 1990). The hypothalamus is the most ventral part of the diencephalon forming the bottom of the 3rd ventricle bordering the optic chiasm caudally.

The basisphenoid bone is strongly developed in pigs with a cranially oriented dorsum sellae forming a rather deep recessus (Sisson 1953). In the horse it is not possible to confirm a recessus. The pituitary gland is positioned on top of the basisphenoid bone, as can be seen in the midsagittal scan of the equine brain (Fig. 72 B).

The pituitary gland of the pig is elongated with a rather long pituitary stalk and points in caudal direction (Fig. 72 A+D, see also Nickel et al. 1992). It is important to mention the blood vessels surrounding the pituitary gland (pg: Fig. 7, Fig. 28-30, Fig. 34-40). The vessels seem to be often collapsed in post mortem MRI scans. Blood can be curdled and oxidized, impacting dramatically on the signal quality. In the scans of the pig brain the vessels are visible as a hypointens area (pointing ventrocaudally). It is known as rete mirabile (rm: Fig. 28-30; Fig. 72, Burbridge et al. 2004). Because of the hypointensity of the signal the structure could be mistaken for an artefact (for example air sucked in during preparation of the skull). The pituitary gland of the pig seems well developed and extends to the rostral end of the pons (Fig. 30, Fig. 72). Its tuber cinerum is difficult to identify in the MR images, but the infundibular recess (ir: Fig. 6) and the mammillary body can be seen (mb: Fig. 28-30, Fig. 38). The mammillary body is divided into two parts in the canine brain but uniform in the other domestic animal species (small ruminants might show a division into two parts) the mammillary body contains two nuclei on either side (Nickel et al. 1992). According to Seeger 1990 the ventromedial hypothalamic nucleus of the pig is the most dominant part of the mammillary body. Unfortunately the individual nuclei could not be visualized in MRI, but a three dimensional study of the pig's hypothalamic nuclei was conducted by Stzeyn et al. 1980, who examined "large white Polish" pigs. A detailed description of the hypothalamic nerve centres of the pig was delivered by Welento (1964).

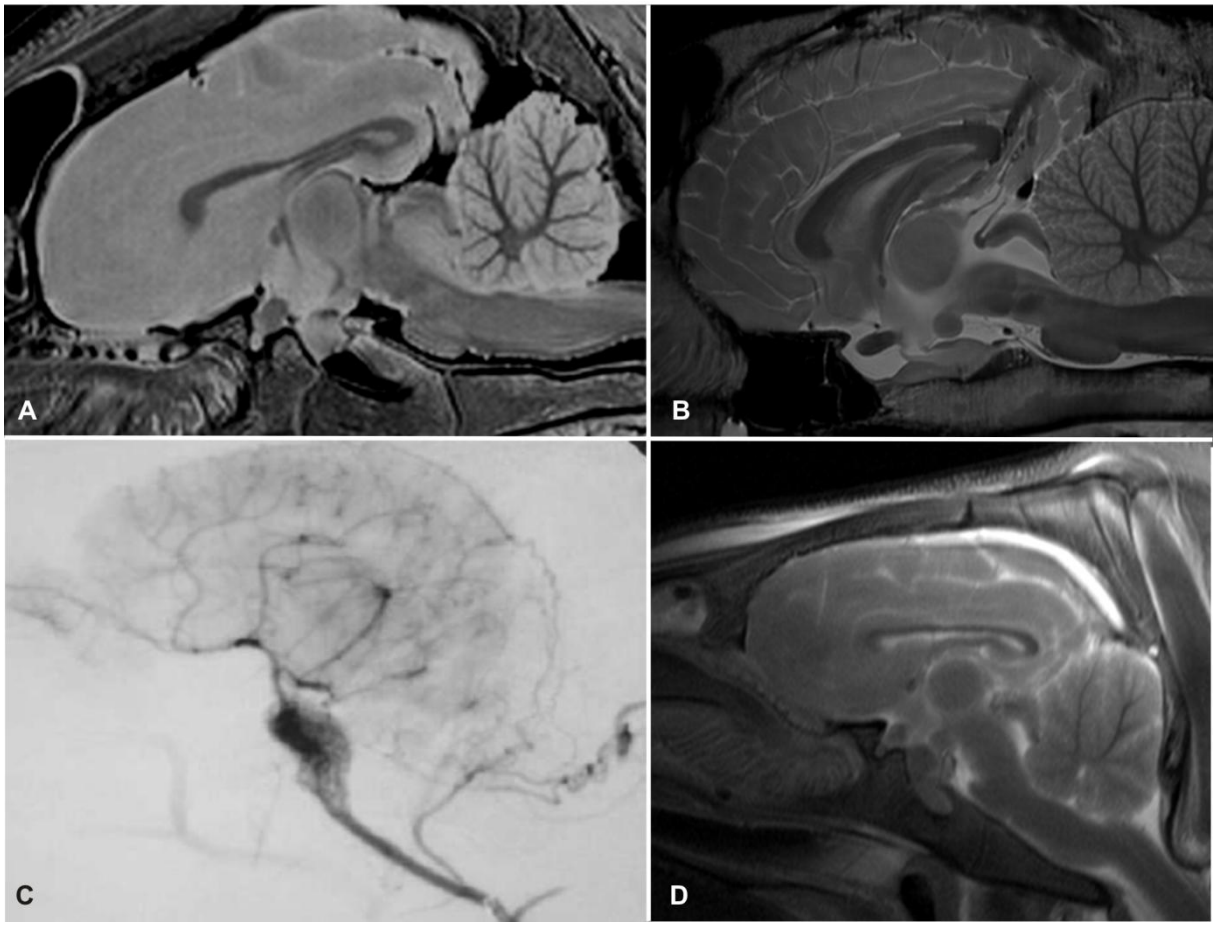

Figure 72

A: midsagittal scan of the porcine brain; B: midsagittal scan of the equine brain C: Angiogram of the right ascending pharyngeal artery in the pig. The lateral projection demonstrates the rete mirabile to better advantage (taken from Burbridge et al. 2004). D: midsagittal scan of the porcine brain (A, B, D courtesy of PD Dr. med.vet. (habil.) M. Schmidt).

5.5.11 Cerebellum

Larsell (1954) studied the morphology of the mammalian cerebellum intensively and describes the organ's homologous design. Since the characteristic shape of the mammalian cerebellum can be traced back to simply structured archetypes, the morphology of this organ is best understood when keeping its simply shaped origins in mind. The cerebellum of amphibians is made up of a single, undivided corpus cerebelli forming the roof of the fourth ventricle (Nickel et al. 1992, Butler and Hodos 2005). In phylogenetically higher ranking specimen the corpus cerebelli is consequently divided through transverse fissures into a number of smaller sections called lobes. The individual sections, the lateral parts in particular, grew larger in the evolutionary process forming the cerebellar hemispheres. The original division into lobes is still preserved in the vermis of the cerebellum throughout the domestic animal species including the pig (Fig. 73 and Fig. 74). The cerebellum also experienced a volume/size growth originating from the vermis towards the hemispheres and in caudal direction. The actual size of the cerebellum is variable amongst vertebrates. Care has to be taken not to simply compare the cerebellar size since animals can vary significantly in body size (Butler and Hodos 2005). The nomenclature still treats the vermis (due to its prominence) as a singular, morphologically separate structure. The individual parts of the hemispheres are named without taking the morphological and functional connection with the vermis into consideration (Nickel et al. 1992). Unlike the vermis of the human brain, the vermis of the domestic animals is very prominent and especially so in the porcine brain. The imposing size of the pig's vermis in our examined specimen is only surpassed by the size of the vermis of the sheep. The vermis nearly equals the hemispheres in size (Fig. 74). Seen from above in the native photograph (Fig. 74 J.) the cerebellum of the pig with its laterally expanding hemispheres appears to be triangular in shape. The cerebellum of the ruminants in comparison is rather round shaped and the cerebellum of the horse seems square (Fig. 74).

The vermis is best examined in the midsagittal scans (Fig. 30, Fig 73) as explained in the result chapter. The rostral lobe is divided from the caudal lobe by the primary cerebellar fissure (Prf: Fig. 27-30, Fig. 73), the first fissure during ontogenesis that divides the primordial cerebellum. It appears to be smaller than the caudal lobe in the fixed pig brain. The formalin fixed specimen in this study was scanned over-night (8

hours) following fixation. Unfortunately there is no data available about the average size of the caudal and rostral lobes, but we suggest that this finding resembles the majority of cases. The hybrid pigs were 5 month old at time of scan. At this point of ontogenesis the juvenile pig brain should resemble the brain of the adult pig (according to Pond et al. 2000). The caudal lobe of the examined sheep's cerebellum is also noticeably larger than the rostral lobe (Fig. 74 C), not unlike the caudal lobe of the fixed pig's cerebellum.

In this study it was possible to identify the most important fissures dividing the cortex and the medulla of the cerebellum using MRI. The names of the subdivisions especially of the vermis are historical and -although controversially discussed (Bradley 1903) - still used today (Nickel et al. 1992). The medulla of the cerebellum is well developed in all our domestic animal species. In the pig and horse the corpus medullare and its branches are relatively thin compared to those of the ruminants' cerebellum (Fig. 74). The similarities between the cerebellum of horse and pig continue with the rather oval (higher than wide) shape of the vermis in midsagittal scans. The cerebelli of the ruminants in the midsagittal scans are round (sheep: Fig. 73 C) and square (calf: Fig. 73 F). The rostral and the caudal lobe of the vermis are similar in size in all featured mammals with exception of the sheep and pig (the rostral lobe is smaller) in the midsagittal images (Fig. 74 C). But looking at the total surface area of the cerebellum, it becomes clear that the rostral lobe in all animals is not as developed as the caudal lobe. The hemispheres are nearly completely extensions of the caudal lobe. The caudal poles of the cerebral hemispheres leave a gap and the cerebellum is positioned in between the hemispheres and not under the cerebrum as seen in the dorsal photographs of the cerebellum (Fig. 74 A,D,G,J). The tentorium cerebelli osseum (see also Fig. 80) is missing in the porcine skull and this facilitates contact between cerebellum and cerebrum. The mesencephalic margin (caudal rim of the cerebrum) of the ruminant's brain overlaps the caudal end of the lamina quadringemina and pushes the caudal colliculi ever so slightly in ventral direction. The mesencephalic margin of the pig's brain and to a certain extend the horses causes a depression of the rostral colliculi (roc: Fig. 13, Fig. 25-30, Fig. 42-45). This can't be interpreted as an intra cranial pressure increase. Whether the recessus tecti of the fourth ventricle of pig (rtv: Fig. 73) and horse are also compressed, can't be confirmed. The lateral extensions of the rostral lobe (lobus anterior) are difficult to identify in the porcine scans. The quadrangular lobule (lobulus quadrangularis) can be detected lateral of the culmen in dorsal photographs (Fig. 74)

because of its cranial extending medullar branches and lobules. The lobulus simplex, the first lobe after the primary fissure that extends from the declive is only weakly developed in the domestic animal species featured (Fig. 73).

The characteristic s-shaped bend of the caudal vermis originates in the declive. There seems to be no rule as to why this shape actually develops. Only Bolk (1906) describes a relationship between the bend of the tuber, folium and declive of the vermis (together forming the median cerebellar lobe) and development and growth of the ansiform lobule (ans: Fig. 11-16, Fig. 21-27, Fig. 47-52). He proposes that the sharper the bend of the median lobe is the smaller the ansiform lobule becomes. This can be seen in the horse (Fig. 73 G-I). This relationship can be more clearly observed in dorsal scans. The caudal crus (crus caudale) of the ansiform lobule extends in ventral direction. The vermis (Fig. 73 j-l) of the pig is straighter and cranial and caudal crus of the ansiform lobule are on one level. In the pig brain the tuber (tu: Fig. 14-16, Fig. 25-26, Fig. 72) of the vermis is different to that of the other species. All of the examined pig brains show a medullar branch that ends right at the surface of the tuber of the vermis. This medullar branch does not seem to be covered by cerebellar cortex. Interestingly this happens in an area of strong development - the region of the tuber vermis. The growth of the tuber results in lateral deviation of the caudal part of the vermis causing an S- shaped bend. This was first observed by Schultz (1953) in his histological examinations of the pig's cerebellum. It has been proposed to be a developmental impediment, thus creating a mechanical barrier due to a lack of space or compression through blood vessels (Cohrs and Schulz 1952). It was also described to be a physiological cortical aplasia (ca: Fig. 28-29; "physiologische Rindenaplasie") that can't be identified in other domestic mammals (Done 1986, Done and Herbert 1986, Nickel et al. 1992). The medulla of the paramedian lobule (pml: Fig. 10-13, Fig. 22-26) merges with the caudal crus of the ansiform lobule (ans: Fig. 11-16, Fig. 21-27, Fig. 47-52) that runs parallel with the medulla of the vermis. The paramedian lobe does not show any interspecific variations, while the shape of the paraflocculus (paf: Fig. 9-13, Fig. 19-21, Fig. 46-52, Fig. 72) is extremely variable. Comparing the relatively simple structure of the lobules of the pig (midsagittal scan) with the midsagittal scans of other domestic ungulate brains, we can see that the lobules branch off from the marrow of the arbor vitae into a number of secondary and tertiary lobules. The cerebelli of the featured ruminants show the most branches. The pig's laminae medullares cerebelli are thin,

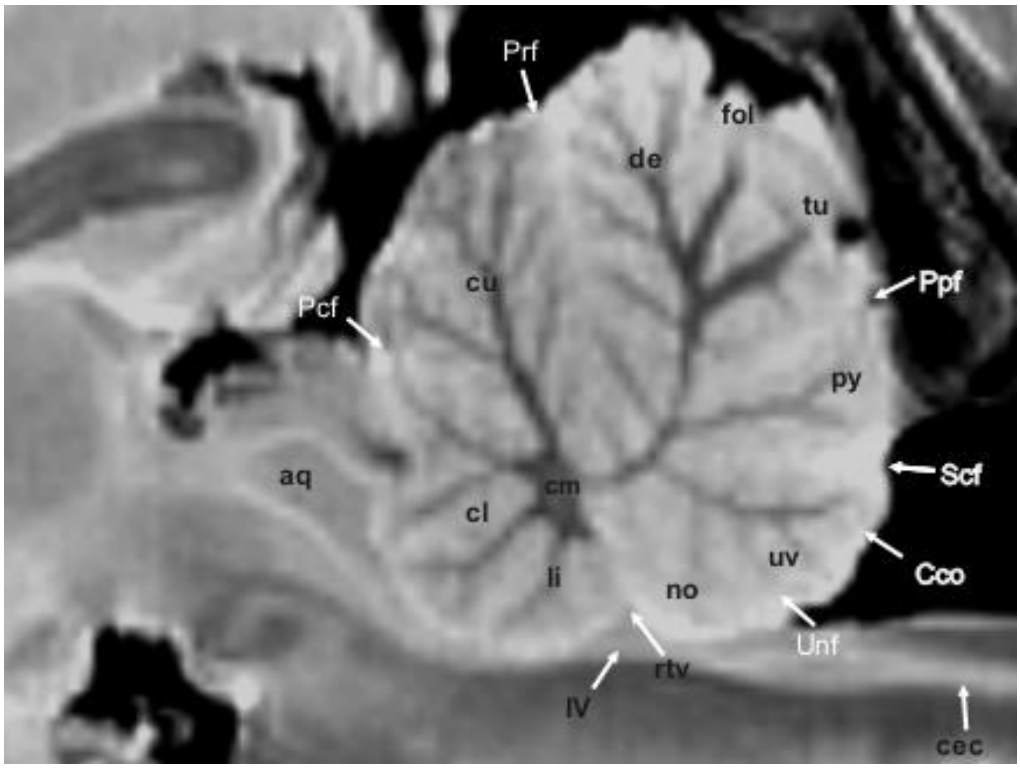

Figure 73
Cerebellum of the pig (sagittal section through the middle of the vermis): aq: mesencephalic aqueduct; Cco: cerebellar cortex; cl: central central lobule; cm: corpus medullare; cu: culmen; de: declive; fol: folium; li: lingula; no: nodulus; Pcf: preculminate fissure; Ppf: prepyramidal fissure; Prf: primary fissure; py: pyramis vermis; rtv: recessus tecti ventriculi quarti; Scf: secondary fissure; tu: tuber; Unf: uvulonodular fissure; uv: uvula; IV: fourth ventricle (picture courtesy of PD Dr. med.vet. (habil.) M. Schmidt).

especially in native scans and the contrast between medulla and cortex is weak. A better contrast can only be achieved through longer scans of the fixed pig brain. The surface of the pig's cerebellum appears to look similar to that of carnivores (like dogs and cats), with its delicate system of gyri and sulci (Nickel et al. 1992). It is connected to the brain stem by the cerebellar peduncles (pcc, pcm, pcr) and the medullary vela (rostral and caudal) and lies dorsal to the pons (po: Fig. 28-30, Fig. 45) and medulla oblongata. It is divided from the cerebral hemispheres by the transverse fissure. The cerebellum of the babirusa appears square. Not unlike the cerebellum of the calf the babirusa's rostral and caudal lobe nearly equal in size (as can be seen in Fig. 63 C). This was also the case in the scanned brachycephalic Wiesenauer minipig (Fig. 63 B). While investigating the cerebellar nuclei and internal grey substance, Bujak (1974) noticed differences between the cerebellar nuclei of domestic pigs and the cerebellar nuclei of the wild boar. The nuclei seem to be more distinctly separable in the wild boar. The MR-images do not reveal differences between the cerebellar nuclei of the domestic pig and the wild boar.

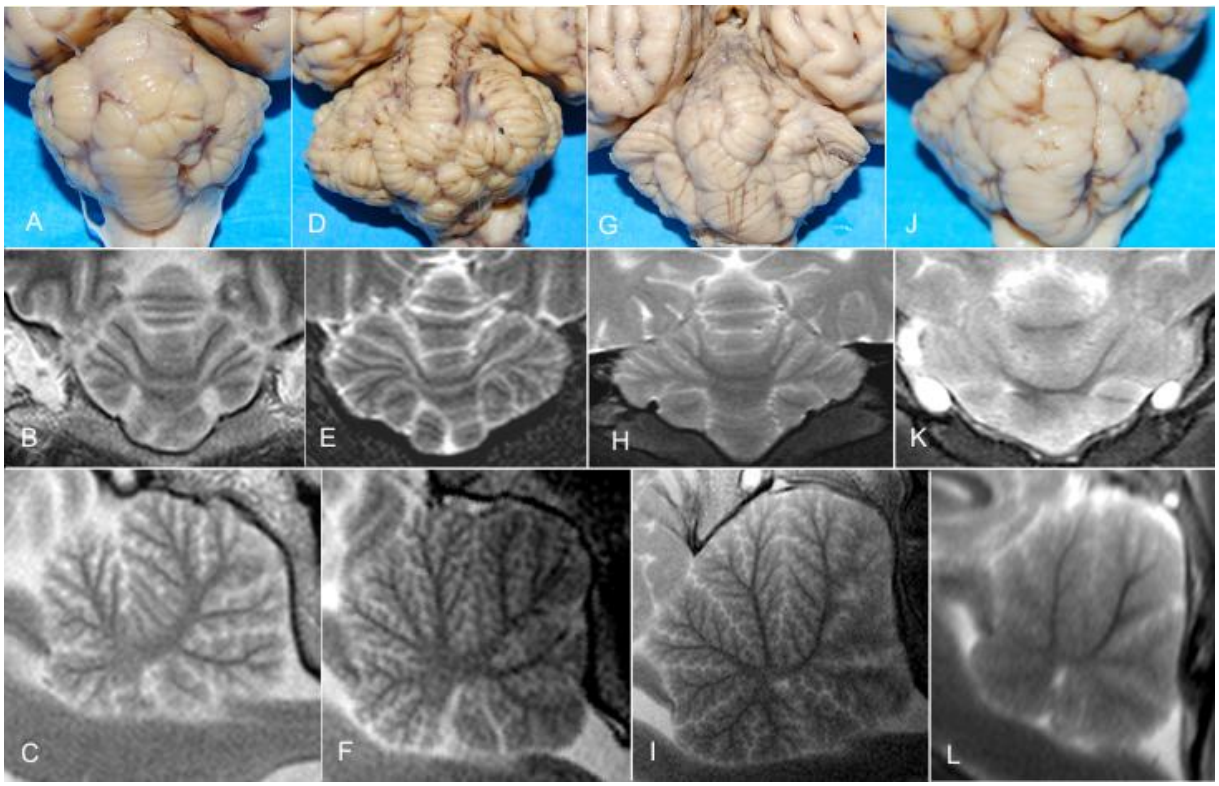

Figure 74

Dorsal photographs (A,D,G,J), dorsal (B,E,H,K) and midsagittal (C,F,I,L) MRI scans.
A-C: ovine cerebellum; D-F: bovine cerebellum (calf); G-H: equine cerebellum; J-L: porcine cerebellum (A-L courtesy of PD Dr. med.vet. (habil.) M. Schmidt).

6 Discussion

Although the main structure (Grundbauplan/blueprint) of the mammalian brain shows a large number of similarities, species differences exist (especially size of the telencephalon, shape etc.) that can make it difficult to differentiate between pathological and physiological structures in brains of specimens that are not regularly examined in MRI (such as the pig). This study aimes describe the brain of the domestic pig (*Sus scrof*a *domestica*) as detailed as possible using a 1 Tesla MRI scanner and is so far the first and most complex textbook MRI-atlas of its kind. It includes 13 dorsal, 12 sagittal and 22 transversal images. In order for a brain atlas to be successful it is important to match the anatomy of the individual specimen with the representation of the anatomy in the atlas (Toga and Thompson 2001). It is therefore vital to scan as many individuals as possible to reflect the anatomy of the majority of individuals. In this study the 10 hybrid pig brains scanned showed little variation in brain structure amongst each other. But every specimen behaved slightly different in MRI as their heads varied slightly in size and also the scans taken did not always capture the exact same plane.

Also the interspecific differences of the brains of different members of the suidae including the wild boar, the Wiesenauer minipig and the babirusa need to be discussed. Where appropriate the pig brain is furthermore compared with brains (in scans and formalin fixed), atlases and studies (Roschig 1907, Anthony and de Grzybowski 1930, Anthony and de Grzybowski1931, Anthony and de Grzybowski 1937, Ciliga 1937, Lauer 1963, Lauer 1982, Cohn and Papez 2004, Schmidt et al. 2009, Schmidt et al. 2011) of domestic animals and ungulates to highlight differences. The brain of the domestic pig in situ is surrounded by the meninges and is positioned within the cranial cavity of the skull. In comparison to the skull the brain of the pig is relatively small and its volume takes up 1/8 of the skull as seen in Fig. 75 (Flatau and Jakobsohn 1899). The cranial cavity in pigs and ruminants is divided by the cruciform eminence (see Fig. 80) and when the brain is in situ, only the membranous tentorium cerebelli divides the cavity into a large rostral part, containing the telencephalon, the diencephalon and the mesencephalon and smaller caudal cavity containing the metencephalon and mylencephalon (Nickel et al. 1992).

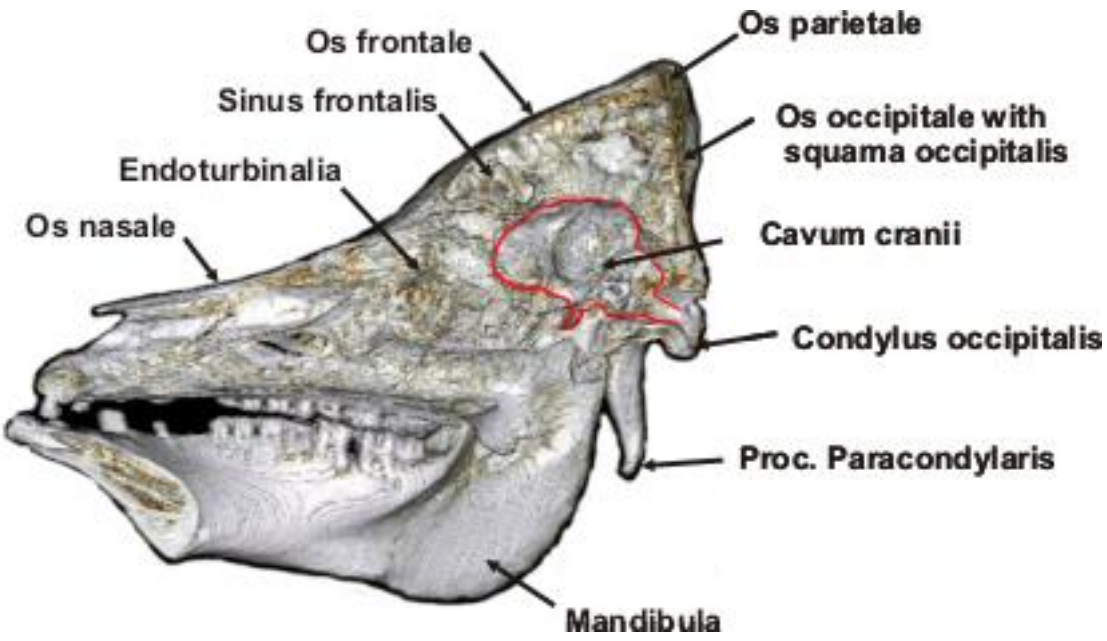

Figure 75
Midsagittal view of the virtual reconstruction of the skull of an adult domestic pig, demonstrating the dimensions of the neurocranium relation to dimensions of the viscerocranium. CT scan © Verena Schmidt

In the pig the cruciform eminence resembles two barely visible ridges that cross over at the most dorsal aspect. In sagittal MR images liquor should be visible between cerebrum and cerebellum and not hypointense bone signal. This can be seen in the native sagittal scan of the babirusa (Fig. 63 C). The tentorium cerebelli is believed to have emerged relatively late in phylogeny as bilateral folds of the dura mater on either side of the brainstem in the cerebro- cerebellar fissure and is ossified in other domestic animals like the horse (Klintworth 1986, Nickel et al. 1992). This in conjunction with the pig's rhienencephalonindex (rhienencephalon in % of neopalliumindex, Nickel et al. 1992) could indicate a lower phylogenetic rank.

6.1 The neocortex of the pig

The MRI study confirms that the brain of the domestic pig is not as convoluted as the brain of other ungulates. It is characterized by la large rhinencephalon and a stable surface pattern as shown in the brain scans of the pig breeds in this study.

It has been postulated that the bigger the neopallium (size, convolution) in relation to the rest of the brain is, the higher the brain is placed in the “phylogenetic hierarchy”. This is known as cerebralization. The artiodactyls (including the domestic pig) and terrestrial herbivores are depending on olfactory signals to interact socially and their intensive olfactory abilities (as macrosmatic animals) are reflected in a well developed rhinencephalon (Lauer 1982, Salazar et al. 2004). A criterion of the degree of cerebralisation is the neopalliumindex. Men, elephants and primates for example have a very high neopalliumindex. Their rhinencephalon is extremely small in relation to the neopallium. The pig’s neopalliumindex is ranked below that of primates, bovines and felines but above the neopalliumindex of canines (Nickel et al. 1992). Interestingly the non-olfactory components of the rhinencephalon - the limbic system (hippocampus), seem not as well developed in relation to the peripheral components of the olfactory system. However, a direct correlation between the dimensions of these brain parts has been questioned (Reep et al. 2007). The hippocampus of the pig is characterised by a general cytoarchitecture, similar to that of other mammals (Saito et al. 1998). The archipallium used to be purely responsible for the correlation of olfactory information with other sensory information. But with the development of the neopallium and reduction of the importance of the olfactory sense the archipallium moved to the medial wall of the hemisphere (Dyce et al. 2002).

It is not possible in this study to determine whether the size of the porcine rhinencephalon can be linked to the pig’s extremely sensitive olfactory sense or to a rather low evolutionary position. Artiodactyls use olfactory cues in a wide variety of social interactions (Hart 1983; Deutsch 1992), but the MRI images are solely able to capture the pig’s large rhinencephalon (and small neopallium) with its dorsally positioned lateral rhinal fissure (Rfi: Fig. 13-14, Fig. 19-22, Fig. 31-48), in comparison to other domestic animal species.

6.2 Gyrification

Among the most distinctive morphological features of vertebrate brains is the evolutionary expansion of the cerebral cortex (Hofman 1985, Barton 2007). By comparing the scans of the pig brain with our scanned brains of sheep, calf, deer, horse and alpaca (Fig. 53) the different degrees of gyrification as well as differences in size and shape of the hemispheres become apparent.

It is known that the level of cortical gyrification varies across mammals of different brain sizes but very little is known about the influences triggering the emergence of the special pattern of grooves and ridges in the brain (Stark 1954). In the ferret (the smallest laboratory animal with a folded cortex) the gyrus formation was studied by firstly investigating the external features of the pallium during the folding process and secondly by describing the histological changes occurring within a gyrus as it develops and grows. It was observed that gyri are formed by longitudinal and radial expansion of the cortical department. Gyri occur between relatively fixed areas which form the sulcal floor. The hemispheres are also subjected to moulding by the growing skull. During that process the frontal pole of the cerebrum becomes pointed while the sulcal walls become closely opposed and the gyral crowns flattened (Smart and Mc Sherry 1986 a, Smart and Mc Sherry 1986 b). Pillay and Manger (2007) examined 25 different mammalian species and support the theory that, with increasing brain size and size of the mammal (actual mass of the periphery serviced by CNS), the gyrencephaly increases (Kuhlenbeck 1927, Stark 1982, Welker 1990, Nieuwenhuys et al. 1998, Danckers 2003). They also found ungulates to be the mammals with the most gyrencephalic brains. When species of similar brain weights were compared ungulate brains were significantly more gyrencephalic. It also seems to be the fact that large brains tend to be more convoluted than small brains due to the disproportionately small changes in cortical thickness (Hofman 1985). Minipigs, when kept under appropriate conditions (e.g. restrictive feeding) remain small, while a fully grown wild boar or landrace pig are larger in size and weight. Allometric growth doesn’t seem to contribute to the emergence of additional cortical areas or a significantly different organisation of the system of gyri and sulci (Fig. 63, Fig. 64-67). This study shows that within the suidae only few differences exist.

Oboussier (1967 and 1971), while investigating phylogenetic relations of different African bovidae, summarises her findings (relation of neocortex surfaces to

bodyweight) as follows: “One must conclude that (amongst *bovidae*) different evolutionary paths were taken 1. Different degree in size of the neocortex surface and 2. The same neocortex surface size is obtained by a) fewer and deeper or b) multiple and more superficial sulci.

Shultz and Dunbar (2006) describe ungulates as a group with relatively simple patterns of resource use but with varied social behaviours. Their statistical study suggests that relative brain size is independently associated with sociality and social complexity and habitat use. The relative neocortex size is associated with social but not with ecological factors (habitat). Barton 2007 comes to the conclusion that the evolution of mammalian cortical structure is closely associated with specialisation for different sensory niches. Barton believes that functionally differentiated cortical areas evolve independently from one another (adaptive specialisation).

Amongst the suidae (as members of the artiodactyls) the brains of European domestic pigs, wild pigs and feral pigs (Galapagos Islands) were examined (Kruska 1988, Kruska et al. 1970, Kruska and Röhrs 1974). The studies reveal that the brain of the wild pig is bigger and more gyrated than the brain of the domestic and feral pig. They also established that the return of the domestic pigs to the wild did not result in a larger brain (in relation to body size) of the feral pig. It seems that the reduction in brain size caused by domestication - domestic pigs have a 33, 6 % smaller brain (Röhrs and Ebinger 1999) - is not reversible. This theory is supported by brain studies of feral dogs (especially the Australian dingo), cats, goats, donkeys and sheep (Kruska 1970, Ebinger 1974, Röhrs and Ebinger 1999). A relationship seems to exist between the degree of cerebralization and reduced brain size due to domestication. Mammals with larger brains (artiodactyls, carnivores) seem to show a greater decrease in brain size during domestication than for example rodents. Comparisons of individuals within an order demonstrate that the level of brain evolution may not be the only factor influencing size reduction due to domestication. Species-specific variations in the level of brain size reduction could result in a gradually different reduction in total function (Kruska 1988).

Renewed interest in the gyrification of the insula region was sparked by the discovery of functions attributed to this area of the cortex such as visceral sensory, visceral motor, somatosensorial and supplementary motor area (Russo et al. 2007). Of the artiodactyl brains compared in this study, the opercularisation appears least advanced in the porcine brain, while it is more advanced in the brain of ruminants. The level of gyrification of the insular region seems to reflect the complexity of the

gastrointestinal tract (Russo et al. 2007). In ruminants we find a complex system of different compartments with highly specified individual functions, while the pig is monogastric. During ontogenesis the insula together with the striate body remain in place, while the pallium growth arch like caudoventrally around this area in order to maximise its mass. As a consequence the temporal lobe is formed. This ontogenetical process is also called temporalisation. Finally the insula can be found at the bottom of the sylvian fissure, often completely obscured by a part of the temporal lobe called operculum (Nickel et al. 1992). The temporal lobe in the pig is clearly formed and develops caudally of the sylvian fissure. Like the temporal lobe of the bovine brain the porcine temporal lobe does not obscure the piriform lobe. The temporal lobe of the canine and feline brain in caudal position to the pseudosylvian fissure covers the piriform lobe laterally almost completely (Nickel et al. 1992).

6.2.1 Discussion of the position and nomenclature of the sulci of the porcine brain

We were able to determine the morphology of the porcine cortex using MRI. During our investigation it became apparent that the terminology of the system of sulci of the porcine brain in literarure is not constant, even though the system of gyri and sulci shows very little variation amongst the studied suidae.

The following chapter discusses the system of sulci of the porcine brain. Pictures in anatomical atlases often consist of two dimensional drawings or illustrations. It is difficult to match drawings of gyri and sulci to actual structures in MRI scans. The identification of sulci in MRI proved less difficult than to establish the position of gyri. The sulci are more defined in the actual two dimensional scans (also noted by Maudgil et al. 1998) and in the three dimensional reconstructions using AMIRA® and AVIZO®.This study therefore concentrates on the identification of the sulci of the pig brain. In order to correctly identify and consequently name the sulci of the pig brain, the MRI images were compared with images and descriptions of a large number of textbooks and studies (Krueg 1878, Franck 1894, Flatau and Jakobsohn 1899, Schellenberg 1900, Martin 1904, Black 1915, Kappers 1921, Rawiel 1939, Ellenberger and Baum 1943, Sisson 1953, Koch 1965, Breazile et al. 1966, Brauer und Schober 1970, Kruska et al. 1970, Lauer 1982, Palmieri et al. 1987, Craner and

Ray 1991 A,B (piglet), Nickel et al. 1992, Watanabe et al. 2001 (minipig), Jelsing et al. 2006 (piglet), Lind et al. 2007 (piglet). In the process of trying to match textbook drawings, histological slices and our MRI scans it became evident, that the nomenclature of the sulci of the pig varies tremendously. This is also true for other species. Lakshminarasimhan (1974 and 1975) investigated the isocortex and the visual cortex of the ox (*bos taurus).* He came across the variability of names for the system of grooves and ridges of the bovine brain. A recent study of the gyration of the feline brain discusses the localisation, terminology and variability of gyri (Pakozdy et al. 2014).

This study demonstrates that there are different reasons for the variable terminology of sulci:

1) Authors copy names from different existing studies of the pig brain.

2) Names for the sulci of the pig brain are copied from anatomical studies of different species (e.g. carnivores, other ungulates, primates). Sulci positioned in similar positions are given the same names. (Schellenberg states for example as early as 1900 that names for a large number of sulci of ungulate brains (including the porcine brain) were borrowed from “The structure of the dog’s brain” by Langley in 1883).

3) Different authors use a different homology concept to establish the names of sulci and use the terminology accordingly.

4) Within the family of suidae the sulci may show variability.

5) Gyri and sulci of the same functional area (motor area, somatosensory area etc.) receive the same names. Again terminology might be copied from already existing studies.

Table 1 gives an overview of the terminology already used for sulci of the pig brain. The reader will also find the Latin name (Nomina Anatomica Veterinaria, *NAV*) and synonymously used terminology (from studies and atlases).

As mentioned above sulci of the pig brain are arranged in a simpler manner than those of ruminant (bovine and ovine) and equine brains. But the pattern of the porcine gyri and sulci is more complex than the system of sulci of dogs and the cat (Schellenberg 1900, Sisson 1953, Nickel et al. 1992). Although the appearance of

the telencephalon in the order of ungulates (including *sus scrofa*) varies tremendously (including the size and the gyral pattern), it has been proposed by Krueg (1878), that ten main sulci (of the dorsal and lateral brain surface) can be constantly identified (in addition to the rhinal and hippocampal sulcus). They are on the lateral surface: the sylvian fissure, the suprasylvian sulcus, the coronal sulcus, the presylvian sulcus, the lateral sulcus, the diagonal sulcus, the caudal ectosylvian sulcus. The deep, long sylvian fissure (Syl: Fig. 14-18, Fig. 19-20, Fig. 33-38, Fig. 57-59) of the pig points caudodorsally. It originates near the middle of the rhinal fissure. The sylvian gyrus obscures the insula almost completely. Some authors describe an anterior ramus that extends in rostral direction along with the rhinal fissure (Flatau und Jakobsohn 1899, Rawiel 1939, Ellenberger und Baum 1943), but this has been questioned by Schellenberg (1900). This study shows that the sylvian fissure of the pig is narrow and flat in comparison to the sylvian fissure of other ungulates. The bovine and equine sylvian fissures are deep and further secondary gyri can be seen inside the furrow (Fig. 57 and Fig. 58, Fig. 60). Caudal to the sylvian sulcus the shorter caudal ectosylvian sulcus (Ecs: Fig. 14-18, Fig. 19, Fig. 35-41, Fig. 57-60) or pars posterior of the ectosylvian sulcus can be identified pointing upwards and backwards nearly parallel to the sylvian fissure. Black (1915) suggests that the term ectosylvian sulcus is misleading because this

Table 1: Main sulci/fissures of the pig brain (dorsal, lateral and medial surface);
Name: names and abbreviation used in this study; NAV: nomina natomica veterinaria
Blue: constant sulci in ungulates (Lauer, Krueg); Green: cruciate /connecting sulcus.
Note: Some of the sulci are divided into cranial-, caudal- and medial parts or have small secondary sulci branching off. The term *"fissure"* is often used instead of sulcus. The term *"fissure"* is used by some authors to indicate a deep incision and the term sulcus for a more superficial groove (Nickel et al.1992). Kreiner (1986) introduced the term *"perfissure"* for fissures that cover gyri and sulci beneath.

Name	*NAV*	Synonym	Position
ansate sulcus (Ans)	*sulcus ansatus*	transverse s., s. transversus (Lauer 1963, Koch 1965, Schellenberg 1900) s.verticalis (Anthony and De Grzybowsky1931), f.cruciata minor (Franck 1894)	from medial to lateral rostral to Spl*/Cru, short and deep extending laterally from Flc, intersected by Cor (Lauer 1963), charachteristic for ungulates (Nickel et al.1992)
coronal sulcus (Cor)	*sulcus coronalis*	s. corona-ansata "since the s. coronalis can be an extension of the s. ansatus" (Kappers 1921)	dorsorostral rostral continuation of s. ansatus (Nickel et al. 1992);
cruciate sulcus (Cru)	*sulcus cruciatus (centralis)*	sulcus centralis (primates),	connection between Spl and Sss (Sisson 1953, Franck 1894, Rawiel 1939 , Kruska 1970, Flatau and Jakobson 1899)

connecting sulcus/ "Verbindungsast" (Spl*)		connecting sulcus , cruciate sulcus, “often described as s. cruciatus” (Martin 1904)	connection between Spl and Sss (Nickel et al. 1992, Ellenberger and Baum 1943, Kappers1921, Martin 1904, Schellenberg 1900)
diagonal sulcus (Dis)	*sulcus diagonalis*	cranial aspect of Ecs (Krueg 1878)	lateral, located between s. coronalis and s. presylvius (Lauer 1963)
ectogenual sulcus (Ecg)	*sulcus ectogenualis*	sulcus rostralis (Lauer 1963, Kappers 1921)	medial, rostral to s. genualis
ectosylvian sulcus (Ecs)	*sulcus ectosylvius*	s. arcuatus (Black 1915), s. postica (Krueg 1878), s. obliqua (Holl 1900)	lateral cranial /pars anterior (not always present) and caudal/posterior part frame the sylvian sulcus
ectomarginal sulcus (Ems)	*sulcus ectomarginalis (ectosagittalis)*	s.ectolateralis (Schellenberg 1900, Koch 1965) s. collateralis (Martin 1904)	lateroventral of marginal sulcus
endomarginal sulcus (Enm)	*sulcus endomarginalis (endosagittalis)*	s.entolateralis (Rawiel 1939, Flatau 1899), confinis (Franck 1894, Flatau 1899)	mediodorsal of marginal sulcus
longitudinal cerebral fissure (Flc)	*fissura longitudinalis cerebri*	interhemispheric fissure (Watanabe et al. 2001)	dorsal, separating the two hemispheres
endogenual sulcus (Eng)	*sulcus endogenualis*	s. entogenualis (Schellenberg 1900)	medial
genual sulcus (Gen)	*sulcus genualis*		mediorostral follows the genu of the corpus callosum
marginal sulcus (Mar)	*sulcus marginalis (sagittalis)*	s.lateralis (Lauer 1963), s. Medilateralis (Franck 1894)	dorsocaudal
presylvian sulcus (Prs)	*sulcus praesylvius*	sulcus presylvius	frontal
lateral rhinal fissure (sulcus) (Rfi)	*sulcus rhinalis lateralis*		lateral
sulcus of the corpus callosum (Scl)	*sulcus corporis callosi*	callosal sulcus	medial, separating the corpus callosum from cortex
splenial sulcus (Spl)	*sulcus splenialis*	s.callosomarginalis= splenial + genual fissure (Sisson 1953, Schellenberg 1900), cranial part= s. cinguli (Nickel et al. 1992)	medial
suprasylvian sulcus (Sss)	*sulcus suprasylvius*		lateral, most extensive sulcus of the lateral surface, parallels the dorsomedial border of hemisphere (Lauer 1963)
sylvian fissure (sulcus) (Syl)	*fissura sylvia (lateralis cerebri)*	fissura lateralis cerebri (Ellenberger and Baum 1943), fissura sylvii (Nickel et al. 1992)	lateral in dorsocaudal direction from rhinal fissure
transverse cerebral fissure	*fissura transversa cerebri*	fissura cerebrocerebellaris	dorsal, separating the cerebrum from the cerebellum

sulcus is not homolog to the ectosylvian sulcus of carnivores and therefore names it “sulcus arcuatus” (Table 1). Cranial to the sylvian fissure the rostral ectosylvian sulcus (pars anterior) can be found. This sulcus is not always present in the porcine brain, but if visible, connects with the diagonal sulcus (Dia: Fig. 15-17, Fig. 21-24, Fig. 57-58), which points dorsal and rostral ending just ventrally to the coronal sulcus (Nickel et al. 1992). A connection between the diagonal sulcus and a rostral part of the ectosylvian sulcus could not be visualised in this study. Nickel et al. 1992 describe the diagonal sulcus as a characteristic feature in the brain of ungulates crossing the rostral part of the lateral surface pointing in caudoventral direction.

The suprasylvian sulcus (Sss: Fig. 14-18, Fig. 19-26, Fig. 31-46, Fig. 57-60) is constantly described in literature and is constant in all featured ungulates. The suprasylvian sulcus is positioned dorsally to the sylvian sulcus and the ectosylvian sulcus. It runs parallel to the mediodorsal border of the hemisphere. The rostral part is the most developed (rostral suprasylvian sulcus) and where the rostral ectosylvian sulcus can’t be found, it may connect with the diagonal sulcus. A dorsal branch of the rostral suprasylvian sulcus (ramus dorsalis) can be regularly identified but is not always present (Nickel et al.1992). This study shows a possible connection between the suprasylvian sulcus and the diagonal sulcus in sagittal images (Fig. 19-22). Further caudal the marginal sulcus (Mar: Fig. 18, Fig. 21-27, Fig. 34-51, Fig. 57-60) can be found, accompanied medially by the endomarginal sulcus and laterally by the ectomarginal sulcus. This sulcus is also very constant and a feature of all scanned specimens. It shows very little variation in shape and length.

The ectomarginal sulcus (Ecm: Fig. 15-18, Fig. 19-21, Fig. 32-40, Fig. 57-60) is positioned dorsocaudally to the suprasylvian sulcus and ventrolaterally to the marginal sulcus. The endomarginal sulcus (Enm: Fig. 18, Fig. 24-25, Fig. 42-51, Fig. 57-60) is positioned mediodorsal to the marginal sulcus. Both sulci can be constantly identified in the scanned pig brains. The positions of the endomarginal and ectomarginal sulci are also not controversially discussed. Still the terminology varies strongly (Table 1). The coronal sulcus (Cor: Fig. 12-18, Fig. 23-26, Fig. 32-33, Fig. 57-58) emerges cranially and connects caudomedially with the ansate sulcus. The cortical area rostral of the coronal sulcus is small in ungulates (1/10 of the total brain surface) indicating a small frontal area (Kappers 1921).

On the medial surface of the hemispheres the following fissures/sulci are constant (Krueg 1878): the splenial sulcus, the genual sulcus and the ectogenual sulcus.

Lauer (1982) adds the callosal sulcus of the medial brain surface to the list of constant sulci. These sulci could be also identified using the 1 Tesla MRI and seem to be constant in our specimen. We also propose that the splenial sulcus, the genual sulcus, the endogenual sulcus and the sulcus of the corpus callosum are constant on the medial brain surface of the pig.

The sulcus of the corpus callosum (Scl: Fig. 30) surrounds the corpus callosum rostrally, dorsally and ventrally separating the corpus callosum from the overlying cortex. It is framed by the dorsal cingulate gyrus. The splenial sulcus (Spl: Fig. 17-18, Fig. 23-30, Fig. 31-48, Fig. 57-60) is described by Sisson (1953). For him the splenial sulcus is part of the callosomarginal fissure that is divided into a posterior (caudal) part named splenial fissure, extending from the tentorial aspect of the hemisphere in a direction parallel with the corpus callosum and the rostral part, called genual fissure that lies in the middle between the rostral aspect of the corpus callosum and the dorsomedial border. Nickel et al. 1992 don't use the name "callosomarginal fissure", but discuss the splenial sulcus and the genual sulcus as separate structures. The caudal splenial sulcus extends around the splenium of the corpus callosum and has a cranial extension over the truncus called cingulate sulcus. The genual sulcus is positioned rostrally and extends around the genu of the corpus callosum.

While Lauer claims that the "sulcus transversus" (in position of the ansatus; Ans: Fig. 76) is variable, Nickel et al. 1992 state that the "sulcus ansatus" (transversus) is characteristic for the ungulate brain. It can be connected to the coronal sulcus. It extends from the dorsomedial to the dorsolateral surface of the cerebrum. The MRI scans in this study do not extend rostrally and dorsally enough to capture this feature in the images of the atlas part.

The most inconsistently named sulcus seems to be the cruciate sulcus (Verbindungsast/Cruciate sulcus; Spl*: Fig. 25-30, Fig. 32-37, Fig. 59) of the porcine (Fig. 76) and indeed the ungulate cortex. Lauer 1982 describes the telencephalon of different ungulate species and proposes that the cruciate sulcus should be described as a characteristic structure of the carnivore brain and that it could be a mistake to try to identify a homologous sulcus in ungulates. Kappers came to the same conclusion in 1921 when he stated: "The frontal sulci of the carnivores are similar to the frontal sulci of the ungulates except the cruciate sulcus. A sure homolog of the cruciate sulcus cannot be found in ungulates" and "some call the dorsomedial incision of the splenial (sulcus) cruciate in ungulates. This is because the cruciate of carnivores such as dogs and cats can have anastomoses with the splenial (sulcus)." A sulcus in

a different position is named “cruciate sulcus” by Nickel et al. 1992. It is supposedly a small structure on the medial surface of the porcine brain - but is pictured in different positions within the same atlas. The sulcus seems to be connected to the splenial sulcus in the first drawing and to the endogenual sulcus in the second. Another group of authors (Franck 1894, Breazile et al. 1966, Brauer and Schober 1970, Palmieri et al. 1987, Craner and Ray 1991 a, Craner and Ray 1991 b, Jelsing et al. 2006, Lind et al 2007) place “their” cruciate sulcus in -what seems to be- the position of the ansate and coronal sulci of other authors. In the MRI images of this atlas, the connection between the splenial sulcus and the suprasylvian sulcus is marked as connecting sulcus (Spl*). It is not the purpose of this study to decide on a correct or incorrect position or definition of the “cruciate sulcus”, but Fig. 76 highlights the need to produce a standard nomenclature of the porcine brain.

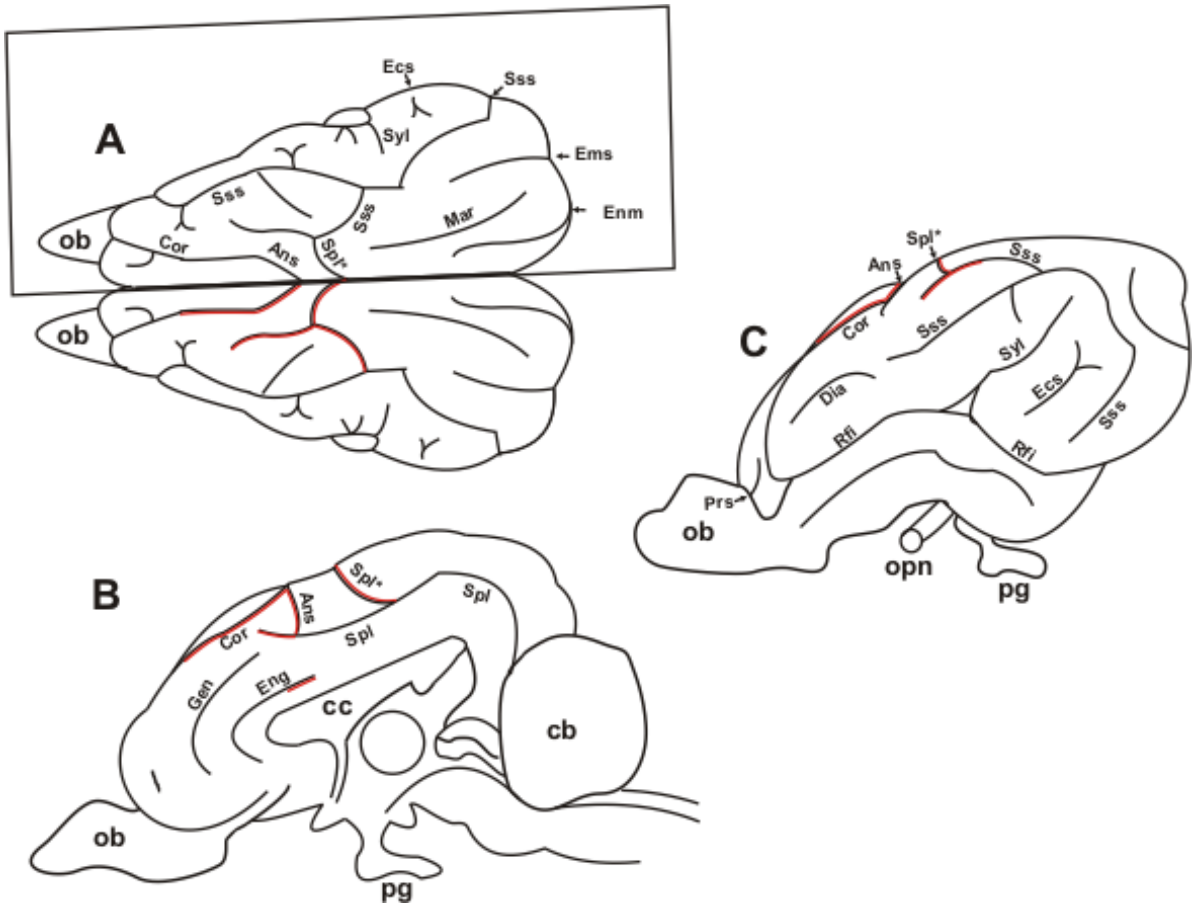

Figure 76

The cruciate sulcus: A: dorsal; B: midsagittal; C: lateral view of the porcine brain. The red areas mark the different positions of the “cruciate sulcus” in the reviewed literature. ©Verena Schmidt.

Ans: ansate sulcus; cb: cerebellum; cc: corpus callosum; Cor: coronal sulcus; Dia: diagonal sulcus; Ecs: ectosylvian sulcus; Ems: ectomarginal sulcus; Eng: endogenual sulcus; Enm: endomarginal sulcus; Gen: genual sulcus; Mar: marginal sulcus; ob: olfactory bulb; opn: optic nerve; pg: pituary gland; Rfi: rhinal fissure; Spl: splenial sulcus; Spl*: connecting sulcus; Sss: suprasylvian sulcus; Syl: sylvian fissure.

6.3 Homology of sulci

The problem of homologies of sulci (and gyri) of the cerebral cortex has been investigated and discussed throughout the 19th century and the beginning of the 20th century (Gegenbauer 1909, Haller v. Hallerstein 1934) without coming to a conclusion. Gegenbauer (1909) believed the homologization of these formations to be impossible and Haller v. Hallerstein (1934) did not believe in the theoretical possibility of homologization of gyri and sulci “since these formations are not organs” (Kreiner 1968). Kreiner (1968) seemed to be of the opinion that it was incorrect to rely on macroscopic morphological observations without investigating the actual architectonics of the cortex. Breazile et al. 1966 suggest that names of gyri and sulci must be reconsidered, if similarities of cortical areas are to be found between the different species. Lind et al. 2007 also recommend further analysis of the system of gyri and sulci, because conclusions and homology assessments of sulci and gyri are variable in scientific studies (“Coronal and cruciate sulci may or may not fusionate or they may be completely separated and the anterior and posterior suprasylvii sulcus may also fusionate”). Lakshminarasimhan (1975), investigating the isocortex of the ox (*Bos taurus)*, realized the need to study the sulci and fissures closely in view of conflicting terminology. In his opinion the criteria for homologizing the sulci of different domesticated animals are often not clearly mentioned. He suggests the study of afferent connections of the sulci, gyri and cortical areas to establish homology. This discussion demonstrates that the term homology is not easily defined and more than just one concept of homology exists (Rehkämper and Zilles 1991, Maudgil et al. 1998, Butler and Hodos 2005). Three current concepts of homology, a phylogenetic, a morphological and a developmental concept compete with each other. The first concept is based on synapomorphy- the inheritance of shared derived features. Synapomorphy has to be established by finding similar structure-function correlations in related species (Maudgil et al. 1998). Care has to be taken to establish homology in this way because there seems to be evidence of parallel evolution of cortical structures in mammalian and avian brains (Rehkämper and Zilles 1991) and the parallel emergence of the cruciate sulcus in dogs and cats (Radinsky 1969). The second concept determines homology through structural similarities such as shape, appearance and position. This can only be established for constant features, which can be reliably identified. The third concept is based on the modus of

structural development, for example developmental origin and cell lineage (Maudgil et al. 1998). In this study MRI is used for morphological research and follows the second concept comparing the form and location of constant features of the porcine brain.

6.4 Variability of the cortical pattern

The system of sulci of the pallium is characterized by individual and breed variability (Nickel et al. 1992). A variety of pig breeds exists, although the percentage of pure bread pigs is getting smaller (Fig: 77). Pigs slaughtered for human consumption are mostly hybrid pigs. Breeders are selecting for performance like meat quality or litter sizes. The conservation of breeds is often neglected (Sambraus 1996).

Variability of sulci has been noted in a variety of other species such as cats (Kawamura 1971) and recently by Pakozdy (2014), dogs (Stark 1954, Oboussier 1949, Oboussier 1950, Oboussier 1955, Lim 1960) and African bovidae (Oboussier 1967, Oboussier 1971).

The variations of cerebral sulci of the cat were investigated by Kawamura (1971) to develop a standard map based upon objective data, because the external appearance of the cat brain had been drawn in multiple ways by a large number of authors (Winkler and Potter 1914, Rose and Woolsey 1948, Crouch 1969, Kawamura and Otani 1970). A division of the cat's sulci into 4 categories is proposed: 1. the most variable, 2. the variable, 3. the stable and 4. the most stable. In his opinion the categorization is necessary to acquire objective data. He also examined as many individuals as possible. 89 feline brains were compared for the study (Kawamura 1971). The left and right hemispheres of the cat brain can also have slight differences in the appearance of sulci (Nickel et al. 1992). Starck (1954) compared the sulci of different canine breeds (Maltese, Pug, Pekinese, Japan Chin, Whippets, Barsoi, Greyhound, Cocker Spaniel and Dachshund). He noticed differences between large, small, brachycephalic and dolichocephalic breeds. The differences include the positions of sulci (ansate and cruciate sulcus) and shape of the brain. Oboussier (Oboussier 1949, Oboussier 1950, Oboussier 1955) examined the sulci of the brains of Whippets and Bulldogs and their first generations offspring (F1). The brains of the animals of the F1 did display characteristic sulci pattern of the mother (Bulldog) and father (Whippet), but neither of them were the same, nor could the pattern be predicted. Also Lim et al. 1960, while developing a stereotactic atlas of the dog's brain**,** found: "the endless variations in size and shape of the dog's head make them unsuitable for research involving accurate cranio-encephalic topography." The study only focuses on light weight (10+/- 2kg), short haired dogs without unduly short or

long noses.

A disadvantage of this study is the relatively small number of individual pigs scanned. A larger number of MRI scans of different specimen could have presented a variability of sulci as well as more differences in the size and shape of the porcine brains. As mentioned above (Table 1) some sulci of the pig brain might fuse (like the coronal and ansate sulcus) or are not constant like the cranial ectosylvian sulcus. We can therefore assume some variability in the sulci of the porcine brain. Rawiel (1939) documented the variability of the appearance of the brain of several domestic pig breeds including Berkshire, Magalitza and German landrace pigs. He states that, although certain structural differences exist between breeds, certain breed characteristics can be occasionally identified in a different porcine breed. In Rawiels opinion age and sex don't seem to have any significant influence on the appearance of sulci of the porcine brain. The main sulci seem to be constant.

A major influence on the shape of the brain seems to be the skull shape -the shorter the base of the skull, the stockier the brain. Therefore mild differences in topography of the sulci exist. The difference of brain shapes are more extensively studied in dog breeds (Stark 1954, Oboussier 1949, Oboussier 1950, Oboussier 1955, Nickel et al. 1992). The dolichocephalic dog breeds are characterised by their elongated brain (sagittal MR images). The olfactory bulbs of the rhinencephalon of dolichocephalic breeds are the most rostrally positioned part of the brain. While the brachycephalic canine brain is round and the olfactory bulbs are shifted caudally under the frontal pole of the hemispheres (Fig. 78). As a result the frontal pole of the brain appears almost round and the olfactory bulbs are moved caudally under the frontal pole of the brain stem seems shortened (Nickel et al. 1992). This is also be the case in porcine breeds and could be visualized in the MRI scans (Fig. 63-64).

Figure 77

Fig.: A variety of pig breeds exists, although the percentage of pure bread pigs is getting smaller. A: Chinese Maishan pig; B: Wild boar; C: Turopolje Pig; D: Landrace pig (above), Potbelly pig (below); E: Magalica pig; F: Angeln Saddleback. ©Verena Schmidt

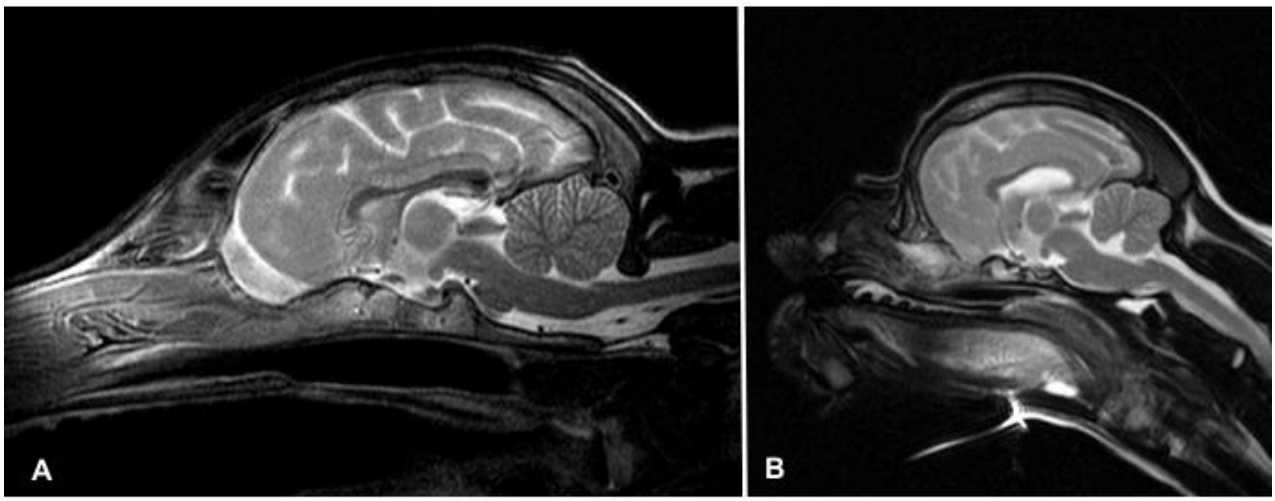

Figure 78

A: Dolichocephalic; B: Brachycephalic (pug) canine breed in midsagittal MRI scan. Note the round shape of the brachycephalic dog compared to the elongated shape of the dolichocephalic specimen. The olfactory bulbs of the pug are moved caudally under the hemispheres of the brain (A+B courtesy PD Dr. med. vet. (habil.) M. Schmidt).

6.5 Influence of skull morphology on the morphology and expansion pattern of the cortex

The brain of ungulates in general expands laterally and is short, similar to the brain of adult cetaceans. Ungulate brains seem to be shortened compared with the brains of most other mammals. Neuroanatomists use the term telescoping. This can be appreciated by a higher inclination angle of the corpus callosum when compared with the inclination angle of the corpus callosum of carnivores (Oelschläger and Kemp 1998, Oelschläger et al. 2010). In the pig the base of the skull does not seem to run parallel to the dorsal surface of the cerebrum. This could be the result of telescoping. During telescoping the brain is shortened along its central axis and the dorsal surface experiences a rostral shift. The hemispheres are drifting apart simultaneously. Telescoping is seen as a mechanism to allow the brain to grow bigger in spite of the restrictions of the skull (Oelschläger et al. 2010). The brain of the pig remains relatively small and is not as gyrencephalic as the brains of other species associated with telescoping (in comparison with brains of other ungulates and cetaceans).

Figure 79
Skeleton of the domestic pig (left). Note the orientation of the head and the rostral tilt of the squama occipitalis compared to the vertical orientation of the squama in the dog. © Verena Schmidt.

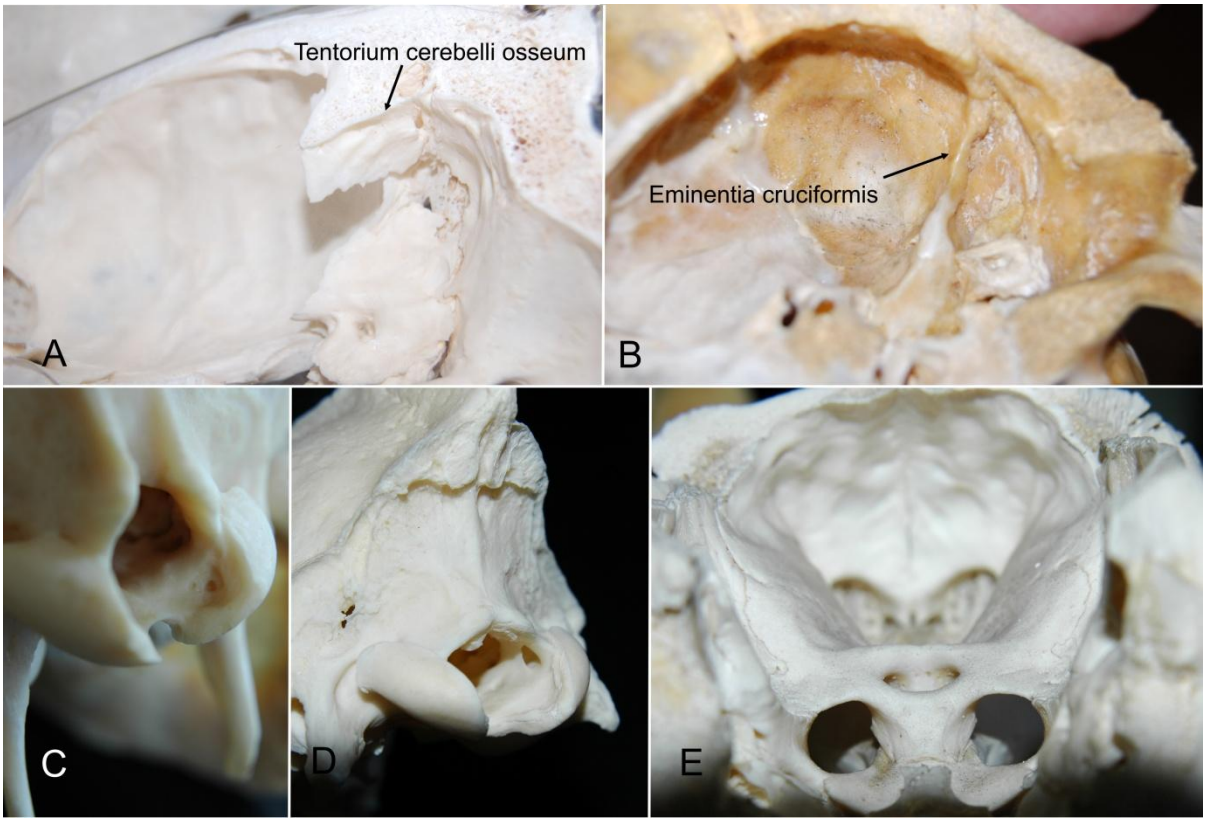

Figure 80

A: tentorium cerebelli osseum of the horse; B: eminentia cruciformis of the pig; C: foramen magnum of the pig; D: strong squama occipitalis of the dog (Cavalier King Charles Spaniel) E: view of the cavum cranii of the pig with top of skull removed (A-E courtesy of PD Dr. med. vet. (habil.) Martin Schmidt).

The porcine brain is elongated in dolichocephalic breeds. We can see in the dorsal scans (atlas) that the hemispheres of the pig brain are positioned in close proximity to each other. Therefore the porcine brain might not experience an increase in size through telescoping. The posture of the pig might give a different explanation for the orientation of the brain stem (Fig. 79). The snout of the pig is pointed rostrally (as adaption to the pigs feeding behaviour). This in turn results in a rostral tilt of the squama occipitalis. Examining the caudal base of the skull, a ventral tilt of the foramen magnum is also visible (Fig. 80). Therefore the medulla oblongata leaves the skull in ventral direction.

6.6 MR-Imaging techniques and their comparability

In veterinary medicine it is common procedure to scan the transverse images at a ninety degree angle to the base of the skull. As a consequence scans of transverse sections of the brain and medulla of the pig are most likely to capture the structures of the brain at a slightly different angle as achieved through other techniques. This in turn influences the appearance -for example length and width- of individual structures, for example nuclei, sulci and gyri. Alternatively internal landmarks such as the rostral and caudal commissures are commonly chosen in MRI to determine the horizontal plane (Andersen et al. 2005). The transverse scans are then taken at a 90º angle as shown in Fig. 81. This is known as the Talairach system (Talairach and Tournoux 1988). In order to compare the shape of nuclei for example it is important to compare scans that were taken in the same plane at a comparable angle. It is important to highlight the fact that standardized scanning regimes in relation to orientation of the scans do not exist in veterinary medicine. In human medicine such regimes are already in place and it would be desirable for veterinarians to establish a uniform system to facilitate easier interpretation of scans. To create reproducible conditions for surgery and biomedical research, stereotactic atlases, such as the stereotactic atlas of the porcine brain (Felix et al. 1999), are of great importance. In this study of the porcine brain, it was challenging to compare histological slices with MRI scans, because of the different orientation of the scans and slices. The shape of structures, as well as the difference in structures captured in one image/slice can differ significantly. Therefore we found the use of stereotactic (Felix et al. 1999) or histological atlases (Yoshikawa 1968) not always practical to help identify structures in MRI.

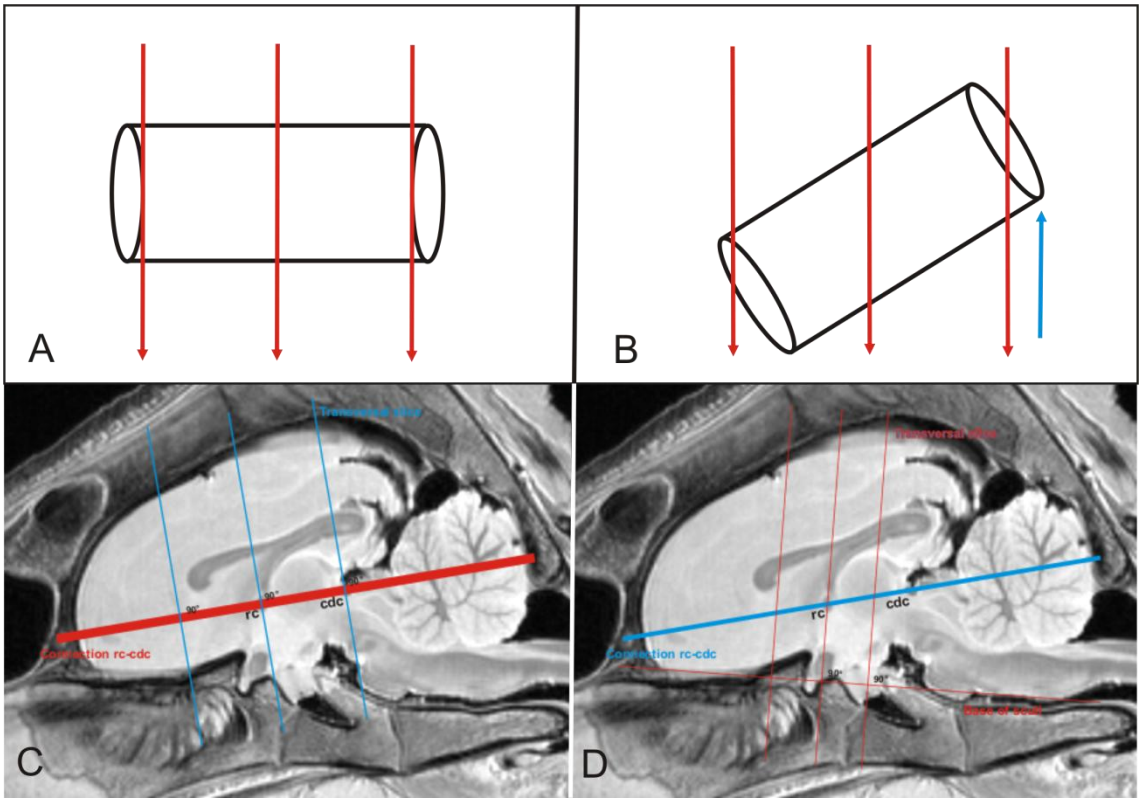

Figure 81
A and B demonstrating the difference in the shape of the objects in slices at different angles. C: Talairach and Tournoux 1988 D: Scanning orientation used in this atlas (transversal scans in 90 degree angle to the base of the scull). © Verena Schmidt.

Nowadays MRI is available to scientists as well as veterinary practitioners, especially to those who are interested in neurological research. Since MRI is more widely accessible and may become less expensive in use, it is most likely that MRI is going to be utilized more frequently for diagnostics in large animals such as horses and other large animal species. Veterinarians and scientists have already started to use MRI as a diagnostic tool for the examination of large animals like sheep and cattle (Karger et al. 1998, Tzuka and Taura 1999, Yamada et al. 2005, Schenk 2007). These animals are not only of economical importance to their owners but more and more often kept as pets. With the MRI data set one can create sections in any desired plane. Being able to see the brain from every angle is of great benefit examining the three-dimensional organisation of the brain (Van der Linden 1998). For this study high quality MRI pictures were taken with a 1.0 T (Tesla) MRI scanner (Phillips) while the pig brain remained in situ. In order to map the brain the PD weighted MRI scans were compared with photographs, histological preparations and drawings of available brain atlases and studies of the pig/ungulate brain (Krueg 1878,

Flatau and Jakobsohn 1899, Schellenberg 1900, Rawiel 1939, Breazile 1967, Breazile 1968, Yoshikawa 1968, Kruska 1970, Lauer 1970, Makita and Tominaga 1987, Palmieri et al. 1987, Brauer and Schober 1970, Félix 1999, Watanabe et al. 2001, Jelsing et al. 2006, Lind et al. 2007,) and anatomical textbooks (Franck and Martin 1894, Martin 1904, Ellenberger and Baum 1942, Sisson 1953, Koch 1965, Nickel et al. 1975, Craner and Ray 1991 a, Craner and Ray 1991, Romer and Parson 1991, Dyce et al. 2002) to aid the identification of structures. The aim was to capture and identify as many details as possible of the porcine brain in all three planes (transverse, dorsal and sagittal). In this study, contrast and spatial resolution were improved and the identification of a large number of delicate brain structures in the MR images of the formalin fixated and native pig brain post mortem was possible by using multiple signal averaging acquisitions. However the field strength of 1.0 T has limitations concerning the image quality. It can be difficult to identify a number of small anatomical details in MRI for example the nuclei of the mesencephalon or the hypothalamus. Higher field strengths are recommended to reveal small anatomical detail (Benveniste and Blackband 2002, Schmidt et al. 2006). The more powerful the magnetic field, the more hydrogen ions inside the brain are exited and produce an intense MR-signal leading to a maximized contrast- and signal-to-noise-ratio (Schmidt 2006). With these field strengths even the central nervous system of embryos can be visualized (spatial resolution ~ 50µm, Schmidt et al. 2009). In these high field scanners however, the size of the coils is a limiting factor, as they are only a few centimetres in diameter (Schmidt et al. 2006, Schmidt et al. 2009). Large brains or whole heads must therefore be scanned with conventional head or surface coils. As a consequence the use of high resolution scanners cannot be applied to brains of mature pigs with an average brain volume of 162cm³ (Hofman 1985) and size about 6cm long x5cm wide x 5cm deep (Hashimoto et al. 1996). The large skull/splanchnocranium of the pig in relation to the actual size of the porcine brain is also a disadvantage when trying to achieve optimal MRI image quality. This is due to the low filling factor that is compromised by the distance between the object (in our case the brain) and the head coil. The longer the distance/the more space between brain and coil the more compromised is the signal to noise ratio. This is frequently a challenge when performing in vivo MRI scans. The pig's skull harbours a large frontal sinus extending from the frontal bone caudally reaching the occipital bone (Nickel et al. 1992) while the human brain for example is positioned directly under the skull (Fig. 82). The frontal sinus of our scanned babirousa female (Fig.83) is even more

impressive and visible as a large air filled cavity that extends far caudally and reaches dorsally over the telencephalon and even the cerebellum (Fig. 83 B). The large frontal sinus is common in animals with an acute olfactory sense. The empty compartments are believed to supply moisture (Negus 1954). Although there are a number of morphological atlases and textbooks available (Frank and Martin 1894, Flatau and Jakobsohn 1899, Martin 1904, Kappers 1921, Ellenberger and Baum 1943, Sisson 1953, Koch 1965, Yoshikawa 1968, Brauer and Schober 1970, Makita and Tominaga 1987, Romer and Parsons 1991, Nickel et al. 1992, Félix et al. 1999, Dyce et al. 2002), so far no textbook atlas exists that can provide information about morphology of the healthy brain of the domestic pig post-mortem, as revealed by high resolution MR imaging. The scanning of fixed brains seems to allow an even better duration of image acquisition (van der Linden et al. 1998).

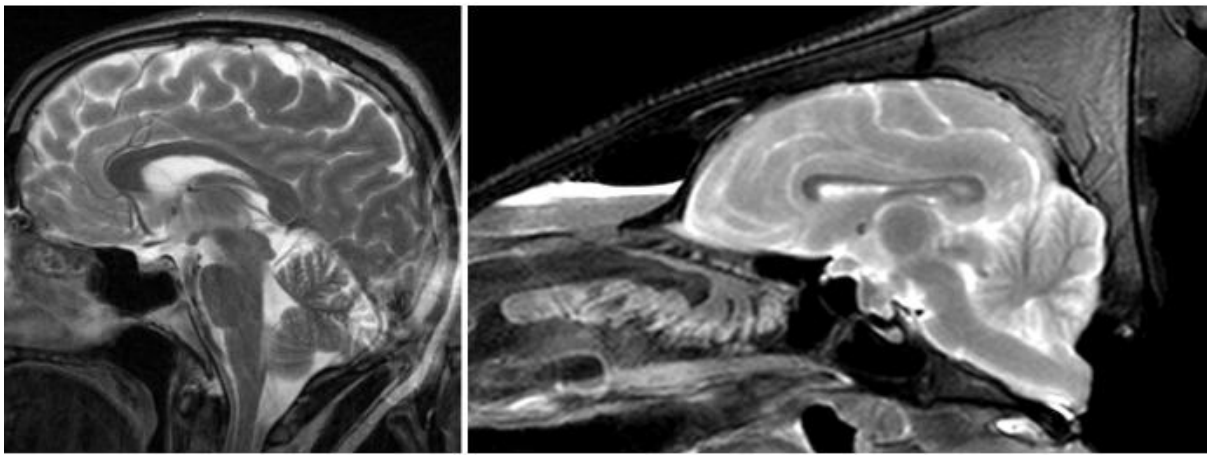

Figure 82
We can compare the human brain (left) and porcine brain (right) in MRI. Note the difference in distance between the brain and the surface of the scull in the human brain compared with the porcine brain. The longer the distance between the head coil and the brain the less optimal the picture quality (picture of human brain courtesy of PD Dr. med.vet. (habil.) M. Schmidt).

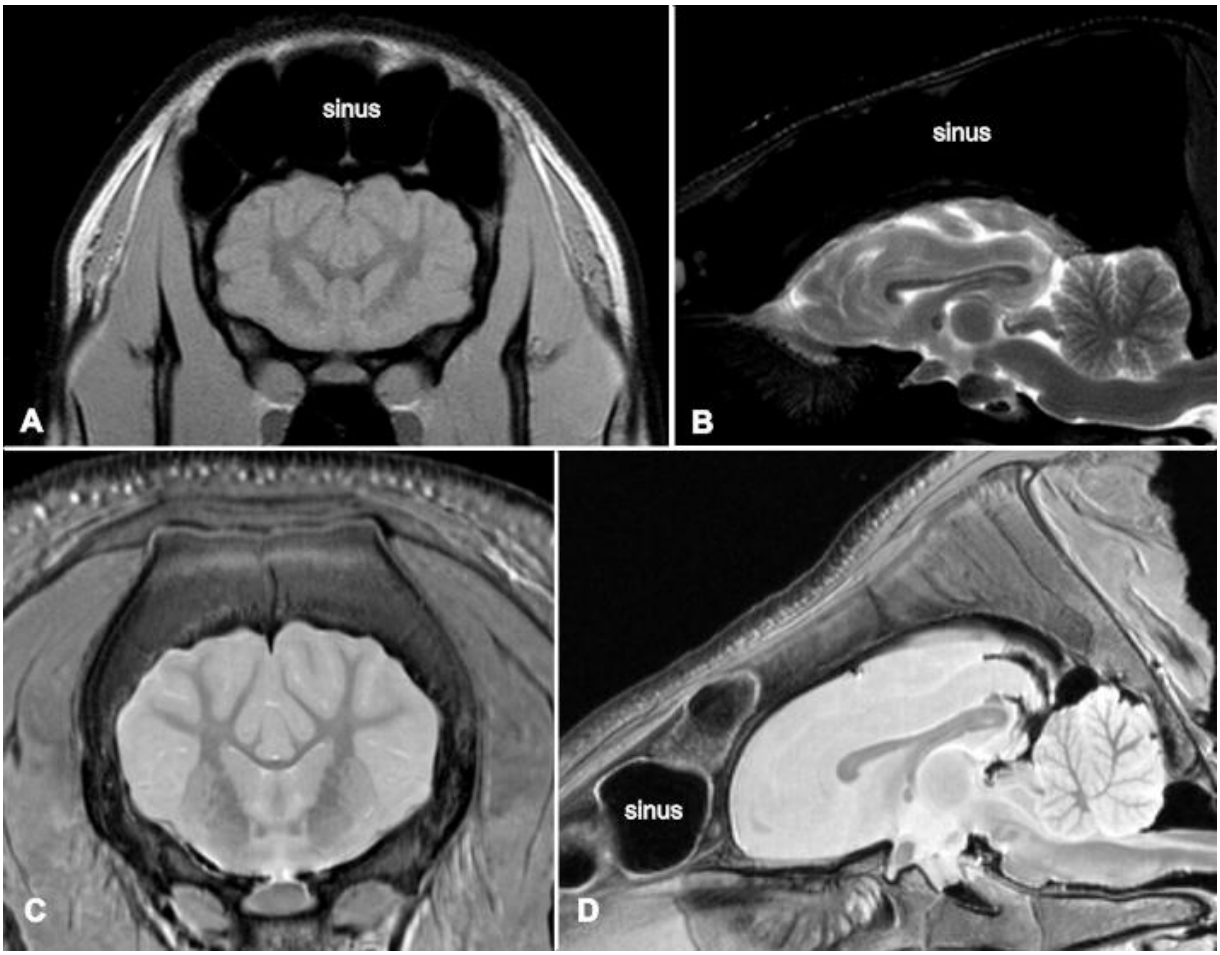

Figure 83
Babirousa (A+B) and Pig (C+D) brain in situ. Transverse (at level of pineal gland) and midsagittal MRI scan. Note the size of the sinus surrounding the brain of the babirousa female. Note also in B: Cerebrospinal fluid (CSF) between telencephalon and cerebellum instead of an osseous tentorium cerebelli seen as hyperintense area (A-D courtesy of PD Dr. med.vet. (habil.) M. Schmidt).

6.6.1 Comparability of MRI scans and histological sections

This study emphasises that it is vital not to interpret MR images in the same way as histological sections, displayed for example by light microscopy. In MRI scans, the shape of a cell group can't be determined by staining features. The shape of the cell group is influenced by differences in water content (concentration of protons) of the tissue and relaxation. Images taken by light microscopy show the characteristic colours of staining methods. Staining methods were developed to improve contrast and details in cells and tissue. They are missing in MR images due to the nature of this technique. Cells with a high contrast due to their staining features in histology

can have similar relaxation times in MR microscopy. A detailed knowledge of the actual morphological details of the subject, in our case the porcine brain, is therefore necessary for the interpretation of corresponding MR images. The MR images are not meant to replace light microscopic images, but aim to complement existing information on brain structures in the third dimension (see also Schmidt et al. 2009). It is complicated and in a number of cases not possible to identify nuclei or small structures in MRI (for example nuclei of the metencephalon or hypothalamus). The interpretation of the MRI images challenges the eye of the interpreter in different ways. The structures and substructures can be so small that more than one signal is combined in one voxel. This makes it difficult to match a single voxel to a single structure. The identification of structures through a signal is often difficult since two different objects in close proximity although separate might not cause a signal difference. This problem can also be experienced when using a microscope where it is often hard to distinguish separate nuclei because they are stained by the same method. This study of the porcine brain describes only structures that can be clearly be identified in the MRI scans.

6.6.2 Orientation

It is important point out the difference in veterinary and human medical terminology when discussing the orientation of brain scans in MRI. The upright posture of humans and the resulting field of view define an anterior and posterior aspect. In veterinary medicine, due to the horizontal position of an animal's spine, the terms cranial (towards the head) rostral (towards the snout) and caudal (towards the tail) are used. Planes parallel to the base of the skull are furthermore defined as dorsal scans (towards the back) as opposed to coronal (Fig.84). In horses, ruminants, dogs and cats the brain stem (truncus encephali) remains in a more horizontal position. The human brain in contrast is bent approximately 90° between diencephalon and mesencephalon, due to the massive cerebrum and the upright posture of men (Nickel et al. 1992, Butler and Hodos 2005). This can also be seen in Fig. 84 B.

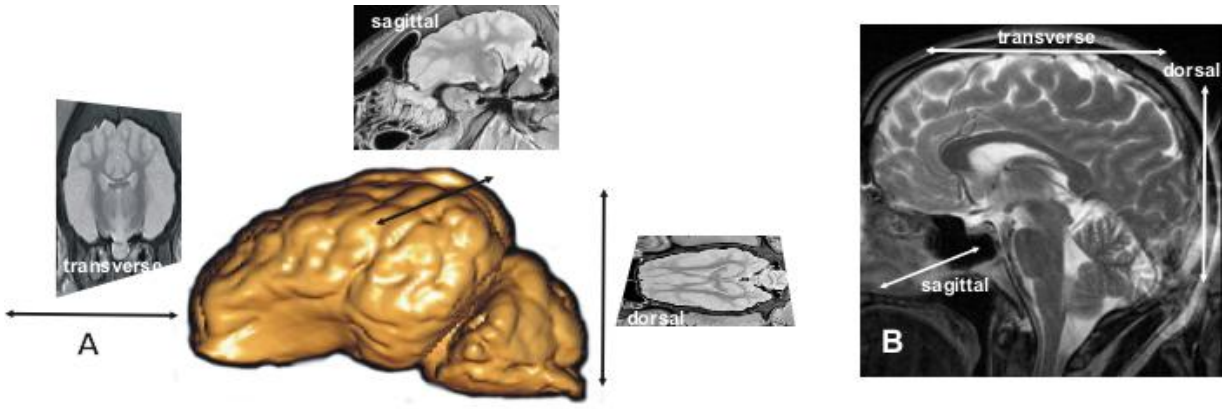

Figure 84
Orientation of the scans in MRI; A: Porcine brain; B: Human brain (picture courtesy of PD Dr. med. vet. (habil.) M. Schmidt). Transversal scan: rostro-caudal orientation. Sagittal scan: latero-lateral orientation. Dorsal scan: dorso-ventral orientation. © Verena Schmidt.

7 Summary

For this study the healthy brains of the domestic pigs are examined post mortem. MRI (magnetic resonance imaging) scans in transverse, sagittal and dorsal orientation (native and formalin fixed) are produced with a 1.0 Tesla scanner.
12 sagittal, 13 dorsal and 22 transverse scans are selected and labelled to produce a MRI picture atlas of the porcine brain. With the aid of the graphical software programs AMIRA® and AVIZO® (Mercury Computer Systems Inc.) it was possible to identify brain structures (like nuclei) and to locate and describe the sulci of the porcine brain in MRI. These graphical software programs make it possible to construct a three dimensional model of the porcine brain and to facilitate simultaneous identification of morphological features in dorsal, transverse and sagittal scans.
In addition to the atlas, MRI scans of a wild boar, a Wiesenauer minipig and a babirusa are produced and compared with the scans of the domestic pig.
An important result of this study is a summary and discussion of the nomenclature of the sulci of the porcine cortex. It is now easier to match functional areas of the cortex with the corresponding structure in the MRI scan, because a standardized nomenclature for the sulci of the porcine brain does not exist so far.
This study also describes special features of the porcine brain. The porcine brain has less gyri than the brains of a variety of other ungulates. The position of the pig's forebrain in relation to the brain stem, the strongly developed pars olfactoria of the rhinencephalon in relation to the limbic system and the topography of the pituitary gland in relation to the diencephalon, are also different from the other featured species. It is furthermore possible to identify a physiological aplasia of the cerebellar cortex of the tuber region in the MRI scans of the porcine brain.
In the featured members of the suidae (pigs and babirusa) the system of gyri and sulci shows little variation. Most sulci and their position are constant. The shape of the brain differs between the brachycephalic breeds (such as the Wiesenauer minipig) and the dolichocephalic hybrid pigs (bread for meat production). The brain of the Wiesenauer minipig is shorter and rounder compared with the brains of the scanned hybrid pigs. However, the surface structures of brachycephalic and

dolichocephalic pig brains show only little difference.

8 Zusammenfassung

Für die vorliegenden Studie wird das gesunde Gehirn des Hausschweines (*sus scrofa domesticus*) post mortem untersucht. Es werden mithilfe eines 1.0 Tesla Scanners MRT (Magnetresonanztomographie) Aufnahmen von Schweinegehirnen in transversaler, sagittaler und dorsaler Ausrichtung erstellt (nativ und formalin fixiert). Für den MRT- Atlas des Schweinegehirnes werden 12 sagittale, 13 dorsale und 22 transversale Bilder ausgewählt. Zur Lokalisation von Gehirnstrukturen, wie z.B. der Kerngebiete oder der Beschreibung des Furchenbildes, werden die Grafikprogramme AMIRA® und AVIZO® (Mercury Computer Systems Inc.) verwendet. Sie ermöglichen eine dreidimensionale Darstellung des Schweinegehirns und die gleichzeitige Identifikation von Gehirnstrukturen in dorsaler, transversaler und sagittaler Schnittebene. Identifizierte Gehirnstrukturen werden in den ausgewählten Scans beschriftet. Es werden ebenfalls Scans von einem Wildschwein, einem Wiesenauer minipig und einem Babirusa angefertigt und mit den Bildern des Hausschweines verglichen.

Ein wichtiges Ergebnis der vorliegenden Arbeit besteht in der Auflistung, der Benennung und Diskussion der Sulci der kortikalen Oberfläche. Sie vereinfacht in Zukunft die Zuordnung funktioneller Abschnitte der Großhirnrinde zur Morphologie im MRT- Schnittbild. Eine standartisierte Nomenklatur existiert bisher nicht.

Das Schweinegehirn ist im Vergleich zu Gehirnen vieler anderer Ungulaten weniger stark gyrifiziert. Weitere Besonderheiten des porcinen Gehirnes sind die Lagebeziehung des Vorderhirnes zum Hirnstamm, die ausgeprägt entwickelte pars olfactoria des Rhinencephalon in Relation zu seiner pars limbica und die topographische Beziehung der Hypophyse zum Diencephalon. Desweiteren kann bei den Masthybriden eine Aplasie der Kleinhirnrinde in der Region des tuber vermis mittels MRI dargestellt werden.

Innerhalb der Suidae (Schweine und Babirusa) weist das System der Gyri und Sulci nur geringe Variationen auf. Die meisten Sulci und deren Lage sind konstant. Unterschiede zwischen den Gehirnen von kurznasigen (Wiesenschwein) und langnasigen (Mehrzahl der Masthybriden) Schweinerassen bestehen in der Stauchung und Abrundung des Gehirnes. Die Oberflächenstruktur der

Grosshirnrinde weist jedoch kaum Unterschiede zwischen den Rassen auf.

9 References

Adrian ED (1943): Afferent areas in the brain of ungulates. Brain, 66:89-103.

Andersen F, Watanabe H, Bjarkam C, Danielsen EH, The DaNeX Study Group, Cumming P (2005): Pig brain stereotaxic standard space: Mapping of cerebral blood flow normative values and effect of MPTP- lesioning. Brain Research Bulletin, 66 (2005) 17-29.

Andrews RJ, Knight RT, Kirby RP (1990): Evoked potential mapping of auditory and somatosensory cortices in the miniature swine. Neuroscience Letters 1990, Vol. 114, no.1, pp. 27-31(15 ref.).

Anthony R, De Grzybowski J (1930): Le néopallium des equides. Étude du développement de ses plissements. Journal of Anatomy, 1930, January; 64 (Pt2): 147-169.

Anthony R, De Grzybowski J (1931): Le neopallium des Suides. Etude de son developpement et interpretation de ses plissements. Archive. de Zool. expe'r. et gen. Volume jubilaire, t. LXXIV, 1931.

Anthony R, De Grzybowski J (1937): Le neopallium du mouton- Étude de son développement et interpretation de ses plissements. Journal of Anatomy, 71,41-53.

Arencibia A, Vazquez JM, Ramirez JA, Ramirez et al. Villar JM, Rivero MA, Alayon S, Gil, F9 (2001): Magnetic resonance imaging of the normal equine brain. Veterinary Radiology and Ultrasound, 5:405-408.

Armstead WM, Kurth CD (1994): Different cerebral hemodynamic responses following fluid percussion brain injury in the newborn and juvenile pig. Journal of Neurotrauma 1994a; 11(5):487-97.

Barbier EL, Marrett S, Danek A, VortmeyerA, van Gelderen P, Duyn J, Bandettini P,

Grafman J,Koretsky AP (2002): Imaging Cortical Anatomy by High-Resolution MR at 3.0T: Detection of the Stripe of Gennari in Visual Area 17. Magnetic Resonance in Medicine, 48:735–738 (2002).

Barton RA (2007): Evolutionary specialisation in mammalian cortical structure. blackwell-synergy. com/doi/abs/10.1111/j.1420-9101.2007.01330.x

Benveniste H, Blackband S (2002): MR-microscopy and high resolution small animal MRI: applications in neuroscience research. Progress in Neurobiology, 67: 5-17.

Bjarkam CR, Cancian G. Larsen M, Rosendahl F, Ettrupp KS, Zeidler D, Blankholm AD, Østergaard L, Sunde N, Sørensen JC (2004): A MRI-compatible stereotaxic localiser box enables high-precision stereotaxic procedures in pigs. Journal of Neuroscience Methods, 139(2004) 293-298.

Black D (1915): A study of the endocanial casts of okapia, giraffa and Samotherium, with special reference to the convolutional pattern in the family of giraffidae. Journal of Comparative Neurology, 25: 320-60

Bolk L (1906): Das Cerebellum der Säugetiere – Eine vergleichende anatomische Untersuchung. Gustav Fischer, Jena, 1906.

Book SA, Bustad LK (1974): The fetal and neonatal pig in biomedical research. Journal of Animal Science 1974.38:997-1002

Bradley OC (1903): On the development and homology of the mammalian cerebellar fissures. Journal of Anatomy and Physiology, Vol.: XXXVII. (N.S. Vol. XVII) - April 1903.

Brant-Zawadski M (1988): MR-Imaging of the brain. Radiology, January 1988.

Brauer K, Schober W (1970): Katalog der Säugetier Gehirne. G. Fischer VEB I.

Breazile JE, Swafford BC, Thompson WD (1966): Study of the motor cortex of the domestic pig. American Journal of Veterinary Research 27, 1369-1373.

Breazile JE, Swafford BC, Biles DR (1966 b): Motorcortex of the horse. American Journal of Veterinary Research, 27, 1605-1609.

Breazile JE (1967): The cytoarchitecture of the brainstem of the domestic pig. Journal of Comparative Neurology, 129, 169-188.

Breazile JE, Kitchell R (1968): Ventrolateral spinal cord afferents to the brain stem in the domestic pig brain. Journal of Comparative Neurology, 133; 363-37.

Bright Funkhouser E (1915): The visual cortex, its localisation, histological structure and physiological function. From the Neurological Institute of the University of Zurich, Zurich, June 1915.

Brodmann K (1909): Vergleichende Lokalisationslehre der Großhirnrinde in ihren Prinzipien dargestellt auf Grund des Zellenbaues. Leipzig: Barth.

Buonnano FS, Pykett IL, Kistler JP, Vielma J, Brady TJ, Hinshaw WS, Goldmann MR, Newhouse JH, Pohost GM (1982): Cranial anatomy and detection of ischemic stroke in the cat by nuclear magnetic resonance imaging. Radiology, 143: 187-193, 1982.

Bujak A (1974): Topography and cytoarchitectonics of the cerebellar nuclei in the boar. Polskie Archiwum Weterynaryjne 17, 43-53, 1974.

Burbridge B, Matt G, Remedios A (2004): Complex intracranial arterial anatomy in swine is unsuitable for cerebral infarction projects. Canadian Association of Radiology Journal, Vol. 55, No 5, 2004.

Buttler AB, Hodos W (2005): Comparative vertebrate neuroanatomy. Evolution and adaption, Wiley – Interscience, second edition, 2005

Campbell AW (1905): Histological studies on the localisation of cerebral function. Cambridge University Press, Cambridge 1905.

Cesta MF, Mozzachino K, Little PB, Olby NJ, Sills RC and Brown TT (2006):

Neuronal ceroid lipofuscinosis in a Vietnamese pot-bellied pig (sus scrofa). Veterinary Pathology, 43(4):556-60, 2006.

Ciliga T (1937): Cerebral convolutions of Ungulates. Veterinarski Arhiv, 7, 509-568, 1937.

Chaffin MK, Walker MA, McArthur NH, Perris EE (1997): Magnetic resonance imaging of the brain of normal neonatal foals. Veterinary Radiology and Ultrasound 38:102-111.

Chang YS, Park WS, Lee M, Kim KS, Shin MS, Choi J-H (1998): Effect of hyperglycemia on brain cell membrane function and energy metabolism during hypoxia-ischemia in newborn piglets. Brain Research 798 (1998) 271-280.

Checkley D, Loveday BE, Waterton JC, Zhu XP, Isherwood I (1987): Detection of myocardial infarction in the minipig using NMR imaging. Magnetic Resonance in Medicine, Vol. 5, Issue 3, p.201-16.

Chromiak M (1963): Topographie und Kernbau des Mesencephalon der Haustiere. Annales Universitatis Marie Curie-Sklodowska, DD 18: 19-31.

Clark TE (1896): The comparative anatomy of the insula. Journal of Comparative Neurology, 6 (1896), pp.59-100.

Cohen ZR, Zaubermann J, Harnof S, Mardor Y, Nass D, Zadicario E, Hananel A, Castel D, Faibel M, Ram Z (2007): Magnetic resonance imaging-guided focused ultrasound for thermal ablation in the brain: a feasibility study in a swine model. Neurosurgery 60:593-600.

Cohn HA, Papez JW (2004): The posterior calcarine fissure in the dog. The Journal of Comparative Neurology, Volume 58, issue 3, pp. 593-602.

Cohrs P, Schulz LC (1952): Entwicklungsmechanisch bedingte partielle Aplasien der Rinde und von Windungsteilen des Kleinhirns beim Schwein. Journal of Neurology 1952, 168: 135-141.

Craner SL, Ray RH (1991 a): Somatosensory cortex of the neonatal pig: 1. Topographic organisation of the primary somatosensory cortex (SI). Journal of Comparative Neurology 306:24-38, 1991.

Craner SL, Ray RH (1991 b): Somatosensory cortex of the neonatal pig: 2. Topographic organisation of the secondary somatosensory cortx. Journal of Comparative Neurology 306: 39-48, 1991.

Dai Y, Vaught TD, Boone J, Chen SH, Phelps CJ, Ball S, Monahan JA, Jobst PM, McCreath KJ, Lamborn AE, Cowell-Lucero JL, Wells KD, Colman A, Polejaeva IA, Ayares DL (2002): Targeted disruption of the alpha1, 3-galactosyltransferase gene in cloned pigs. Nature Biotechnology 20, 251–255.

Crouch JE (1969): Text-atlas of Cat Anatomy. Philadelphia: Lea and Febiger, 1969.

D'Azyr V (1786): Traité d'anatomie et de physiologie. Paris 1786.

Dalmose AL, Bjarcam R and Djurhuus JC (2005): Stereotactic electrical stimulation of the pontine micturition centre in the pig. Blackwell Synergie-BJU Int., Volume 95 Issue 6 page 886.

Danielsen EH, Smith D, Hermansen F, Gjedde A, Cumming P (2001): Acute neuroleptic stimulates DOPA decarboxylase in porcine brain in vivo. Synapse, Volume 41, Issue 2, pages 172-175.

Danckers J (2003): Cytoarchitektonische Arealisierungen des Neocortex beim Mink (*Mustela vison*) und vergleichend-quantitative Untersuchungen zwischen der Wild- und Haustierform. Dissertation zur Erlangung des Doktorgrades der Mathematisch-Naturwissenschaftlichen Fakultät der Christian-Albrechts-Universität, Kiel.

Dellman HD, McClure RC (1975): Porcine nervous system. The Anatomy of Domestic Animals. W.B. Saunders Co., Philadelphia.

Deutsch JC (1992): Olfactory cues influence female choice in two lek-breeding antelopes. Nature 356: 596–598.

Dickerson JWT, Dobbing J (1967): Prenatal and postnatal growth and development of the central nervous system of the pig. Proceedings of the Royal Society London 1967;166:384/95.

Dilberovic F, Secerov D, Tomic V (1986): Morphological charachteristics of the gyrus dentatus in some animal species and in man. Anatomischer Anzeiger 161,231-238

Done JT, Herbert CN (1968): The growth of the cerebellum in the foetal pig. Research in Veterinary Science 9, 143-148

Done JT (1968): Congenital nervous diseases of the pig. Laboratory animal (1986) 2, 207-217.

Douglas WR (1972): Of pigs and men and research: A review of applications and analogies of the pig, *sus scrofa*, in human medical research. Space Life Sciences 3 (1972) 226-234.

Dow RS (1942): The evolution and anatomy of the cerebellum. Biological reviews, 17,179-220.

Duhaime A-C, Margulies SS, Durham SR, O'Rouke MM, Golden JA, Marwaha S, et al (2000): Maturition dependant response of the piglet brain to scaled cortical impact. Journal of Neurosurgery 93: 455-462, 2000

Duhaime A-C, Hunter JV, Grate LL, Kim A, Golden J, Demidenko E, et al (2003): Magnetic resonance imaging studies of age- dependant responses to scaled focal brain injury in the piglet. Journal of Neurosurgery 99: 542-548, 2003

Duhaime A-C, et al. (2006): Functional magnetic resonance imaging of the primary somatosensory cortex in piglets. Journal of Neurosurgery: Paediatrics/Volume 104/April 2006

Dyce KM, Sack WO, Wensing CJG (2002): Textbook of veterinary anatomy (3rd edition). Elsevier Science (USA) 2002, 1996, 1987

Ebinger P (1974): A cytoarchitectonic volumetric comparison of brains in wild and domestic sheep. Zeitschrift für Anatomie und Entwicklungsgeschichte, 144, 267-302 (1974)

Edgar A, Bedford SM (1904): The early history of the olfactory nerve in swine. Journal of Comparative Neurology, 14, pp. 390-410.

Ellenberger W, Baum H (1943): Handbuch der vergleichenden Anatomie der Haustiere, 18. Auflage, Berlin: Springer-Verlag

Fang M, Lorke DE, Li J, Gong X, Yew JCC, Yew DT (2005 a): Postnatal changes in functional activities of the pig's brain: A combined functional Magnetic Resonance Imaging and immunohistochemical study. Neurosignals 2005; 14:222-223 (DOI: 10.1159/000088638).

Fang M, Zhang L, Li J, Wang C, Chung C, Wai S, Yew D (2005 b): The postnatal development of the cerebellum - A f MRI and silver study. Cellular and Molecular Neurobiology, Volume 25, Number 6, September 2005, pp. 1043-1050 (8).

Fang M, Li J, Rudd JA, Wai SM, Yew JC, Yew DT (2006): fMRI mapping of cortical centres following visual stimulation in postnatal pigs of different ages. Life Sciences 78, 1197-1201.

Félix B, Leger M-E, Albe- Fessard D, Marcilloux J-C, Rampin O, Laplace J-P (1999): Stereotaxic atlas of the pig brain. Brain Research Bulletin, Vol. 49, Nos.1/2, pp.1-138, 1999.

Flatau E, Jakobsohn C (1899): Handbuch der Anatomie des Centralnervensystems der Säugetiere. 1-Makroskopischer Teil. Berlin : Verlag von S. Karger

Förstl H (2005): Frontalhirn, Funktionen und Erkrankungen. 2. Auflage, Springer Medizinverlag Heidelberrg, 2005.

Franck L, Martin P (1894): Handbuch der Anatomie der Haustiere mit besonderer

Berücksichtigung des Pferdes. Zweiter Band. Stuttgart 1894, Verlag von Schickhardt & Ebner.

Freund E (1969): Cytoarchitectonics of the mesencephalon and pons in the domestic pig (sus scrofa domestica). Anatomischer Anzeiger 125,345-362

Freund E (1973): Myeloarchitecture of the mesencephalon in the domestic swine. Anatomischer Anzeiger 134, 445-459

Gegenbauer C (1909): Vergleichende Anatomie der Wirbeltiere. Wilhelm Engelmann, Leipzig 1909.

Gillian LA (1943): The nuclear pattern of the non-tectal portions of the midbrain and isthmus in ungulates. The Journal of Comparative Neurology 78(3): 289-364.

Gizewski ER, Schanze T, Bolle I, de Greiff A, Forsting M, Laube T (2007): Visualization of the visual cortex in minipigs using fMRI. Research in veterinary Science 82 (2007) 281-286.

Glauser EM (1966): Advantages of piglets as experimental animals in pediatric research. Experimental Medicine and Surgery 24,181-190 1966.

Gordon PJ, Dennis R. (1995): Magnetic resonance imaging for the ante mortem diagnosis of cerebellar hypoplasia in a Holstein calf. Veterinary Record 23:671-672.

Grate LL, Golden JA, Hoopes PJ, Hunter JV, Duhaime A-C (2003): Traumatic brain injury in piglets of different ages : techniques for lesion analysis using histology and magnetic resonance imaging. Journal of Neuroscience Methods 123 (2003) 201-206.w

Gross CG (1998): Galen and the squealing pig. Neuroscientist 1998; 4; 216

Hadziselimovic H, Dilberovic F (1977): Appearance of the wild boar brain. Acta Anatomica (Basel) 98, 14-20.

Haller v. Hallerstein V (1934): Äussere Gliederung des Zentralnervensystems. Handbuch der vergleichenden Anatomie der Wirbeltiere. Urban & Schwarzenberg, Berlin/Wien 1934.

Harper JW, Maser JD (1975): A macroscopic study of the brain of *Bison bison bison* the American plains buffalo. Anatomical Record, 148: 187-202.

Hart BL (1983): Flehmen behavior and vomeronasal organ function. Chemical Signals in Vertebrates III, pp 87–103. New York: Plenum Press.

Hashimoto I, Papuaashvili N, Xu C, Okada YC (1996): Neuronal activitiesfrom a deepsubcortical structure can be detected magnetically outside the brain in the porcine preparation. Neuroscience letters 206 (1996)25-28, Elsevier.

Hata N, Dohi T, Warfield S, Wells III W, Kikinis R, Jolesz FA (2007): Multimodality deformable registration of pre- and intraoperative images for MRI- guided brain surgery. Springer Berlin, Volume 1496/ 1998

Hereć S (1967): Structure of the olfactory tubercle and nucleus of the diagonal fasciculus of Broca in the pig. Folia Morphologica (Poland) 1967,Vol 26(issue4):pp 499-506.

Herre W, Stephan H (1954): Zur postnatalen Morphogenese des Hirnes verschiedener Haushunderassen. Morph. Jb.69, 210-264 (1955).

Hofman MA (1985): Size and shape of the cerebral cortex in mammals I. The cortical surface, Brain Behaviour Evolution 27, 28-40.

Holl (1900): Über die Insel des Ungulatengehirnes. Archiv für Anatomie und Physiologie, anatomische Abteilung 1900.

Hudson LC, Cauzinille L, Kornegay JN, Tompkins MB (1995): Magnetic resonance imaging of the normal feline brain. Veterinary Radiology and Ultrasound, Vol. 36, No. 4, 1995, pp 267-275.

Imai H, Konno K, Nakamura M, Shimizu T, Kubota C, Seki K, Honda F, Tomizawa S, Tanaka Y, Hata H, Saito N (2006): A new model of focal cerebral ischemia in the miniature pig. Journal of Neurosurgery. 2006 Feb; 104(2 Suppl):123-32.

Jelsing J, Olsen AK, Cunning P, Gjedde A, Hansen AK, Arnfred S, Hemmingsen R, Pakkenberg B (2005): A volumetric screening procedure for the Göttingen minipig brain. Experimental Brain research, (2005) 162: 428-435.

Jelsing J, Hay-Schmidt A, Dyrby T, Hemmingsen R, Uylings HBM, Pakkenberg B (2006 a): The prefrontal cortex in the Goettingen minipig brain defined by neural projectioncriteria and cytoarchitecture. Brain Research Bulletin 70, (2006) 322-336 Elsevier.

Jelsing J, Nilsen R, Olsen AK, Grand A, Hemmingsen R and Pakkenberg B (2006 b): The postnatal development of neocortical neurons and glia cells in the Göttingen minipig and the domestic pig brain. The Journal of Experimental Biologists 2006 doi:10.1242/jeb.02141.

Jelsing J, Gundersen HJG, Nielsen R, Hemmingsen R, Pakkenberg B (2006 c): The postnatal development of cerebellar Purkinje cells in the Göttingen minipig estimated with a new stereological sampling technique- the vertical bar fractionator. Blackwell Synergy- Journal of Anatomy, Volume 209 Issue 3 Page 321-331, Sept. 2006

Kappers CU (1921): Die vergleichende Anatomie des Nervensystems der Wirbeltiere und des Menschen. Haarlem, De Erven F. Bohn, 1921.

Karamanlidis AN, Magras J (1972): Retinal projections in domestic ungulates I. The retinal projections in the sheep and in the pig. Brain Research, 44(1972)127-145.

Karger B, Puskas Z, Ruwald B, Teige K, Schuirer G (1998): Morphological findings in the brain after experimental gunshots using radiology, pathology and histology. International Journal of Legal Medicine (1998), Volume 111, No. 6: 314-319.

Kawamura K, Otani K (1970): Corticocortical fibre connections in the cat cerebrum: The frontal regions. Journal of Comparative Neurology, 139:423-48.

Kawamura K (1971): Variations of the cerebral sulci in the cat. Acta Anatomica, 80: 204-221 (1971).

Klintworth GK (1968): The comparative anatomy and phylogeny of the tentorium cerebelli. Anatomical Record 160: 635-642.

Koch T (1965): Lehrbuch der Veterinär-Anatomie. Band III: Die großen Versorgungs- und Steuerungssysteme. VEB Gustav Fischer Verlag Jena 1965.

Kraft SL, Gavin PR, Wendling LR, Reddy VK (1989): Canine brain anatomy on magnetic resonance images. Volume 30, Issue 4, pages 147-158, July 1989.

Krueg J (1878): Über die Furchung der Grosshirnrinde der Ungulaten. Z. F. Wissensch. Zoologie. Bd.31, 297-345 (1878).

Kruska D, Röhrs M, Herre W (1970): Vergleichend zytoarchitektonische Untersuchungen an Gehirnen von Wild- und Hausschweinen. Zeitschrift für Anatomie und Entwicklungs Geschichte,131,291-324 (1970).

Kruska D, Röhrs M (1974): Comparative-quantitative investigations on brains of feral pigs from Galapagos Islands and European domestic pigs. Zeitschrift Anatomie und Entwicklungsgeschichte, 144, 61-73, Springer Verlag 1974.

Kruska D (1982): Über das Gehirn des Zwergwildschweins, Sus (Porcula) salvanius Hodgson, 1847- Ein Beitrag zur Problematik vergleichender Hirnuntersuchungen bei Säugetieren unterschiedlicher Körpergrösse. Zeitschrift für Zoologische Systematik und Evolutionsforschung, 20 (1982) 1-12.

Kruska D (1988): Effects of domestication on brain structure and behaviour in mammals. Human Evolution, Vol. 3,- N. 6 (473-485) 1988.

Kuhlenbeck H (1927): Vorlesungen über das Zentralnervensystem der Wirbeltiere. Verlag von Gustav Fischer. Jena.

Lai L Kolber-Simonds D, Park KW, Cheong HT, Greenstein JL, Im GS, Samuel M, Bonk A, Rieke A, Day BN, Murphy CN, Carter DB, Hawley RJ, Prather RS (2002): Production of alpha-1,3-galactosyltransferase knockout pigs by nuclear transfer cloning. Science 295, 1089–1092.

Lakshminarasimhan A (1974): The visual cortex of the ox (*Bos taurus*). Journal für Hirnforschung, Bd. 15, Heft 5/6 1974.

Lakshminarasimhan A (1975): The isocortex of the ox (*Bos taurus*) I. The sulci and gyri. Journal für Hirnforschung, 16, (1975), 293-306.

Landy JJ, Growdon JH, Sandburg R (1961): Use of large germfree animals in medical research. Journal of the American Medical Association, 178:1084-1087.

Langley J (1883): The structure of the dog's brain. Journal of Physiologie, IV 1883.

Larsen M, Bjarkam CR, Ostergaard K, West MJ, Sorensen JC (2004): The anatomy of the subthalamic nucleus evaluated with immunohistochemistry and design-based stereology. Anatomy and Embryology (Berlin) 208, 239-247

Larsell O (1954): The development of the cerebellum of the pig. Anatomical Record 1954, 118(1):73-107.

Lassek AM (1941): The pyramidal tract. A fiber and numerical analysis in a series of non-digital mammals (ungulates). Journal of Comparative Neurology, 77: 399-404.

Lauer EW (1963): The rhinencephalon of Ungulates: Gross morphology. Elsevier Amsterdam, Volume 3, pp. 218-229 (1963).

Lauer EW (1982): Telencephalon of Ungulates. Crosby E.L. & H.N. Schnitzlein: Comparative correlative neuroanatomy of the vertebrate telencephalon,501-524, Macmillan, NY.

Leigh EJ, Mackillop E, Robertson ID, Hudson L (2008): Clinical anatomy of the canine brain using magnetic resonance imaging. Veterinary Radiology and

Ultrasound, Vol. 49, No.2, 2008,pp 113-121.

Leshin LS, Kineman RD, Crim JW, Rampacek GB, Kraeling RR (1991): Immunecytochemical localization of luteinizing hormone-releasing hormone within the olfactory bulb of pigs. Biology of Reproduction 44, 299-304 (1991).

Lidegran MK, Frenckner B, Mosskin M, Nordell B, Palmer K and Linden VB (2006): MRI of the brain and Thorax during extracorporeal membrane oxygenation: Preliminary report from a pig model. American Society for Artificial Internal Organs Journal 2006 doi: 10.1097/01.mat.0000194058.62228.56.

Lind NM, Moustgaard A, Jelsing J, Vajta G, Cumming P, Hansen AK (2007): The use of pigs in neuroscience: Modeling brain disorders. Neuroscience and Biobehavioural Reviews 31(2007) 728-751.

Lim RKS, Liu C-N, Moffitt RL (1960): A stereotaxic atlas of the dog's brain. Charles C Thomas Publisher, Springfield Illinois U.S.A.

Lodygensky GA, Inder TE, Neil JJ (2008): Application of magnetic resonance imaging in animal models of perinatal hypoxic-ischemic cerebral injury. International Journal of Developmental Neuroscience (2008), (1): 13-25.

Mäkiranta MJ, Jauhiainen JP, Oikarinen JT, Suominen K, Tervonen O, Alahuhta S, et al (2002): Funktional magnetic resonance imaging of swine brain during change in thiopental anesthesia into EEG burst- suppression level- a preliminary study. MAGMA 15 (2002) 27-35

Makita T, Tominaga M (1987): Regional anatomy of swine V. Cross section of brain of swine (Part I).The Yamaguchi Journal of Veterinary Medicine., No.14:49-66 1987.

Makita T, Ishida T, Tominaga M, Kagabu S, Mamba K (1988): Computed tomography of the brain of swine and wild boar. The Yamaguchi Journal of Veterinary Medicine, No.15:49-60.1988

Marcilloux J-C, Felix M-B, Rampin O, Stoffels C, Ibazizen M-T, Cabanis EA, Laplace J-P and Albe-Fessard D (1993): Preliminary results of a magnetic resonance imaging (MRI) study of the pig brain placed in stereotaxic conditions. Neuroscience Letters, 156 (1993) 113-116.

Marcilloux J-C, Felix M-B, Laplace J-P, Albe- Fessard D (1989): A stereotaxic apparatus for the study of the central nervous structures in the pig. Brain Research Bulletin, 22:591-597; 1989.

Marino L, Murphy TL, Gozal L, Johnson JI (2001): Magnetic resonance imaging and three dimensional reconstruction of the brain of the fetal common dolphin. Anatomy and Embryology, 203:393-402.

Marquis DG (1934): Effects of removal of teh visual cortex in mammals, with observations on the retentionof light discrimination in dogs. Association for research in nervous and mental diseases: Research publications, 13, 558-592.

Martin P (1904): Lehrbuch der Anatomie der Haustiere. II. Band: Beschreibende Anatomie der einzelnen Haustierarten. Stuttgart 1904 : Verlag von Schickhardt und Ebner.

Maudgil DD, Free SL, Sisodiya SM, Lemieux L, Woermann FG, Fish DR,Shorvon SD (1998): Identifying homologous anatomical landmarks on reconstructed magnetic resonance images of the human cerebral cortical surface. Journal of Anatomy, (1998) 193, pp. 559-571.

McCellan RO (1968): Applications of swine in biomedical research. Laboratory Animal Care 18,120-126.

Meyer RC, Bohl EH, Kohler EM (1964): Procurement and maintenance of germ-free swine for microbiological investigations. Applied Microbiology, Vol.12, No. 4, p. 295-300, 1964.

Moxon-Lester L, Sinclair K, Burke C, Cowin GJ, Rose SE, Colditz P (2007): Increased cerebral lactade during hypoxia may be neuroprotective in newborn piglets

with intrauterine growth restriction. Brain Research 1179 (2007) 79-88.

Mun-Bryce S, Wilkerson AC, Papuashvili N, Okada YC (2001): Recurring episodes of spreading depression are spontaneously elicted by an intracerebral hemorrhage in the swine. Brain Research, 888:248-255, 2001.

Munkeby BH, Smith H-J, Winther-Larssen EH, Bjornerud A and Bjerkas I (2006): Magnetic resonance imaging of the Harderian gland in piglets. Journal of Anatomy, (2006) 209, pp 699-705.

Natt O, Watanabe T, Boretius S, Radulovic J, Frahm J, Michaelis T (2002): High resolution 3D MRI of mouse brain reveals small cerebral structures in vivo. Journal of Neuroscience Methods, 120, (2002), 203- 209.

Negus VE, Street H (1954): The function of the paranasal sinuses. Acta Oto-Laryngologica, Vol. 44: 408-426 (1954)

Nickel R, Schummer A, Seiferle E (1992): Lehrbuch der Anatomie der Haustiere Vol. IV, 3. Auflage, Verlag Paul Parey.

Nielsen MS, Sørensen JC, Bjarcam CR (2009): The substantia nigra pars compacta of the Göttingen minipig: an anatomical and Stereological study. Brain Structure and Function, 213:481-488 (2009).

Nieuwenhuys R, ten Donkelaar HJ, Nicholson C (1998): The central nervous system of vertebrates 3, Springer Verlag Berlin, Heidelberg.

Oelschläger HHA, Kemp B (1998): Ontogenesis of the Sperm Whale Brain. The Journal of Comparative Neurology 399:210–228 (1998).

Oelschläger HHA, Ridgway SH, Knauth M (2010): Cetacean Brain Evolution: Dwarf Sperm Whale *(Kogia sima)* and Common Dolphin *(Delphinus delphis)* – An Investigation with High-Resolution 3D MRI. Brain Behaviour Evolution, 2010; 75:33–62.

Oboussier H (1949): Über Unterschiede des Hirnfurchenbildes beim Hunde.

Verhandlungen der Deutschen Zoologischen Gesellschaft, Mainz 1949.

Oboussier H (1950): Zur Frage der Erblichkeit der Hirnfurchen. Untersuchungen an Kreuzungen extremer Rassetypen des Hundes. Zeitschrift für Menschliche Verebungs – und Konstitutionslehre, Bd. 29, S.831-864 (1950).

Oboussier H (1955)**:** Das Verhalten des Hirnfurchenbildes bei Kreuzungen extremer Rassetypen des Hundes. (Whippet ♀ x Bulldogge ♂). Zeitschrift für Menschliche Vererbungs - und Konstitutionslehre, Bd. 33, S. 1-9 (1955).

Oboussier H (1967): Das Grosshirnfurchenbild als Hinweis auf die Verwandtschaftsbeziehungen der heutigen afrikanischen *Bovidae*. Acta Anatomica, 68:577-596 (1967).

Oboussier H (1971): Quantitative und morphologische Studien am Hirn der Bovidae, ein Beitrag zur Kenntnis der Phylogenie. Gegenbaurs Morphologisches Jahrbuch., Leipzig 117 (1971) 2, S. 162-168.

Okada Y, Lahteenmaki A, Xu C (1999): Comparison of MEG and EEG on the basis of somatic evoked responses elicted by stimulation of the snout in the juvenile swine. Clinical Neurophysiology, 110:214-229, 1999.

Olivares R, Montiel Juan, Aboitiz F (2001): Species differences and similarities in the fine structure of the mammalian corpus callosum. Brain Behaviour Evolution, 2001; 57:98-105.

Otabe JS, Horowitz A (1970): Morphologie and cytoarchitecture of the red nucleus of the domestic pig (sus scrofa) Journal of Comparative Neurology, 138: 373-390.

Oto Ç, Ekİm O, Algin O, Şenel OO, İnce N, Haziroglu RM (2011): 3 Tesla Magnetic resonance imaging and multiplanar reconstruction of the brain and its associated structures in pig. Ankara Üniversitesi Veteriner Fakültesi Dergisi, 58, 73-78, 2011.

Palmieri G, Farina V, Panu R, Asole A, Sanna L, de Riu PL, Gabbi C (1987): Course and termination of the pyramidal tract in the pig. Archives of Anatatomy, Microscopy

and Experimental Morphology, 1987; 75:167-76.

Pakozdy A, Angerer C, Klang A, König EH, Probst A (2014): Gyration of the feline brain: Localisation, terminology and variability. Anatomia, Histologia, Embryologia DOi: 10.1111/ ahe.12153, Blackwell Verlag GmbH, 2014.

Pillay P, Manger PR (2007): Order- specific quantitative patterns of cortical gyrification. European Journal of Neuroscience, Vol. 25, pp. 2705-2712, 2007.

Pillay P (2007): Are there order specific patterns of cortical gyrification and if so why? Thesis for the degree of Masters of Science, Johannesburg 2007.

Pinto Hamuy T, Bromiley RB, Woolsey CN (1956): Somatic afferent areas I and II of dog's cerebral cortex. Journal of neurophysiology, 19, 485-499.

Plogmann D, Kruska D, (1990): Volumetric comparison of auditory structures in the brains of European wild boars (sus scrofa) and domestic pigs (sus scrofa f.dom.) Brain Behavioural Evolution 35, 146-155.

Poceta JS, Hamlin MN, Haack DW, Bohr DF (1981): Stereotaxic placement of cannulae in cerebral ventricle of the pig. The Anatomical Record 200:349-356 (1981).

Pond WG, Boleman SL, Fiorotto ML, Ho H, Knabe DA, Mersmann HJ, Savell JW, Su DR (2000): Perinatal ontogeny of brain growth in the domestic pig. Proceedings of the Society for Experimental Biology and Medicine, 223,102-108.

Radinsky LB (1969): Outlines of canid and felid brain evolution. Annals New York Academy of Sciences, Vol. 167¸issue1, pp. 277-292.

Raghupathi R, Margulies SS (2002): Traumatic axonal injury after closed head injury in the neonatal pig. Journal of Neutotrauma, July 1, 2002, 19(7): 843-853.

Rajimehr R, Tootell RBH (2009): Does Retinotopy Influence Cortical Folding in Primate Visual Cortex? The Journal of Neuroscience, September 9, 2009 • 29(36):11149 –11152 • 11149.

Rawiel F (1939): Untersuchungen an Hirnen von Wild und Hausschweinen. Zeitschrift für Anatomie und Entwicklungsgeschichte, 110, 344-371.

Reep RL, Finlay BL, Darlington RB (2007): The limbic system in mammalian brain evolution. Brain Behaviour Evolution 2007, 70:57-70.

Rehkämper G, Zilles K (1991): Parallel evolution in mammalian and avian brains: comparative cytoarchitectonic cytochemical analysis. Cell Tissue Research 263:3-28.

Rhode V, Rhode I, Thiex R, Küker W, Ince A, Gilsbach JM, Nimsky C, Fahlbusch R, Black PM, Drummond K (2001): The role of intraoperative magnetic resonance imaging for the detection of hemorrhagic complications during surgery for intracerebral lesions: An experimental approach. Surgical Neurology (Surg. neurol.) ISSN 0090-3019, 2001, vol.56,no4,pp.266-275 (47 ref.).

Robinson EM, Mackensie IS, Freemont A, Jasani MK (1988): High resolution magnetic resonance imaging of the pig knees at 4.7T. Magnetic Resonance Imaging, Vol. 6, Issue 5, p. 591-4.

Röhrs M, Ebinger P (1999): Verwildert ist nicht gleich wild: Die Hirngewichte verwildeter Haussäugetiere. Berl. Münch. Tierärztl. Wschr. 112,234-238 (1999).

Roland PE and Zilles K (1994): Brain atlases- a new research tool. Trends Neurosciences, 17(11):458-67.

Romer AS, Parsons TS (1991): Vergleichende Anatomie der Wirbeltiere. Parey-Verlag.

Roohey T, Raju TN, Moustogiannis AN (1997) Animal models for the study of perinatal hypoxic-ischemic encephalopathy: a critical analysis. Early Human Development **47**, 115–146.

Roschig G (1907): Untersuchungen über die Verschiedenheiten der Grosshirnfurchen beim Rinde. Inaugural-Dissertation. Medizinische Fakultät der

Grossherzoglich Hessischen Ludwigs-Universität Giessen 1907.

Rose JE, Woolsey CN (1948): The orbitofrontal cortex and its connections with the mediodorsal nucleus in rabbit, sheep and cat. Association for Reasearch in nervous and Mental Disease. 27: 210-232.

Rosen CL, Schecter WS, Mellins RB, Haddad GG (1992): Effect of acute hypoxia on metabolism and ventilation in awake piglets. Respiration Physiology, 91 (1993) 307-319.

Rosendal F, Pedersen M, Sangill R, Stodkilde-Jorgensen H, Slot Nielsen M, Bjarkam CR, Sunde N, Sorensen JC (2009): MRI protocol for *in vivo* visualization of the Gottingen minipig brain improves targeting in experimental functional neurosurgery. Brain Research Bulletin 79 (2009) 41–45.

Russo D, Paparcone R, Genovese A (2008): A cytoarchitectonic and myeloarchitectonic study of the insular cortex of the bull, *Bos taurus*. Acta Histochemica,110 (2008) 245-255.

Saito T, Bjarkam CR, Nakamura M, Nemoto T (1998): Determination of stereotaxic coordinates for the hippocampus in the domestic pig. Journal of Neuroscience Methods, ISSI 0165-0270, 1998, vol. 80 pp. 29-36 (39 ref.)

Salazar I, Quinteiro PS, Lombardero M, Aleman N, Fernández de Trocóniz P (2004): The prenatal maturity of the accessory olfactory bulb in pigs. Chemical Senses 29: 3–11, 2004.

Salinas-Zeballos ME, Zeballos GA, Gootman PM (1986): A stereotaxic atlas of the developing swine (*Sus scrofa*) forebrain. Plenum Press, 1986: 887-906.

Sakoh M, Gjedde A (2003): Neuroprotection in hypothermia linked to redistribution of oxygen in brain. American Journal of Physiology, Heart and Circulatory Physiology, 285: H17-H25, 2003.

Sambraus HH (1996): Atlas der Nutztierrassen, 5. Auflage. Eugen Ulmer GmbH &

Co. 1986.

Scarpelli M, Salvolini U, Diamanti L, Montironi R, Chiaromoni, Maricotti M (1994): MRI and pathological examination of post-mortem brains: the problem of white matter high signal areas. Neuroradiologie (1994) 36:393-398.

Schellenberg K (1900): Untersuchungen über das Grosshirnmark der Ungulaten. Inaugural-Dissertation. Gustav Fischer Jena 1900.

Schenk H, Ganter M, Seehusen F, Schoeder C, Gerdwilker A, Baumgaertner W, Tipold A (2007): Magnetic resonance imaging findings in metabolic and toxic disorders in three small ruminants. Journalof Veterinary Medical science 61, 865-871.

Schmidt MJ, Pilatus U, Wigger A, Kramer M, Oelschläger HA (2009): Neuroanatomie of the calf brain as revealed by high-resolution magnetic resonance imaging.Journal of Morphology 270: 745-758 2009

Schmidt MJ, Langen N, Klumpp S, Nasirimanesh F, Shirvanchi P, Ondreka N, Kramer M (2011): A study of the comparative anatomy of the brain of domestic ruminants using magnetic resonance imaging. The Veterinary Journal (2011), doi: 10.1016/j.tvjl.2010.12.026.

Schulz LC (1953): Entwicklugsmechanisch bedingte physiologische Aplasien in der Kleinhirnrinde beim Haus und Wildschwein. Inaugural Dissertation, Tierärztliche Hochschule , Hanover 1953.

Seeger J (1990): Zytoarchitektur und Topographie ausgewaehlter Kerngebiete des ventromedialen hypothalamus des Schweines (*sus scrofa domestica*). J. Hirnforschung 1990; 31: 601-11.

Shultz S, Dunbar RIM (2006): Both social and ecological factors predict ungulate brain size. Proceedings of the Royal Society B: Biological sciences (2006) 273, 207-215.

Sisson S (1953): The anatomy of the domestic animals. Revised by Grossmann JD 4th ed. Philadelphia and London: WB Saunders Company.

Smart IHM, Mc Sherry GM (1986 a): Gyrus formation in the cerebral cortex in the ferret. I. Description of the external changes. Journal of Anatomy (1986), 146, pp. 141-152.

Smart IHM, Mc Sherry GM (1986 b): Gyrus formation in the cerebral cortex in the ferret. II. Description of the internal histological changes. Journal of Anatomy (1986), 147, pp 27-43.

Smith JM, James MF, Bockhorst KHJ, Smith MI, Bradley DP, Papadakis NG, Carpenter TA, Parsons AA, Leslie RA, Hall LD, Huang CL-H (2001): Investigation of feline brain anatomy for the detection of cortical spreading depression with magnetic resonance imaging. Journal of Anatomy (2001) 198, pp. 537- 554.

Solnitzky O (1937): The thalamic nuclei of sus scrofa. The Journal of Comparative Neurology, Volume 69, Issue 1, Pages 121-169, published online Oct. 2004 Accepted for publiction Dec. 6,1937

Solnitzky O (1939): The hypothalamus and subthalamus of sus scrofa. Journal of Comparative Neurology. 70, 191-229.

Sørensen JC, Bjarkam CR, Danielsen EH, Simonsen CZ, Geneser FA (2000): Oriented sectioning of irregular tissue blocks in relation to computerized scanning modalities : Results from the domestic pig brain. Journal of Neuroscience Methods, 104 (2000) 93-98.

Starck D (1954): Die äussere Morphologie des Grosshirns zwergwüchsiger und kurzköpfiger Haushunde. Ein Beitrag zur Entstehung des Furchungstyps. Gazeta Médica Portugesa, Vol I-N.º 12, Secção Neurologia e Psiquiatria.1954.

Starck D (1982): Vergleichende Anatomie der Wirbeltiere. Bd. 3: Organe des aktiven Bewegungsapparates, der Koordination, der Umweltbeziehung, des Stoffwechsels und der Fortpflanzung. Springer Verlag - Berlin, Heidelberg, New York.

Stephan H (1951): Vergleichende Untersuchungen ueber den Feinbau des Hirnes von Wild und Haustieren (nach Studien am Schwein und Schaf). Zoologische Jahrbücher Abteilung für Anatomie und Ontogenie der Tiere 1951;71:487-586.

Striedter GF (2002): Brain homology and funktion: An uneasy alliance. Brain Research Bulletin, Vol. 57, Nos. 3/4, pp. 239–242, 2002.

Swindle MM, Smith AC, Laber-Laird K, Dungan L (1994): Swine in biomedical research: Management and models. Institute for Laboratory Animal Research Journal, V36 (1)1994.

Swindle MM (1998): Surgery, anesthesia and experimental techniques in swine. CRC (Chemical Rubber Company) Press Boca Raton, Florida USA.

Szteyn S, Galert D, Dynowski J, Hoczyk W, (1980): The stereotaxic configuration of hypothalamus nerve centres in the pig. Anatomischer Anzeiger 147,12-32.

Talairach J, Tournoux P (1988): Coplanar stereotactic atlas of the human brain. Thieme- Verlag.

Thomas JM, Beamer JL (1971): Age-weight relationships of selected organs and body weight for miniature swine. Growth 1971; 35:259 /72.

Tindal JS, Knaggs GS, Turvey A (1968): The forebrain of the goat in stereotaxic coordinates. Journal of Anatomy, (1968), 103, 3pp.457-469.

Toga AW, Mazziotta JC (1996): Brain mapping: The methods. Academic Press, Inc. 1996.

Toga AW, Thompson P (2001): Maps of the brain. The Anatomical Record (New Anat.) 265:37-53, 2001.

Tumbleson ME (1986): Swine in Biomedical Research. Vol 1-3. New York: Plenum Press, 1986.

Tunturi AR (1950): Physiological determination of the arrangement of teh afferent connections to the middle ectosylvian auditory area in the dog. American journal of physiology 162, 489-205.

Tzuka T, Taura Y (1999): Abscess of bovine brain stem diagnosed by contrast MRI examinations, Journal of Veterinary Medical Science, 61: 425-427.

Uylings HBM, van Eden CB (1990): Qualitative and quantitative comparison of the prefrontal cortex in rat and in primates, including humans, Prog.Brain Res. 85 (1990) 31–62.

Van der Linden A, Verhoye M, Van Audekerke, Peeters R, Eens M, Newman SW, Smulders T, Balthazart J, De Voogd TJ (1998): Non invasive in vivo anatomical studies of the oscine brain by high resolution MRI microscopy. Jounal of Neuroscience Methods, 81 (1998) 45-52.

Vodička P, Smetana K, Dvořánková B, Emerick T, Xu YZ, Ourednik J,Ourednik V, Motlik J (2005): The miniature pig as an animal model in biomedical research. Annals of the New York Academy of Sciences, 1049: 1161-171 (2005)

Wagner R, Xi G, Hua Y, Kleinholz M, de Courten –Meyers GM, Myers RE, Broderick JP, Brott TG (1996): Lobar intracerebral hemorrhage model in pigs (rapid edema development in perihematomal white matter).Stroke. 1996 ;27: 490-497.

Watanabe H, Andersen F, Simonsdn CZ, Evans SM, Gjedde A, Cumming P, DaNeX Study Group (2001): MR-based statistical atlas of the Göttingen Minipig brain. Neuroimage Journal, 14, 1089-1096 (2001).

Waters KA, Beardsmore CS, Paquette J, Meehan B, Cote A, Moss IR (1996): Respiratory responses to rapid-onset, repetitive vs. continuous hypoxia in piglets. Respiration Physiology 105 (1996) 135-142.

Welento J (1964): Structure and topography of the diencephalon nuclei of the pig Part 11. Nuclei of the posterior group of the thalamus and nuclei of the

hypothalamus. Annalea Universitatis Mariae Curie-Sklowdowska. Sectio D. Medicina 19, 143-160.

Welker W (1990): Why does cerebral cortex fissure and fold? A review determinants of gyri and sulci. Jones, E.G., & Peters, A. (Eds), Cerebral Cortex: Vol. 8B, Comparative Structure and Evolution of Cerebral Cortex, Part II. Plenum Press, New York & London, pp. 3-110.

Winkler C, Potter A (1914): An anatomical guide to experimental researches on the cat's brain. Amsterdam, Versluys, 1914, 35pl.

Woolsey CN, Fairman D (1946): Contralateral, ipsilateral and bilateral representation of cutaneous receptors in somatic areas I and II of the cerebral cortex of pig, sheep and other mammals. Surgery 19:684-702.

Woolsey CN, Settlage PH, Meyer DR, Spencer W, Hamuy TP, Travis AM (1952):Patterns of localisation in precentral and "supplymentary" motor areas and their relation to the concept of a premotor area. Association for research in nervous and mental disease: research publications 30, 238-264.

Woolsey CN (1960): Some observations on brain fissuration in relation to cortical localisation of function. Structure and function of the cerebral cortex, p.64-68. Elsevier.

Yamada K, Ishiara K, Yasutomi I, Kobayashi Y, Ueno H, Miyahara K, Furuoka H (2005): Extracranial meningioma in a dairy cow. The Veterinary Record, 156, 652-653, 2005.

Yoshikawa T (1968): The brain of the pig (Yorkshire breed): Atlas of the brains of domestic animals. London: University Press Tokyo and Pennsylvnia State Univ., Tokyo and University Park.

Ziehen T (1899): Anatomie des Centralnervensysthems. Handbuch der Anatomie von Bardeleben und Eggeling, Fischer, Jena 1899.

Erklärung

Ich erkläre: „Ich habe die vorgelegte Dissertation selbstständig und ohne unerlaubte fremde Hilfe und nur mit den Hilfen angefertigt, die ich in der Dissertation angegeben habe. Alle Textstellen, die wörtlich oder sinngemäß aus veröffentlichten oder nicht veröffentlichten Schriften entnommen sind, und alle Angaben, die auf mündlichen Auskünften beruhen, sind als solche kenntlich gemacht. Bei den von mir durchgeführten und in der Dissertation erwähnten Untersuchungen habe ich die Grundsätze guter wissenschaftlicher Praxis, wie sie in der „Satzung der Justus-Liebig-Universität Gießen zur Sicherung guter wissenschaftlicher Praxis“ niedergelegt sind, eingehalten.“

(Verena Schmidt)

Danksagung

Ich möchte mich bei allen Menschen bedanken, die mich bei der Erstellung dieser Doktorarbeit begleitet haben.
Mein besonderer Dank gilt PD Dr. med. vet. (habil.) M. Schmidt für das Angebot des interessanten Themas, der Anleitung und der hervorragenden Betreuung und Prof. Dr. Dr. hc. M. Kramer für die anhaltende Unterstützung und konstuktive Kritik beim Erstellen der Doktorarbeit.
Danken möchte ich auch Payam Shirvanchi und Faranak Nasirimanesh für die Überwachung und Hilfe bei der Erstellung der MR- Bilder während der langen Aufnahmezeiten und Sylke Gralla für ihre Hilfe bei Computerfragen.
Vielen Dank an Dr. Markus Müller für das Wildschwein und an das Hessische Untesuchungsamt für das Babirusa.
Vielen Dank an Frank O'Leary und alle Kollegen von T.F. O'Leary and associates und alle meine Freunde in Irland für Zuspruch in guten und in schlechten Zeiten – go raibh maith agat.
Meinem Rudel möchte ich für Freundschaft und Halt danken (durch Prüfungszeiten und darüber hinaus).
Zuletzt möchte ich meiner Familie für die Liebe und Unterstützung danken, ohne die ich meine Ziele nicht verwirklichen könnte.

édition scientifique
VVB LAUFERSWEILER VERLAG

VVB LAUFERSWEILER VERLAG
STAUFENBERGRING 15
D-35396 GIESSEN

Tel: 0641-5599888 Fax: -5599890
redaktion@doktorverlag.de
www.doktorverlag.de

ISBN: 978-3-8359-6246-0